Natural Organic Matter (NOM) in South African water sources and its removal using ceramic membranes in water treatment plants

---

By

WELLDONE MOYO

Thesis in fulfilment of the requirement for the degree

Doctor of Philosophy

in the

COLLEGE OF SCIENCE, ENGINEERING AND TECHNOLOGY

of the

UNIVERSITY OF SOUTH AFRICA

Supervisor	**:**	**Prof. THABO T.I NKAMBULE**
Co-supervisors	**:**	**Prof. SEBASTIAAN G.J HEIJMAN**
		Prof. TITUS A.M MSAGATI
		Prof. BHEKIE B. MAMBA

DECEMBER 2019

DECLARATION

Name: Welldone Moyo

Student number: 46564195

Degree: PhD: SET

I declare that this thesis is my own work and all sources quoted or used were indicated and acknowledged by complete references.

SIGNATURE DATE

DEDICATION

To my children: Langelihle, Thabo and Aminata

The bar is set…….you have no choice

ACKNOWLEDGEMENTS

To God be the glory for making this possible.

I am grateful to be directed and mentored by the specialists in the area of natural organic matter (NOM) in South Africa.

I would like to express my deepest gratitude to the following individuals and institutions:

- Prof. Thabo T.I Nkambule my supervisor for always making time and offering sound advice on all aspects of this work. Prof S.G.J Heijman, Prof T.A.M Msagati and Prof B.B Mamba my co-supervisors, for their continuous encouragement throughout this research work and for having faith in what I am capable of accomplishing.
- My late parents, mother (Tracey) and father (Patrick), thank you for loving and supporting me in many ways than one. May your souls rest in peace.
- My wife Nozipho, thank you for tolerating my abnormal working hours, my many episodes in absentia and in many instances having to take care of the kids all by yourself.
- Prof. N Chaukura and Dr M.M Motsa of the Nanotechnology and Water Sustainability (NanoWS) Research Unit at UNISA for their guidance in the experimental designs and write up.
- Water Research Commission (WRC) of South Africa, National Research Fund (NRF) of South Africa and UNISA (through the NanoWS Research Unit of the College of Science Engineering and Technology), for providing financial support.
- The Editing Doctor® for providing specialist academic editing and proofreading services to get this thesis ready for submission and examination.
- All the water treatment plants in Gauteng, Limpopo, Kwa-Zulu Natal, North-West and Western Cape for allowing us to take samples.
- My colleagues and friends at NanoWS research unit and more specifically the NOM group, for providing support and assistance in many ways I could not have imagined.
- My colleagues at TU Delft thank you for impacting knowledge and skills on ceramic membrane technology. Also thank you making my six months residency in the Netherlands memorable.

PUBLICATIONS AND PRESENTATIONS

The research work presented in this thesis has been presented at local and international conferences. Parts thereof have also been submitted or published in peer-reviewed journals.

Published manuscripts

1. **Moyo W**, Motsa M.M, Chaukura N, Msagati T.A.M, Mamba B.B, Heijman S.J.G and Nkambule T.T.I (2020). Investigating the fate of natural organic matter at a drinking water treatment plant in South Africa using optical spectroscopy and chemometric analysis. *Water SA*, **46**(1), 131-140.
2. **Moyo W**, Chaukura N, Msagati T.A.M, Mamba B.B, Heijman S.J.G and Nkambule T.T.I (2019). The properties and removal efficacies of natural organic matter fractions by South African drinking water treatment plants. *Journal of Environmental Chemical Engineering,* ***7***(3), 103101*.*
3. **Moyo W**, Motsa M.M, Chaukura N, Msagati T.A.M, Mamba B.B, Heijman S.J.G and Nkambule T.T.I (2019). Fundamental fouling mechanisms of dissolved organic matter fractions and their implications on the surface modifications of ceramic nanofiltration membranes. Insights from a laboratory application. *Water Science and Technology*, **80**(9), 1702-1714.
4. **Moyo W,** Motsa M.M, Chaukura N, Msagati T.A.M, Mamba B.B, Heijman S.J.G and Nkambule T.T.I. The synergistic fouling of ceramic membranes by particles and natural organic matter fractions using different surface waters in South Africa*. Journal of Membrane Science and Research. In press.*
5. **Moyo W**, Msagati T.A.M, Chaukura N, Heijman S.J.G, Mamba B.B and Nkambule T.T.I. Defects in the active layer of ceramic membranes: A facile characterization approach. Water Institute of Southern Africa, 2018, Cape Town, South Africa, 24 – 27 June 2018 (**ISBN** 978-0-6399369-2-5 pp.104).

Manuscripts under peer review

6. **Moyo W**, Motsa M.M, Chaukura N, Msagati T.A.M, Mamba B.B, Heijman S.J.G and Nkambule T.T.I. Selective removal of natural organic matter fractions by ceramic membranes from water samples obtained from a drinking water treatment plant in South Africa. *Journal of Membrane Science (Submitted: 30 November 2019).*
7. **Moyo W**, Motsa M.M, Chaukura N, Msagati T.A.M, Mamba B.B, Heijman S.J.G and Nkambule T.T.I. Characterisation of natural organic matter in South African drinking water treatment plants: Towards integrating ceramic membrane filtration. *Water Science and Engineering (Submitted: 26 February 2020).*
8. **Moyo W**, Motsa M.M, Chaukura N, Msagati T.A.M, Mamba B.B, Heijman S.J.G and Nkambule T.T.I. Monitoring the characteristics and removal of natural organic matter fractions in selected South African water treatment plants. *Water Practise and Technology* (Submitted: *02 May 2020*).

Manuscript under preparation

9. **Moyo W**, Chaukura N, Motsa M.M, Msagati T.A.M, Mamba B.B, Heijman S.J.G and Nkambule T.T.I. Membrane filtration for drinking water treatment: An African perspective.

Other related publications not referenced in this thesis

10. Chaukura N, **Moyo W**, Mamba B.B and Nkambule T.T.I (2018). Abatement of humic acid from aqueous solution using a carbonaceous conjugated microporous polymer derived from waste polystyrene. *Environmental Science and Pollution Research*, **25** (4), 3291-3300.
11. Chaukura N, **Moyo W**, Mamba B.B and Nkambule T.T.I (2018). Removal of dissolved organic matter from raw water using zero valent iron-carbonaceous conjugated microporous polymer nanocomposites. *Physics and Chemistry of the Earth*, Parts A/B/C **107**, 38-44

12. Chaukura N, Ndlangamandla N.G, **Moyo W**, Msagati T.A.M, Mamba B.B and Nkambule T.T.I (2018). Natural organic matter in aquatic systems–a South African perspective. *Water SA,* **44** (4), 624-635.
13. Chaukura N, Marais S.S, **Moyo W**, Mbali N, Thakalekoala L.C, Ingwani T, Mamba B.B, Jarvis P and Nkambule T.T.I. Contemporary issues on the occurrence and removal of disinfection by-products in drinking water – a review. *Journal of Chemical Environmental Science*, **8**(2) 103659.
14. Tshindane P, Mamba P.P, Moss L, Swana U.U, **Moyo W**, Motsa M.M, Chaukura N, Mamba B.B and Nkambule T.T.I (2019). The occurrence of natural organic matter in South African water treatment plants. *Journal of Water Process Engineerin*g **31**, 100809.
15. Chaukura N, Chiworeso R, Gwenzi W, Motsa M.M, Munzeiwa W, **Moyo W**, Chikurunhe I and Nkambule T.T.I (2020). A new generation low-cost biochar-clay composite 'biscuit' ceramic filter for point-of-use water treatment. *Applied Clay Sciences*, **185** (2020), 105409
16. Chaukura N, **Moyo W**, Ndiweni S.N, Ingwani T, Gwenzi W and Nkambule T.T.I. A comparative assessment of the removal efficiency of natural organic matter in conventional water treatment plants in Zimbabwe and South Africa. *Water Environment Research* (*Submitted: 15 June 2020)*
17. Ingwani T, Ndiweni S.N, **Moyo W**, Chaukura N, Mamba B.B, Nkambule T.I.T and Gilmore A.M. Water quality analysis using simultaneous absorbance and fluorescence excitation-emission mapping: A review of fundamental research and industrial applications and trends. *Methods and Applications in Fluorescence (Submitted: 28 May 2020).*

Technical Reports

18. Marais S.S, Ndlangamandla N.G, Bopape D.A, Strydom W.F, **Moyo W**, Chaukura N, Kuvarega A.T, de Kock L, Mamba B.B, Msagati T.A.M and Nkambule T.T.I. (2018). Natural organic matter (NOM) in South African waters. Volume I: NOM fractionation, characterization and formation of disinfection by-products. Report No. 2468/1/18, Water Research Commission, South Africa, 2018 (**ISBN**: 978-1-4312-0993-4).

19. Marais S.S, Ndlangamandla N.G, Bopape D.A, Strydom W.F, **Moyo W**, Chaukura N, Kuvarega A.T, de Kock L, Mamba B.B, Msagati T.A.M and Nkambule T.T.I. (2018). Natural organic matter (NOM) in South African waters. Volume II: Conventional and advanced processes for natural organic matter (NOM) removal. Report No. 2468/1/18, Water Research Commission, South Africa, 2018 (**ISBN**: 978-0-6392-0106-1).
20. Chaukura N, Strydom W.F, **Moyo W**, Marais S.S, Ndiweni SN, de Kock L, Msagati T.A.M, Mamba B.B, Nkambule T.T.I (2017). Stakeholder engagement workshops on natural organic matter (NOM) in South African Waters. A technical report for the Water Research Commission of South Africa.

Conference Presentations

Oral

1. **Moyo W**, Msagati T.A.M, Mamba B.B, Heijman S.J.G and Nkambule T.T.I. *Synergism between particulate and dissolved organic matter on ceramic membrane fouling using South African surface waters.* International Water Association (IWA) Specialist Conference on Particle Separation, Massachusetts, United States of America, 13 - 15 November 2019.
2. **Moyo W**, Msagati T.A.M, Mamba B.B, Heijman S.J.G and Nkambule T.T.I. *Combined optical methods for tracking NOM properties and removal efficacies by South African drinking water treatment plants*. International Water Association (IWA) Specialist Conference on Natural Organic Matter in Drinking Water, Tokyo, Japan, 7 - 10 October 2019.
3. **Moyo W**, Msagati T.A.M, Mamba B.B, Heijman S.J.G and Nkambule T.T.I. *Fate of natural organic matter at a full scale drinking water treatment plant in the Gauteng province of South Africa: Insights from optical spectroscopy coupled with chemometric analysis*. 2nd International Symposium on Environment and Energy, Science and Technology, ISEEST-2. Misty Hills, Johannesburg, South Africa, 18 – 21 August 2019.
4. **Moyo W**, Msagati T.A.M, Mamba B.B, Heijman S.J.G and Nkambule T.T.I. *Fate of natural organic matter at a full scale drinking water treatment plant in the Gauteng province of South Africa: Insights from optical spectroscopy*

coupled with chemometric analysis. US-Africa Forum on Nanotechnology Convergence for Sustainable Energy, Water and Environment, Glenburn Lodge in Johannesburg, South Africa, 11 – 15 August 2019.

5. **Moyo W**, Msagati T.A.M, Mamba B.B, Heijman S.J.G and Nkambule T.T.I. *Fundamental fouling mechanisms of DOM fractions and their implications on the surface modifications of ceramic nanofiltration membranes*. International Water Association (IWA) Regional Membrane Technology Conference, Vadodara, India, 10-13 December 2018.
6. **Moyo W**, Msagati T.A.M, Mamba B.B, Heijman S.J.G and Nkambule T.T.I. *Defects in the active layer of ceramic nanofiltration membranes: A facile characterization approach.* Oral presentation. Water Institute of Southern Africa (WISA) 2018 Biennial Conference, Cape Town, South Africa, 15 - 19 June 2018.
7. **Moyo W**, Msagati T.A.M, Mamba B.B, Heijman S.J.G and Nkambule T.T.I. *Natural Organic Matter (NOM) in South African water sources and its removal using ceramic membranes in water treatment plants.* Water Research Commission (WRC) Workshop on natural organic matter (NOM) in South African waters, University of KwaZulu Natal (UKZN), Durban, South Africa, 9 June 2017.
8. **Moyo W**, Msagati T.A.M, Mamba B.B, Heijman S.J.G and Nkambule T.T.I. *Natural Organic Matter (NOM) in South African water sources and its removal using ceramic membranes in water treatment plants.* Water Research Commission (WRC) Workshop on natural organic matter (NOM) in South African waters, University of Cape Town (UCT), Cape Town, South Africa, 7 June 2017.
9. **Moyo W**, Msagati T.A.M, Mamba B.B, Heijman S.J.G and Nkambule T.T.I. *Natural Organic Matter (NOM) in South African water sources and its removal using ceramic membranes in water treatment plants.* Water Research Commission (WRC) Workshop on natural organic matter (NOM) in South African waters, UNISA, Florida Sciences Campus, Roodepoort, South Africa, 23 May 2017.

Poster Presentation

1. **Moyo W**, Motsa M.M, Chaukura N, Msagati T.A.M, Mamba B.B, Heijman S.J.G and Nkambule T.I (2019). *Monitoring the characteristics and removal of natural organic matter fractions in selected South African water treatment plants*. Workshop on natural organic matter (NOM) in South African waters, UNISA, Florida Sciences Campus, Roodepoort, South Africa, 20 November 2019.

ABSTRACT

South African water treatment plants employ the conventional water treatment processes which include processes such as coagulation/flocculation, sedimentation, filtration and disinfection. However, these traditional unit processes do not effectively remove natural organic matter (NOM) (around 35% at conventional pH). Detrimental to water treatment and distribution, NOM is the major contributor to the fouling of all membrane types (MF, UF, NF and RO), is a precursor to the formation of disinfection by-products (DBPs), impacts on the organoleptic properties, accelerates the clogging of the pores of activated carbon and thus decreases their effectiveness to remove pollutants, and certain fractions of NOM promote biological growth in the distribution. Previous research showed good correlation of NOM reactivity and treatability by employing comprehensive and sensitive analytical approaches such as biodegradable dissolved organic carbon (BDOC), polarity rapid assessment matrix (PRAM), fluorescent excitation emission matrix (FEEM), and synchronous fluorescence scan (SFS). Coupling the aforementioned techniques with chemometric methods such as parallel factor component analysis (PARAFAC), fluorescent regional integration (FRI), two dimensional correlation spectroscopy (2D-COR), spectroscopic indices such as humification index (HIX), freshness index (β:α) and fluorescence index (FI) would provide even deeper information on otherwise latent features of NOM fractions. There has not been a comprehensive study in South Africa pooling these analytical methods and chemometric techniques for characterization of NOM found in drinking water sources of South Africa. Additionally, there are no studies in South Africa that seek to introduce advanced treatment process such as ceramic membrane filtration to complement the conventional treatment process.

To achieve the principal aim of assessing the applicability of ceramic membranes for the removal of NOM, it required that the NOM character and the extent of NOM removal by conventional methods be established. Data from the eleven drinking water plants spatially located in the five water quality regions of South Africa were pooled and a PARAFAC model fitting four components was established and validated based on the slit half criteria, and the distribution of the components at each water source was quantified using their maximum fluorescence intensities

(F_{max}). The value of F_{max} was higher for terrestrial humic-like (C1) and fulvic like (C2) components in comparison to humic-like (C3) and protein-like (C4) components. It was established that coagulation was more effective for the removal of the humic-like fractions when compared with the other fractions. In the rapid sand filtration stage (RSF), bulk NOM removal (in terms of UV_{254}) was found to be higher than that of fluorescent natural organic matter (FNOM) fraction, regardless of location of the plant. This suggests that non-FNOM fractions were removed much more effectively than FNOM fraction during the RSF stage.

The selectivity of ceramic membranes was further explored by using ceramic membranes of different molecular weight cut off (MWCO) within the nanofiltration range so as to identify latent removal efficacies of ceramic membranes within a narrow range. Ceramic NF membranes with a disc configuration of 90 mm diameter, 2.5 mm thickness, and an effective filtration area of 0.00563 m^2, with a porosity of 30% were used. It was established that higher MWCO (750 Da) membranes rejected FNOM fractions more compared to lower MWCO (450 Da) membranes. This was attributed to the effect of permeation drag. The results indicated that FNOM fractions could effectively be removed by higher MWCO membranes than lower MWCO membranes. In addition, higher MWCO membranes were particularly selective towards the removal of tryptophan (TPL) and humic like (HL) fractions of FNOM. Further, by employing 2D-Shige modelling technique it was deduced that the HL and TPL like fractions were more susceptible to removal than the fulvic-like (FL) fraction. These findings corroborated FNOM removal studies, which suggest that the rate of removal of FNOM fractions (TPL and HL, in particular) was higher than that of other fractions.

The propensity to fouling, (i.e the deposition of NOM on the membrane surface and inside the membrane pores consequently leading to the reduction of flux) by model NOM fractions on ceramic membranes was investigated. The effect of membrane surface modification on fouling resistance was also studied by comparing the performance of both TiO_2 atomic layer deposited (ALD)-coated and pristine membranes. Using model NOM foulants, the results showed that sodium alginate (SAL) caused the most extensive fouling on pristine membranes, and the ALD coating reduced the fouling potential of SAL by 35%. Cake filtration was

found to be the least significant fouling mechanism occurring in feed solutions composed of bovine serum albumin (BSA) and SAL, and the most significant fouling mechanism of feed solution made up of humic acid (HA) and SAL. The fouling mechanisms were almost similar for both the coated and the pristine membranes. For the coated membrane the propensity to fouling correlated with complete blocking, standard blocking and intermediate blocking (R^2 = 0.74; 0.74 and 0.40, respectively). For the pristine membrane, R^2 values of 0.76; 0.75 and 0.60 were established for the respective fouling mechanisms of complete blocking, standard blocking, and intermediate blocking. However, cake filtration was found to be the most significant fouling mechanism for the coated membrane (R^2 = 0.99), and the least significant fouling mechanism for the pristine membrane (R^2 = 0.37). Coating was found to increase the hydrophilicity of the ceramic membranes; this was evidenced by the contact angle measurements, which showed a 23% decline in hydrophobicity of the coated membrane relative to the uncoated membrane.

TABLE OF CONTENTS

LIST OF FIGURES

LIST OF TABLES

LIST OF ABBREVIATIONS

ALD	Atomic Layer Deposition
AOC	Assimilable Organic Carbon
AOP	Advanced Oxidation Processes
ASTM	American Society for Testing and Materials
ATP	Adenosine Triphosphate
BAC	Biological Activated Sand
BDOC	Biodegradable Dissolved Organic Carbon
BSA	Bovine Serum Albumin
CAPEX	Capital Expenditure
C18	Octadecylsilane
CN	Cyanopropyl
CVD	Chemical Vapour Deposition
DBP(s)	Disinfection by-product(s)
DBPFP	Disinfection by-product Formation Potential
DOC	Dissolved Organic Carbon
DWTP	Drinking Water Treatment Plant
EEM	Excitation Emission Matrix
EPA	Environmental Protection Agency
FEEM	Fluorescence Excitation Emission Matrix
FI	Fluorescence Intensity
FL	Fulvic acid Like
FNOM	Fluorescent Natural Organic Matter
FRI	Fluorescence Regional Integration
GC	Gas Chromatography
GC-ECD	Gas Chromatography-Electron Capture Detector
HA	Humic acid
HAA(s)	Haloacetic acid(s)
HIX	Humification Index
HPI	Hydrophilic
HPIA	Hydrophilic acids
HPIB	Hydrophilic bases
HPIN	Hydrophilic neutrals
HPLC	High Performance Liquid Chromatography
HPO	Hydrophobic
HPOA	Hydrophobic acids
HPOB	Hydrophobic bases
HPSEC	High Performance Size Exclusion Chromatography
LC-OCD	Liquid Chromatography with Organic Carbon Detector
MBP	Microbial By-Product like
MF	Micro-filtration
MIEX	Magnetic Ion Exchange
m-PRAM	Modified Polarity Rapid Assessment Method
MWCO	Molecular Weight Cut Off
NF	Nano-filtration
NOM	Natural Organic Matter
OPEX	Operational Expenditure
PARAFAC	Parallel Factor

PCA	Principal Component Analysis
PRAM	Polarity Rapid Assessment Method
RSF	Rapid Sand Filters
RO	Reverse Osmosis
SAL	Sodium Alginate
SEC	Size Exclusion Chromatography
SPE	Solid Phase Extraction
SANS	South African National Standards
SUVA	Specific Ultraviolet Absorbance
THM	Trihalomethane
THMFP	Trihalomethane Formation Potential
TOC	Total Organic Carbon
TPL	Tryptophan Like
TPI	Transphilic
TYL	Tyrosine Like
UF	Ultra-filtration
UV_{254}	Ultra Violet absorbance at wavelength of 254 nm
WHO	World Health Organization
WRC	Water Research Commission
WTP	Water Treatment Plant

CHAPTER 1*:*
INTRODUCTION

1.1 BACKGROUND

Competing anthropogenic activities and natural catastrophes have put a strain on the quality and quantity of water usable for basic needs. Compounding these problems is the emergency of water borne diseases especially in third world countries where water companies or municipalities are not able to meet the demand to supply good quality water for domestic use [1]. Rapid industrialization and population growth has exacerbated the concentrations of concoctions of mixed organic pollutants that find their way into the drinking water system.

Organic pollutants are broadly classified into naturally occurring organic and man-made organic pollutants. Man-made organic pollutants are further sub-categorized into: Industrial chemicals and pharmaceuticals (e.g. trichloroethylene, carbon tetrachloride and caffeine); Hydrocarbons, (e.g. benzene, xylene and toluene); pesticides (e.g. aldicarb and chlordane); and herbicides (e.g. alachor and silvex) [2]. Natural organics, which are collectively known as natural organic matter (NOM) result from the degradation of the remains of animal (e.g. carcasses), plant (e.g. falling branches and leaves) and microorganism (e.g. microbial excretions) [3]. When present in natural waters, NOM poses no harm; however, its occurrence in potable water has proven to be a challenge for water treatment utilities and municipalities [4]. Therefore, it is imperative that NOM is removed from drinking water because its presence gives the water undesirable repulsive organoleptic properties (taste, odour, visual).

The disinfectants (mainly chlorine and ozone) used in the water treatment process react with NOM to produce carcinogenic disinfection by-products (DBP), which are probable human carcinogens. The DBPs include halogenated organics (e.g. trihalomethanes (THM) and haloacetic acid (HAA)). Therefore, the measurement, monitoring and control or removal NOM from water sources is very important. For

this to be realized, the character of NOM must be established upfront so that rapid protocols are formulated and implemented.

Commonly used NOM characterization techniques include: Specific Ultraviolet Absorbance (SUVA) calculations, Ultraviolet (UV) absorbance measurements at a wavelength of 254 nm, Dissolved Organic Carbon (DOC) measurements, Liquid Chromatography coupled to an Organic Carbon Detector (LC-OCD), Size Exclusion Chromatography (SEC), Fluorescence Excitation-Emission Matrices (FEEM) as well as techniques that employ membrane filtration and ion exchange resins. Each of these characterization techniques yields their own unique information on NOM. Therefore, when employed individually, each of these methods does not give conclusive data on the character of NOM. For this reason, a series of characterization techniques is often employed to give detailed information about the character of NOM under investigation. As already alluded to in the preceding paragraph, it is very important that the characterization of the NOM is undertaken upfront. Not only will the type of the organic pollutant such as NOM determine the choice of treatment process, it will also influence the performance and efficiency of the selected treatment process [6].

The most commonly used treatment process for the removal of NOM include: coagulation, ion exchange (IEX), granular activated carbon (GAC) adsorption, filtration membranes (micro (MF), ultra (UF), nano (NF) and reverse osmosis(RO)) and ion exchange processes. However, these methods are either not very efficient in the removal of NOM and its fractions or they are energy consuming and generate sludge which causes problems with disposal.

1.2 PROBLEM STATEMENT.

The nature and quantity of NOM is affected by the bio-geophysical activities that are characteristic of that watershed or in the periphery of the water source and within the water source itself. To this end, NOM varies from one water source to another both with respect to time (season) and space (watershed characteristics) [5]. There are roughly five geographical water quality regions in South Africa, which reflect the combined effect of climate (i.e. rainfall, evaporation and temperature), geological formation, soil type, anthropogenic activities and

vegetation pattern [1]. However, the data on the nature and composition of NOM occurring in these geographical regions is largely unknown. A multifaceted NOM characterization approach is required to learn of the nature of NOM in these regions for the purposes of optimizing unit operations and determining the best technology or technology mix for better NOM removal.

1.3 LIMITATIONS OF CHARACTERIZATION TECHNIQUES

For the effective determination of NOM, it is necessary to characterize NOM in terms of spatial and temporal variations so as to allow the predictive tools for rapid assessment protocols to be formulated [6]. However, NOM characterisation techniques and parameters (SUVA, UV, DOC, BDOC, EEM, SEC, LC-OCD) possess specific inherent limitations. Although they allow partial characterization of NOM to be undertaken, they do not delve into the compositional properties of the NOM. Only when the composition of NOM is known then can site specific protocols targeting NOM characteristics that are specific to that particular area and season be formulated and implemented. Most studies undertaken on South African waters have reported isolated characterization parameters with very little or no attention on multi-faceted characterization techniques for the purposes of capturing the multi-dimensional nature of NOM.

1.4 LIMITATIONS OF NOM REMOVAL TECHNIQUES

The most commonly applied treatment process for the removal of NOM include: coagulation, granular activated carbon (GAC) adsorption, filtration membranes (nano (NF) and reverse osmosis (RO)) and ion exchange processes. It must be noted that NOM is mostly dissolved and that dissolved NOM can be removed directly or by conversion to particulate form via coagulation membrane filtration methods such as micro (MF), ultra (UF). However, the aforementioned techniques have their drawbacks. For example, iron or aluminium based inorganic coagulants do not completely remove all fractions of NOM but just in part. Additionally, conventional and advanced NOM removal techniques may not be cost effective nor environmentally friendly. The disposal of sludge generated from NOM removal may require costly disposal means such as energy for incineration or disposal on land. Sedimentation/ flotation and filtration preceded by coagulation/ flocculation are generally considered to be the most common and economically feasible

process for the removal of NOM. Although NOM can be removed by coagulation, the technique is less effective in the removal of hydrophilic low molecular weight (LMW) fractions of NOM when compared with hydrophobic high molecular weight (HMW) fractions. Membrane filtration (NF and RO) is energy and operationally intensive and it is primarily effective towards the removal of low molecular weight (LMW) NOM. For these reasons, this technology is not economically viable at a commercial scale, especially in developing countries [7]. Despite adsorption techniques such as GAC being effective in the removal of NOM, their effectiveness is hampered by the presence of other species, which often decrease uptake capacity for a trace contaminant such as atrazine. compete for the adsorption sites [8]. The shortcomings listed above are compounded by the pH of waters found in some parts of South Africa, which are detrimental to the treatment plants infrastructure and/or the functionality of specific steps of the water treatment processes.

1.5 JUSTIFICATION OF THE RESEARCH STUDY

Over the past two decades, increased focus has been directed towards the application of pressure driven filtration membranes in drinking water treatment, polymeric membranes in particular [9]. Polymeric membranes are commonly used in water treatment because they are cheap compared to the inorganic membranes. Organic membranes are generally manufactured from polymers such as cellulose acetate (CA), polysulfone (PS), polyamide (PA), polyethersulfone (PES), polypropylene (PP), and polyvinylidene fluoride (PVDF) [94]. Although these membranes offer promising solutions in the water treatment, they suffer drawbacks relating to the synthetic organic polymeric material used for the fabrication of such membranes. This type of material functions optimally in medium with a neutral to slightly acidic pH [9]. In contrast, inorganic membranes are generally fabricated from oxides of titanium, zirconium, aluminum and silicon carbide [95]. Inorganic membranes are beginning to find application in water treatment because of their durability and low operational expenditure (OPEX) costs compared to the polymeric membranes. Therefore, ceramic membranes provide a good alternative for targeting, in this case, the removal of organic pollutants from any aqueous medium. Furthermore, because of their inherent

mechanical stability, ceramic membranes can be modified to enhance their filtration function without altering their mechanical strength [10].

Ceramic membranes are used in European countries for the treatment of drinking water. However, the organic matter load in European countries is fairly uniform thus making the operational conditions to be fairly uniform. In South Africa, the different water quality types found in the country give rise to a non-uniform organic load, which by extension gives non-uniform physico-chemical conditions. No studies have been undertaken on the application of ceramic membranes for the removal of organic pollutants from South African waters (i.e. for drinking water purposes). In addition, the coupling of membrane filtration to unit operations (such as coagulation/flocculation, GAC, Ion exchange) for purposes of removing NOM fractions has not been explored in the South African context. To this end, the coupling mix that gives the best efficiency and cost effectiveness has not yet been established. It is envisioned that the data generated from this study will appraise the application of ceramic membranes to augment the existing water treatment methods in South Africa.

The challenge that is inherent to membrane technology is the phenomenon of fouling. Fouling is the deposition of pollutants on the membrane surface, which results in the blockage of pores or pore channels and ultimately causing a reduction in the flux (i.e. increase in TMP needed to maintain constant flux). Zheng et al [11] has reported that the organic water content in a particular season determines the type and extent of membrane fouling. In South Africa, research on the contribution of organic pollutants towards fouling is at its infancy. Additionally, most of the research on fouling is focused on the behaviour of polymeric membranes, and preliminary findings indicate that the fouling behaviour of ceramic membranes is dissimilar to that of polymeric membranes under similar fouling conditions [12]. Prior to investigating real water samples, model foulants that mimic organic pollutants that are prevalent in drinking water will be used to model the fouling behavior.

1.6 AIM, OBJECTIVES AND RESEARCH QUESTIONS

The aim of this study was to characterise NOM found in South African water systems and then apply both pristine and modified ceramic membranes to target

NOM and its fractions. In order to achieve this, the aim was broken down into the following objectives:

(i) Characterize NOM found in South African surface waters using advanced methods (i.e. (Fluorescent excitation emission matrix (FEEM), modified polarity rapid assessment method (mPRAM), biodegradable dissolved organic carbon (BDOC), parallel factor component analysis (PARAFAC) using SOLO software and SUVA)

(ii) To investigate the occurrence, distribution and behavior of NOM fractions found in South Africa for the purpose of investigating the effectiveness of ceramic membranes filtration in the removal of NOM fractions using multi-faceted characterization techniques. The overall goal here was to gain a deeper understanding of the changes of NOM composition upon treatment by ceramic membranes.

(iii) Conduct a comparative analysis of the fouling of ceramic membranes by model NOM pollutants on modified membranes and pristine ceramic membranes under similar hydrodynamic conditions.

(iv) Investigate the selectivity of ceramic membranes towards removal of specific NOM fractions and the impact of coupling ceramic membranes to unit operations (e.g.DAFF, dissolved air floatation filtration) for the purposes of removing problematic NOM fractions.

Therefore, this research study aimed at addressing the following research questions:

1. To what extent are NOM fractions removed at each treatment stage?
2. To what extent can spectroscopic indices be used as predictors for NOM removal efficiency by conventional unit processes?
3. What is the removal efficiency of the NOM characteristics (DOC, UV_{254} FNOM, BDOC) found in South African surface waters by ceramic membranes?
4. What is the dominant fouling mechanism for ceramic membranes by waters from different water quality sources of South Africa?
5. Which model NOM fraction has the highest propensity to foul the membranes and why?

6. How does the extent of fouling on the modified ceramic membrane compare with that of pristine membranes?
7. What is the extent of selective removal of specific NOM fractions by ceramic membranes (i.e. BDOC, chromophoric, fluorescent and biogenic fractions) from raw and partially treated waters?
8. To what extent does coupling of the membrane to unit processes improve the effectiveness of the removal of DBP precursors?
9. What are other opportunities for development of simple methods of characterizing ceramic membrane?

The novelty of this study is in the following ways:

1. Tracking the compositional transformations of NOM fractions throughout the water treatment train has not been carried out extensively on full-scale treatment plants in South Africa.
2. Ceramic membranes have not been used for the purposes of removing NOM in drinking water in South Africa. This is expected to be a first in South Africa. This research aims at giving a better and superior alternative.
3. Studies in coupling ceramic membranes with unit operations (e.g DAFF or coagulation) for the purposes of removing DBP precursors have not been explored in the South African context.

1.7 THESIS OUTLINE

The remainder of this thesis is structured as follows:

Chapter 2 – Literature review

Chapter 2 provides an in-depth discussion on the occurrence, distribution and fate of NOM within the water treatment plants, treatability of NOM during potable water treatment and challenges associated with currently available NOM characterization and removal techniques. Furthermore, membrane technology, in particular ceramic membranes filtration, is discussed in terms of its strengths, limitations and opportunities for NOM removal in single and integrated systems.

Chapter 3 – Experimental methodology

A concise description of experimental and analytical methods employed to achieve the objectives of this research study is presented in this chapter.

Chapter 4 – The properties and removal efficacies of natural organic matter fractions by South African drinking water treatment plants

This chapter is presented in the form of papers, one is published in the *Journal of Environmental Chemical Engineering* and the other is submitted to the journal *Water Practice and Technology*. Work presented in this chapter involves an assessment of the efficiency of treatment processes that use conventional and advanced drinking water treatment technologies for the removal of NOM. This chapter is dedicated to the response of research questions 1 and 2.

Chapter 5 – Characterization of natural organic matter of South Africa: Towards an integrated ceramic membrane filtration system

This chapter is presented in the form of a paper that is submitted to the *Water Science and Engineering Journal*. The applicability of ceramic membranes in the removal of NOM fractions is explored using water samples abstracted from different water quality regions of South Africa. Specifically, an emphasis is placed on determining the extent and dynamics of NOM character reduction due to ceramic membrane filtration (polarity, BDOC, SUVA, fluorescence, DOC etc). Research questions 3 and 4 are addressed by this chapter.

Chapter 6 – Fundamental fouling mechanisms of DOM fractions and their implications on the surface modifications of ceramic nanofiltration membranes

This chapter is presented in the form of papers, one is published in the journal *Water Science and Technology* and the other is in press in the *Journal of Membrane Science and Research*. Fundamental factors influencing foulant - foulant and foulant - membrane interactions during simulated dissolved organic matter (DOM) fractions and removal using ceramic nanofiltration (NF) is investigated in this chapter. The impact of membrane ceramic modification by

atomic layer deposition (ALD) on fouling mitigation is also assessed. Research questions 5 and 6 are addressed by this chapter.

Chapter 7 – Selective removal of natural organic matter fractions by ceramic nanofiltration membranes at a full-scale drinking water treatment plant in South Africa

This chapter is presented in the form of papers, one is published in the journal *Water SA* and the other is submitted to the *Journal of Membrane Science*. This chapter explores the selectivity of ceramic membrane of NOM fraction removal from samples collected after each treatment stage from a full-scale drinking water treatment plant (DWTP). Research questions 7 and 8 are addressed by this chapter

Chapter 8 – Defects in the active layer of ceramic nanofiltration membranes: a facile characterization approach

This chapter is presented in the form of a paper presented in a refereed conference proceeding of the Water Institute of Southern Africa. Chapter 8 explores a facile nondestructive defect characterization approach using ceramic membranes of deferent degrees of defects. Research question 9 is addressed by this chapter.

Chapter 9 – Conclusion and Recommendations

The conclusion, perspectives and recommendations for future work is presented in Chapter 9.

References – All references used are listed at the end of each particular chapter.

Appendix – Supplementary tables and figures of results generated in this

1.8 REFERENCES

[1] CSIR (2010). *A CSIR perspective on water in South Africa*.

[2] P. R. Hunter, A. M. MacDonald, and R. C. Carter (2010). Water Supply and Health. *PLoS Med,* **7**(11).

[3] E. Lavonen (2015). *Tracking Changes in Dissolved Natural Organic Matter Composition*. Doctoral Thesis, Swedish University of Agricultural Sciences.

[4] J. Haarhoff, B. Mamba, R. Krause, and S. Van Staden (2013). Natural Organic Matter in Drinking Water Sources : Its Characterisation and Treatability. *WRC* Report No. 1883 2013.

[5] Z.Dladla (2013). The effect of natural organic matter on ultrafiltration and reverse osmosis membrane performance at komati power station. MSc Dissertation. University of Pretoria.

[6] K. P. Lobanga (2014). Natural organic matter removal from surface waters by enhanced coagulation, granular activated carbon adsorption and ion exchange.PhD Thesis, University of Johannesburg.

[7] S. Metsämuuronen, M. Sillanpää, A. Bhatnagar, and M. Mänttäri (2014). Natural Organic Matter Removal from Drinking Water by Membrane Technology. *Sep. Purif. Technol,* **43**(July),1–61.

[8] H. Wang, A. A. Keller, and F. Li (2010). Natural Organic Matter Removal by Adsorption onto Carbonaceous Nanoparticles and Coagulation. *J. Environ. Eng,*October, 1075–1081.

[9] T. Nguyen, F. A. Roddick, and L. Fan (2012). Biofouling of water treatment membranes: A review of the underlying causes, monitoring techniques and control measures. *Membranes*, **2**(4) 804–840.

[10] R. Shang (2014). *Ceramic Ultra- and Nanofiltration for Municipal Wastewater Reuse*. PhD Thesis. Technical University of Delft.

[11] S. Hong and M. Elimelech (2007). Chemical and physical aspects of natural organic matter (NOM) fouling of nanofiltration membranes. *J. Memb. Sci,* **132**(2),159–181.

[12] B. Hofs, J. Ogier, D. Vries, E. F. Beerendonk, and E. R. Cornelissen (2011). Comparison of ceramic and polymeric membrane permeability and fouling using surface water. *Sep. Purif. Technol,* **79** (3), 365–374.

CHAPTER 2*:*
LITERATURE REVIEW

In this chapter, literature review is presented in order to identify the knowledge gaps/deficiencies in order to establish the key research questions for this work. The following aspects are covered in this literature review: (i) characteristics of natural organic matter with emphasis on South African water sources; (ii) methods of NOM removal in conventional and advanced processes; (iii) application of membrane technology in water treatment; and (iv) membrane fouling and fouling mitigation approaches.

2.1 INTRODUCTION

Natural organic matter (NOM) is a heterogeneous complex mixture of compounds occurring naturally and in abundance in natural waters. The origins of NOM emanates from living and decaying debris of animals, plants and microorganisms, and from the degraded end-product of these sources [1]. The source of the organic matter has a greater bearing on the concentration, composition and chemistry of NOM. Water treatment processes such as adsorption, coagulation, membrane filtration and oxidation are compromised by the presence of NOM in the source waters. These problems are compounded by the fact that NOM impacts the organoleptic parameters of colour, taste and odour. Further, NOM serves as the main precursor in the formation of disinfection by-products; early exhaustion of activated carbon is accelerated by the presence of NOM due to clogging of pores; NOM is the major foulant of membranes, and corrosion and microbial recolonisation in the distribution system is promoted by NOM [1]. Therefore, a robust characterisation approach is needed in order to identify the problematic NOM fractions thereafter NOM removal protocols can then be formulated to target those problematic fractions. To achieve this goal, it would be mandatory to monitor the transformation of NOM fractions as they traverse the treatment train.

The last few decades have witnessed a sharp increase in the application of membrane technology for the production of potable water [2]–[5]. By replacing or

complimenting conventional treatment steps (such as: coagulation, sedimentation, rapid sand filtration and disinfection) with membrane filtration (although costly), a more effective, robust and reliable treatment method is availed. In comparison to conventional treatment methods, additional advantages of membrane technology include a constant permeate quality under changing feed water quality streams, a smaller carbon footprint, and highly automated operation [6].

Several studies on membrane technology have focused on the application of polymeric membranes in pilot and full scale installations [7]–[9]. However, very few studies on the application of ceramic membranes for water treatment could be found world-wide. In fact, no studies in Sub-Saharan Africa are yet to be conducted. Additionally, given the spatial variability of NOM, the treatability and fouling behaviour of NOM fractions of surface waters on ceramic membranes has largely been unexplored. This slow drive towards the research and application of ceramic membranesdespite their promising physical properties is mainly due to higher investment costs[6].

2.1.1 Structure and Composition of Natural Organic Matter

Natural organic matter is ubiquitous in natural pedological (terrestrial) and aquatic environments. In general, NOM is a complex heterogeneous mixture whose chemistry is influenced the by the functional groups such as carboxcylate, phenolate, amine etc present e.g humic or fulvic acids (**Figure 2.1**).

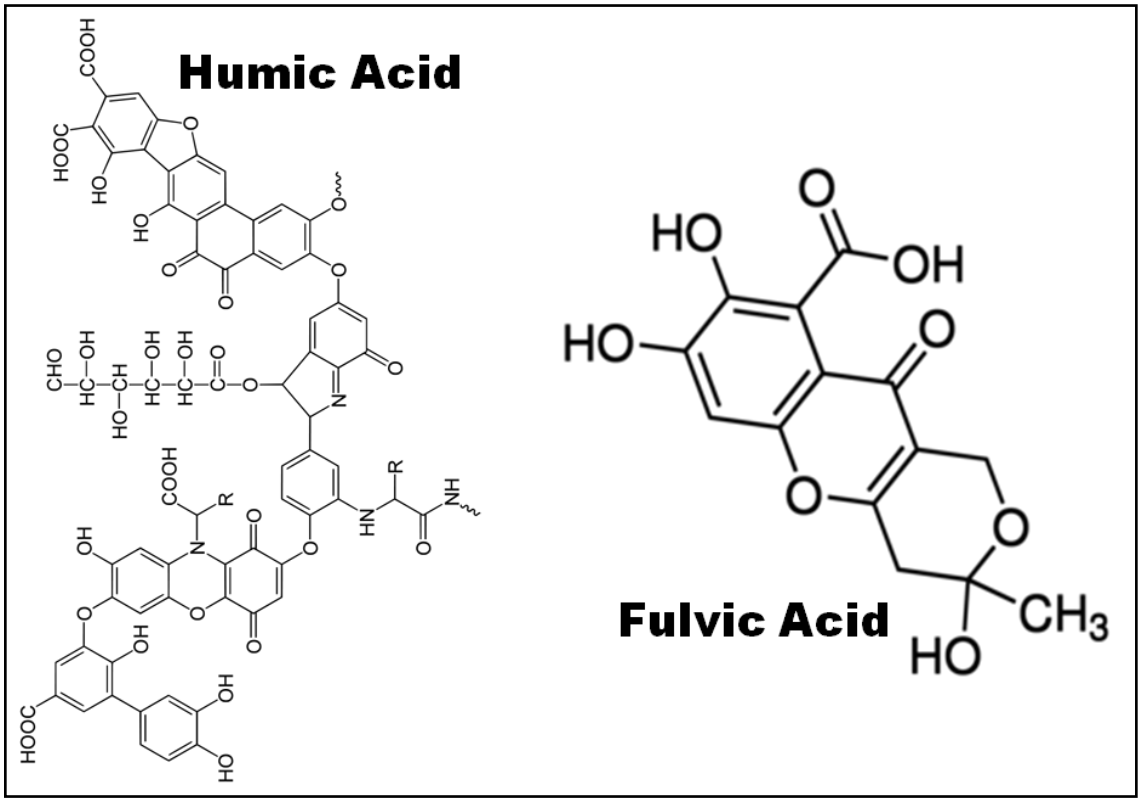

Figure 2. 1: General molecular structure of fulvic and humic [10]**.**

NOM is functionally separated into two distinct groups, which are non-humic and humic substances. Humic substances (HS) are the components that give NOM colour (often yellow to brown), while non-humic substances are composed of hydrophilic acids, amino acids, proteins, lipids, carbohydrates, polysaccharides and hydrocarbons [10]–[14]. HS are further broken down into three main sub-fractions, namely fulvic acid, humin and humic acid. Humic acid is the fraction of NOM that is soluble in a base and insoluble at pH < 2. Fulvic acid is soluble in all pH ranges [12]. Humic acid is considered to be larger between the two, with molecular mass ranging from 1.5 to 5 kDa in aquatic environments and from 50 to 500 kDa in pedological environments. Fulvic acid molecular weight range from 0.6 to 1 kDa in water and 1 kDa to 5 kDa in soils [15].

The composition of humic and fulvic substances in surface waters varies spatially and temporally. Research has shown that the dissolved organic carbon (DOC) in surface water contain about 40% fulvic acid, 10% humic acid, 30% low molecular weight (LMW) acids (<0.6 kDa), 10% carbohydrates, 7% carboxylic acid and 3% amino acids [16]–[18]. Also, humic acid constitutes approximately 40 to 75% of

DOC, whilst fulvic acid constitutes approximately 20 to 80% of DOC, depending on the water sources such as ground water or surface water [19], [20]. As a result of this discrepancy, various methods are employed in a bid to standardize NOM characterization and quantification. These methods include:

i. Application of ion exchange to partition NOM into major fractions due to preferential adsorption/desorption on particular resins.
ii. Quantifying the fraction of NOM responsible for biological re-growth, such as biodegradable dissolved organic carbon (BDOC) or assimilable organic carbon (AOC).
iii. Measuring UV absorbance in the range 200 – 600 nm with particular emphasis on the absorbance at wavelength, λ = 254 nm.
iv. Application of liquid chromatography with organic carbon detection to partition NOM into biopolymers (polysaccharides, proteins, amino-sugars, and organic colloids), HS and low molecular weight compounds.
v. Calculating composite indicators such the specific UV absorbance (SUVA), which is the ratio of UV absorbance at 254 nm (per meter of path length) per unit dissolved organic carbon (DOC) (in mg/L).
vi. Measuring specific formation potentials of organic species, such as trihalomethanes (THM) or haloacetic acids (HAA).
vii. Fractionation of NOM into different molecular weight categories using pressure filtration through a series of ultrafiltration membranes.
viii. Fractionation of fluorescent NOM moieties into five groups, namely: humic like, fulvic like, tyrosine like, tryptophan like and soluble microbial by-product like.

The physico-chemical parameters of a water body such as pH, concentration and ionic strength impacts on the structure and reactivity of NOM. For example, a coiled morphology of NOM is exhibited at high concentration (>1 $g.L^{-1}$), or at high electrolyte concentration (NaCl ≥ 0.05 M) [21], [22]. In contrast, a quasi linear morphology of NOM is exhibited at low concentration, high pH or at lower electrolyte concentration (NaCl ≤ 0.01 M) [21], [22]. This is because at high pH, more acidic functional groups become deprotonated, leading to mutual repulsion of negative charges on the humic molecules resulting in a coiled geometric

morphology of the molecules [23]. It is therefore paramount to study the NOM composition and reactivity taking into cognizance the *in situ* physico-chemical parameters.

2.1.2 Significance of NOM in drinking water treatment

Operational costs, poor unit process performance and poor finished water quality are exacerbated by the presence on NOM in drinking water. NOM impacts the efficiency of water treatment process and the produced water quality in the following manner [21]–[27].

i. Active site or pores for adsorption in activated carbon are preferentially filled by NOM leaving little to no room for targeted micropollutants to adsorb thus impacting both the adsorption kinetics and adsorption capacity of the targeted organic micropollutants.
ii. The dose or demand of disinfectants, coagulants and oxidants and disinfectants required for drinking water treatment is increased in the presence of NOM.
iii. The potential of microbial re-growth in the distribution system is compounded by insufficient disinfectant residual is in the distribution system and the presence of the biodegradable fraction of NOM.
iv. Organoleptic properties (colour, taste and odour) are impacted upon by the presence of NOM in the finished water.
v. Carcinogenic or mutagenic disinfection by-products (DBPs) are produced when a disinfectant such as ozone or chlorine reacts with residual NOM at the disinfection stage.
vi. The presence of NOM affects membrane technology by increasing the fouling rate thereby reducing specific flux and increasing energy consumption and the frequency of backwashing or cleaning of membranes.
vii. In cooling waters, the presence of NOM leads to the production of corrosive organic acids, which affect the construction material thus leading to increased costs of replacing the pipes.

2.2 CHARACTERISATION OF NOM

2.2.1 General Sampling Protocol and Measurement of NOM

For reproducibility and standardisation, NOM sampling and analysis must follow appropriate standard procedures (e.g. SANS 241, EPA or ASTM standards for water testing) for:

- Sample container preparation;
- Actual sampling;
- Sample preservation; and
- Analysis and reporting.

Sample container preparation and sampling procedure should be adhered to so as to minimise external contamination during sampling and sample handling. Collected samples that cannot be analysed soon after sampling should be preserved at a temperature of 4 °C, and analysis should be carried out at ambient temperatures. However, it is recommended that samples for biodegradable dissolved organic carbon (BDOC) analysis should be carried out immediately so as to minimise hydrolysis of some components of NOM and/or biodegradation. [28].

Sample containers with hard plastic screw caps with a teflon, polypropylene (PP) or polyethylene (PE) lining should be used. Prior to sampling, sample containers should be washed with deionised (DI) water, rinsed with HNO_3 and thereafter flushed with DI water prior to being dried overnight in the oven. Other precautionary measures include:

- Sampling bottles should be labelled correctly.
- At the sampling point, the sample container should be rinsed at least three times with the analyte sample prior to collection of the final sample.
- Depending on the forthcoming analysis, the samples should not be treated with any additives or preservatives.

Cooler boxes should be used for the shipment of samples and for non-cooled samples analysis should be carried out within 24 hours of sampling and the cooled samples should be chilled for at most 72 hours before analysis [12]. For purposes of quality assurance and auditing, the method of shipment, analysis on site (i.e. measurements of temperature, pH, and conductivity at the sampling site using field meters), method of sampling (grab, composite), date of sampling and arrival at the lab for analysis should be noted and recorded.

2.2.2 Bulk Characterisation

Bulk characterisation involves the measurement of UV-vis, TOC, turbidity, conductivity, pH and alkalinity. These techniques are discussed individually in the sub-sections that follow.

2.2.2.1 Total organic carbon (TOC)

TOC is a quantitative technique that measures the organic carbon content of the bulk NOM in a sample. Operationally, TOC is the sum of particulate organic carbon (POC) and dissolved organic carbon (DOC). DOC is the permeate obtained from filtering a sample through a 0.45 µm filter [29]. Since TOC is a bulk analysis technique, it does not reveal the behaviour and character of NOM in the sample [30].

2.2.2.2 Ultraviolet-visible (UV-Vis) absorption spectroscopy

Ultraviolet (UV) absorption spectroscopy measures the light attenuation as it passes through a water sample. UV absorbance at λ = 254 nm (UV_{254}) is associated with aromatic organic carbon [31]. The amplitude of absorbance is a measure of the quantity of aromatic organics or conjugation (C=C) [32]. Absorbance at λ = 254 nm is used as a surrogate parameter for disinfection by-product formation potential (DBPFP) [33]. This is because conjugated bonds (C=C) react with disinfectants and oxidants by donating electrons [31]. Besides the information obtained at λ = 254 nm, UV-visible spectra are usually monotonous, broad and featureless [31]. Thus, many researchers have limited their data collection to monitoring the absorbance at a single wavelength (e.g. 254 nm) to provide an indication of the overall NOM concentration. However, the UV spectra could be embedding a wealth of information, therefore relying on one value or certain points for the interpretation of absorbance of the UV spectra denies the

users opportunities to access substantial information obtainable from the rest of the UV spectra.

2.2.2.3 Specific ultraviolet absorbance (SUVA)

SUVA is a ratio of UV_{254} absorbance (per cm) per unit DOC (mg/ L) concentration multiplied by 100 (**Equation 2.1**). The SUVA ratio gives an indication of the dominant NOM type in the sample classified as humic matter, non-humic matter or a combination thereof. SUVA values are indicative of the effectiveness of the coagulation process in the removal of DOC. Previous reports indicate the major fraction of NOM in the water is of non-humic substances when SUVA < 2 L/mg.C, and of humic substances when SUVA > 4 L/mg.C. SUVA values ranging 2 - 4 L/m-mg.C indicate a mixture of aquatic humics, i.e. a mixture of hydrophilic and hydrophobic NOM and of varying molecular weights [21]. The expected removal efficiencies by coagulation as reflected by the SUVA values are shown in **Table 2.1**. When the SUVA values are greater than 4 $Lmg^{-1}m^{-1}$, a DOC removal greater than 50 % is expected. Further, when SUVA values are less than 2 $Lmg^{-1}m^{-1}$, DOC removal rates of less than 25 % are expected [34]. It must be noted, it is misleading to assume similar SUVA value translates to similar reactivity. The distribution around an average value from respective samples maybe different [35]. Therefore, it is not enough to base the treatability of NOM using SUVA values, sensitive and comprehensive analytical methods are necessary for fuller details.

.

$$SUVA(L/mg.m) = \frac{UV_{254}(cm^{-1})}{DOC(mg/L)} \times 100 \qquad (2.1)$$

Table 2. 1: Guiding SUVA values for the determination of the nature of NOM and expected DOC removals by coagulation [21]**.**

DOC removals	Coagulation	Composition	SUVA $L.mg^{-1}m^{-1}$
>50%	NOM Controls Good DOC removal	Mostly aquatic humic High hydrophobicity High molecular weigh	**>4**
25-50%	NOM influences DOC removals satisfactorily	Mixture of aquatic humic substances and other NOM Mixture of hydrophobic and hydrophilic NOM Mixture of molecular weights	**2 - 4**
<25%	NOM has little Influence Poor DOC removal	Mostly non-humic substances Low hydrophobicity Low molecular weight	**<2**

2.2.3 Advanced Characterisation

Bulk characterization of NOM, do not give deeper insights on the nature and reactivity of individual NOM fractions. Thus, it is envisioned that advanced characterization techniques can be employed to give more detailed data suitable to make operational and or strategic decisions for the best methods for NOM removal

2.2.3.1 Size Exclusion Chromatography (SEC)

High performance liquid chromatographic (HPLC) separation method is mimicked by size exclusion chromatography (SEC) in principles of operation. The column packing material is aligned to give progressive and precisely controlled pores and the fractionation *modus operandi* is strictly due to size or hydrodynamic volume differences [12]. Lower molecular weight (LMW) molecules are retained for a

longer period of time compared to larger molecules because LMW molecules penetrate the pores of the column packing material and elute later in time. In this method NOM can be successfully fractionated according to size, starting with the higher molecular weight fractions down to the LMW fractions. The data obtained can be used to provide a molecular weight (MW) or molecular size (MS) profile in terms MW distribution (Daltons) or retention time (**Figure 2.2**).

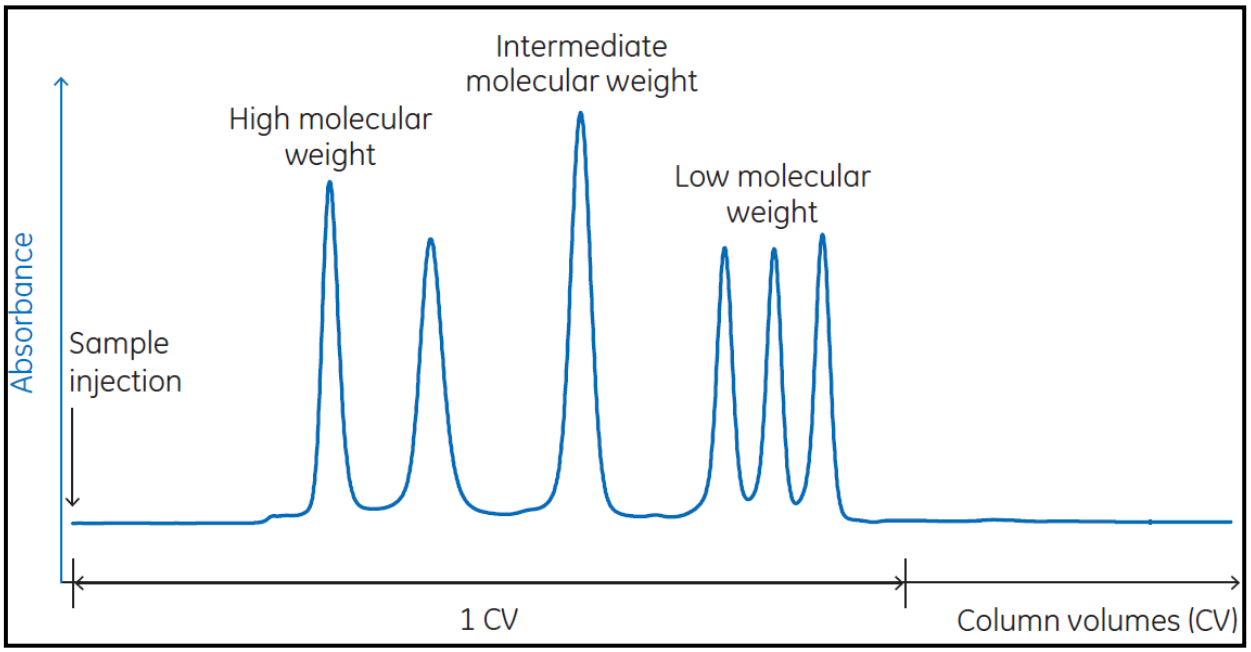

Figure 2. 2: A typical SEC chromatogram [12]**.**

Historically, the exclusive reliance on a single wavelength value of UV detector set to detect at λ = 254 nm used in SEC to determine MW/MS of NOM was somehow misleading. Detection at this wavelength is appropriate for humic substances and i less effective for NOM fractions with no chromophoric activity at the set wavelength such as non-humic components (e.g.: simple sugars and polysaccharides) [36]. It is also necessary to quantify non-humic components of NOM (e.g. polysaccharides) since they have been reported to be major membrane foulants [12]. This problem is compounded by factors such as steric effects, charge, hydrophobicity and molecular structure, which also influence the retention capacity of the material of the column packing [12].

2.2.3.2 Liquid Chromatography coupled with Organic Carbon Detector (LC-OCD)

Liquid Chromatography (LC) coupled with organic carbon detection (OCD) is a fractionation technique that employs various size exclusion chromatography (SEC) columns to separate organic carbon into different molecular sized fractions. Five fractions are specifically identified and quantified by this method [37], namely:

- Low molecular weight neutral compounds (such as aldehydes, alcohols, amino acids and ketones).
- low molecular weight (LMW) humic substances and acids;
- building blocks (hydrolysates of humic substances);
- humic substances (humic and fulvic acids) and
- Biopolymers (such as polypeptides, polysaccharides, amino sugars and proteins).

The original system has received further upgrades by the addition of an organic nitrogen detector. The system can now detect and quantify organically bound nitrogen (e.g. bound to biopolymers or humic substances) [38]. LC-OCD chromatography has shed more light into the efficacy and selectivity of water treatment steps to remove NOM fractions [38]. However, LC-OCD is relatively expensive and time consuming and out of reach for researchers in developing countries. For these reasons, LC-OCD is less commonly used for studying NOM fractionation.

2.2.3.3 XAD Resin Fractionation

This method fractionates NOM by taking advantage of its varied polarities (hydrophilic/hydrophobic); neutral, acid, or base properties; specific compound characteristics; structural complex characteristics and compound-class characteristics [39]. This method relies on the sorption of polarity fractions on non-ionic resin sorbents such as Amberlite XAD (polymethyl methacrylate). Humic substances such as humics and fulvics adsorb onto the XAD-8 resin column, and this forms the basis for fractionating drinking water NOM into humic and non-humic [40]. When operated in series with the XAD-4, NOM is fractionated further. The XAD-8 resins return the less polar hydrophobic organic acids, mainly composed primarily of humic and fulvic acids. On the other hand, the XAD-4 resins return the more polar hydrophilic organic acids [40] (see **Figure 2.3**). However, the

XAD method cannot be carried out under ambient environmental conditions; the method requires that the sample be acidified, thus changing the morphology and chemistry of the original NOM contained in the sample [41].

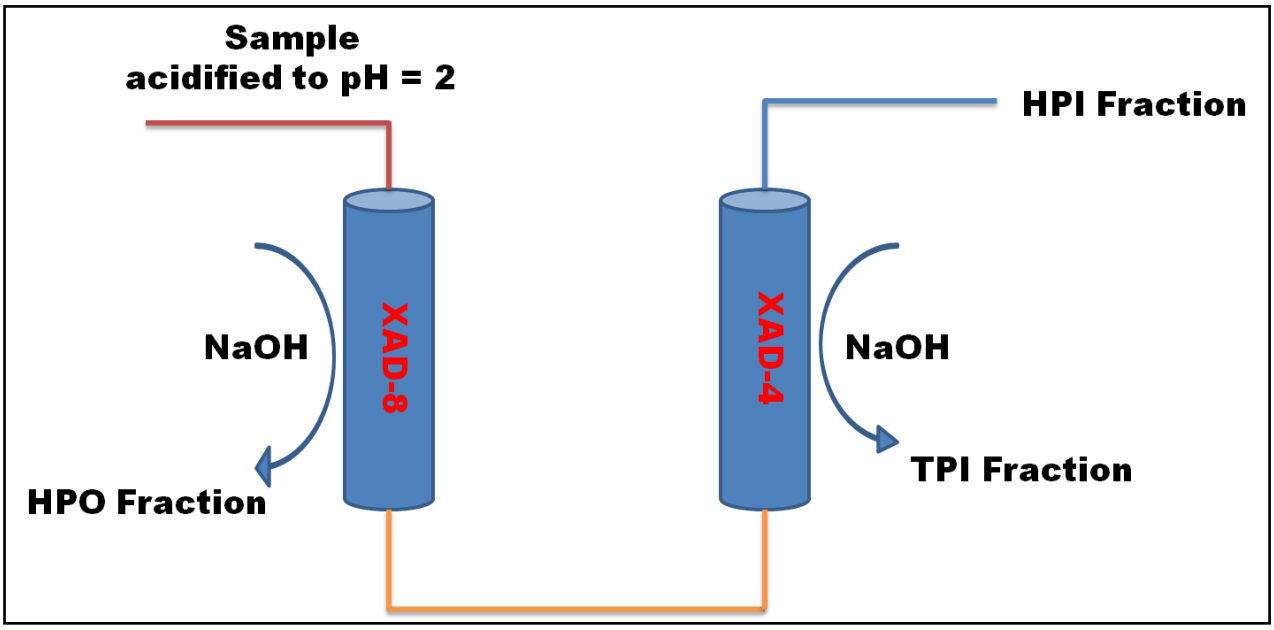

Figure 2. 3: Schematics of XAD fractionation technique [42]

2.2.2.4 Polarity Rapid Assessment Method (PRAM)

Another method that fractionates NOM in terms of polarity is the polarity rapid assessment method (PRAM) [43]. This method categorises NOM based on sorption on solid phase extraction cartridges placed in parallel. Non-polar sorbents (C2, C18) return the hydrophobic fraction of NOM, the polar sorbents (CN, diol and silica) return the hydrophilic fraction of NOM while the anion exchange sorbents (SAX and NH2) return the transphilic portion of NOM, which is essentially a mixture of hydrophilic and hydrophobic fractions of NOM [43]. The quantity of NOM fraction adsorbed by a specific SPE sorbent is determined by using concentration measured as DOC or UVA_{254}. Thereafter breakthrough concentration is determined by the breakthrough curves (i.e. the quotient of break-through concentration and the concentration of the initial sample). The retention coefficient (RC) describes the retention capacity for each NOM fraction by each SPE sorbent; operationally RC is defined as sum of one minus the quotient of the normalized maximum breakthrough level achieved (**Equation 2.2**). In most PRAM

based studies, UV_{254} absorbance is used due to ease of use, minimum interferences and high sensitivity [27], [43], [44]. The use of DOC as a measure of retention coefficient is deterred by the leaching of carbon from the SPE sorbents

$$RC = 1 - \frac{C_{max}}{C_o} \qquad (2.2)$$

Where, C_{max} and C_o defines the maximum breakthrough concentrations and initial concentration of the sample, respectively

The original PRAM has undergone modification by Nkambule et al (2012) [41]. Instead of the original parallel set-up, the modified method involves an alignment of three SPE sorbents in series (C18, CN and NH_2 sorbents) (see **Figure 2.4**).

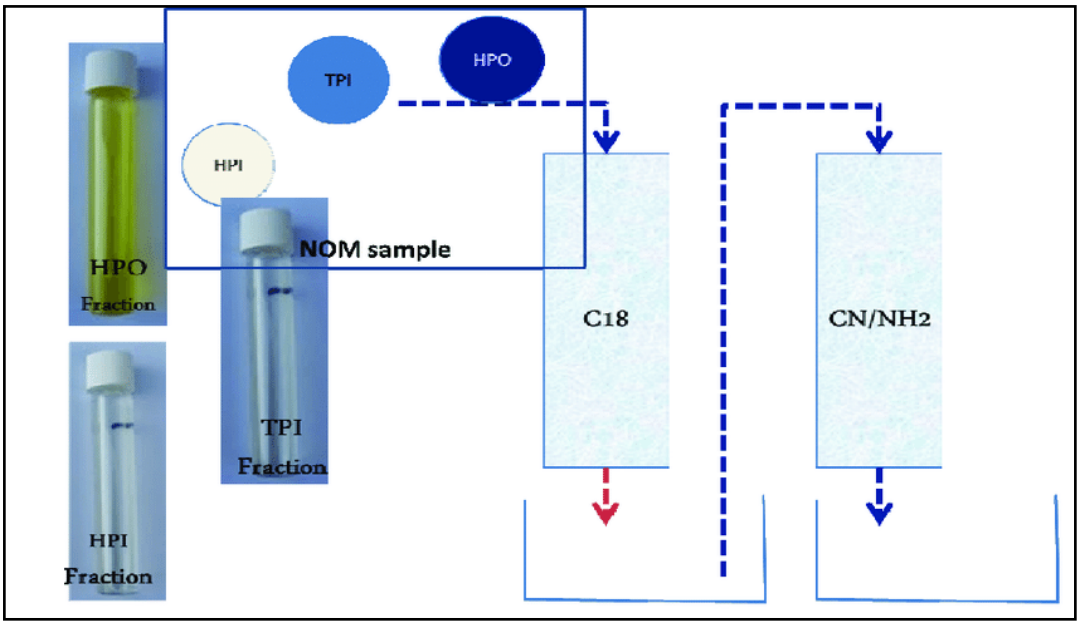

Figure 2. 4: The modified polarity rapid assessment method flow diagram [41]

In the modified method (mPRAM) method, 0.1 M NaOH was used for the elution of the HPI and HPO fractions using the CN and C18 cartridges, respectively [41]. Filtrates from the C18 and CN cartridge were passed through the NH_2 sorbent to generate a transphilic (TPI) fraction, which is a combination of HPO and HPI components. Not only did the modified method reduce the number of SPE sorbents used, it also reduced the time required to run the experiment whilst capturing the full picture of polarity fractions in a given sample. The validity of the

new method was confirmed by comparing Fluorescence Excitation-emission Matrix (FEEM) spectroscopic data and the results obtained from the modified PRAM (m-PRAM) technique utilising only three sorbents (C18, CN, NH2).

Overall, when compared with XAD, PRAM has the advantage of not requiring sample pre-treatment and allowing the experiment to be run under ambient conditions. Furthermore, many PRAM runs can be carried out relatively quickly due to the small sample volume (about 20 mL) requirement. However, like the XAD method, the disadvantage of PRAM is it is a terminating technique, i.e. no other successive or follow up analytical techniques such as as ^{13}C NMR and FTIR can be carried out from the collected NOM fraction [45].

2.2.2.5 Fluorescence Excitation Emission Matrices (FEEM)

Fluorescence spectroscopy is a robust tool for characterizing fluorescent dissolved organic matter (FDOM) in various engineered and natural aquatic systems [46]–[48]. Owing to simplicity in application, FEEM has shown promise in the prediction of the removal of NOM during both advanced and conventional drinking water treatment processes [49]. Typically, this characterization technique involves the identification of fluorophores by identifying the location of maximum excitation-emission wavelength pairs (i.e. fluorescence peak in the FEEM contour plots) [50]. The magnitude and location of the EEM peaks vary with the concentration and composition of NOM. Even though the fluorescence initially increases with DOC, the absorbance of different DOC molecules does not increase linearly, particularly at higher concentrations [47]. Factors such as photo-bleaching and photon quenching exaggerate or diminish the fluorescence profile due to absorbing molecules ions such as nitrate and fluorescent metal complexes in the DOC matrices. To cater for these anomalies, inner filter and Raman scattering correction is applied [51].

The main NOM fraction peaks identified by the FEEM are those of protein-like (< 350 nm) characterized by emission found in the shorter wavelengths and humics (> 350 nm), characterized by emission in the longer wavelengths. **Figure 2.5** shows a contour plot typical of FEEMs of surface water sample identifying previously determined fluorescence intensity peaks location: C (humic-like), B

(tyrosine-like, protein-like), M (humic-like, marine humic-like) and T (tryptophan-like, protein-like) [55]. The coupling of this method with multivariate statistical methods such as self-organizing maps (SOM), parallel factor analysis (PARAFAC), principal filter analysis (PFA), and fluorescence regional integration (FRI) can provide further insight into the environmental dynamics of NOM in diverse aquatic ecosystems.

However, fluorescence intensity can be affected by factors such as pH, solvent polarity, temperature, interactions with organic substances (other or synthetic) and metal ions, redox potential of the medium [51]. Therefore, proceeding characterization that follow and require pretreatment such as pH correction can greatly affect the fluorescence properties of the original sample.

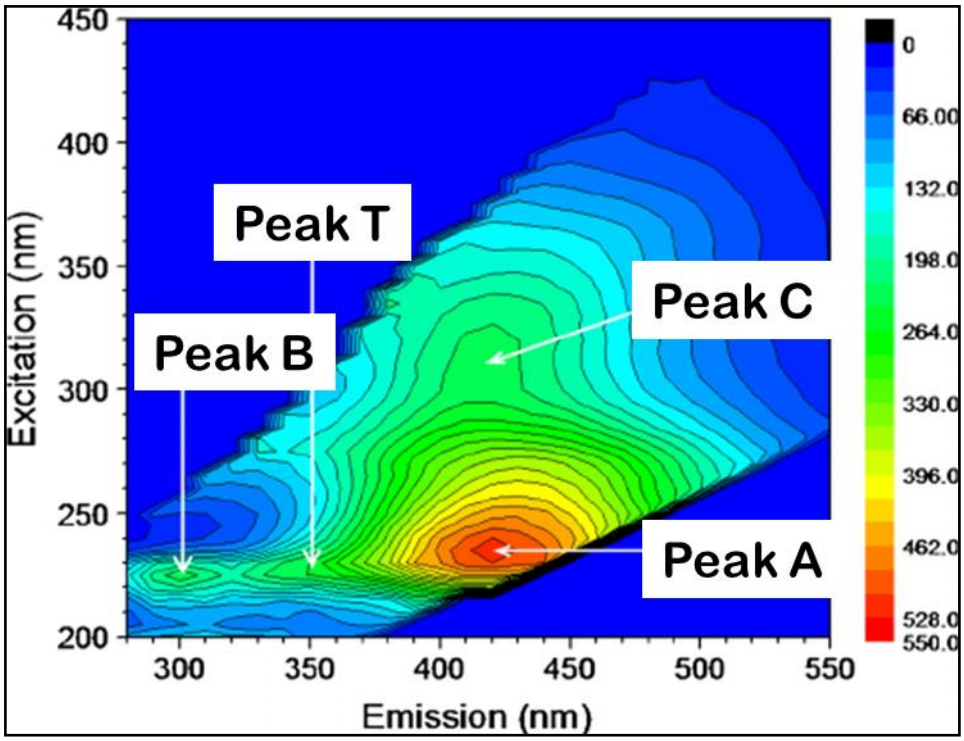

Figure 2. 5: A typical EEM contour plot from a surface water source showing the location of fluorescence intensity peaks: A, B, C and T [55].

2.2.3.6 Biodegradable Dissolved Organic Carbon (BDOC)

The source or substrate for energy and nutrients for heterotrophic bacteria is provided by the BDOC is the fraction of NOM [31]. The quantity of BDOC available for assimilation by heterotrophic bacteria is measured by determining the reduction

of DOC after a predefined time frame (**Figure 2.6)**. The time frame can range from several days to weeks depending on *inter alia* [31], [56]–[58]:

- Incubation time-frame, size, vessel type and type (flow-through bioreactor, batch culture).
- Change in DOC over time relative to initial DOC concentration.
- Additives or supplementary nutrient inclusion.
- Amount of inoculums, monitored biodegradation product and type of bacterial strain.
- Frequency of measurements and temperature.

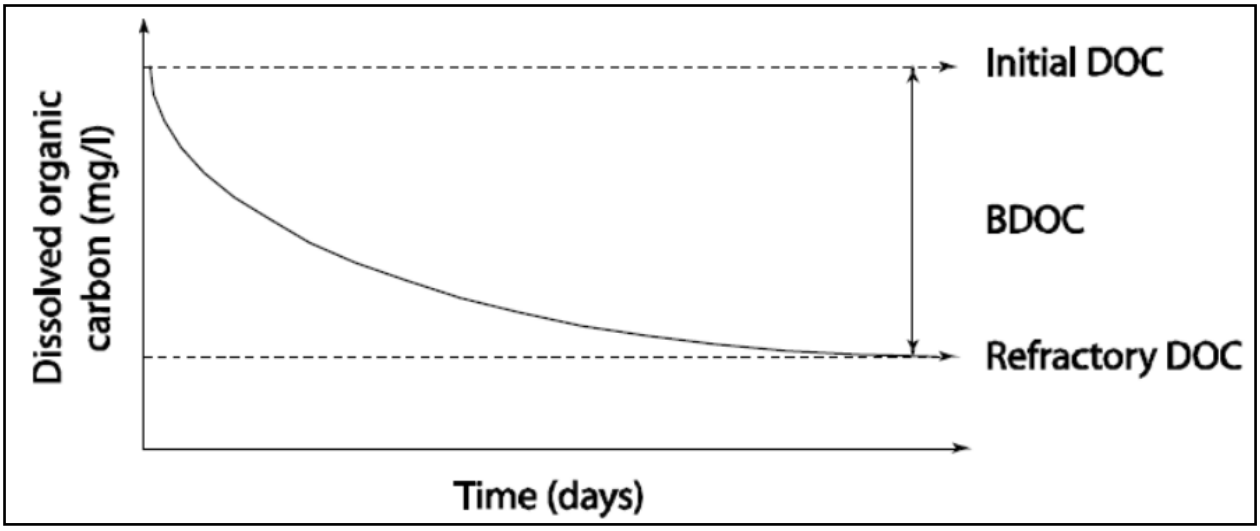

Figure 2. 6: A typical biodegradable dissolved organic carbon decay graph [59]

However, the measurement of the reduction of DOC as the sole determinant of BDOC is insufficient because DOC is a bulky NOM parameter, with a wide continuum of carbon (e.g, conjugated and aromatic; non-fluorescent and fluorescent; saturated and aliphatic) [60]. Deeper insights on the character of the labile NOM fraction readily assimilable by heterotrophic bacteria are needed so as to adjust the water treatment parameters for the targeting of the problematic fraction conversely starving the bacteria.

2.2.3.7 Assimilable organic carbon (AOC)

Complementing the BDOC method is the assimilable organic carbon (AOC) method, which is a water quality parameter that influences the microbiological stability of drinking water [61]. AOC is the fraction of NOM that is used by

heterotrophic microbial organisms for energy and biomass growth, and it can be measured via either a plate count or through adenosine triphosphate (ATP) measurements [61]. The commonly used strains of bacteria used in this test include *Spirillum* NOX and *Pseudomonas fluorescens* P17. The yield values for acetate measured as the maximum colony counts for these bacterial strains is used to calculate AOC. Also, other standard bacteria and natural flora are commonly used for the determination of AOC [56].

2.2.4 Modeling Techniques for Deeper Insights on NOM Character

2.2.4.1 PeakFit®

Characterisation techniques such as a full UV-Vis scan of a water sample usually from 600 – 200 nm provides a monotonous and featureless exponentially decaying graph [33]. For this reason, most researches are mainly interested in absorbance at a single wavelength, or ratios thereof [31], [33], [62]–[64]. Gaussian fitting using the PeakFit® software deconvulates a given spectra to identify hidden peaks that are not responsible for a local maximum in the data stream [49]. The energy, intensity and location of the maxima of each Gaussian peak has been used to characterize the efficiency of each treatment step in a wastewater treatment plant [49]. Previous research has revealed that the deconvulated peaks are Gaussian in nature when expressed in terms of the photon energy parameter shown in **Equation 2.2** [73], [74].

$$E(eV) = \frac{1240}{\lambda}(nm) \qquad (2.2)$$

The data containing one local maximum peak and two hidden peaks is depicted in **Figure 2.7** [67]. The shoulder on the left produces a local maximum and gives a hidden peak. The Peakfit® software is able to pick up a local maximum at what was previously far less apparent in the data stream positioned on the right of the principal peak.

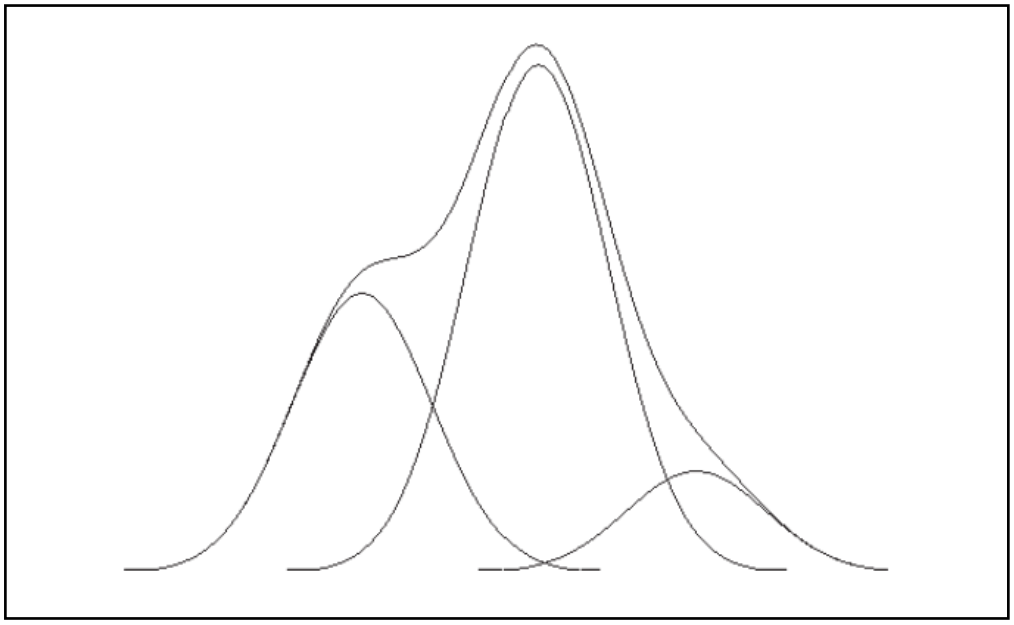

Figure 2. 7: A typical monotonous graph with hidden peaks

2.2.4.1.1 Methods for finding hidden peaks using the Peakfit® software

The Peakfit® software is endowed with different mathematical algorithms for identifying peaks depending on the needs of the user. Below is a discussion of some of the methods of determining hidden peaks.

- **Residuals Method** – The residual method depicted by **Equation 2.1** allows for identification of peaks by placing peaks whose sum of the area equals to that of the data. As shown in **Figure 2.8(a**), five local maxima and two hidden peaks can be observed on the upper graph. When conservation of data area is applied the hidden peaks in the bottom of the graph are revealed as the residuals obtained from initial five local maxima peaks.

  Residual = (y-value of data point) – (data of component peaks obtained at x-value of data point) (2.1)

- **Second Derivative Method** - A local minima at peak position is observed when a smoothed second derivative of the data is applied. Hidden peaks, which ordinarily show no local maxima in the original data stream, appear as local minima when a smoothed second derivative method is applied. As illustrated in the lower graph of **Figure 2.8 (b)**, the same data set was plotted/used to produce five local maxima and two hidden peaks. The

smoothened second derivative revealed the two hidden peaks (see lower graph in **Figure 2.8 (b)**).

- **Deconvolution Method** - Instrumental artefacts such as smearing or broadening of peaks can be corrected by deconvolution. Peaks are sharpened when an instruments' response function is deconvoluted from the data. After the data has been filtered and deconvoluted, hidden peaks that did not originally exhibit any local maxima begin to do so. As shown in **Figure 2.8(c),** when the same data set was used to produce five local maxima and two sharpened peaks, the resultant deconvoluted and filtered peaks are sharpened and the two previously hidden peaks exhibit a local maximum.

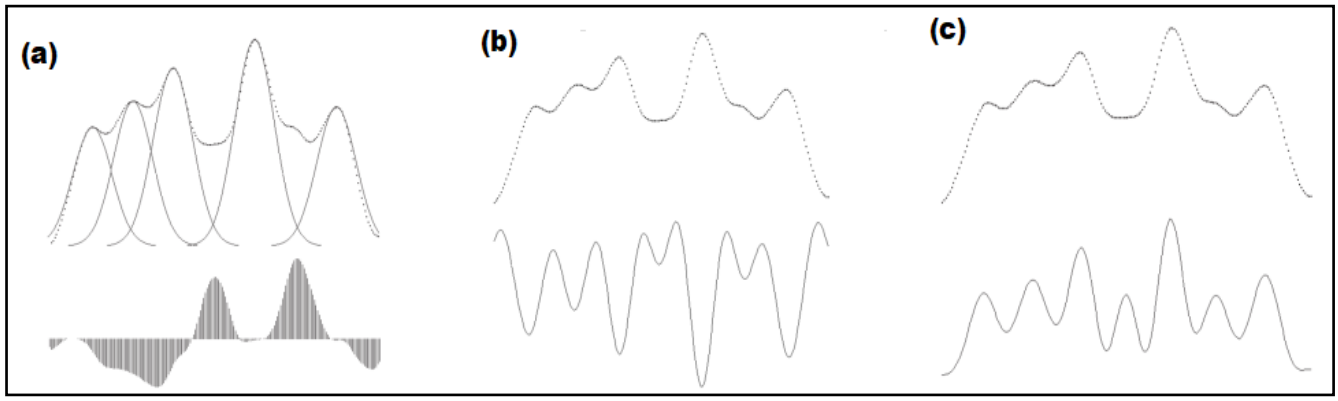

Figure 2. 8: Methods for finding hidden peaks [75] (a) Residuals method, (b) Second derivative method and (c) Deconvolution method

Given the wealth of data obtainable from the application of this software, no study has, to the best of our knowledge, been conducted using the Peakfit® software to study the water treatment efficacy for the removal of chromophoric NOM.

2.2.4.2 Two dimensional correlation spectroscopy

Two dimensional correlation spectroscopy (2D-COS) is acquired as a response by the system to an external perturbation, which gives rise to perturbation-induced experimental spectrum *A(v,s)* [68] (**Figure 2.9**). External perturbations can results from changes in temperature, time, pressure, pH, concentration, or changes of the spatial coordinates.

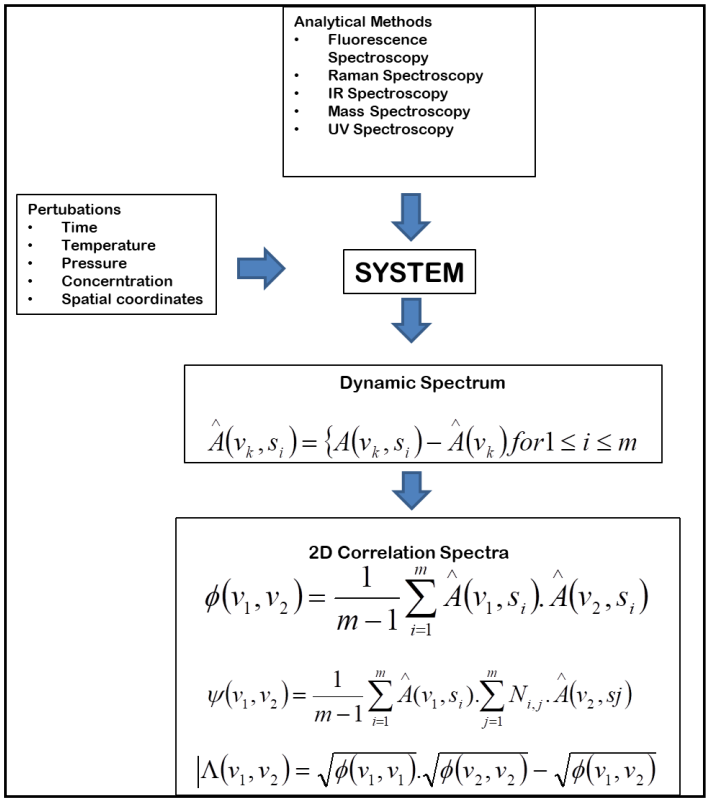

Figure 2. 9: Generalized 2D-COS, scheme for obtaining 2D correlation spectra [68]

In the application of 2D-COS, the dynamic spectrum Ã *(v,s)* contains a series of *m* spectra and is formally defined in the following way:

$$\tilde{A}(v_k, s_i) = \begin{cases} A(v_t, s_i) & \text{for } 1 \le l \le m \\ 0 & \end{cases} \qquad (2.3)$$

Where variables *v* and *s* represent the spectral and perturbation responses, respectively.

Specifically, Ã(v_k) denotes the reference spectrum, often an average spectrum or the first or the last spectrum of a given spectral series. In the same vein, Ã(v_k, s_i) denotes the perturbation-induced variations spectra and are systematically examined by a cross-correlation analysis [69]. The synchronous and asynchronous 2D-COS spectra $\phi(v_1,v_2)$ and $\Psi(v_1,v_2)$ are then given by the following equations [70]:

$$\Phi(v1,v2) = \frac{1}{m-1}\sum_{i=1}^{m} \tilde{A}(v_1 s_i).\tilde{A}(v_2 s_i) \quad (\mathbf{2.4})$$

$$\Psi(v1,v2) = \frac{1}{m-1}\sum_{i=1}^{m} \tilde{A}(v_1 s_i).\sum_{i=1}^{m} N_{i,j}\tilde{A}(v_2 s_{ij}) \quad (\mathbf{2.5})$$

The Hilbert–Noda transformation matrix is denoted by the variable $N_{i,j}$ given by the following equation [70]:

$$N_{i,j} = \begin{cases} 0 & \text{for } i = j \\ \frac{1}{\pi(j-i)} & \end{cases} \quad (\mathbf{2.6})$$

The intensity of the synchronous 2D correlation spectrum $\phi(v_1,v_2)$ can be considered a comparative measure of the similarity of spectral intensity variations at spectral variable positions v_1 and v_2. It can be shown that the intensities in synchronous 2D correlation spectra correspond to the covariance of spectral variations [70]. The intensity of the asynchronous 2D correlation spectrum $\Psi(v_1,v_2)$ represents the dissimilarity or, more accurately, a phase difference of these changes, and is thus useful when analyzing the sequential order of spectral events.

2D-COS was used to track changes in composition of NOM polarity fractions along the river, which passed through sections affected by different anthropogenic activities [71]. It was shown that 2D-COS can track the succession of changes in composition of each NOM polarity fraction. Such knowledge is essential in modelling the NOM compositional dynamics when an external perturbation is applied (e.g. a different water treatment process or varying MWCO of filtration membranes).

2.2.4.3 Parallel Factor Analysis (PARAFAC)

Parallel factor analysis (PARAFAC) has proven to be the most robust multivariate analytical technique for the analysis of NOM in diverse aquatic systems [30], [51], [80]. PARAFAC is largely promoted by advances and developments of algorithms for multilinear data decomposition by statistical parallel factor analysis. NOM fluorescent fractions that are humic-, fulvic- and protein-like have been

successfully identified and quantified in relative terms using PARAFAC [12], [51], [69], [73], [74].

In brevity, the EEM dataset is decomposed into residual arrays and trilinear terms by PARAFAC [51] (see **Figure 2.10 and Equation 2.7**).

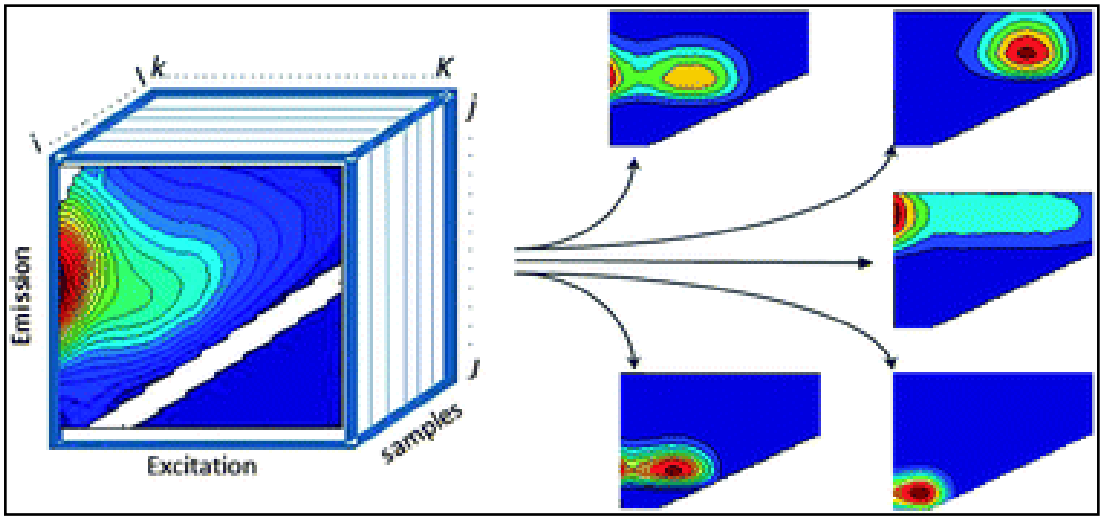

Figure 2. 10: A typical FEEM graph deconvoluted via PARAFAC to reveal undelaying components [51]

The goodness of fit of the model to the experimental data and the maximum fluorescence intensities *(F_{max})* is obtained through alternating least squares regression procedure.

$$x_{ijk} = \sum_{f=1}^{F} a_{if} b_{jk} c_{kf} + e_{ijk} \qquad (\mathbf{2.7})$$

Where: k= 1……..K , i = 1……..I and j = 1……..J

The variable x_{ijk} is the *i*th sample denotes fluorescence intensity at excitation:emission wavelength pair (*k:j)*. The parameter a_{if} contained in the *i*th sample (score) is determined by the quantity of the *f*th fluorophore, and the emission:excitation spectrum of the *f*th fluorophore are given by the parameters b_{jk} and c_{kf}, respectively (loadings). The residual variables of model are denoted by the variable e_{ijk},, The sum of components making up the fluorophore is denoted by the variable *F*.

The model is fitted by using alternating least squares regression procedure. The number of components defining the EEM dataset of samples of unknown fluorophore composition is determined by the predefined goodness of fit [51].

According to Murphy et al. [51], the PARAFAC model is validated using a series of the following predetermined criteria:

(i) Core consistency examination;
(ii) Spectral loading shape evaluation;
(iii) Contribution of the influence of specific sample or wavelengths on the leverage;
(iv) Analysis of the residual, and
(v) The split half-criterion.

After validation, the maximum fluorescence intensities (F_{max}) and distribution at each treatment stage can be a tool to measure the efficacy of each treatment step in removing the particular component. In-depth information on the PARAFAC model can be accessed in accordance with a procedure by Murphy and Stedmon [73].

2.3 DRINKING WATER TREATMENT METHODS FOR THE REMOVAL OF NOM FRACTIONS

NOM exists as a complex heterogeneous mixture of macro-structures with variable chemistries and characteristics and variations that occur seasonally [76]. This predicament impacts on the effective removal of NOM, and it has remained a long lasting challenge to the drinking water industry all over the world. The available technologies for NOM removal include coagulation by converting dissolved NOM to particles which are subsequently removed, adsorption using activated carbon, anion exchange and membrane filtration (NF and RO). Coagulation is the most commonly used method for removing the bulk of NOM and the most effective in the removal of NOM of high humics content. Subsequently, activated carbon, membrane filtration or ion exchange are usually used for NOM removal at polishing stages. This section explores the strengths, weaknesses and opportunities relating to the removal of NOM fractions using some of the available treatment options depicted in **Figure 2.11**.

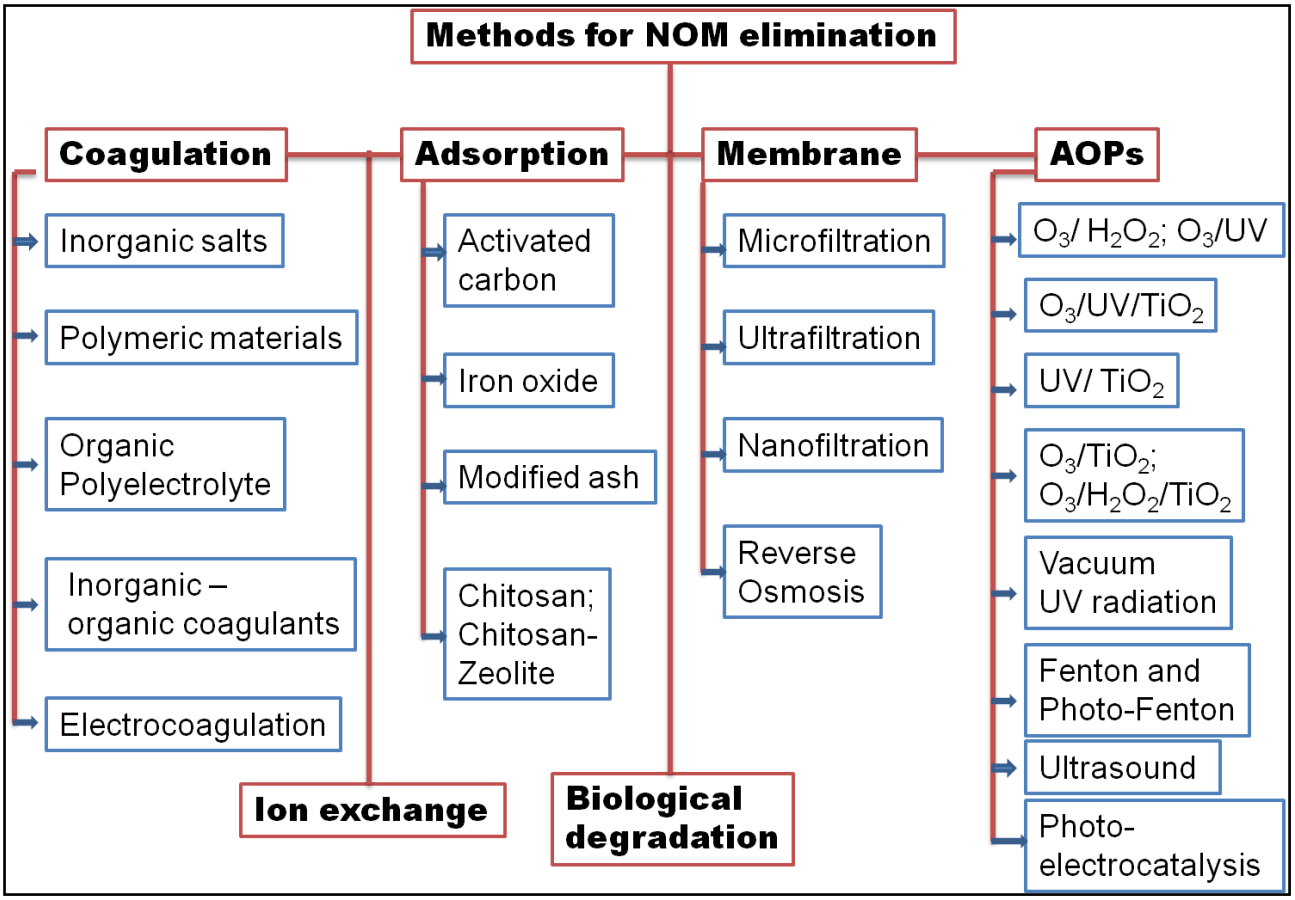

Figure 2. 11: Methods for NOM elimination [77]

2.3.1 Coagulation

Coagulation converts dissolved NOM to particulate NOM via direct precipitation by complexation between coagulant species and NOM species or by soprtion of NOM to precipitated inorganic metal hydroxides. Subsequent particle removal does the actual NOM removal [78]. Coagulation is achieved by reducing the double layer of the colloids at the solid-liquid interface thereby conversely reducing the repulsive potential and leading to the formation of micro-flocs. The collision of the micro-flocs with each other leads to agglomeration into larger aggregates [28]. The mechanisms of removal of NOM by coagulation include: entrapment, destabilisation, adsorption and complexation [79] (**Figure 2.12**).

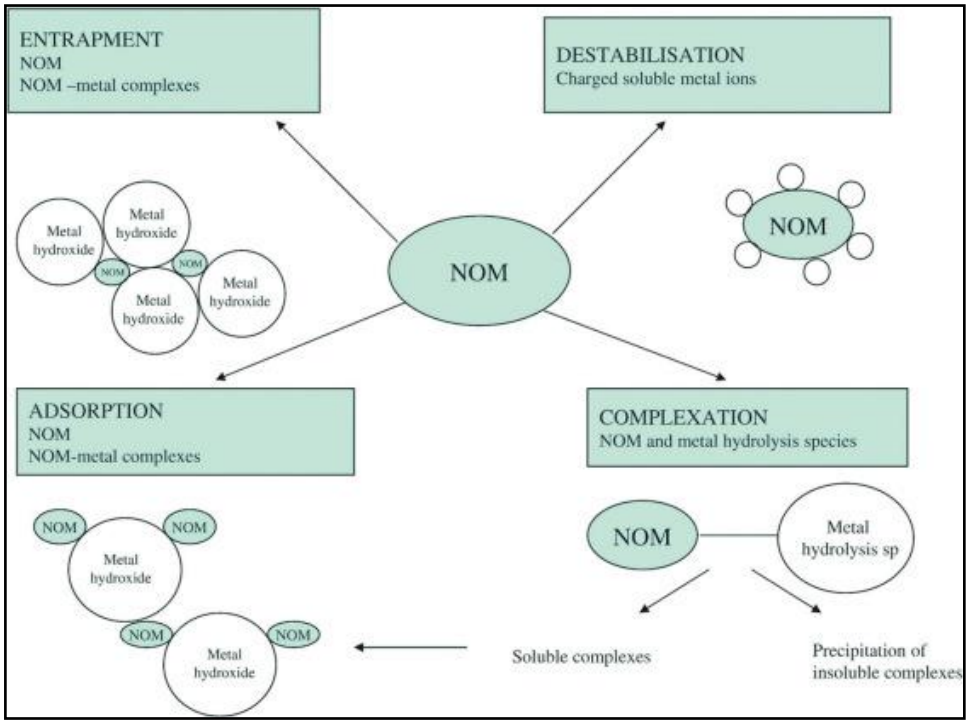

Figure 2. 12: Removal mechanisms of natural organic matter, NOM, during coagulation [80].

Prehydrolysed coagulants (such as polyferric chloride, polyferric sulphate, and polyaluminum chloride (PACl)) have been found to improve the coagulation performance due to their stability under different pH and temperature conditions [30]. Common coagulants used in water treatment include aluminium and iron salts [81], [82]. At very low pH these hydrolyzed salts form highly reactive ions, which adsorb onto the negatively charged NOM in the water [83]. However, at the pHs used in coagulation, hydroxyl-metal complexes are the dominant dissolved species, as well as polymers for the pre-hydrolyzed products. The effectiveness of coagulants to form easily removable flocs depends on coagulant type, dosage, temperature, and pH; and NOM properties [84]. In general, coagulation effectively removes high molecular weight hydrophobic fraction of NOM better than the low molecular weight hydrophilic fraction. This selective phenomenon is attributed to the fact that hydrophobic fractions are mainly composed of aromatic functional groups, which form complexes with hydrolysed metal coagulants [85].

Due to low capital costs and ease of operation, the coagulation process is the most favoured technology for the removal of NOM, especially in developing

countries [85]. However, inherent to the coagulation process is the production of waste sludge, which poses environmental problems upon disposal. In addition, despite its ability to remove DBP precursors to a greater extent, it does not completely convert all dissolved NOM and its fractions to particulate matter which is subsequently removed [22].

2.3.2 Adsorptive Techniques

In drinking water treatment, odour causing compounds such as phenol and phenolic compounds are removed to a great extent by powdered activated carbon (PAC) and granulated activated carbon (GAC) [86]. The adsorption process of these odour causing compounds is determined by carbon pore size, pore size distribution and the molecular weight distribution of the targeted organic matter [79]. The adsorption of the low to intermediate molecular weight organic matter is much better than that of higher molecular weight organic matter. It has been reported that microbial communities coexisting in the pores of unregenerated activated carbon can symbiotically degrade biodegradable organic compounds [87]. NOM-rich waters have to go through a pretreatment stage prior to treatment with activated carbon. The pretreatment step is necessary to avoid the early impregnation and blockage of the pores of the activated carbon with organic matter. Therefore, the activated carbon process is usually placed as a polishing step in water treatment process with the aim of targeting mainly the low molecular weight hydrophilic NOM fraction [86]. The performance and longevity of GAC and PAC are dependent on morphology, concentration and physico-chemical characteristics of the NOM in raw water, the type of activated carbon, and the availability of active sites for adsorption [79]. The downside of this technology is the regeneration process and disposal of the used activated carbon pose an environmental concern in addition to increased operational cost.

2.3.3 Ion Exchange

Ion exchange involves the interchange of ions that occurs reversibly from the solid-liquid interphase with no long-lasting structural changes of the solid [88]. Ion exchange resins act as the solid phase whilst water acts as the liquid phase. The inter ion exchange between the liquid and solid phases, is illustrated in **Figure 2.13**, shows: (1) the exchange of ions occurs at the surface of the solid; and (2) an

interchange of phases from solid to liquid or vice versa by the ions [88]. To this end, the sorption process is defined by the two above-mentioned characteristics. Under ambient conditions, the pH range of natural waters renders NOM to be negatively charged [82]. Therefore, anionic exchange resins can effectively remove NOM.

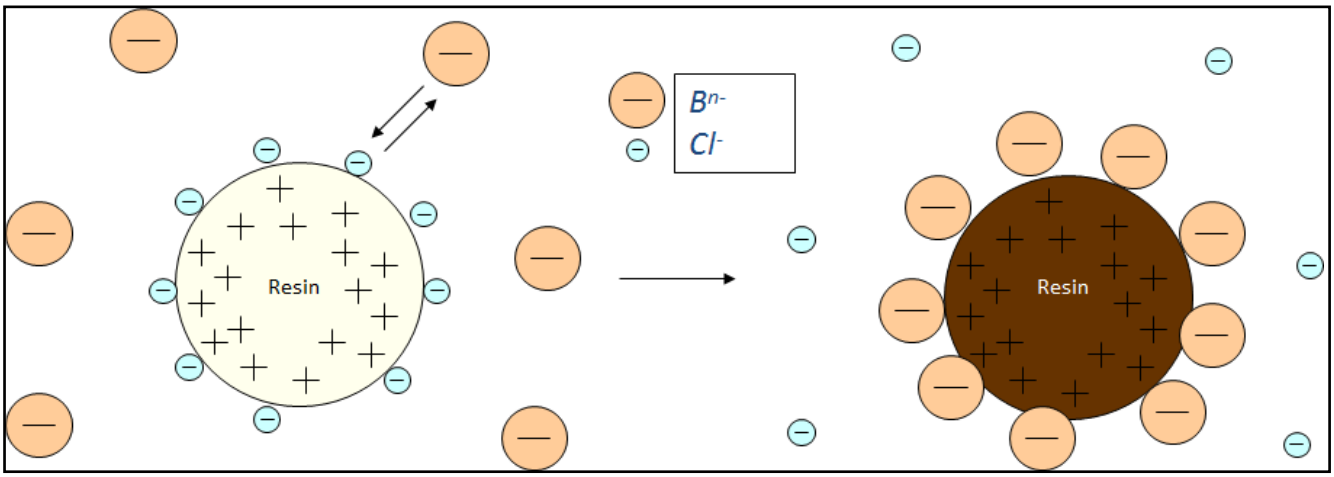

Figure 2. 13: Inter ion exchange between the liquid and solid phases [88]

2.3.4 Membrane Filtration

Membrane filtration technology has many applications, including water treatment. The application of membrane technology in water treatment is driven mainly by [6], [89]–[92]:

- low energy use (MF and UF);
- small carbon footprint;
- simple maintenance and operation;
- capability to cope with feed waters of fluctuating quality; and
- capability of producing water of high quality.

Membrane filtration is classified according to pore size into four categories, namely microfiltration (MF), ultrafiltration (UF), nanofiltration (NF) and reverse osmosis (RO) (**Figure 2.14**). The food and beverages industries as well as water and waste water treatment processes utilize mainly the UF and MF. On the other hand, NF and RO are used mainly as a polishing stage following MF and UF filtration [90]. The driving force in membrane filtration is due to factors such as pressure

differences, concentration gradients, hydrophobic interactions, size exclusion and charge repulsion [87].

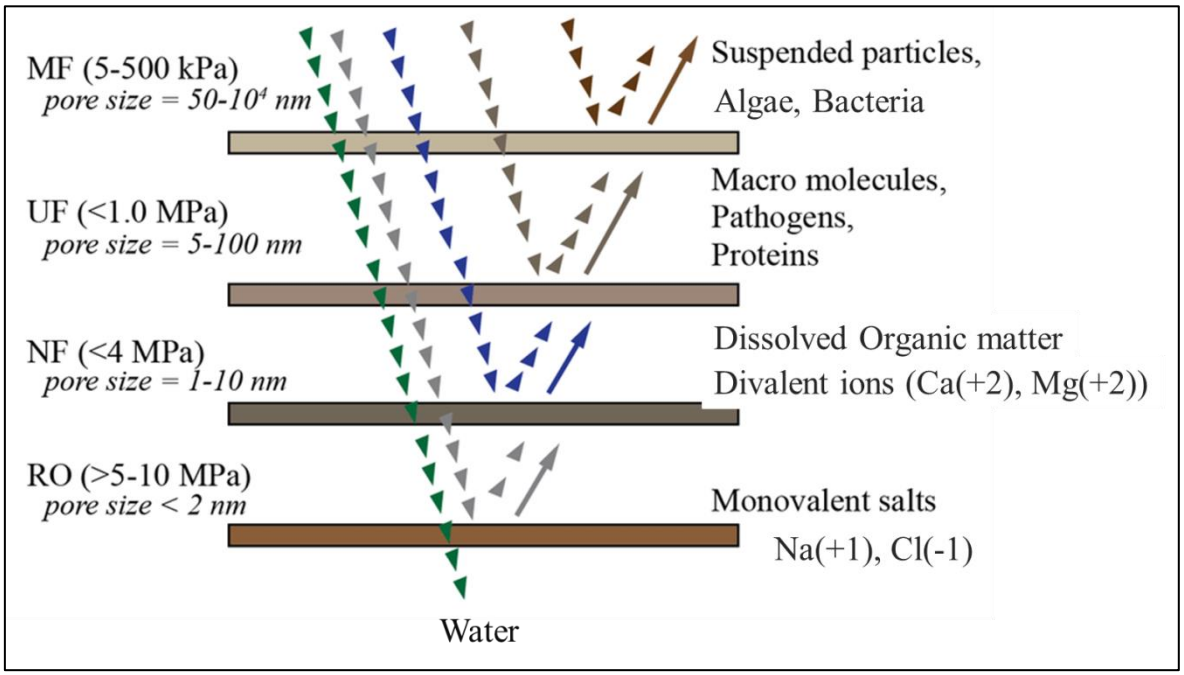

Figure 2. 14: Categories of membranes according to pore size [96]

Membrane material and design is dependent on the intended use; the membrane employed may be composed of a single composite or mixture of organic (polymers), inorganic or metallic substances. Polymeric membranes are commonly used in water treatment because they are cheap compared to the inorganic membranes. Polymeric membranes are usually manufactured from polymers such as polysulfone (PS), cellulose acetate (CA), polyamide (PA), polypropylene (PP), polyethersulfone (PES) and polyvinylidene fluoride (PVDF) [94]. In contrast, inorganic membranes are generally fabricated from oxides of titanium, zirconium, aluminum and silicon carbide [95]. Inorganic membranes are beginning to find application in water treatment because of their durability and low operational expenditure (OPEX) costs compared to the polymeric membranes.

The major hindering factor to cost effective application of membrane technology is fouling. Fouling is the accumulation of rejected particles on the surface of the membrane or the internal pore structure [96]. This phenomenon can eventually lower the lifetime of the membrane resulting in increased overall OPEX cost and ultimately increasing the unit price of the produced water.

The nature and extent of membrane fouling by NOM is dependent on several factors such as the hydrodynamic conditions, nature of the NOM, physico-chemical properties of the feed water and the membrane [97]. Procedures for MF and UF membrane fouling control include backwash, air scouring, forward flush, chemical wash or cleaning in place [87]. Albeit, frequent cleaning compromises the membrane integrity leading to significant increase in process costs and ultimately the price of produced water [87].

2.3.5 Oxidation Methods

The methods discussed above show significant effectiveness in NOM removal. However, the recalcitrant NOM fractions responsible for DBP and other upstream problems still persist. This challenge has motivated scientists and engineers to explore other alternative technologies for NOM degradation and removal for drinking water treatment. One of the emerging and promising technologies under critical consideration is the advanced oxidation processes (AOPs), which include various catalytic and photochemical methods. The major advantage of AOP methods over conventional processes is their ability to transform NOM to intermediates that can be easily by removed by downstream processes [98]. Complete mineralization of NOM by AOP methods would be energy intensive. The hydroxyl radical (OH●) generated in AOP is responsible for the partial mineralisation of organic matter.

The mineralisation process is categorized into homogeneous photodegradation and heterogeneous catalysis. In the homogeneous photodegradation process, the oxidant and organic matter are in the same state of matter. On the other hand, heterogenous catalysis involves an oxidant and the organic matter that are not in the same phase [28].

The most commonly used homogeneous photodegration oxidants are hydrogen peroxide (H_2O_2) and ozone (O_3) jointly or singularly irradiated by UV. The UV irradiation fast tracks the production of the OH● radicals. At an irradiation wavelength below 360 nm, H_2O_2 dissociates forming the highly oxidizing OH● radicals, which attack the organic matter [99]. Compared to the H_2O_2 system, the formation of reactive radicals is slower with O_3 and leads to greater production of

carcinogenic trihalomethanes (THM). However, research has shown that the combinations of H_2O_2 and O_3 and/or UV irradiation improves the rate of mineralization and reduces the THM formation potential [77].

In heterogenous photocatalysis, semicondictors such as titanium dioxide (TiO_2), tungsten oxide (WO_3) and zinc oxide (ZnO) are UV irradiated to induce the production of OH● radicals, which are able to oxidise organic compounds [100]. When light is irradiated on the semiconductor surface, electrons in the valence band are excited to the conduction band and thus leave holes. Water molecules adsorbed onto the semiconductor surface are then oxidized by these holes producing the OH● radicals, which in turn oxidise organic matter [101] (**Figure 2.15**).

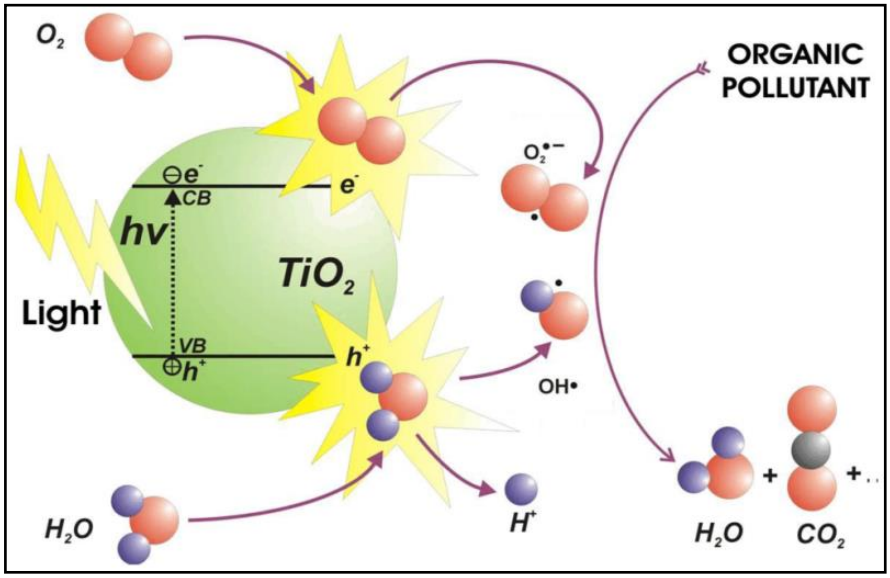

Figure 2. 15: Heterogeneous photocatalysis processes for the oxidation of organic pollutants [102]

Although AOPs show great potential in water treatment for the eradication of organic compounds, some drawbacks of this technology such as slow rate of degradation, high energy consumption for the photoactivation and production of equally carcinogenic oxidation by-products are known. In this regard, some of the drawbacks of AOPs are [102]:

- The application of AOPs is hindered by high capital and operational cost. Such application requires a continuous input of chemical reagents and the disposal of residual hazardous chemicals since the quantity of pollutants to

be removed is proportional to the OH● radicals and other important reagents. .

- There is a need for pre-treatment to ensure that ions such as carbonates (HCO_3^-) are stripped off the water to be treated. The presence of HCO_3^- reduces the concentration of OH● radicals brought about by the scavenging of the radicals.
- AOPs are usually employed at polishing stages after an appreciable amount of organics are removed by upstream processes. Therefore, AOPs are not cost effective when used solely for handling large amounts of water.

2.4 NOM CHARACTER AND REMOVAL: LESSONS FROM SOUTH AFRICA

Thus far, the literature review has demonstrated that:

- NOM has deleterious effects in drinking water for various reasons such as a being a precursor for the formation of THMs;
- NOM monitoring and control in water treatment plants (WTPs) is hampered due to exorbitant cost of treatment equipment; and
- The conventional and advanced techniques for NOM removal are neither completely environmentally friendly nor cost effective.

This section discusses the occurrence and distribution of common NOM fractions and methods used to treat NOM together with their strengths and limitations. Although the character and removal efficiency of NOM by various techniques is fairly well researched, especially in the developed world [30] [21], the available body of knowledge on South Africa is not sufficient to substantiate the removal and occurrence of NOM and its fractions in aquatic systems of South African. This section is, therefore, aimed at:

- evaluating the efficiency of NOM removal by different water treatment plants found in South Africas' water quality regions; and
- proposing newer methods that can be adopted for the removal of NOM in South Africa

The South African landscape is divided into roughly six geographical location-based water quality regions [103], [104] (**Fig. 2.16**). These regions are:

A. The north-eastern part of the country - The source waters in this region are clear to turbid, with fairly high amounts of NOM.
B. The northwestern part – The source waters in this region are mostly turbid rivers with variable salt levels.
C. The central part – The source waters in this region has high levels of suspended salts and clay.
D. Western Cape – The source waters in this region has clear acidic waters.
E. The Southern Cape – The source waters in this region has dark brown waters due to the presence of humic and fulvic compounds.
F. The Free State – The source waters in this region are from the highlands of Lesotho, mostly oligotrophic water and transparent with low dissolved salt levels.

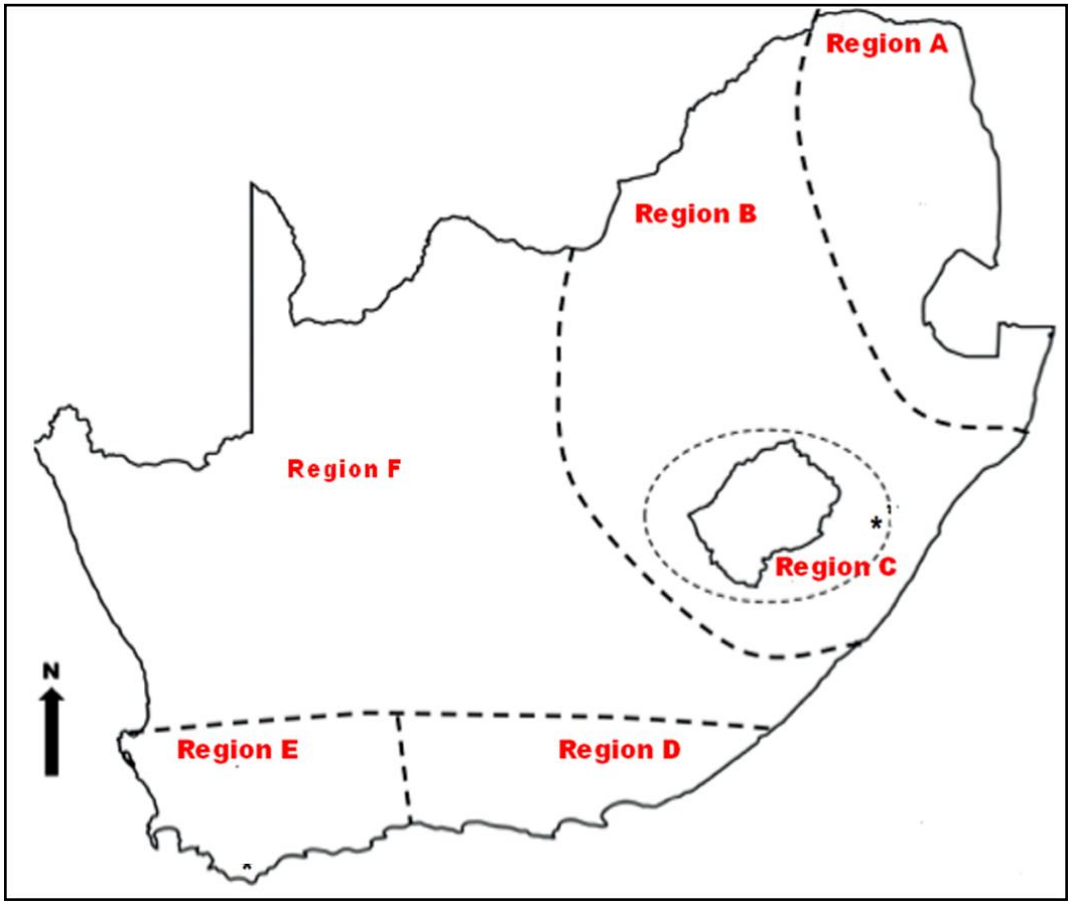

Figure 2. 16: Water quality regions of South Africa, showing A – North Eastern region; B – North Western region; C – Central region; D – Western Cape region; E – Southern Cape region; F – Free State region [104].

De facto water recycling is inevitable because South Africa is a water stressed country. Dilapidated wastewater treatment infrastructure in most parts of the country has resulted in partially treated waste water reaching many streams and rivers and ultimately into drinking water treatment plants [41]. Thus effluent NOM (EfNOM) influences the quality of water reaching drinking WTPs and also the quality of the produced water. The physico – chemical properties of NOM is influenced by factors such as: (i) climatic and hydrological conditions (ii) anthropogenic activities and (iii) geological formation [22].

Therefore, it is expected that the NOM concentration and composition is variable throughout the water quality regions of South Africa. This means it would be futile to prescribe a particular treatment process for all regions. Additionally, each treatment process impacts on the NOM composition differently, hence its expected the removal efficiency at each treatment step to be different. This means the efficacy of a particular treatment process varies in transforming NOM concentration and composition throughout the country. Water treatment methods that are known remove NOM and other organics in large quantities include membrane filtration, coagulation, adsorption and ozonation in combination with bio-filtration [16]. However, these methods have, in the South African context, not gained wide use because they attract high capital costs (CAPEX) and OPEX implications. Furthermore, the fact that research on NOM in South Africa is at its infancy blinds water practitioners and water treatment companies with respect to the urgency and need of additional steps to combat NOM. Surveys sponsored mainly by the Water Research Commission (WRC) on the NOM removal efficiencies of South African water treatment plants show that the efficacy of removal of NOM is not consistent countrywide mainly because of (i) variability in NOM concentration and composition found in raw waters supplying respective water treatment; and (ii) the difference in water treatment processes configuration of each WTP (**Table 2.2**). Overall, South African research shows that the majority of WTPs are neither adequately designed nor capable of adequately removing NOM (**Table 2.2**).

Table 2. 2: NOM removal capacities of different techniques employed by respective WTPs in South Africa [104]

Region	Plant Name	*NOM removal efficiency (%)				Remarks	Reference
		Autumn	Winter	Spring	Summer		
A	Lepelle Plants:					Conventional treatment processes** are used in these plants, except for Ebenezer, which has an aeration stage after raw water abstraction. The drought of 2016 resulted in low water levels and concentrated NOM in summer.	[41] [105] [103]
	Ebenezer	100	100		58		
	Olifantspoort	23	26		15		
	Flag Boshielo	13	14		23		
B	Rietvlei		26	18	28	Rietvlei uses an additional GAC and DAFF*** stage.	[10]
	Vereening	61	61	56	49		
	Stilfontein		50	31	35		
	Lourie		16	21	48		
	Magalies:		30	51	46	Magalies Plants use prechlorination with chlorine dioxide and a post-ozonation step.	[105]
	Plant 1	38	38	25			
	Plant 2	31	34				
	Plant 3	36	29	33			
C						Research in this region is underway.	
D	Preekstoel		65	93		These plants treat highly coloured borehole water using biologically active sand with microorganisms attached to the grain surfaces for Fe and Mn removal.	
	Hermanus						
E	Plettenberg Bay		85	63	58	These plants follow a conventional method	[41]
	Plettenberg Bay		83	92			
	Umzoniana		25	26	37		
F	Umgeni plants::					Umgeni plants use conventional treatment methods to treat water impacted by agricultural activities especially sugarcane plantations.	[105] [106]
	Wiggins		29	22	64		
	Amanzimtoti			22			
	Umzinto		85	27			
	Hazelmere			33			
	Mtwalume		12	34			

**Measured as % DOC removal*
***Conventional water treatment processes involve coagulation, flocculation, filtration, and disinfection*
****DAFF is dissolved air floatation filtration.*

Therefore, it is crucial to conduct new research into technologies and new materials that can ameliorate the NOM related health risks. One of the emerging technologies in water treatment is based on membrane processes. Whereas research in this area is quite advanced in developed countries [94][107], such research in South Africa is at its infancy. Very few studies are at pilot or industrial scale, and the research is dominated mainly by laboratory-scale studies. Future research efforts should be focussed on opportunities of up-scaling current research technologies which are mainly at laboratory scale, to pilot scale. This should be done for the purposes of learning process and reactor dynamics for the ultimate goal of up scaling to industrial scale.

2.5 MEMBRANE FILTRATION IN WATER TREATMENT.

Membrane technology provides the following advantages in water treatment [108]:

- Consistent water quality in terms of microorganism and particle removal.
- Less labour intensive and automation.
- Compatible with conventional treatment processes requiring limited space.

Membranes are classified broadly by point of use and the driving forces that result in the movement of materials across the membrane barrier [108]:

- Concentration gradient (e.g. Dialysis, pervaporation, osmosis).
- Temperature gradient (e.g. membrane distillation).
- Electrical potential (e.g. Electrodialysis, electro-osmosis).
- Pressure gradient (e.g. MF, UF, NF and RO).

The inception of membrane technology bore many advantages in the water treatment industry because of its ease in compatibility with conventional treatment processes; can be used as a pretreatment stage for the more sensitive advanced treatment process and can be placed at the end of the treatment train to act as a polishing stage. The removal potential of various compounds and particles by membranes overlaps regardless of their intended use [96]. The membrane pore sizes and their different applications are summarized in **Table 2.3**.

Table 2. 3: Pore sizes of membranes and their application [93]

	Pore size	Pressure (bar)	Pollutants retained
MF	0.1 – 5 µ	0.1 - 3	Particles in suspension (fine dust, blood cells)
UF	20 – 0.1 µ	2 – 10	A Selection of macromolecules (proteins, endotoxins, viruses, silica)
NF	>1 nm	5 - 30	Small solutes and multivalent salts (salts, sugars and synthetic dyes)
RO	0.1 – 1 nm	10 - 100	Salts

2.5.1 Factors Governing the Removal of NOM by Pressure Driven Membranes

The wider application of membranes in the water industry is hindered by their propensity to foul and costs (capital and operation). The extent of fouling is influenced by membrane synthesis materials, physico - chemical properties, solution chemistry (i.e. temperature, ionic strength and pH), character (in this case NOM hydrophilicity/hydrophobicity) and the hydrodynamic conditions and solute concentration of the feed [109]. Wang et al. [110] investigated a range of MF, UF and NF membrane modules for the reason of determining the fouling of the membranes due to the presence of NOM. They reported when the model foulant was humic acid, hydrodynamic conditions and feed stream solution chemistry are the major contributor to the extent of fouling [110]. Divalent cations such as Ca^{2+} and Mg^{2+} were reported to adhere onto the NF membrane surface preferentially over monovalent and divalent anions. The divalent cations act as bridging ligands between the humic acid and the membrane surface. This is achieved by the cations ability to form bonds with the OH group inherent to ceramic membranes surface and the carboxylic groups of the humic acid. Further, intra- and inter-molecular binding is promoted by the presence of the cations as they bind negatively charged humic acid molecules that are not in contact with the membrane thus forming a compacted fouling layer on the membrane. Fouling by the presence of Ca^{2+} was mitigated by increasing the crossflow velocity thus reducing the residence time of Ca^{2+} on the membrane surface [110]. According to Roddrik *et al*., [4], the rate of fouling of polymeric or ceramic membranes by NOM

is influenced by its character. The inherent presence of the –OH groups on the surfaces of the ceramic membranes surface interact with the polar groups such as phenolic and carboxylic groups, an abundance of these groups determines the extent of fouling on the membrane surface and pores [52]. The fouling potential of NOM fractions of NOM follows the order: hydrophilic charged < transphilic acids < hydrophobic acids < hydrophilic neutral. Filtration methods are key processes for the removal of colloidal and particulate matter in the water treatment industry. Currently, research is centered on the two membrane materials of choice, which are broadly classified as either polymeric or ceramic. This study seeks to extend the technologies of drinking water treatment in South Africa by exploiting the many advantages of ceramic membranes, given the variable water quality in the country.

2.6 CERAMIC MEMBRANES

The materials of choice for ceramic membranes are oxides of alumina, silica, titania, and zirconia as well as silicon carbide. As illustrated in **Figure 2.17**, the porous multi-strata of ceramic membrane consist of at least two to three layers which are: (i) micro-porous also known as the filtering layer or active layer; (ii) meso-porous that is sometimes referred to as the intermediate layer; and (iii) macro-porous also known as the support layer.

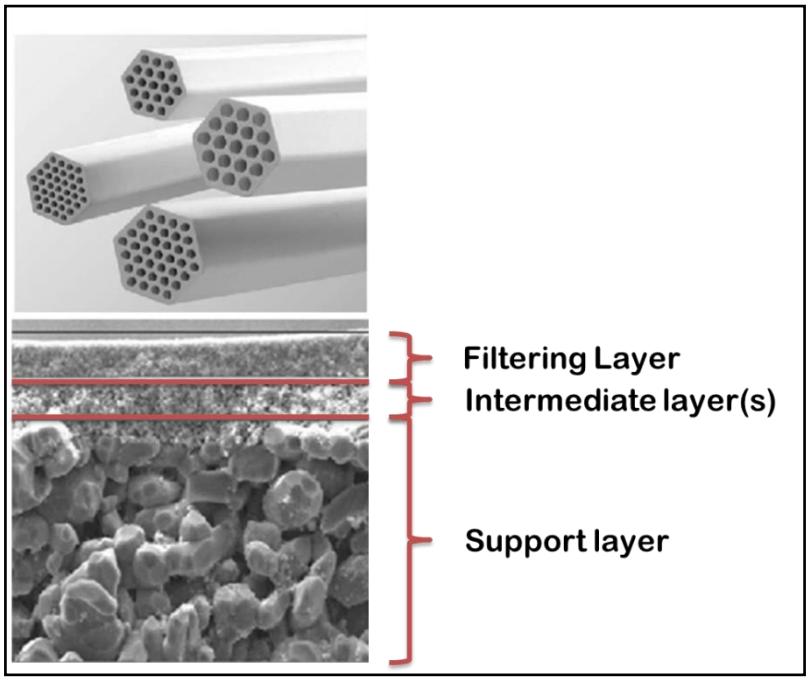

Figure 2. 17: A typical ceramic membrane and its cross sectional structure [111].

The active layer is responsible for providing effective selectivity and separation because of its direct proximity to the aquatic contaminants contained in the feed stream. The macro-porous layer provides the mechanical strength needed to support the membrane. The function of the intermediate layers is to act as a bridge between the filtering layer and the support layer [112].

Intrinsic features of the ceramic membranes place them at an advantage point over the polymeric membranes. Characteristics such as chemically stable even in aggressive environments, membrane regeneration, mechanical and thermal stability make ceramic membranes an attractive option in water treatment, more especially when treating water of variable physico – chemical properties due to seasonal changes or flush flood event [113]. Furthermore, AOPs such as catalytic or photocatalytic ozonation can easily be coupled with ceramic membranes, whereas polymeric membranes easily degenerate in the presence of hydroxyl radicals. [114]. Climatic, seasonal variations and load, water characteristics (i.e. pH, temperature, presence of natural oxidants) fluctuations are tolerated by ceramic membranes whereas organic membranes would simply collapse [115]. Additional properties of hydrophilicity and porosity make ceramic membranes the technology of choice in waters which NOM laden [116]. Hofs et al [116] reported that the substitution of conventional steps in water treatment (i.e. coagulation, sedimentation, and filtration) with ceramic membranes is more advantageous and equally effective in the removal of particulate matter by MF and UF membranes.

2.6.1 Types of Ceramic Membranes

Ceramic membranes are categorized into two, namely porous and dense membranes. Porous membranes are characterised by pore size, thickness and surface porosity. The types of ceramic membranes and their related pore sizes are described in **Table 2.4**. Dense membranes are mainly applied in gas separation (GS) such as the high temperature oxygen permeation through zirconium oxide membrane. In this type of ceramic membrane, the gas diffuses through the membrane before desorbing from the membrane.

Table 2. 4: Types of Ceramic membranes [117].

Type of ceramic membrane	Application	Pore size (nm)
Macro - porous	MF,UF	> 50
Meso - porous	Gas separation (GS), NF,UF	2 - 50
Micro - porous	GS	< 2
Dense	reaction, GS	-

2.6.2 Geometrical Configuration of Ceramic Membranes

The morphology of the ceramic membranes is determined by the intended application. The geometrical configuration of ceramic membranes [118] are discussed briefly in the following sub-sections.

2.6.2.1 Tubular / straw membranes

These types of membranes are generally used for highly turbid water with excessive particulate matter content. The *modus operandi* involves the passing of the feed water through the membrane core and the collection of the permeate in the tubular housing.

2.6.2.2 Hollow fiber membranes

The internal diameter of these membranes, which is less than 0.5 mm, increases plugging chances. Therefore, this type of membrane is useful for treating water with low suspended solids content. The feed water is pumped into the open core area of the fibers, and the cartridge area encompassing the fibres collects the permeate.The collection of the permeate can be carried out in two modes, namely inside out or outside in.

2.6.2.3 Capillary membranes

The *modus oparandi* of capillary membranes rests on the membrane selectivity. Therefore the membrane can operate in either an “inside-out” or “outside-in” mode. When compared to the hollow membrane, capillary membranes internal diameter is much smaller; the chances of plugging are, therefore, much higher.

2.6.2.4 Plate and frame (pillow-shaped) membranes

The membranes are packed in such a way that they form a pillow shape. Within the packing module, the content of the waters' dissolved solids determine the separation membranes in the module. The feed water is pumped through the membranes on an inside-out basis, and the permeate is collected from the spaces between the membranes.

2.6.3 Synthesis of Ceramic Membranes.

As depicted in **Figure 2.18**, the general synthetic procedures of ceramic membranes involve [119]:

- **Suspension preparation** – A binding liquid is used to dissolve and mix the starting powders.
- **Forming** – the dough from the previously prepared suspension is shaped according to a predefined method.
- **Heat treatment** – Preset firing temperatures are applied on to the membrane particles to increase binding of particles through a sintering process.

The number of coatings onto the support layer of the membrane determines the active layer (e.g. chemical vapour deposition (CVD) and sol-gel) before the firing step. The number of layers formed determines the porosity of the active layer.

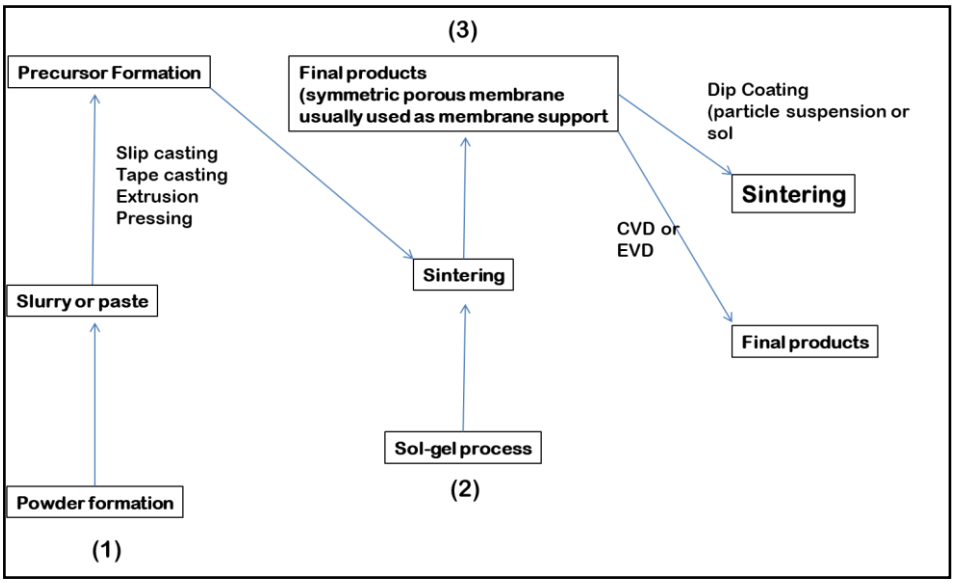

Figure 2. 18: General procedures for the synthesis of ceramic membranes [6].

2.6.3.1 Slip casting method

In this process, the powder precursor is mixed and thereafter poured into a porous mold to facilitate gel formation by precipitation of solvents on the internal surface of the mold. The slip casting process may be optimized through the density of the slip, the temperature of the slip, process technology parameters such as pressure and time, and utilization of chemical auxiliaries [120].

2.6.3.2 Tape casting method

Flat sheet ceramic membranes are produced by this method. A stationary casting knife is used to control the thickness of the cast layer. This is achieved by predetermining the distance between the moving carrier and the blade. This method can be optimized by controlling the powder suspension viscosity, the reservoir depth, knife blade and the gap between moving carrier [120].

2.6.3.3 Pressing method

Ceramic membranes for gas separation are fabricated using this method. Pressure of up to 100 MPa on the slurry is applied by a press machine. This method can be optimized by varying the pressure so as to control the pore sizes.

2.6.3.4 Extrusion method

This is the most popular way of producing porous ceramic membranes. A homogeneously prepared paste is forced through a nozzle to form the final green membrane. To maintain the integrity of the membrane, any remaining binder, solvent, and plasticizer is evaporated.

2.6.3.5 Sol-gel method

This method has the advantage of stringent control of pore size distribution and the sizes of the pores.

2.6.3.6 Dip coating method

The dip coated substrate is calcinated before it is in contact with the atmosphere.

2.6.3.7 Chemical vapour deposition (CVD) method

In this method, very thin and uniform layers of coat are applied on to the substrate. The CVD method can be modified by layering similar or different compositions of the coat onto the substrate. A gas phase chemical reaction at elevated temperatures can be used for this process [6].

2.6.4 Suitability of Ceramic Membranes for NOM Removal

The hallmark of successful membrane performance is determined by the membranes ability to resist fouling and at the same time maintaining a steady permeate flux over extend time. The presence of NOM remains a long lasting limitation to this achievement. Factors which exacerbate fouling by NOM include: the membranes' charge, surface roughness and hydrophobicity [4], the physic-chemical properties of NOM such as charge, hydrophobicity and size [121], the hydrodynamics conditions such as surface shear and solution and the solution chemistry (ionic strength, hardness ion concentration and pH) [122]. Numerous literature reports indicate under identical conditions ceramic membranes of similar pore size outperform polymeric membranes in terms of extent of fouling [116][123][124]. Furthermore, the mechanisms and dynamics of ceramic membrane fouling are dissimilar to those of polymeric membranes [116].

2.6.5 Role of NOM in Ceramic Membrane Fouling

Membrane technology has found application in water and wastewater sector. In particular, ultrafiltration/nanofiltration has shown to be an efficient process for the removal of DOM and other macromolecules such as humic substances, sugars and proteins. As water is separated from contaminants, the continual interaction between the solutes and membrane surface eventually leads to the deposition of the solutes forming a cake layer, blocking the membrane pores and further constricting the pores of the membrane. This fouling process results in an increased operational pressure and cleaning frequency and concomitant decline in the membrane separation performance [125][90].

The major organic foulant from surface waters on membrane processes is NOM [126]. The extent and severity of NOM fouling in simulated and environmental conditions are broadly classified under foulant-membrane and foulant-foulant interactions. Studies on membrane fouling mechanisms are well documented for polymeric membranes [96] [127]. However, conflicting reports on NOM fractions contributing more to membrane fouling have been reported. Some studies indicate that colloidal NOM fractions are the major contributor to membrane fouling [128]. Some researchers have reported hydrophobic or aromatic compounds (fulvic humic acids) to be the major NOM foulants of UF/NF membranes [129]. In

contrast, other investigators have reported polysaccharides as major contributors to membrane fouling. Furthermore, macromolecular biopolymers such as dextran and sodium aliginate increase the severity of fouling especially in the presence of inorganic particles [24]. Interestingly, the sole presence of inorganic particles present have been reported not to increase the severity of membrane fouling [130]. Moreover, many simulated studies have focused on investigating the fouling behaviour of polymeric membranes by mono-dispersed foulants possessing homogeneous physico-chemical properties and a defined character. Be that as it may, investigations of fouling by mono-dispersed foulants cannot be confidently extrapolated to real water and/or wastewater treatment systems where a mixture of foulants exist in solution and fouling cannot be fully attributed to a single foulant.

Polymeric membranes are the most common commercially available type and the mostly widely applied for water treatment purposes. However, most of polymeric membranes have a limited pH application range, are very prone to fouling by organic species and are not very tolerant of chlorine-based chemicals (chlorine attack) making them vulnerable to chemical cleaning [96]. Therefore, the development of new materials that can withstand chlorine (tolerant to severe cleaning procedures) and harsh conditions have attracted significant attention from material scientists. Among the studied materials are ceramics, motivated by their chemical, thermal and mechanical stability [112]. With an application span of more than two decades in the water treatment industry, little is known about ceramic membranes' fouling behaviour by organic macromolecules. it is paramount to fully understand the fundamental fouling mechanisms involved during the filtration process for further advancement of ceramic membranes in water treatment industry..

2.6.6 Mechanism and Characteristic of Membrane Fouling

The phenomenon of membrane fouling is best illustrated by studying the underlying promoters such as: membrane – solute interactions, membrane surface chemistry and solute – solute interactions. The adsorption of solute in the pores of the membrane and onto the surface of the membrane is best understood by studying the membrane−solute interactions. The propensity of solute fouling is governed by membrane property, solute or particle property and hydrodynamic

conditions under which the experiment is carried out. The methods of solute or particle fouling are [131]:

(i) Adsorption – this occurs as a result of attraction interactive forces between particles/solute and the surface of the membrane. A monolayer of solutes or particles begins to develop even at zero to negligible permeation flux resulting in more hydraulic resistance. Concentration polarisation occurs if the extent of adsorption is dependent on concentration; this increases the amount of adsorption.

(ii) Pore blockage – When the pores of the membranes are blocked or partially blocked results in reduction of flux and an increase in hydraulic resistance.

(iii) Deposit – Also known as cake resistance. This results as more and more monolayers of particles are deposited onto the membrane surface consequently increasing the hydraulic resistance.

(iv) Gel - When extracellular polymeric substances (EPS) or any other macromolecules deposit onto the surface of the membrane via concentration polarisation on to the membrane they form a gelatinous layer which exacerbates hydraulic resistance and loss in permeation flux.

The fouling types are schematically shown in **Figure 2.19** [132].

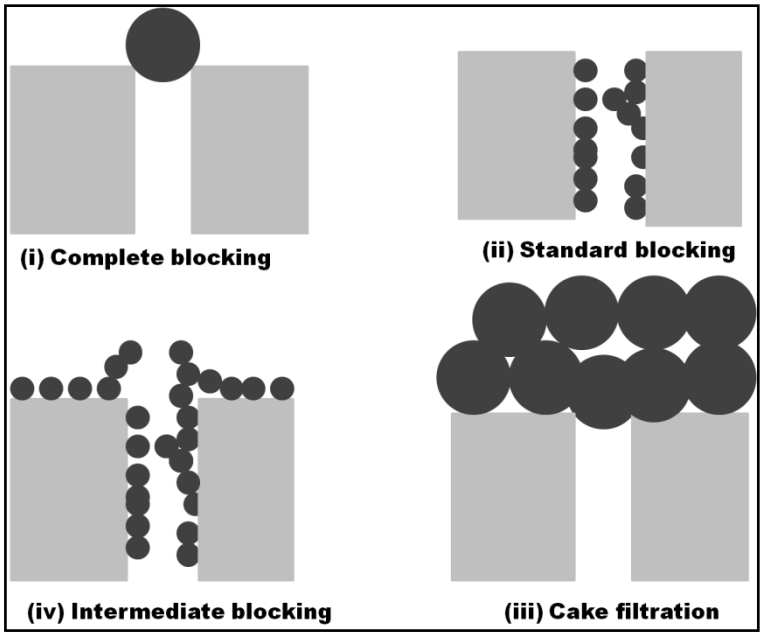

Figure 2. 19: The typical foulant deposit mechanism [132]

The fouling mechanisms can be further elucidated using the model equations shown in **Box 2.1**.

(1). $J = J_0 e^{-At}$	$A = K_A u_0$
(2). $J = \frac{J_0}{(1+Bt)^2}$	$B = K_B u_0$
(3). $J = \frac{J_0}{(1+At)}$	
(4). $J = \frac{J_0}{\sqrt{1+Ct}}$	$C = (2R_r) K_c u_0$

Box 2.1: Models to describe mechanisms of fouling: (1) complete blocking, (2) standard blocking, (3) intermediate blocking, and (4) cake filtration, respectively [132]**.**

where, J_0 and J are initial and final flux respectively; u_o average initial filtrate velocity; R_r denotes the resistance of cake filtration by the clean membrane; K_A denotes the quotient of the blocked membrane surface and volume of permeated water through the pores of the membrane; K_B denotes the extent of internal membrane pore area constriction due to particle deposition as a quotient total volume permeated; K_C denotes the quotient of permeated volume and membrane area.

Linear relationships can be obtained from the four fouling models and the goodness of fit coefficient (R^2) is used to identify the main operational fouling mechanism.

2.6.7. Methods for Fouling Control

Physical methods for fouling control include seeding particles, fluid shear, air scour, mechanical shear and the use of electric field. The added particles act as a centre for nucleation of dissolved macromolecules, thus creating larger non settling particles repelling them away from the surface of the membrane. The function of the electric field is to facilitate charged molecules to migrate away from the surface of the membrane and the magnitude of separation depends on the applied electric field, increasing flux at the same time minimising the extent of concentration polarization [133]. Surface membrane chemistry modification can be

manipulated so as to mitigate solute or particle deposition. This can be done by introducing charge or some degree of hydrophobicity so as to weaken membrane solute/particle attractive forces or increase the repulsive forces to completely repel solute/particle settling or adhering onto the membrane surface [134]. The feed stream chemistry can be altered so as to mitigate fouling. This can be done by adjusting ionic strength and pH. The morphology of NOM is dependent on pH and ionic strength (IS), high pH and low IS promote a coiled morphology whereas at low pH and high IS a linear morphology is promoted. Again pH and IS influence extent of complexation and chelation of cations with NOM [135].

2.6.7.1 Membrane Cleaning

The industrially economic method of maintaining constant membrane flux after extended operations is through membrane cleaning. Pointers signaling the need of membrane cleaning include (1) significant permeate flux reduction; (2) reduction in salt rejection (for NF or RO); and (3) the need to adjust trans-membrane pressure in order to maintain a desired permeate flux. In brief, membrane cleaning the ability to dislodge foulants on the surface and inside the pores of the membrane, using physical or chemical means. The knowledge of interaction of membrane surface and foulants dictates the method of cleaning to be applied. Membrane cleaning can be classified into physical and chemical cleaning with the former including pneumatic, hydraulic and electrical field applications, and mechanical processes and, and the latter involving the use of chemicals such as bases, acids, surfactants and oxidants and surfactants. Irreversible fouling is the extent of fouling not mitigated by the cleaning procedures; it is termed hydraulically irreversible or chemically irreversible depending on the cleaning mechanism employed.

(a) Physical Cleaning

Back pulsing/backwashing and flushing are the most common hydraulic cleaning techniques for mitigating hydraulically reversible fouling [121]. Regular Intermittent backwashing dislodges the foulants off the membrane surface and pores consequently reducing concentration polarization [4]. While non-adhesive foulants are effectively dislodged by rapid backwashing effectively from the surface of the membrane surfaces and consequently reducing reversible fouling. Pneumatic

cleaning includes air lifting, air sparging, air bubbling and air scouring [121]. The advantages of pneumatic cleaning include easy integration into the membrane system, low maintenance costs and no chemicals are required.

(b) Chemical Cleaning

Chemically reversible fouling is mitigated through the use of chemicals such as acids, metal chelating agents, alkalis, enzymes and surfactants [133]. Additionally, sequestration agents such as hypochlorite and hydrogen peroxide, EDTA and sodium bisulphite or oxidants and disinfectants are commonly used in membrane cleaning. The usual chemical membrane cleaning agents: caustic (KOH, NaOH, NH_4OH), acidic (HNO_3, HCl, H_3PO_3, H_2SO_4, citric, oxalic), complexing/sequestering (EDTA), surfactant/detergent (sodium dodecyl sulphate , alkyl sulphate, cetyl trimethyl ammonium bromide), enzymatic (CP-T , α-CT, peroxidase), disinfectants/oxidants (H_2O_2, NaOCl, $KMnO_4$) and cleaning blends (e.g., TRiclean®, 4 Aqua clean®, Ultrasil®/Aquaclean®) [121]. The effectiveness of chemical cleaning depends on the type of the cleaning agent and its concentration, and the operating conditions such as pressure, cross flow velocity, turbulence near the membrane surface, pH, temperature and cleaning time [134].

(c) Cleaning Efficiency

The effectiveness of cleaning is commonly measured by determining the clean water flux after cleaning at a defined trans-membrane pressure, circulation velocity and temperature. Other cleaning efficiency measurements entail: (a) ultrapure water flux recovery; (b) ratio of the volume of water used to wash the membrane and the produced water volume and (c) ratio of total solids before and after cleaning.

2.6.8 Atomic Layer Deposition Route for Ceramic Membrane Surface Modifications

The usual fabrication method for ceramic membranes is the sol-gel method. However, this method returns a challenge in the development of tight ceramic NF membranes. Atomic layer deposition (ALD) is a gas phase self-limiting atomic layer coating technique for growing atomic-scale thin layers. ALD has been used to address the challenges of the sol – gel method, and it’s a promising technique

of modifying ceramic membranes by inferring the surface of the membrane a desirable chemistry to serve a particular purpose [95]. The alternating, self-limiting saturation surface reactions of the ALD results in exquisitely uniform and conformal pinhole free 3-D coatings of metal oxides on the membrane surface and pore walls, resulting in the predetermined pore size. In a study by Song et al. [136], TiO_2 loose NF membranes fabricated by the sol-gel method from a pore size of 20 nm to 1 nm via the ALD method were fabricated. Intriguingly, the clean water permeability of ALD-modified NF membranes was 48 L m^{-2} h^{-1} bar^{-1}, which is about two times higher than that of the unmodified sol-gel-made NF [137]. Despite the ALD modified membranes showing promise in increased water permeability, a demonstration of the impact of fouling or the mechanism fouling on these membranes compared to the unmodified counterparts has not been reported.

The ALD technique involves a sequential deposition of the precursors unlike its predecessor chemical vapour deposition (CVD) whereby the precursors are introduced simultaneously onto the surface [95]. In the ALD technique, the precursors are introduced into the reactor chamber sequentially resulting in an atomic level thin film deposition due to self-saturating reactions with exposed surface groups, thus leading to a successive self-limited growth of a (sub) monolayer of material. The process of TiO_2 deposition on a ceramic membrane substrate by an ALD process is illustrated in **Figure 2.20**.

The process of a single cycle deposition is as follows [95]:

1. Firstly, the introduction and the formation of a monolayer of the first precursor onto the surface on the membrane.
2. Excess amounts of the first precursor and other by-products are purged off the reaction chamber.
3. The second precursor is introduced into the reaction chamber.
4. Again excess amounts of the second precursor and other by-products are purged off the reaction chamber.

5. The required thickness or in this case pore size is achieved by repeating steps 1 to 4.

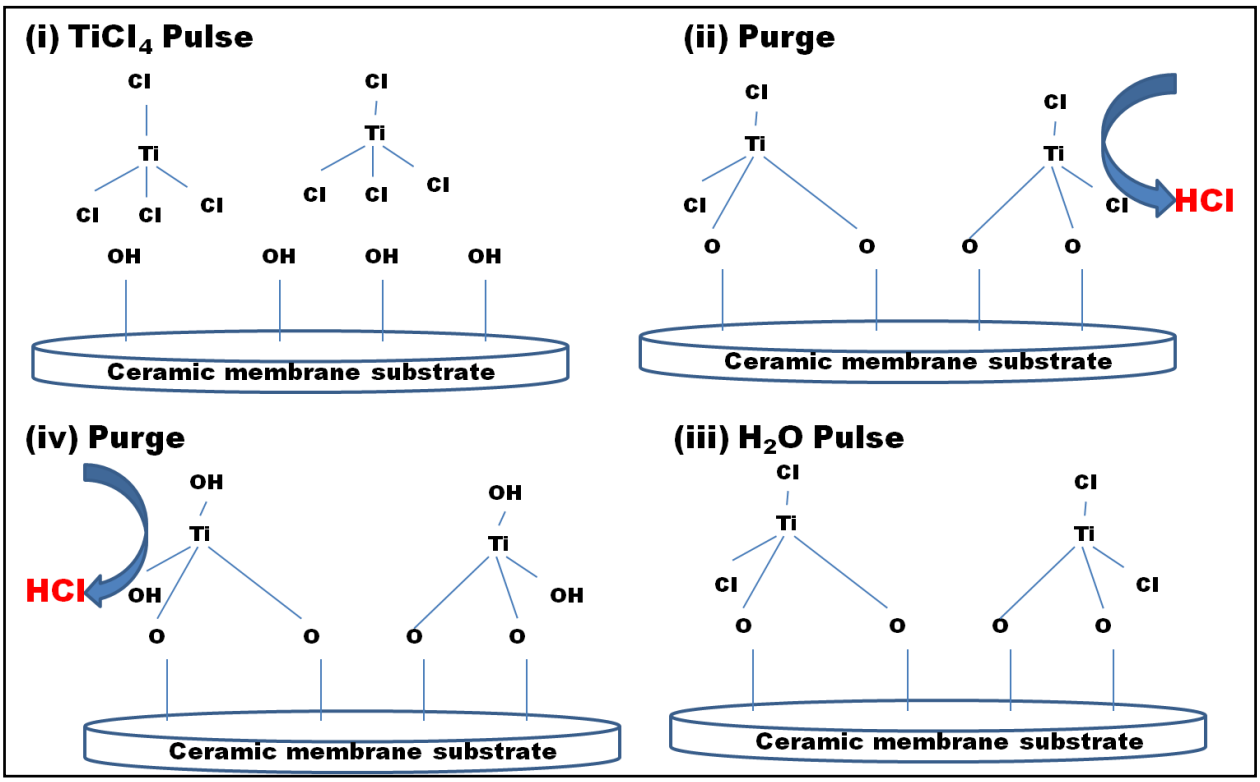

Figure 2. 20: ALD method for the coating of ceramic membranes [95]

2.8 DEFECTS

The most popular synthesis route for ceramic membranes is the sol-gel method because of its simplicity, controllability and homogeneous dispersion of particles that gives homogeneity to the physical properties to the layers of the membrane [112]. However, the major limitation to this synthetic route is the occurrence of defects. A defect is a crack or pinhole that can occur during membrane fabrication (gelling, drying or firing steps), or during membrane utilization (sealing or thermal cycling of the membrane) [138]. Defect nomenclature classifies defects according to size and site of occurrence. For example, a defect in a microporous membrane of a diameter *(d_p)* that is less than 2 nm is considered a crack or a pinhole on the membrane surface. The presence of any pores that belong to the mesopore region (2 nm < d_p < 50 nm) on a microporous membrane surface is also classified as a defect [139]. The presence of super-micropores (0.7 nm < d_p < 2 nm) instead of

ultra-micropores (d_p < 0.7 nm) can also be considered as defects depending on the intended application. The presence of a small number of defects, even in the nanometer range, in the active layer can drastically reduce the selectivity of the membranes [139].

The basic and qualitative method of analyzing defects in ceramic membranes is the application of transmission electron microscopy (TEM) or scanning electron microscopy (SEM) images. However, it is difficult to get a general picture of defect size distribution due to limited area of analysis (ca. 100 μm^2) [139]. In addition, given the brittle nature of ceramic membranes, any attempt to break a small piece for SEM/ TEM defect analysis is likely to result in the total destruction of the whole membrane. The most popular quantitative method for characterizing and analyzing defects in membranes is permporometry, which is based on monitoring a flow of a non-condensable gas (e.g. helium) as a function of relative pressure of a strong adsorbing compound (e.g. n-hexane). Using this method to characterize the flow through micro-pores in modified fouling index (MFI) membranes, Korelskiy et al. [140] reported 0.7 % of the total area of the membrane was defective as determined by using n-hexane, and 97% of the defects had a with a width below 1 nm for the best membrane. This method was also used to check for nano-defects by examining if SF_6 (kinetic diameter 0.55nm) can permeate through sol-gel silica membranes, and permselectivity varied between 3.2 and 52. After chemical vapour infiltration (CVI) treatment to remove the defects, the permselectivity increased to 68 – 308 [141][142]. Although these results are promising, the very nature of permporometry relies on the permeation of gases through the pores and does not distinguish the layers and the associated pore sizes that are characteristic of each layer in ceramic membrane morphology [140]. Despite the crucial effect of defects on membrane performance, this problem has not been thoroughly examined on water/wastewater filtration membranes because most of the studies are focussed mainly on defects on gas separation membranes [143].

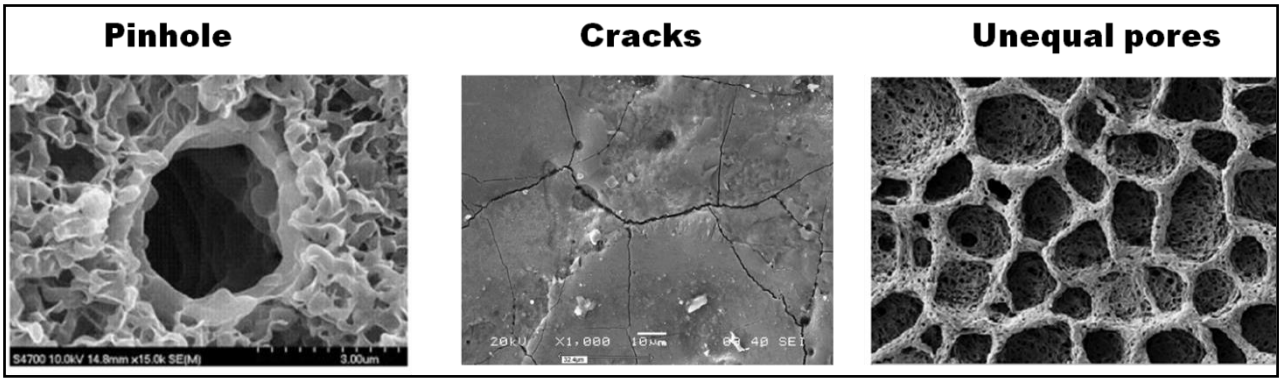

Figure 2. 21: Typical defects on the surface of ceramic membranes [144]

2.8 CONCLUSION

This literature review has demonstrated the challenges associated with the presence of natural organic matter in water. The importance and necessity of effective NOM removal prior to distribution was highlighted. The physicochemical characteristics of NOM vary depending on age, source and season. This variability and complex chemistries of NOM play a significant role towards its treatability by water treatment processes. Therefore, it is paramount to learn of its characteristics at source prior to water treatment process in order to improve the removal efficiency as well as to reduce the disinfection by-products formation downstream. Stringent water quality regulations and high variability of raw water have necessitated the development of a new and/or improved treatment strategy for effective NOM removal. Coagulation is the most popular unit process for the removal of NOM worldwide. However, this process leads to the production of large quantities sludge, low and/or ineffective removal efficiency of certain NOM fractions are still the major problems in the coagulation technology. Recently, AOPs are fast gaining recognition as an attractive solution for NOM removal, mainly due to its ability to transform NOM. Nevertheless, the application of AOP in water treatment process is still limited due to slow reaction kinetics, costs, chemicals, environmental hazards and separation challenges. Ceramic membrane filtration offer many advantages as an alternative process for drinking water purification such as low fouling rate, superior mechanical properties, and ease of operation and maintenance. However, the application of ceramic membranes is limited mainly because of high capital costs. Thus, the next few chapters of this

thesis will describe the effort undertaken to develop and apply ceramic membranes to remove NOM in South African waters.

2.9 REFERENCES

[1] Y. Hu, L. Tan, S.H Zhang, Y. T Zuo, X. Han, N. Liu, W.Q Lu and A. L Liu (2017). Detection of genotoxic effects of drinking water disinfection by-products using Vicia faba bioassay. *Environ. Sci. Pollut. Res*, **24**(2), 1509–1517.

[2] B. Teychene, G. Collet, and H. Gallard (2016). Modeling of combined particles and natural organic matter fouling of ultrafiltration membrane," *J. Memb. Sci.*, **505**(August),185–193.

[3] J.Z Hamad, C. Ha, M.D Kennedy and G. L Amy (2013). Application of ceramic membranes for seawater reverse osmosis (SWRO) pre-treatment. Desalination and Water Treatment., **51**(25-27), 4881 - 4891.

[4] T. Nguyen, F. A. Roddick, and L. Fan (2012). Biofouling of water treatment membranes: A review of the underlying causes, monitoring techniques and control measures. *Membranes*, **2**(4), 804–840.

[5] S. G. Lehman and L. Liu (2009). Application of ceramic membranes with pre-ozonation for treatment of secondary wastewater effluent. *Water Res.*,**43**(7), 2020–2028.

[6] R. J. Ciora and P. K. T. Liu (2003). Ceramic Membranes for Environmental Related Applications. *Fluid/Particle Sep. J.*, **15**, 51–60.

[7] G. Mustafa, K. Wyns, A. Buekenhoudt, and V. Meynen (2016). Antifouling grafting of ceramic membranes validated in a variety of challenging wastewaters. *Water Res.*, **104**, 242–253.

[8] T. O. Mahlangu, T. A. M. Msagati, E. M. V. Hoek, A. R. D. Verliefde, and B. B. Mamba (2015). Rejection of pharmaceuticals by nanofiltration (NF) membranes: Effect of fouling on rejection behaviour. *Phys. Chem. Earth, Parts A/B/C*, **76**(January), 28–34.

[9] E. Lavonen, K. M. Persson, and M. Larson (2016). Integrity breaches in a

hollow fiber nano filter: Effects on natural organic matter and virus-like particle removal. **105**, 231–240.

[10] T. I. Nkambule, R. W. M. Krause, J. Haarhoff, and B. B. Mamba (2012). Natural organic matter (NOM) in South African waters : NOM characterisation using combined assessment techniques. *Water SA* **38**(5),697–706, 2012.

[11] Y. Zhang, M. Li, S. Wu, and Q. Zhang (2016). Research on hydrophilicity and hydrophobicity of adsorption of NOM on metal oxide / water interface. *Desalin. Wat. Treat.* **3994**(December), 1940-1948.

[12] S. A. Baghoth, S. K. Sharma, and G. L. Amy (2010).Tracking natural organic matter (NOM) in a drinking water treatment plant using fluorescence excitation e emission matrices and PARAFAC. *Water Res.*, **45**(2),797–809.

[13] E.N Hidayah, Y.C Chou and H.H Yeh (2016). Using HPSEC to identify NOM fraction removal and the correlation with disinfection by-product precursors," *Water Science and Tech*.,**16**(2), 305–313.

[14] A. Bhatnagar (2017). Removal of natural organic matter (NOM) and its constituents from water by adsorption: A review. *Chemosphere*., **166**(January), 497-510.

[15] G. Kastl, A. Sathasivan, and I. Fisher (2016). A selection framework for NOM removal process for drinking water treatment. *Desalin. Water Treat.*, **3994**(December), 1–11.

[16] T. I. Nkambule (2012). Natural Organic Matter (Nom) in South African Waters: Characterization of Nom, Treatability and Method Development for Effective Nom Removal From Water. PhD Thesis, University of Johannesburg.

[17] S. A. Parsons, B. Jefferson, E. H. Goslan, P. R. Jarvis, and D. A. Fearing, (2004). Natural organic matter – the relationship between character and treatability. *Water Supply*, **4**(5-6),43–48.

[18] Z. Filip, W. Pecher, and J. Berthelin (2000). Microbial utilization and transformation of humic acid-like substances extracted from a mixture of municipal refuse and sewage sludge disposed of in a landfill. *Environ. Pollut.*, **109**(1), 83–89.

[19] F. L. Rosario-Ortiz, S. Snyder, and I. H. Suffet (2007). Characterization of the polarity of natural organic matter under ambient conditions by the Polarity Rapid Assessment Method (PRAM). *Environ. Sci. Technol.*, **41**(14), 4895–4900.

[20] E Vasyukova, R Proft, J Jousten, I Slavik (2013). Removal of natural organic matter and trihalomethane formation potential in a full-scale drinking water treatment plant. *Water Science and Supply*, 2, 1099–1108.

[21] K. ??zdemr (2014). Characterization of natural organic matter in conventional water treatment processes and evaluation of THM formation with chlorine. *Sci. World J.*, **2014**, 2014.

[22] K. P. Lobanga (2012). Natural organic matter removal from surface waters by enhanced coagulation, granular activated carbon adsorption and ion exchange. Ph.D Thesis, University of Johannesburg.

[23] B. Jefferson and E. H. Goslan (2004). Natural Organic Matter – the Relationship between Character and Treatability. *Water Sci. Technol. Water Supply*, **5**(July), 43–48.

[24] H. Yamamura, K. Okimoto, K. Kimura, and Y. Watanabe (2014). Hydrophilic fraction of natural organic matter causing irreversible fouling of microfiltration and ultrafiltration membranes. *Water Res.*, **54**, 123–136.

[25] J.F Koprivnjak (2007). Natural organic matter: isolation and bioavailability. PhD Thesis, Geogia Institute of Technology.

[26] E. E. Lavonen, D. N. Kothawala, L. J. Tranvik, M. Gonsior, and P. Schmitt-kopplin (2015). Tracking changes in the optical properties and molecular composition of dissolved organic matter during drinking water

production.*Water Res*., **85** (November), 286–294.

[27] X. Liao, E. Bei, S. Li, Y. Ouyang, J. Wang and C. Chen (2015). Applying the polarity rapid assessment method to characterize nitrosamine precursors and to understand their removal by drinking water treatment processes. *Water Res.*,**87**, 292–298.

[28] S. A. Baghoth (2012). Characterizing natural organic matter in drinking water treatment processes and trains saeed abdallah baghoth. PhD Thesis, Technical University of Delft.

[29] J. C. Rodr (2013). Natural organic matter quantification in the waters of a semiarid freshwater wetland (Tablas de Daimiel , Spain).*J. Env. Sci*., 25(1), 114-123.

[30] A. Matilainen, N. Lindqvist, S. Korhonen, and T. Tuhkanen (2002). Removal of NOM in the different stages of the water treatment process. *Environ. Int.*, **28** (6), 457–465.

[31] W. T. Li. (2017). Application of UV absorbance and fluorescence indicators to assess the formation of biodegradable dissolved organic carbon and bromate during ozonation. *Water Res.*,**111** (March), 154-162.

[32] K Kalbitz, W Geyer and S Geyer (1999). Spectroscopic properties of dissolved h u m i c substances - a reflection of land use history in a fen area. *Biogeochemistry*, **47**, 219–238.

[33] J. L. Cortina and S. Gonz (2016). Integration of Ultraviolet e Visible spectral and physicochemical data in chemometrics analysis for improved discrimination of water sources and blends for application to the complex drinking water distribution network of Barcelona. *J. Clen. Prod*., **112**(January), 4789–4798.

[34] E. Lavonen (2015). *Tracking Changes in Dissolved Natural Organic Matter Composition*. Doctoral Thesis, Swedish University of Agricultural Sciences.

[35] Y. Shutova, A. Baker, J. Bridgeman, and R. K. Henderson (2014).

Spectroscopic characterisation of dissolved organic matter changes in drinking water treatment : From PARAFAC analysis to online monitoring wavelengths. *Water Res.*,**54**, 159–169.

[36] D Ridder, A.R.D. Verliefde, S.G.J. Heijman, S Gelin, M.F.R. Pereira, R. P. Rocha, J.L. Figueiredo, G.L. Amy, H.C. Dijk (2012). A thermodynamic approach to assess organic solute adsorption onto activated carbon in water. *Carbon*.,**50**, 3774-3781.

[37] K. Kimura and Y. Oki (2017). Efficient control of membrane fouling in MF by removal of biopolymers: Comparison of various pretreatments. *Water Res.*, **115**,172–179.

[38] K. Kimura, K. Shikato, Y. Oki, K. Kume, and S. A. Huber (2018). Surface water biopolymer fractionation for fouling mitigation in low-pressure membranes. *J. Memb. Sci.*, **554**(November) 83–89.

[39] W. Chen, P. Westerhoff, J. A. Leenheer, and K. Booksh (2003). Fluorescence Excitation-Emission Matrix Regional Integration to Quantify Spectra for Dissolved Organic Matter. *Environ. Sci. Technol.*, **37** (24), 5701–5710.

[40] G. Hua, D. A. Reckhow, and I. Abusallout (2015). Correlation between SUVA and DBP formation during chlorination and chloramination of NOM fractions from different sources. *Chemosphere*, **130**.

[41] T. I. Nkambule(2012). Natural Organic Matter (NOM) in South African Waters: Characterization of Nom, Treatability and Method Development for Effective Nom Removal From Water. PhD Thesis, University of Johannesburg.

[42] E. H. Goslan, D. Wilson, J. Banks, P. Hillis, A. Campbell, and S. A. Parsons, (2004). Natural organic matter fractionation : XAD resins versus UF membranes . An investigation into THM formation.*Water Supply*., **4**(5-6), 113-119.

[43] F. L. Rosario-Ortiz, K. Kosawa, H. N. Al-Samarrai, F. W. Gerringer, C. J. Gabelich, and I. H. Suffet (2004). Characterization of the changes in polarity of natural organic matter using solid-phase extraction: Introducing the NOM polarity rapid assessment method (NOM-PRAM). *Water Sci. Technol. Water Supply*, **4**(4),11–18, 2004.

[44] M. Philibert, S. Bush, F. L. Rosario-Ortiz, and I. H. Suffet (2008). Advances in the characterization of the polarity of DOM under ambient water quality conditions using the polarity rapid assessment method. *Water Sci. Technol. Water Supply*, **8**(6), 725–733.

[45] X. Liao (2015). Applying the polarity rapid assessment method to characterize nitrosamine precursors and to understand their removal by drinking water treatment processes. *Water Res.*, **87**(July), 292–298.

[46] N. P. Sanchez, A. T. Skeriotis, and C. M. Miller (2013). Assessment of dissolved organic matter fluorescence PARAFAC components before and after coagulation e filtration in a full scale water treatment plant. *Water Res.*, **47**(4), 1679–1690.

[47] L. Guo, M. Lu, Q. Li, J. Zhang, Y. Zong, and Z. She (2014).Three-dimensional fluorescence excitation–emission matrix (EEM) spectroscopy with regional integration analysis for assessing waste sludge hydrolysis treated with multi-enzyme and thermophilic bacteria. *Bioresour. Technol.*, **171**, 22–28.

[48] Jean-Phillipe Croue, Gregory V. Korshin, Mark M. Benjamin, AWWARF (2000). Characterization of Natural Organic Matter in Drinking Water. American Water Works Association, Nature

[49] X. Yang, Z. Zhou, M. N. Raju, X. Cai, and F. Meng (2017). Selective elimination of chromophoric and fluorescent dissolved organic matter in a full-scale municipal wastewater treatment plant," *J. Environ. Sci. (China)*, **57**, 150–161.

[50] J. Boehme, P. Coble, R. Conmy, and A. Stovall-leonard (2004). Examining

CDOM fluorescence variability using principal component analysis : seasonal and regional modeling of three-dimensional fluorescence in the Gulf of Mexico. **89**, 3–14.

[51] K. R. Murphy, C. A. Stedmon, D. Graeber, and R. Bro (2013). Fluorescence spectroscopy and multi-way techniques. PARAFAC. *Anal. Methods*, **5** (23),6557.

[52] J. A. Korak, A. D. Dotson, R. S. Summers, and F. L. Rosario-ortiz, (2013). Critical analysis of commonly used fluorescence metrics to characterize dissolved organic matter. *Water Res.*, **49**, 327–338.

[53] R. K. Henderson, A. Baker, K. R. Murphy, A. Hambly, R. M. Stuetz, and S. J. Khan (2009). Fluorescence as a potential monitoring tool for recycled water systems : A review. *Water Res.*, **43**(4), 863–881.

[54] M. Bieroza, A. Baker, and J. Bridgeman (2011). Exploratory analysis of excitation – emission matrix fluorescence spectra with self-organizing maps — A tutorial. *Educ. Chem. Eng.*, **7**, (1), 22–31.

[55] U. J. Wünsch, K. R. Murphy, and C. A. Stedmon (2015). Fluorescence Quantum Yields of Natural Organic Matter and Organic Compounds : Implications for the Fluorescence-based Interpretation of Organic Matter Composition. *Front. Mar. Sci.*, **2**(November), 1–15.

[56] W. H. Mcdowell (2006). A comparison of methods to determine the biodegradable dissolved organic carbon from different terrestrial sources. *Soil. Bio. Biochem*.,**38**(7), 1933–1942.

[57] L. G. Terry and R. S. Summers (2018). Biodegradable organic matter and rapid-rate bio fi lter performance : A review. *Water Res.*, **128**, 234–245.

[58] C. J. Volk, A. Reserche, C. Gcncrale, M. Laffitte, C. B. Volk, and L. A. Kaplan (1997). Chemical composition of biodegradable dissolved organic matter in streamwater.*Limnol. Oceonogr.*, **42**(l), 39–44.

[59] T. I. Nkambule, R. W. M. Krause, J. Haarhoff, and B. B. Mamba (2012). A

three step approach for removing organic matter from South African water sources and treatment plants. *Phys. Chem. Earth*, **50–52**,132–139.

[60] J. Van Leeuwen, C. Chow, R. Fabris, N. Withers, D. Page, and M. Drikas, (1998). Application of a fractionation technique for better understanding of the removal of natural organic matter by alum coagulation. *Water Supply*., **2**(5-6), 427–433.

[61] M. Vital, D. Stucki, T. Egli, and F. Hammes (2010). Evaluating the growth potential of pathogenic bacteria in water. *Appl. Environ. Microbiol.*,**76** (19), 6477–84.

[62] M. Zhou, Z. Zhou, and F. Meng (2017). Using UV – vis spectral parameters to characterize the cleaning e ffi cacy and mechanism of sodium hypochlorite (NaOCl) on fouled membranes. *J. Memb. Sci.*, **527**(September) 18–25.

[63] J. L. Maldonado and J. L. Pichardo-molina (2007). UV – vis absorption spectroscopy and multivariate analysis as a method to discriminate tequila. *Spec. Acta*., **66**(1), 129–134.

[64] F. J. Rodríguez, P. Schlenger, and M. García-valverde (2016). Monitoring changes in the structure and properties of humic substances following ozonation using UV – Vis , FTIR and 1 H NMR techniques. *Sci. Total Environ.*, **541**, 623–637.

[65] D. J. Dryer, G. V Korshin, A. Heitz, and C. Joll (2008). Characterization of proton and copper binding properties of natural organic matter from an Australian drinking water source by differential absorbance spectroscopy. *Water Supply.,* **8**(6), 611–614.

[66] D. J. Dryer, G. V. Korshin, and M. Fabbricino (2008). In situ examination of the protonation behavior of fulvic acids using differential absorbance spectroscopy. *Environ. Sci. Technol.*, **42**(17), 6644–6649.

[68] T. Pazderka and V. Kopeck. 2D correlation spectroscopy and its application

in vibrational spectroscopy using matlab computation of 2d spectra.

[69] T. Maqbool and J. Hur (2016). Changes in fluorescent dissolved organic matter upon interaction with anionic surfactant as revealed by EEM-PARAFAC and two dimensional correlation spectroscopy. *Chemosphere*, **161**, 190–199.

[70] J. Hur, K. Jung, and Y. Mee (2011). Characterization of spectral responses of humic substances upon UV irradiation using two-dimensional correlation spectroscopy. *Water Res.*, **45**(9), 2965–2974.

[71] B. Su, Z. Qu, X. He, Y. Song, and L. Jia (2016). Characterizing the compositional variation of dissolved organic matter over hydrophobicity and polarity using fluorescence spectra combined with principal component analysis and two-dimensional correlation technique. *Environ. Sci. Pollut. Res.*,**23**,9237–9244.

[72] B. Carlson, D. Reckhow, F. Rosario, and I. Suffet (2007). PRAM : Polarity Rapid Assessment Method. 8–10.

[73] U. J. Wu, K. R. Murphy, and C. A. Stedmon (2017). The One-Sample PARAFAC Approach Reveals Molecular Size Distributions of Fluorescent Components in Dissolved Organic Matter. *Environ. Sci. Technol*., **51**(20), 11900-11908

[74] B. Aftab and J. Hur (2017). Fast tracking the molecular weight changes of humic substances in coagulation / flocculation processes via fluorescence EEM-PARAFAC. *Chemosphere*, **178**, 317–324.

[75] V. A. Online, K. R. Murphy, C. A. Stedmon, P. Wenig, and R. Bro (2014). Analytical Methods OpenFluor – an online spectral library of auto- fl uorescence by organic compounds in the environment. *Anal. Methods* **6**(3), 658–661.

[76] J. Haarhoff, B. Mamba, R. Krause, and S. Van Staden (2013). Natural Organic Matter in Drinking Water Sources : Its Characterisation and

Treatability, no. 1883. NOM WRCreport.

[77] I. Ivančev-Tumbas (2014). The fate and importance of organics in drinking water treatment: a review. *Environ. Sci. Pollut. Res.*, **21**(20), 11794–11810, 2014.

[78] L. Xing (2012). Characterization of organic matter in alum treated drinking water using high performance liquid chromatography and resin fractionation. *Chem. Eng. J.*, **192**, 186–191.

[79] M. C. Ncibi and A. Matilainen (2018). Removal of natural organic matter in drinking water treatment by coagulation : A comprehensive review. Chemosphere., **190**, 54–71.

[80] P. Jarvis (2004). The Impact of Natural Organic Matter on Floc Structure. PhD Thesis, Cranfield University.

[81] Z. Su, T. Liu, W. Yu, X. Li, and N. J. D. Graham (2017). Coagulation of surface water: Observations on the significance of biopolymers. *Water Res.*, **126**, 144–152.

[82] J. P. Ritson, N. J. D. Graham, M. R. Templeton, J. M. Clark, R. Gough, and C. Freeman (2014). The impact of climate change on the treatability of dissolved organic matter (DOM) in upland water supplies: A UK perspective. *Science of the Total Environment*, 473–474.

[83] C. S. Uyguner-Demirel and M. Bekbolet (2011). Significance of analytical parameters for the understanding of natural organic matter in relation to photocatalytic oxidation. *Chemosphere*, **84**(8), 1009–1031.

[84] J. Awad, J. Van Leeuwen, J. Liffner, C. Chow, and M. Drikas (2016). Treatability of organic matter derived from surface and subsurface waters of drinking water catchments. *Chemosphere*, **144**, 1193–1200.

[85] S. S. Marais, E. J. Ncube, T. A. M. Msagati, J. Haarhoff, T. I. Nkambule, and B. B. Mamba (2015). Investigation of natural organic matter (NOM) character and its removal in a chlorinated and chloraminated system at

Rand Water, South Africa. *Water Supply*., **17**(5), 1287-1297

[86] M. Clements (2002). Granular Activated Carbon Management At a Water Treatment Plant. MSc Dissertation, University of Johannesburg.

[87] S. Metsämuuronen, M. Sillanpää, A. Bhatnagar, and M. Mänttäri (2014). Natural Organic Matter Removal from Drinking Water by Membrane Technology. *Sep. Purif. Technol.*,**43**(July),1–61.

[88] A. Grefte, M. Dignum, E. R. Cornelissen, and L. C. Rietveld (2013). Natural organic matter removal by ion exchange at different positions in the drinking water treatment lane. *Drink. Water Eng. Sci.*, **6**(1),375-400.

[89] H. C. Kim, J. H. Hong, and S. Lee (2006). The fouling of ultrafiltration membranes by natural organic matter after chemical coagulation treatment with different initial mixing conditions. *Water Supply*., **6**(4) 17–124.

[90] M. M. Motsa, B. B. Mamba, and A. R. D. Verliefde (2015). Combined colloidal and organic fouling of FO membranes: The influence of foulant–foulant interactions and ionic strength. *J. Memb. Sci.*, **493**, (July), 539–548.

[91] R. Shang *(2015).* Hydraulically irreversible fouling on ceramic MF / UF membranes : Comparison of fouling indices , foulant composition and irreversible pore narrowing. *Sep. Purif. Technol.*,**147**, 303–310.

[92] H. Song, J. Shao, Y. He, J. Hou, and W. Chao (2011). Natural organic matter removal and flux decline with charged ultrafiltration and nanofiltration membranes. *J. Memb. Sci.*, **376**(1–2), 179–187.

[93] B. Tylkowski and I. Tsibranska (2015). Overview of main techniques used for membrane characterization. *J. Chem. Technol. Metall.*, **50**(1), 3–12.

[94] M. M. Pendergast and E. M. V. Hoek (2011). A review of water treatment membrane nanotechnologies. *Energy Environ. Sci.*,**4**(6),1946.

[95] R. Shang, A. Goulas, C. Y. Tang, X. de Frias Serra, L. C. Rietveld, and S. G. J. Heijman (2017). Atmospheric pressure atomic layer deposition for tight

ceramic nanofiltration membranes: Synthesis and application in water purification. *J. Memb. Sci.*, **528**(January),163–170.

[96] A. I. Schäfer (1999). Natural Organics Removal Using Membranes.

[97] Q. Li and M. Elimelech (2003). Natural organic matter fouling and chemical cleaning of nanofiltration membranes. *Wat. Sci. Tech: Water Supply*., **4**(5), 245–252.

[98] J. Brame, M. Long, Q. Li, and P. Alvarez (2015). Inhibitory effect of natural organic matter or other background constituents on photocatalytic advanced oxidation processes: Mechanistic model development and validation. *Water Res.*, **84**(August), 362–37.

[99] J. Kim, S. H. R. Davies, M. J. Baumann, V. V Tarabara, and S. J. Masten, (2008). Effect of ozone dosage and hydrodynamic conditions on the permeate flux in a hybrid ozonation – ceramic ultrafiltration system treating natural waters. J*. Memb. Sci*., **311**(1-2), 165–172.

[100] L. Song, B. Zhu, S. Gray, M. Duke, and S. Muthukumaran (2016). Hybrid Processes Combining Photocatalysis and Ceramic Membrane Filtration for Degradation of Humic Acids in Saline Water. *Membranes*., **6**(1)18

[101] M. Rajca (2016). Photocatalytic oxidation of natural organic matter enhanced with microfiltration and nanofiltration. *Desalin. Water Treat.*, **57**(3), 1132–1138.

[102] J. O. Tijani, O. O. Fatoba, G. Madzivire, and L. F. Petrik (2014). A review of combined advanced oxidation technologies for the removal of organic pollutants from water. *Water. Air. Soil Pollut.*, **225**(9), 2014.

[103] P. Tshindane (2019). Journal of Water Process Engineering The occurrence of natural organic matter in South African water treatment plants. *J. Water Process Eng.*, **31**(March),100809.

[104] N. Chaukura, N. G. Ndlangamandla, W. Moyo, T. A. M. Msagati, B. B. Mamba, and T. T. I. Nkambule (2018). Natural organic matter in aquatic

systems – a South African perspective. *Water SA*.,**44**(4), 624–635.

[105] S. S. Marais *(2017).* Natural organic matter (NOM) in south african waters volume i : nom fractionation , characterisation and formation of disinfection by-products by. WRC report.no. 2468.

[106] W. Moyo, N. Chaukura, T. A. M. Msagati, and B. B. Mamba (2019).The properties and removal efficacies of natural organic matter fractions by South African drinking water treatment plants. *J. Environ. Chem. Eng.*, **7**(3), 103101.

[107] Yue Zhang , Xinhua Zhao , Xinbo Zhang and Sen Peng (2015). A review of different drinking water treatments for natural organic matter removal. Water Supply., **15**(3), 442–455.

[108] Z. Dlahla (2013). The Effect Of Natural Organic Matter On Ultrafiltration And Reverse Osmosis Membrane Performance At Komati Power Station. MSc Dissertation, University of Pretoria.

[109] H. Wang, A. A. Keller, and F. Li (2010). Natural Organic Matter Removal by Adsorption onto Carbonaceous Nanoparticles and Coagulation. *J. Environ. Eng.*,(October),1075–1081.

[110] G. S. Wang and S. T. Hsieh (2001).Monitoring natural organic matter in water with scanning spectrophotometer. *Environ. Int.*, vol. **26**(4), 205–212.

[111] U. Mueller, G. Biwer, and G. Baldauf (2010). Ceramic membranes for water treatment. *Wat. Sci. Tech*: *Water Supply*., **10**(6),987–994.

[112] J. Malzbender (2016). Mechanical aspects of ceramic membrane materials," *Ceramics International*, **42**(7), 1.

[113] M. Kabsch-korbutowicz and A. Urbanowska (2010). Water Treatment in Integrated Process Using Ceramic Membranes," Polish J. of Environ. Stud, **19**(4),731–737.

[114] S. G. Lehman, S. Adham, and L. Liu (2008). Performance of new

Generation Ceramic Membarnes using Hybrid Coagulation Pretreatment. *J. Environ. Eng. Manag.*, **18**(4), 257–260.

[115] Observatory Nano (2011). Nanoenhanced membranes for improved water treatment briefing no.16 environment. (16), 1–4.

[116] B. Hofs, J. Ogier, D. Vries, E. F. Beerendonk, and E. R. Cornelissen (2011). Comparison of ceramic and polymeric membrane permeability and fouling using surface water. *Sep. Purif. Technol.*, 79(3), 365–374.

[119] R. Liu, T. Xu, and C. an Wang (2015). A review of fabrication strategies and applications of porous ceramics prepared by freeze-casting method. *Ceram. Int.*, **42**(2), 2907–2925.

[120] Z. Schimmer and Schwarz (2000). Additives for the Optimisation of the Pressure-Casting Process. *Keramische Zeitschrift*, 1–10.

[121] L. Oligny, P. R. Bérubé, and B. Barbeau (2016). Impact of PAC Fines in Fouling of Polymeric and Ceramic Low-Pressure Membranes for Drinking Water Treatment. *Membranes* **6**(3), 38 no. 2012.

[122] D. Zheng, R. C. Andrews, S. A. Andrews, and L. Taylor-Edmonds (2015). Effects of coagulation on the removal of natural organic matter, genotoxicity, and precursors to halogenated furanones. *Water Res.*, vol. 70, pp. 118–129, 2015.

[123] J. M. Benito, M. J. Sánchez, P. Pena, and M. A. Rodríguez (2007). Development of a new high porosity ceramic membrane for the treatment of bilge water," *Desal.*, **214**(1–3),91–101.

[124] I. Gonzalo-Juan (2012). Synthesis and dispersion of yttria-stabilized zirconia (YSZ) nanoparticles in supercritical water. *Mater. Chem. Phys.*, **134**(1), 451–458.

[125] T. O. Mahlangu, E. M. V Hoek, B. B. Mamba, and A. R. D. Verliefde (2014). Influence of organic, colloidal and combined fouling on NF rejection of NaCl and carbamazepine: Role of solute-foulant-membrane interactions and

cake-enhanced concentration polarisation. *J. Memb. Sci.*, **471**(July), 35–46.

[126] K. Kim and A. Jang (2016). Fouling characteristics of NOM during the ceramic membrane microfiltration process for water treatment. *Desalin. Water Treat.*, **3994**(December),1–9.

[127] T. O. Mahlangu, J. M. Thwala, B. B. Mamba, A. D'Haese, and A. R. D. Verliefde (2015). Factors governing combined fouling by organic and colloidal foulants in cross-flow nanofiltration. *J. Memb. Sci.*, **491**(July), 53–62.

[128] H. C. Kim and B. A. Dempsey (2013). Membrane fouling due to alginate, SMP, EfOM, humic acid, and NOM. *J. Memb. Sci.*, **428**, 2013.

[129] D. R. Ã, M. Rodrı, M. Leo, and D. Prats (2008). Removal of natural organic matter and THM formation potential by ultra- and nanofiltration of surface water. Wat. Res. **42**(3), 714–722.

[130] H. Yu (2015). Understanding ultrafiltration membrane fouling by soluble microbial product and effluent organic matter using fluorescence excitation-emission matrix coupled with parallel factor analysis. *Int. Biodeterior. Biodegrad.*, **102**, 2015.

[131] H. Budman (2010). Identifying fouling events in a membrane-based drinking water treatment process using principal component analysis of fluorescence excitation-emission matrices. *Water Res.*, **44**(1), 185–194.

[132] L. De Angelis, M. Marta, and F. De Cortalezzi (2013). Ceramic membrane filtration of organic compounds : Effect of concentration , pH , and mixtures interactions on fouling. *Sep. Purif. Technol.*, **118**, 762–775.

[133] X. Zhang (2014). Characterisation and Mitigation of the Fouling of Ceramic Microfiltration Membranes Caused by Algal Organic Matter Released from Cyanobacteria. MSc Thesis, RMIT University..

[134] W. Yu, T. Liu, J. Crawshaw, T. Liu, and N. Graham (2018). Ultrafiltration and nanofiltration membrane fouling by natural organic matter: Mechanisms and

mitigation by pre-ozonation and pH. *Water Res.*, **139**(August), 353-362.

[135] J. Xing (2018). Combined effects of coagulation and adsorption on ultrafiltration membrane fouling control and subsequent disinfection in drinking water treatment. *Environ. Sci. Pollut. Res.*, **26**, 1–11.

[136] Z. Song, M. Fathizadeh, Y. Huang, K. Hoon, and Y. Yoon (2016). TiO 2 nano fi ltration membranes prepared by molecular layer deposition for water puri fi cation. J. Memb. Sci., **510** (July). 72–78.

[137] P. Puhlfürß, A. Voigt, R. Weber, and M. Morbé (2000). Microporous TiO 2 membranes with a cut off < 500 Da. J. Memb. Sci., **174** (1) 123–133.

[138] S. P. Cardoso, I. S. Azenha, Z. Lin, I. Portugal, A. E. Rodrigues, and C. M. Silva (2017). Inorganic Membranes for Hydrogen Separation. *Sep. Purif. Rev.*, **47**(3), 1–38.

[139] L. Zheng, H. Li, T. Xu, F. Bao, and H. Xu (2016). Defect size analysis approach combined with silicate gel/ceramic particles for defect repair of Pd composite membranes. *Int. J. Hydrogen Energy*., **41**(41), 18522–18532.

[140] D. Korelskiy, P. Ye, H. Zhou, J. Mouzon, and J. Hedlund (2014). Reprint of: An experimental study of micropore defects in MFI membranes. *Microporous Mesoporous Mater.*,**192**, 69–75.

[141] D. Koutsonikolas, S. Kaldis, G. P. Sakellaropoulos, M. H. Van Loon, R. W. J. Dirrix, and R. A. Terpstra (2010). Defects in microporous silica membranes: Analysis and repair. *Sep. Purif. Technol.*,**73**(1), 20–24.

[142] D. Koutsonikolas, S. Kaldis, and G. P. Sakellaropoulos (2009). A low-temperature CVI method for pore modification of sol-gel silica membranes. *J. Memb. Sci.*, **342**(1–2), pp. 131–137.

[143] K. H. Kim, P. G. Ingole, and H. K. Lee (2017). Membrane dehumidification process using defect-free hollow fiber membrane. *Int. J. Hydrogen Energy*, **42**(38), 24205–24212, 2017.

[144] J. Yu, J. Zhang, C. Bao, H. Li, H. Xu, and J. Sun (2017). Confined and in-situ zeolite synthesis: A novel strategy for defect reparation over dense Pd membranes for hydrogen separation. *Sep. Purif. Technol.*, **184**, 43–53.

CHAPTER 3*:*

EXPERIMENTAL METHODOLOGY

3.1 INTRODUCTION

This chapter provides detailed descriptions of experimental procedures conducted in order to fulfill the objectives of this study.

3.2 SAMPLING

Samples were abstracted in triplicates after each water treatment step using clean 1 L glass bottles which had Teflon-lined screw caps. Samples were collected at each point of the treatment train, and suitable sample collection methods were used. For example, for collection of the samples, a 1L bucket was either hooked to a rod or rope or the sample was simply scooped or collected from a sampling tap located at designated parts of the water treatment train. Prior to collection of each water sample, specific care was taken for the sample container to be rinsed at least three times with the targeted water sample. Samples for membrane research work were collected in 25 L plastic containers.

3.3 SAMPLING SITES

Sample collection was carried out at eleven water treatment plants, which represent the five water quality regions of South Africa, the sixth water quality region was left out due to logistical and budgetary constraints (**Figure 3.1**). The water treatment plants located in the first water quality regions that were selected for this study are Ebenezer (EB), Flag Boshielo (FB) and Olifantspoort (OL) plants. These inland plants, which are operated and managed by Lepelle Northern Water Company, supply potable water to the entire province of Limpopo including its farming and mining communities. NOM found in this region is impacted by agricultural and mining activities due to surface runoff in combination with other catchment dynamics.

The plants located in the second water quality region were Rietvlei (RV) and Midvaal (MV) water treatment plants. RV is operated by the Tshwane Municipality and has a maximum treatment output of 42 ML/day, and the treatment processes involve coagulation/flocculation using a combination of ferric sulphate and a

commercial organic flocculant with pH correction using lime, followed by dissolved air floatation filtration (DAFF) through sand beds, and finally chlorination. While MV in addition to those treatment steps of RV also employs advanced methods such as pre and post ozonation. RV is located in a metropolitan region, therefore its sources of pollution that impact the nature of NOM are mainly anthropogenic activities. MV is located in the mining regions of the North West province of South Africa. This region is mainly a surface and subsurface mining area; therefore the character of NOM is greatly affected by mining activities due to acid mine drainage, metal contamination, and increased sediment levels in streams.

The treatment plants located in the third water quality region, which were selected for this study, are Mtwalume (MT), Amanzimtoti (AM), Umzinto (UM) and Hezelmere (HL). Although located in the eastern part of the country and operated by the Umgeni Water Company, these coastal plants and supply potable water to the greater KwaZulu Province and specific parts of the Eastern Cape Province. The relatively pristine source water for these coastal plants emanate from the highlands of Lesotho [1]. Commercial sugarcane plantations found in this region tend to influence the type of NOM reaching the plants due to surface runoff.

Plants located in fourth and fifth water quality types are located in the south east coast water quality region of the country. These plants are: Preekstoel (H) and Plettenburg Bay (P) water treatment plants, respectively, which are operated by Veolia Water Company and the local municipality, respectively. These water treatment plants are located in regions which experiences episodes of extended droughts. Unlike the rest of the country, the south east coastal plants experience a hot and dry summer seasons similar to Mediterranean climate, mild to warm spring and autumn seasons and rainy winter seasons [2]. Thus, NOM found in this region is greatly influenced by climatic conditions.

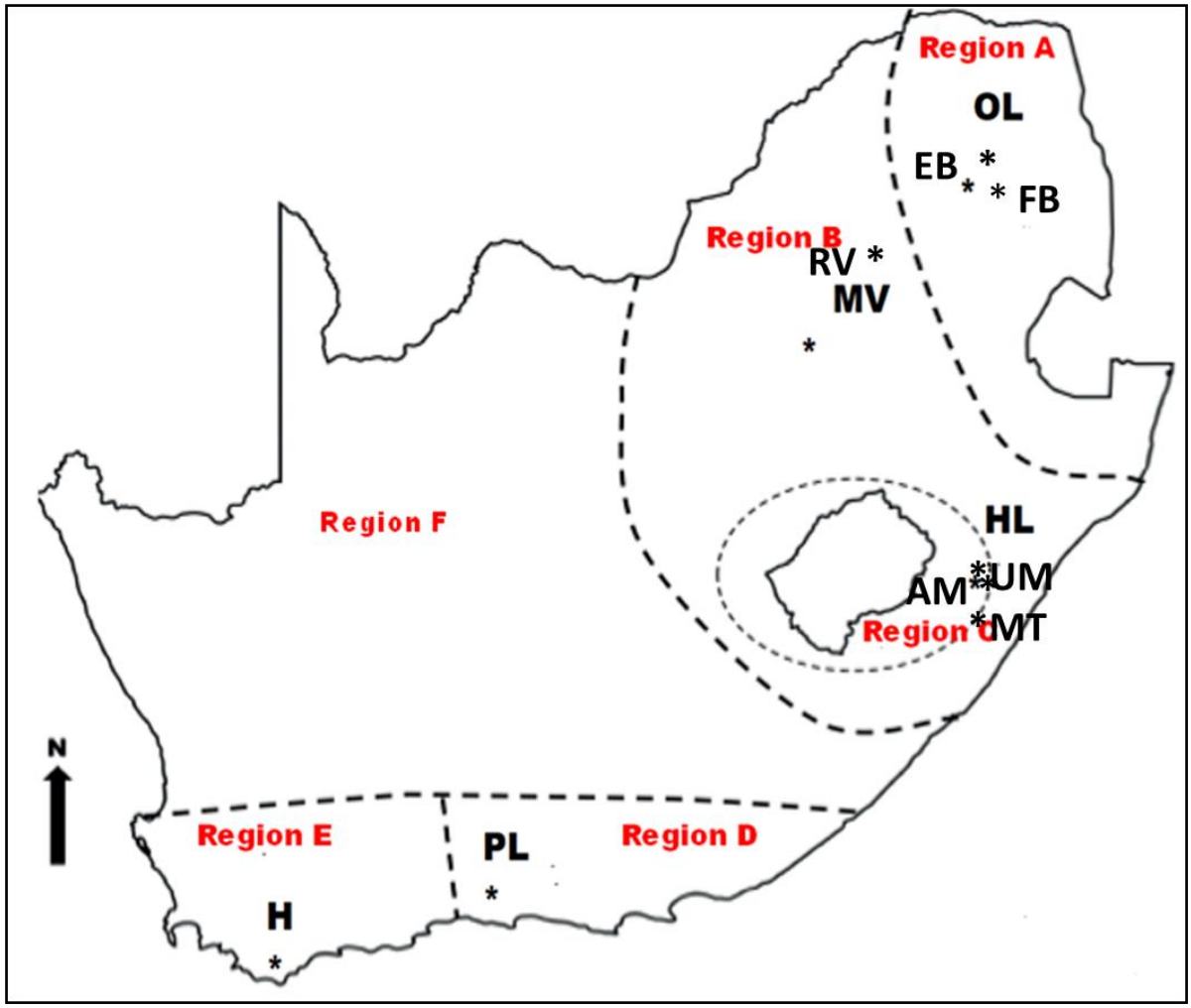

Figure 3. 1: The location of the sampled water treatment plants within the water quality regions of South Africa.

3.4 QUANTITATIVE (BULK) NOM CHARACTERIZATION

Basic water quality parameters such as pH, conductivity and turbidity were measured on site. Chemical parameters such as pH are important because they can be used for determining the morphology of NOM. Whereas NOM tends to acquire a compact morphology at low pH, it generally has a linear morphology at higher pH. This information is particularly important for water treatment plants that use membrane technology since the morphology determines the mechanism and ultimately the extent of membrane fouling. Additionally, pH plays an important role when determining the optimal coagulant required for the removal of NOM.

Another important parameter for assessing the viability of membrane technologies is conductivity. Conductivity is an indirect measure of ionic strength (IS), which determines electrical activity of the water. At high IS, NOM assumes a coiled morphology and at low IS, NOM assumes a linear morphology [3]. Further, turbidity was measured onsite, turbidity is an indicator of the quantity of colloidal and particulate matter in a sample and is the primary determinant of the coagulant demand when turbidity is very high. The treatment conditions of the sampled plants are summarised in **Table 3.1**.

Table 3. 1: Treatment conditions of sampled treatment plants

Raw		Coagulation		Clarification			Filtration		Disinfection		Finished Water
Sample	**Source**	**Type**	**Dosage**	**Basin**	**DAF**	**DAFF**	**RSF**	**DAFF**	**Type**	**Dosage**	
EB	Ebenezer Dam	Polymer U3800	0.5 mg/l				X		Chlorine	1.02 mg/l	51.41 ML/d
OL	Lepelle River	Polymer 3456	4 mg/l	X			X		Chlorine	2.19 mg/l	65.66 ML/d
FB	Flag Bosheilo Dam	Polymer U38100	144 mg/l	X			X		Chlorine	1.9 mg/l	11 ML/d
UM	Umzinto River E.J Smith Dam	Zeta floc 553	4 mg/l	X			X		Chlorine	0.17 mg/l	13.97 ML/d
AM	Nungwane Dam	Polymer U3500	8.55 mg/l	X			X		Chlorine	1.7 mg/l	6.7 ML/d
HL (New plant)	Hezelmere River	Polymer 3.3 mg/l		X			X		Chlorine 1.5 mg/l		4.3 ML/d
HL (Old plant)				X			X				
MT	Mthwalume River	Zeta-floc	4.6 mg/l	X			X		Chlorine	1.5 mg/l	9.43 ML/d
H	Debose Dam	Alum	0.061 g/l	X			X		Chlorine	4 mg/l	11 ML/d
H	**Borehole:** (Out of Commission)			X			**Iron Filter:** **Manganese Filter:**		Chlorine		
P	**Keurbooms River**	SUD-floc	0.006 g/l		X		X		Chlorine	0.6 mg/l	

3.5 LABORATORY ANALYSIS AND CHARACTERIZATION

Sample analysis was undertaken within 72 hours after collection. No chemical preservatives where used because of their contribution to the alteration of the chemical composition of NOM. Parameters such as DOC, UV_{254}, FEEM, SUVA, PRAM and BDOC procedures are discussed individually in the sub-sections that follow.

3.5.1 Dissolved Organic Carbon (DOC)

Prior to analysis, samples were filtered with a 0.45 µm GF/F filter. Thereafter, the a total organic carbon (TOC) analyser (Teledyne Tekmar, TOC combustion) was used to analyse the DOC of the samples. Hydrogen phthalate (KHP) standards of concentrations ranging from 1, 5, 10, 20 to 30 mg/L were used to calibrate the instrument. DOC measurement was carried out in triplicates. Removal efficacies of respective treatment stages were quantified as the percentage DOC reduction after the various treatment steps (i.e. coagulation, sedimentation, sand filtration and disinfection). The membrane rejection of DOC (r_{DOC}) was calculated **(Equation 3.1)** [5]:

$$r_{DOC} = \frac{\left(C_0 - C_p\right)}{C_0} \qquad (3.1)$$

where, C_0 is initial *DOC* concentration in the raw water feed, and C_p is the concentration of *DOC* in the permeate.

3.5.2 Fluorescence and Ultraviolet Absorbance at 254 nm (UV_{254})

After temperature stabilization at 25 ^{o}C, the samples were passed through 0.45 µm GF/F filters before analysis. A fluorescence spectrometer (Aqualog, HORIBA, Jobin Yvon) was used to measure EEMs, simulated SFS at Δλ = 60 nm and UV-Vis absorbance spectra in the wavelength range 200 – 800 nm. The excitation interval was set at 2 nm while the emission interval was set at 3.28 nm, respectively, and emission was recorded in the wavelength range 248.58-830.59 nm. The area under the peak was obtained by exciting the Raman water standard at 350 nm and measuring the emission between 248.58 - 830 nm [34]. Raman units (RU) were obtained by conversion using the area under the peak of the reference Raman water sample. Ultraviolet absorbance at λ = 254 nm (UV_{254}) measurements were performed on the NOM fractions

(hydrophobic (HPO), hydrophilic (HPI), transhpilic (TPI)) obtained after the modified polarity rapid assessment method (mPRAM).

3.5.3 Specific Ultraviolet Absorbance (SUVA)

SUVA is the quotient of DOC and UV_{254} (**Equation 3.2**). SUVA is an indicator of the hydrophobicity of a sample and it is used to determine the relative amount of humic substances present in organic matter relative to non-humic substances [4]. Whereas SUVA values greater than 4 $L.mg^{-1}.m^{-1}$ indicate NOM of a hydrophobic nature, SUVA values in the range of 2 to 4 $L.mg^{-1}.m^{-1}$ indicate transphilic NOM. Any SUVA values that are less than 2 $Lmg^{-1}m^{-1}$ are indicative of NOM that is hydrophilic in nature [4].

$$SUVA(L/mg.m) = \frac{UV_{254}(cm^{-1})}{DOC(mg/L)} \times 100 \quad (3.2)$$

3.5.4 Polarity Rapid Assessment Method

The m-PRAM method was used to fractionate NOM into 3 fractions, namely; TPI, HPO and HPI following a method by Nkambule et al. (2012)[3]. Briefly, a vacuum pump operated at 5 inches Hg, 0.1 bar was connected to a 24 position vacuum manifold (Sigma Aldrich, Germany) equipped with 20 mL glass vials for collecting the filtrate. Solid phase extraction (SPE) cartridges (i.e., NH_2 (weakly anionic), C18 (non-polar) and CN (polar)), each of 6 mL volume and 500 mg size were placed on the vacuum manifold and operated in series to collect the TPI, HPO and HPI, respectively. Quality assurance for reproducible results was guaranteed by allowing sufficient clean-up of the cartridges to eliminate carbon leaching. Firstly, Methanol (15 mL) was passed through each cartridge at a rate of 1 ml/s until a methanol head of about 1-2 mm. Secondly, loosely bound organic matter and residual methanol was washed off using 500 mL deionized water in 100 mL aliquots until a constant UV_{254} absorption was obtained. Water samples (20 mL) were introduced into the cartridges placed in series in the order C18, CN and NH_2, respectively. The permeate of the first cartridge was introduced into the second cartridge and in turn the permeate thereof was then introduced into the third cartridge. The elution of the HPI and HPO was achieved by filtrating 0.1 M NaOH (10 mL) through

the CN and C18 cartridges, respectively. The fraction not retained by the NH_2 cartridge was designated the TPI fraction.

3.5.5 Biodegradable Dissolved Organic Carbon

DAFF beds at the WTP were sampled for an inoculum heterotrophic bacterium contained in the biologically active sand (BAS). The sand was washed in 0.1 M sodium thiosulphate to remove excess carbon. The sand sample was further rinsed with deionized water. The supernatant was then analyzed for UV254, DOC and fluorescence, and the data obtained used as the baseline. The washed sand (100 g) was placed in 500 mL Erlenmeyer flasks, to which 300 mL of water sample was added and covered with aluminum foil. Glucose solutions of concentrations 5, 8, and 10 mg/L, respectively were used as control. Both samples and control were kept in the dark for 5 days in an incubated water bath at 22˚C, and daily measurements of UV254, DOC and fluorescence were obtained.

3.5.6 Sulphuric acid-UV Absorbance Method for Polysaccharide Quantification

A modified method reported by Albalasmeh (2013)[38] for the measurement of polysaccharides was used. In brevity, 3 mL of 95 % sulphuric acid was added to 1 mL aliquot of sample from the feed and permeates of respective membranes. The samples were then vortexed for 30 s and UV absorbance was measured using a UV-Vis spectrophotometer (Lambda 650S, Perkin Elmer). Known concentrations of glucose were used as calibration standards. The peak area was assumed to be proportional to the sum of biopolymer derivatives absorbing in that region.

3.6 MODELING TECHNIQUES EMPLOYED TO TRACK NOM COMPOSITION AND DYNAMICS

3.6.1 Log-Transformed Absorbance Spectrum

The Naperian form of absorbance data was obtained by determining the natural logarithm of the absorbance values (LnA) measured at respective treatment stages. The difference in LnA values of successive treatment stages was denoted as the differential log-transformed absorbance *(DLnA)* [5] (**Equation 3.3**):

$$DLnA(\lambda_i) = LnA_{i-1} - LnA_i(\lambda) \quad (3.3)$$

where, $A_{i-1}(\lambda)$ and $A_i(\lambda)$ are the absorbance intensities measured from samples from two successive treatment process at a wavelength of interest, respectively.

3.6.2 Fluorescence Regional Integration (FRI) of Removed Fractions

Five wavelength-dependent regions of the EEM spectrum representing specific components of NOM (i.e. tyrosine-like (TYL), tryptophan-like (TPL), fulvic-like (FL), microbial by-products like (MBP) and humic-like (HL)) were determined [7]. The volume under the respective region in the EEM map gives an indication of the quantity of the respective component (**Box 3.1**) [8].

$$\theta = \sum_{ex} \sum_{em} I(\lambda_{ex}\lambda_{ex})\Delta d\lambda_{ex}\Delta d\lambda_{em}$$

$$\theta_{Tot,5} = \sum_{i=1}^{5} \theta i_{i,5}$$

$$P_{i,n} = \frac{\theta_{i,5}}{\theta_{Tot,5}} \times 100\%$$

Box 3.1: Equations used to determine the quantitative contribution of each region.

where θ_i denotes the volume bound by region *i* and $\theta_{Tot,5}$ is the sum of volume bound by all five regions; *n* denotes the respective region; and $P_{i,n}$ denotes the percentage contribution of the respective region *i*.

The components making up the BDOC fraction was determined by the application of the FRI method.

$$BDOC_{EEM} = EEM_{day1} - EEM_{day7} \quad (3.4)$$

3.6.3 PARAFAC Modelling

PARAFAC modelling was carried by the using the inbuilt SOLO software (Eigenvector Inc) contained in Aqualog instrument using the method described by Ndiweni et al. (2019) [4]. In brevity, PARAFAC is a modelling technique which relies on statistics to

decompose a dataset of EEMs into a residual array and a set of trilinear terms [4] (**Equation 3.5**):

The goodness of fit of the model to the experimental data and the maximum fluorescence intensities *(F_{max})* is obtained through alternating least squares regression procedure.

$$x_{ijk} = \sum_{f=1}^{F} a_{if} b_{jk} c_{kf} + e_{ijk} \qquad (\mathbf{3.5})$$

Where: k= 1……..K , i = 1……..I and j = 1……..J

The variable x_{ijk} is the *i*th sample denotes fluorescence intensity at excitation:emission wavelength pair (*k*:*j)*. The parameter a_{if} contained in the *i*th sample (score) is determined by the quantity of the *f*th fluorophore, and the emission:excitation spectrum of the *f*th fluorophore are given by the parameters b_{jk} and c_{kf}, respectively (loadings). The residual variables of model are denoted by the variable e_{ijk},, The sum of components making up the fluorophore is denoted by the variable *F*.

The model was fitted by using alternating least squares regression procedure. The number of components defining the EEM dataset of samples of unknown fluorophore composition was determined by the predefined goodness of fit [10]. According to Murphy et al. [10], the PARAFAC model is validated using a series of the following predetermined criteria: (1) Core consistency examination; (2) Spectral loading shape evaluation; (3) Contribution of the influence of specific sample or wavelengths on the leverage; (4) Analysis of the residual, and (5) The split half-criterion. After validation, the maximum fluorescence intensities (F_{max}) and distribution at each treatment stage was used to measure the efficacy of each treatment step in removing the particular component. In-depth information on the PARAFAC model can be accessed in accordance with a procedure by Murphy et al. [10].

3.6.4 Gaussian Fitting

Gaussian fitting using the PeakFit® software was used to deconvulate the UV-Vis spectrum to identify hidden peaks. The energy, intensity and location of the maxima of each Gaussian peak was used to characterize the efficiency of the treatment step. Previous research has revealed that the deconvulated peaks are Gaussian in nature when expressed in terms of the photon energy parameter shown in **Equation 3.4** [11].

$$E(eV) = \frac{1240}{\lambda}(nm) \qquad (2.2)$$

3.6.5 Two Dimensional Correlation Spectroscopy

The 2D-Shige software (Kwansei-Gakuin University, Japan) was used to track the rate of compositional variation of NOM as it was treated by the ceramic membranes. The SFS from the permeates from the membranes was inputted into the software and the order of MWCO of the membranes was the external perturbation producing the synchronous and asynchronous maps. Briefly, Noda's rules states that cross peaks can either be negative or positive while auto peaks are positive only. A positive cross peak in the synchronous spectra with the wavelength pair λ1/λ2 means changes occurring at λ1 and λ2 are concurrent or synchronous, whilst a negative cross peak of wavelength pair of λ1/λ2 in the synchronous spectra means changes occurring at λ1 and λ2 are inverse or asynchronous. Asynchronous spectra contains cross peaks only and a positive cross peak of λ1/λ2 wavelength pair means the pace of change occurring at wavelength λ1 is faster than that at λ2. While a negative cross peak of λ1/λ2 wavelength pair in the asynchronous spectra implies the changes happening at λ1 are slow paced than that at λ2.

3.6.6 Determination of Spectroscopic indices

Box 3.1 shows the equations used in the determination of spectroscopic indices: SUVA, freshness index *(β:α)*, humification index *(HIX)* and fluorescence index *(FI)*.

$$SUVA\left(\frac{L}{mg.m}\right)=\frac{UV_{254}\left(cm^{-1}\right)}{DOC\left(\frac{mg}{L}\right)}\times 100$$

$$HIX=\sum I_{435\to480}\Big/\left(\sum I_{300\to345}+\sum I_{435\to480}\right)$$

$$FI=Em_{470}/Em_{520}$$

$$\beta:\alpha=Em_{380}/\max\left(Em_{420\to435}\right)$$

Box 3.1: Spectroscopic indices for NOM characterisation

3.7 MODIFICATION AND CHARACTERISATION OF CERAMIC MEMBRANES FOR NOM FRACTION REMOVAL IN WATER.

3.7.1 Substrate Membranes

Commercial ceramic NF membranes purchased from TAMI, France, were used in these experiments. The membranes had a disc configuration of 90 mm diameter, 2.5 mm thickness, and an effective filtration area of 0.00563 m^2, with a porosity of 30% and MWCO of 450 Da (loose NF). The active and support layer of the as received membrane was made of TiO_2 and Al_2O_3, respectively. A field emission scanning electron microscope (JSM-IT300, JEOL, Oxford) with and energy dispersive X-ray (EDX) detector was used to analyse the surface morphology and elemental mappings of the membrane.

3.7.2 Contact angle and surface energetics

A sessile drop method was used to determine the contact angle (θ). In this method three liquids with well-characterized surface tension components, namely: Milli-Q water, diiodomethane and glycerol, were used. At least 10 drops per liquid was deposited on the membrane using a microlite syringe, from which the contact angle was determined (Fig. A5). The θ was then used to calculate surface tension and interfacial free energies of interactions. Briefly, the sum of the Liftshitz-van der Waals component (γ^{LW}) and Lewis acid–base components γ^{AB} ($\gamma^{AB} = 2\sqrt{(\gamma^+ \gamma^-)}$ with γ^+ and γ^- denote the electron

acceptor and electron donor, respectively was used to determine the total surface tension [37].

3.7.3 Membrane surface characterisation.

Surface topology was determined in air using an atomic force microscope (AFM) (Alpha300 microscope by WITEc Focus Innovations, Germany) in the non-contact mode (Fig. A6). Five different sites of dimensions 20 µm×20 µm on each membrane were scanned at a rate of 0.5 Hz and averaged. AFM height data and roughness were determined using the in-built Nanoscope software (Nanoscope 5.30 r3 sr3, Veeco Instruments, CA). A scanning electron microscope (JSM-IT300, JEOL, Tokyo, Japan) and an energy dispersive spectroscopy were used to analyse the surface morphology and elemental mappings of the membrane, respectively

3.7.4 Molecular Weight Determination

Unless stated otherwise, the purity of reagents used in this work was > 95 %, and all reagents were sourced from Sigma Aldrich, Germany. Polyethylene glycols (PEG) (0.6 g/L) of average molecular weights 200-1000 Da were prepared by dissolving PEG (18 g) in deionised water (30 L). A PEG feed solution was filtered through each membrane at room temperature at cross-flow mode and velocity of 1 ms^{-1} and at a constant trans-membrane pressure (TMP) of 3 bars.

MWCO was determined by analyzing the retention of PEG molecules from both the feed and permeate solutions using a high-performance liquid chromatography (HPLC) system (Shimadzu, Japan). The size exclusion chromatography (SEC) columns (5 µm 30 Å) coupled to the HPLC were obtained from PSS Polymer Standards Service GmbH, Germany. The rejection rate of PEG *(r_{PEG})* of a specific molecular weight were used to plot the retention curves (**Equation 3.7**) [3];[12]:

$$r_{PEG} = \frac{C_{feed} - C_{permeate}}{C_{feed}} \tag{3.7}$$

Where C_{feed} and $C_{permeate}$ are concentrations of PEG in the feed and permeate, respectively.

Thereafter, the log normal model was created by plotting MW vs. MWCO from the data of the experimental rejection curves (**Equation 3.8**) [12].

$$\sigma(MW_s) = \int_0^{MW_s} \frac{1}{S_{MW}\sqrt{2\pi}} \frac{1}{MW} \exp\left[\frac{-((In(MW) - In(MWCO) + 0.56S_{MW}))^2}{2S_{MW}^2}\right] \quad (3.8)$$

Where $\sigma\ (MW_S)$ denotes the reflection coefficient for a PEG of molecular weight MW_S, MW is the molecular weight distribution and its standard deviation is denoted by S_{MW}

Basing on the premise that the retention of PEG molecules is solely through steric exclusion with insignificant solute diffusion, the MWCO was taken to be the value at which 90% of PEGs are retained [3];[12].

3.8 FILTRATION EQUIPMENT SET UP AND OPERATION

3.8.1 Filtration Equipment

The filtration equipment consisted of a pump operated at 1100-1180 rpm (revolutions per minute) to circulate the feed. The membrane was housed in a circular disc module (TAMI, Germany), and the system was pressurized by altering the concentrate feed valve (**Figure 3.2**). The actual membrane filtration laboratory set up is shown in **Figure 3.3**. Measurements were run under a TMP of 3 bar and a feed flow of 175 L/h. After equilibration, membranes were conditioned for 5 min for deionised water permeability and 1 h for raw water permeability before sampling both the feed and permeate.

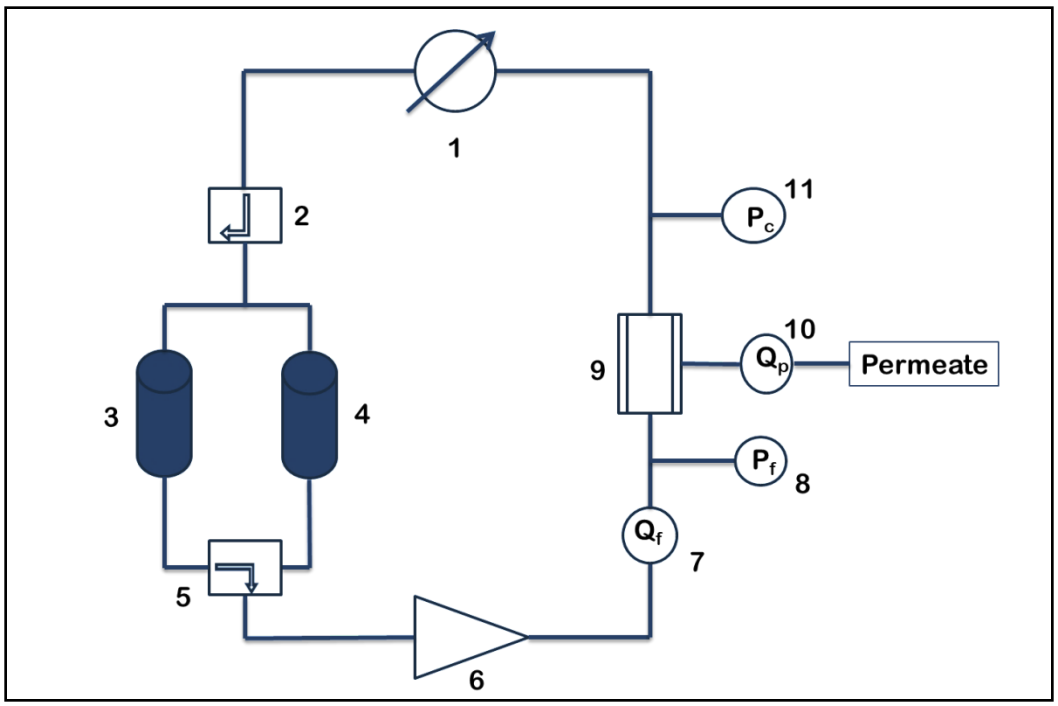

Figure 3. 2: The schematic layout of the filtration set up. The cross flow mode was maintained by opening the concentrate valve and equilibrating the TMP at 3 bars. (1-concentrate valve; 2-flow direction valve; 3-deionised water tank; 4-PEG/Feed water tank; 5-flow direction valve; 6-pump; 7-flow speed meter; 8-feed pressure meter, 9-membrane housing; 10-permeate pressure meter; 11-concerntrate pressure meter.)

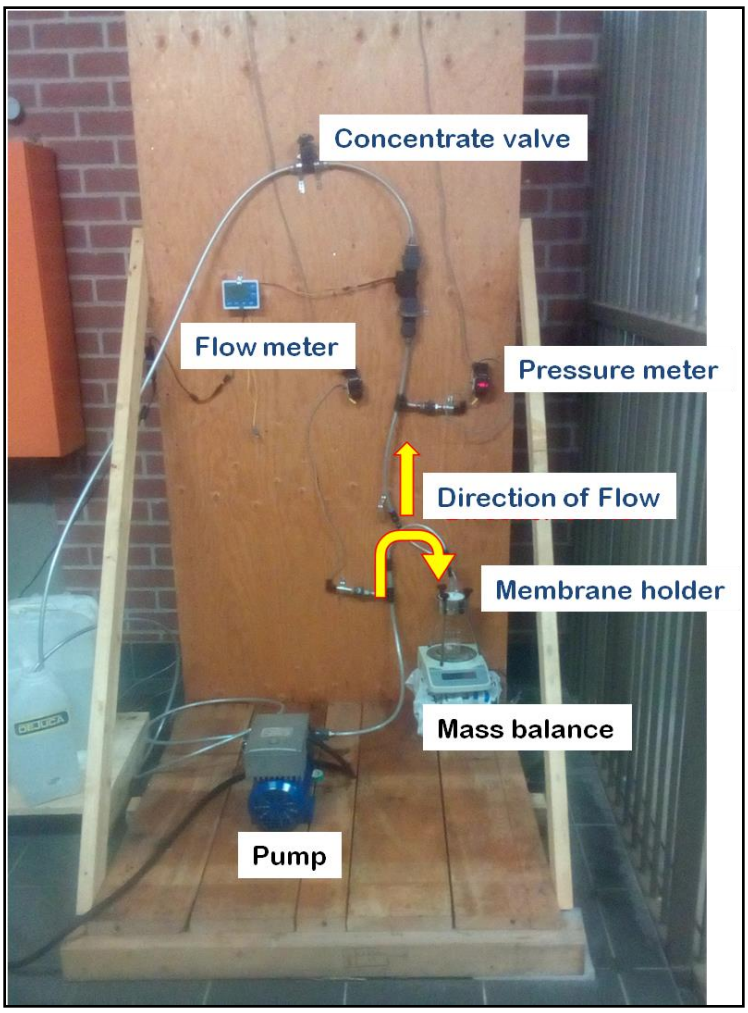

Figure 3. 3: Filtration set up in the laboratory

Membrane fluxes and water temperature were monitored. The flow rate was correlated to the sample mass, and the flux and temperature-corrected permeability were determined (**Box 3.2**)[12]:

$$v_s = \frac{(M_{SC} - M_C)}{(T_f \times 60)/1000}$$

$$\Delta P = \frac{P_f + P_c}{2}$$

$$J = \frac{v_s}{A}$$

$$L_{p,20^oC} = \frac{J}{\Delta P} \cdot \frac{\eta_T}{\eta_{20}} = \frac{J.e^{-0.0289.(T-20)}}{\Delta P}$$

Box 3.2: Mass flow equations

Where v_s is the flow rate, M_{sc} and M_c is the mass (g) of the sample container plus permeate sample and the mass (g) of the empty container respectively, T_f is the temperature of water *(^oC), ΔP* is the measured TMP (bar), P_f (bar) is the feed pressure and P_c (bar) is the concentrate pressure*, J* is the obtained membrane flux ($Lm^{-2}h^{-1}$), *A* is the effective membrane filtration area, $L_{p,20}{}^{o}{}_{C}$ is the permeability at 20 ^oC ($Lm^{-2}h^{-1}bar^{-1}$) and η_{20} and η_T are the permeate viscosities at 20 ^oC and at the measured water temperature, respectively.

3.8.2 Determination of Fouling Mechanisms

The fouling mechanisms were determined using the model equations in **Box 3.3**. The goodness of fit (R^2) of the plot of time (*t*) versus $\text{Ln}\left(\frac{J}{J_o}\right)$ in the first 2 hours was used as a measure of dominancy of complete blocking mechanism. The goodness of fit (R^2) in the first 2 hours of the plot of time (*t*) versus $\left(\frac{J_o}{J}\right)^{\frac{1}{2}} - 1$ was used as a measure of dominancy of standard blocking mechanism. The goodness of fit (R^2) between 2 to 4 hours of the plot of time (*t*) versus $\left(\frac{J_o}{J}\right) - 1$ was used as a measure of dominancy of intermediate blocking mechanism. The goodness of fit (R^2) in the last 2 hours of the plot of time (*t*) versus $\left(\frac{J_o}{J}\right)^{2} - 1$ was used as a measure of dominancy of cake filtration mechanism.

(1).	$J = J_0 e^{-At}$	$A = K_A u_0$
(2).	$J = \frac{J_0}{(1+Bt)^2}$	$B = K_B u_0$
(3).	$J = \frac{J_0}{(1+At)}$	
(4).	$J = \frac{J_0}{\sqrt{1+Ct}}$	$C = (2R_r)K_c u_0$

Box 3.3: Models to describe fouling mechanisms: (1) complete blocking, (2) standard blocking, (3) intermediate blocking, and (4) cake filtration, respectively.

where, J_0 and J are initial and final flux respectively; u_o average initial filtrate velocity; R_r denotes the resistance of cake filtration by the clean membrane; K_A denotes the quotient of the blocked membrane surface and volume of permeated water through the pores of the membrane; K_B denotes the extent of internal membrane pore area constriction due to particle deposition as a quotient total volume permeated; K_C denotes the quotient of permeated volume and membrane area.

3.9. REFERENCES

[1] T. I. Nkambule (2012). Natural Organic Matter (Nom) in South African Waters: Characterization of Nom, Treatability and Method Development for Effective Nom Removal From Water. PhD Thesis, University of Johannesburg.

[2] X. Booi (2013). Perfluorinated Compounds and Trihalomethanes in Drinking Water Sources of the Western Cape, South Africa. MSc Dissertation.

[3] N. Shamsuddin, D. B. Das, and V. M. Starov (2015). Filtration of natural organic matter using ultrafiltration membranes for drinking water purposes: Circular cross-flow compared with stirred dead end flow. *Chemical Engineering Journal*, **276**(August), 331–339.

[4] S.N Ndiweni, M Chys, C Nhamo, S. W.H van Hulle, T.T.I Nkambule (2019). Assessing the impact of environmental activities on natural organic matter in South Africa and Belgium. *Environmental Technology*, **40**(13), 1756-1768.

[5] P. Li and J. Hur (2017). Utilization of UV-Vis spectroscopy and related data analyses for dissolved organic matter (DOM) studies: A review. *Crit. Rev. Environmental Science and Technology*, **47**(3), 131–154.

[6] B. Hu (2017). The effect of anthropogenic impoundment on dissolved organic matter characteristics and copper binding af fi nity : Insights from fl uorescence spectroscopy. *Chemosphere*, **188**(1), 424–433.

[7] E. Ejarque (2017). Quality and reactivity of dissolved organic matter in a Mediterranean river across hydrological and spatial gradients. *Science of the Total Environment*., **600**,1802–1812.

[8] X. S. He (2013). Fluorescence excitation-emission matrix spectra coupled with parallel factor and regional integration analysis to characterize organic matter humification. *Chemosphere*, **93**(9), 2208–2215.

[9] K. R. Murphy, C. A. Stedmon, D. Graeber, and R. Bro (2013). Fluorescence

spectroscopy and multi-way techniques. PARAFAC. *Analytical Methods*, **5**(23), 6557.

[10] U. J. Wu, K. R. Murphy, and C. A. Stedmon (2017). The One-Sample PARAFAC Approach Reveals Molecular Size Distributions of Fluorescent Components in Dissolved Organic Matter. *Environmental Science and Technology*, **51**(20), 11900–11908.

[11] Z. Chen, M. Li, Q. Wen, and N. Ren (2017). Evolution of molecular weight and fluorescence of effluent organic matter (EfOM) during oxidation processes revealed by advanced spectrographic and chromatographic tools.*Water Research,* **124**, 566–575.

[12] R. Shang, A. Goulas, C. Y. Tang, X. de Frias Serra, L. C. Rietveld, and S. G. J. Heijman (2017). Atmospheric pressure atomic layer deposition for tight ceramic nanofiltration membranes: Synthesis and application in water purification. *Journal of Membrane Science*, **528**(January), 163–170.

CHAPTER 4*:...*

The properties and removal efficacies of natural organic matter fractions by South African drinking water treatment plants

---

4.1 INTRODUCTION

The effective removal of NOM has cost and environmental implications, hence the urgent need to track changes in its quality using real time monitoring techniques. This study explores spectroscopic approaches to shed more insight into NOM reactivity and treatability. Fluorescence spectroscopy is a robust tool for characterizing fluorescent dissolved organic matter (FDOM) in various natural and engineered aquatic systems [1]–[5]. Owing to its simplicity in application, EEM fluorescence spectroscopy has shown promise in the prediction of the removal of NOM during both conventional and advanced drinking water treatment processes [3], [6]–[8]. Coupled with chemometric methods such as parallel factor analysis (PARAFAC), 2D-correlation spectroscopy and fluorescence regional integration (FRI), EEMs have been used to identify NOM components and have thus provided further insight into the environmental dynamics of NOM in diverse aquatic ecosystems. In this chapter, the assessment of NOM using spectroscopic methods at source and the dynamics of NOM character changes throughout the treatment train using WTPs representative of the five water quality regions of South Africa are explored (*vide supra*).

This chapter is based on:

Moyo W, Chaukura N, Msagati T.A.M, Mamba B.B, Heijman S.J.G and Nkambule T.T.I (2019). The properties and removal efficacies of natural organic matter fractions by South African drinking water treatment plants. *Journal of Environmental Chemical Engineering*, **7**(3). doi.org/10.1016/j.jece.2019.103101

Moyo W, Motsa M.M, Chaukura N, Msagati T.A.M, Mamba B.B, Heijman S.J.G and Nkambule T.T.I . Monitoring the characteristics and removal of natural organic matter fractions in selected South African water treatment plants. *Water Practice and Technology* (Submitted: 02 May 2020)

4.2 MATERIALS AND METHODS

The research presented in this chapter is divided into two distinct phases. The first phase reports on the raw water characteristics of water collected from different parts of South Africa. The second phase discusses the efficacies of NOM treatment by unit processes from the respective water treatment plants of South Africa.

4.2.1 Sampling and Sample sites

Samples were collected from nine different water treatment plants spatially distributed throughout the five water quality regions of South Africa. Samples were collected using 1L Teflon capped glass bottles (**Section 3.2; Figure 3.1**). Sampling was carried out in triplicates at each major treatment stage, namely: disinfection, rapid sand filtration, coagulation/flocculation and raw (**Appendix A1**). Potable millimetres were used to measure conductivity, temperature, pH and turbidity. Immediately after sampling, the samples were couriered in ice boxes and upon arrival at the laboratory the samples were filtered using a 0.45 µm GF/F filters and analysed immediately. Samples or further analysis were stored at 4 ^{0}C before analysis within 48 h.

4.2.2 Bulk NOM Characterisation

UV, synchronous spectra, DOC and SUVA were analysed according to the method outlined in **sections 3.51; 3.52 and 3.53.**

4.2.3 Determination of biogenic NOM fraction

Section 3.5.6 describes in detail the method carried out in the determination of biogenic NOM fraction.

4.2.4 Modelling techniques

Section 3.6.1 describes the log-transformed absorbance spectra modelling technique for the determination of latent UV characteristics. **Section 3.6.2** describes the fluorescence regional integration method for the quantification of fluorescent NOM fractions removed by respective water treatment processes. **Section 3.6.3** describes the parallel factor analysis for the identification and quantification of fluorescent NOM fractions from a pool of data obtained from all the water sources under this study.

4.2.5 Determination of Spectroscopic indices

The determination of spectroscopic indices such as freshness index, fluorescence index and humification index is detailed in **section 3.56**

4.3 RESULTS AND DISCUSSION

4.3.1 Raw water characteristics

The mechanism of NOM removal from water by specific treatment processes is better elucidated when the chemistry and composition of NOM at source is delineated. DOC measurement is a bulk measurement method and is one of the main methods of explaining the nature and extent of NOM removal because such a measurement gives the amount of NOM as “carbon” in the sample. No further insight into the removal of specific or problematic fractions of NOM is obtained from such a measurement. Nevertheless, DOC analysis provides a starting point in any NOM studies because it gives a general overview of a particular treatment step ability to remove NOM (**Appendix A1**). Then again the nature of NOM at the source determines its removability by specific treatment steps.

4.3.2 Assessment of Conventional Parameters to Evaluate the Treatability of NOM at Source

Data on physico-chemical properties of NOM is key for the comprehension of its treatability. DOC values in the range 2.60-12.51 mg/L were found for source waters (**Table 4.1**) These values seem to be in agreement with previous research that suggests that the quantity and quality of NOM have spatial and temporal variability [10]. The measured DOC is what is detected as carbon dioxide after the photo-oxidation of carbon containing organic matter. Therefore, not all the natural sources of carbon are measured, and runoff of dyes, pesticides and synthetic polymers can potentially exaggerate the obtained values. Needless to say that further characterization of NOM found in surface water is necessary. NOM found in natural waters is the main light absorbing component in the visible range [11]. As expected, the coloured raw water laden with humic substances feeding plants H and P showed high UV_{254} absorbance (**Table 4.1**). Absorbances from non-humic substances with high *UV-Vis* absorbance such as inorganic compounds for example peroxides, nitrates, ammonium were also recorded on the full *UV* scans [11]. As a result, *UV* absorbance data in the region < 240

nm is excluded, and UV absorbance at 254 nm is instead used an as indicator for aromaticity [12].

Table 4. 1: Dissolved organic carbon and spectrophotometric parameters for raw water sources *(n=3)*

	C1	F_{max} (RU) C2	C3	C4	tCDOM (nm/cm)	a315 (/cm)	TotAbs / DOC (nm.mg/ L.cm)	SUVA (L/mg.m)	UV254 (/cm)	DOC (mg/L)
FB	0.010 ± 0.001	0.007 ± 0.0001	0.003 ± 0.0001	0.001 ± 0.0001	5.882 ± 0.9	0.514 ± 0.03	1.061 ± 0.08	1.692 ± 0.1	0.094 ± 0.001	5.544 ± 0.9
UM	0.009 ± 0.001	0.007 ± 0.0001	0.003 ± 0.0001	0.001 ± 0.0001	9.360 ± 0.8	0.578 ± 0.02	1.242 ± 0.07	1.872 ± 0.3	0.141 ± 0.001	7.535 ± 0.8
OL	0.009 ± 0.001	0.005 ± 0.0001	0.003 ± 0.0001	0.002 ± 0.0001	16.351 ± 1.2	0.497 ± 0.02	2.723 ± 0.07	3.018 ± 0.6	0.181 ± 0.002	6.005 ± 0.8
AM	0.005 ± 0.001	0.008 ± 0.0002	0.001 ± 0.0001	0.001 ± 0.0001	16.224 ± 1.1	0.638 ± 0.03	3.436 ± 0.09	3.896 ± 0.7	0.184 ± 0.002	4.721 ± 0.5
HL	0.009 ± 0.002	0.008 ± 0.0002	0.003 ± 0.0001	0.001 ± 0.0001	12.768 ± 0.9	0.558 ± 0.03	4.912 ± 0.09	6.339 ± 0.9	0.165 ± 0.001	2.600 ± 0.3
MT	0.007 ± 0.001	0.008 ± 0.0002	0.003 ± 0.0001	0.001 ± 0.0001	12.012 ± 0.9	0.463 ± 0.03	0.960 ± 0.002	1.117 ± 0.09	0.140 ± 0.002	12.509 ± 0.9
H	0.006 ± 0.001	0.010 ± 0.001	0.004 ± 0.0001	0.000 ± 0	35.935 ± 2.2	0.674 ± 0.02	5.960 ± 0.12	7.988 ± 0.98	0.482 ± 0.001	6.030 ± 0.9
P	0.004 ± 0.001	0.010 ± 0.001	0.004 ± 0.001	0.000 ± 0	19.572 ± 1.9	0.643 ± 0.03	3.328 ± 0.09	4.379 ± 0.1	0.258 ± 0.002	5.881 ± 0.8

High UV_{254} absorbances implying high aromatic content were recorded for Coastal plants H and P. It has been demonstrated through other studies that *SUVA* gives an indication of NOM composition and hence treatment processes can be tailored for its removal [13]. Research has shown that *SUVA* < 2 L/(mgM) implies the major fraction of NOM in the water is of non-humic substances, and *SUVA* > 4 L/(mgM) indicates humic substances. Furthermore, whereas *DOC* > 50% is expected to be removed when *SUVA*

> 4, *DOC* < 25% should be removed when *SUVA* < *2* [14]. To this end, coagulation was expected to remove *DOC* > 50% in coastal plants H, HL and P; and < 25% from plants FB, UM and MT. A correlation matrix (**Figure 4.1**) was generated from data analysis using Spearman correlation on Xlstat statistical software. As expected, the correlations of spectroscopic parameters were found to be higher with UV_{254} than *DOC*. This is because the non-dispersive infra-red detector (NDIR) that quantifies the *DOC* measures the concentration of carbon released as carbon dioxide, while UV_{254} and spectroscopic ratios measure organic matter moieties that absorb and/or fluoresce in the *UV-Vis* range [2].

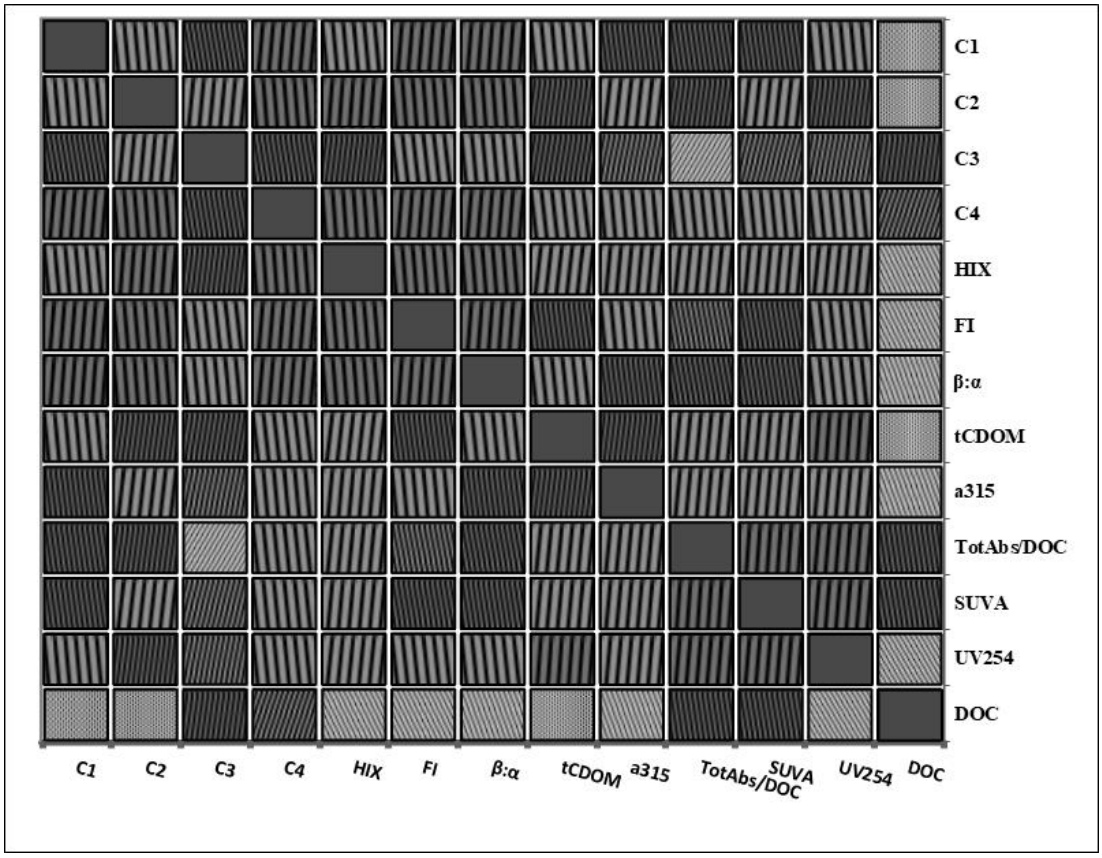

Figure 4. 1: Correlation map relating NOM compositions and its spectroscopic parameters. N.B: Correlation map uses patterns to identify both the sign and the intensity of the correlations: lines that go from the bottom left to the top right correspond to positive correlations, and vice versa; the tighter the lines, the closer the correlation to 0.

4.3.3 Relating Optical Indices at Source to the Treatability of Natural Organic Matter

A good correlation between *HIX* at source and UV_{254} removal across the treatments plants (Table A1) was established (R^2 = 0.80) (**Figure 4.2a**). The index *HIX* in the raw water gives an indication of NOM removal efficiency, with a high *HIX* value meaning that the NOM sample contains high quantities of humic substances (HS) [15]. These HS are easily removed by coagulation in conventional water treatment processes [2]. Thus, higher *HIX* should lead to a larger NOM removal. At the same time, the freshness index *(β:α)* was correlated to UV_{254} removal (R^2 = 0.79) (**Figure 4.2b**). A low *β:α* value indicates aged and condensed humic substances susceptible to removal by conventional processes such as coagulation [16]–[18]. Microbially derived NOM (*FI* < 1.3) showed greater susceptibility to removal than the terrestrially derived NOM (*FI* >1.7) (**Figure 4.2c**). Similar findings have been reported by Lidén et al. (2017) [9]. Interestingly, the correlation of *FI* and *β:α* followed a similar trend, thus suggesting that both parameters are influenced by microbial derived NOM, either by source (*FI*) or degree of degradation *(β:α).* Specific UV absorbance displayed a mild relationship to the UVA reduction (R^2= 0.75) (**Figure 4.2d**).

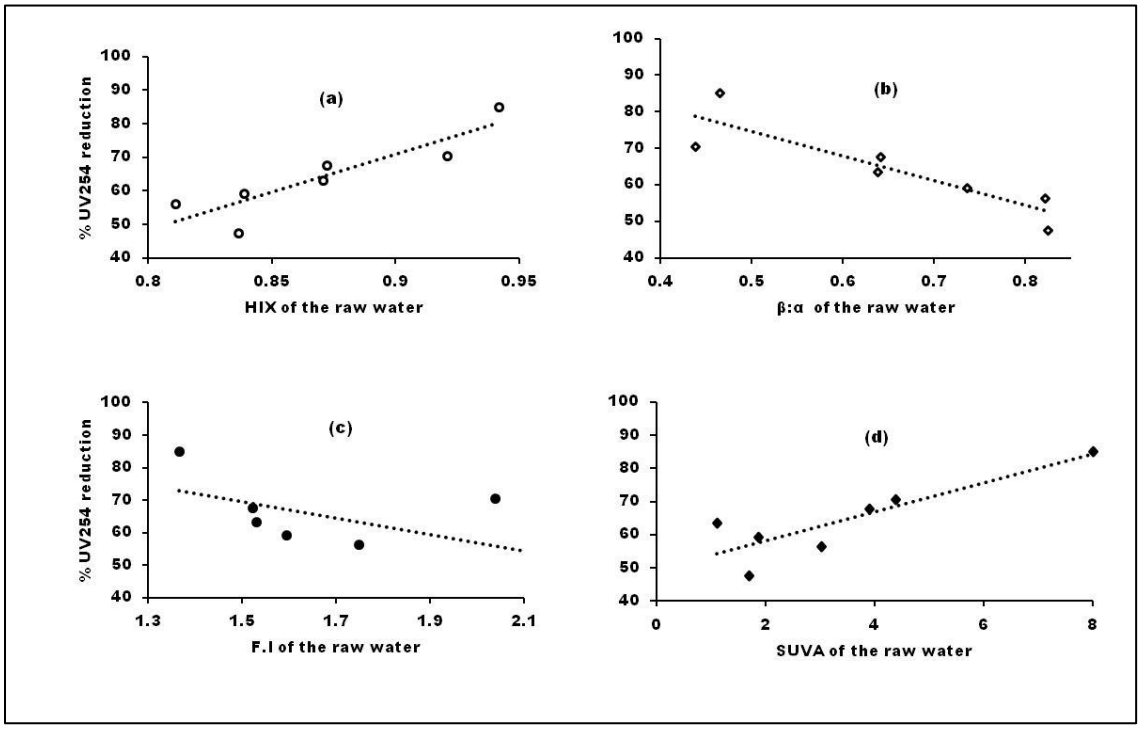

Figure 4. 2: The variation of UV_{254} reduction as a function of (a) HIX, (b) β:α, (c) FI, and (d) SUVA for the raw water samples

4.3.4 Application of Synchronous Fluorescence Spectra (SFS) to Quantify Fluorescent NOM Fractions for Raw Water Samples

Using SFS scans, one major peak and three broad shoulders were observed for all water sources (**Figure 4.3a**). The protein like fluorescence (PLF) peak, which is associated with the presence of tyrosine-like and tryptophan-like components, appeared in the wavelength region 260 - 314 nm [19]. Whereas the first shoulder appearing in the wavelength range 314-355 nm microbial was assigned to the microbial humic-like fluorescence (MHLF) component [20], the second shoulder (355 - 420 nm) is attributable to the fulvic-like fluorescence (FLF) component (Yu et al., 2011). The third and weak shoulder appearing in the range 420 - 500 nm is indicative of the presence of the humic-like fluorescence (HLF) component [22]. Resolution of the one peak and three shoulders, which are defined as PLF, MHLF, FLF, and HLF, respectively, was achieved through the SFS scan. The area under each fluorescent region is known to be proportional to the relative abundance of the fluorescent component in that region [23] [20].

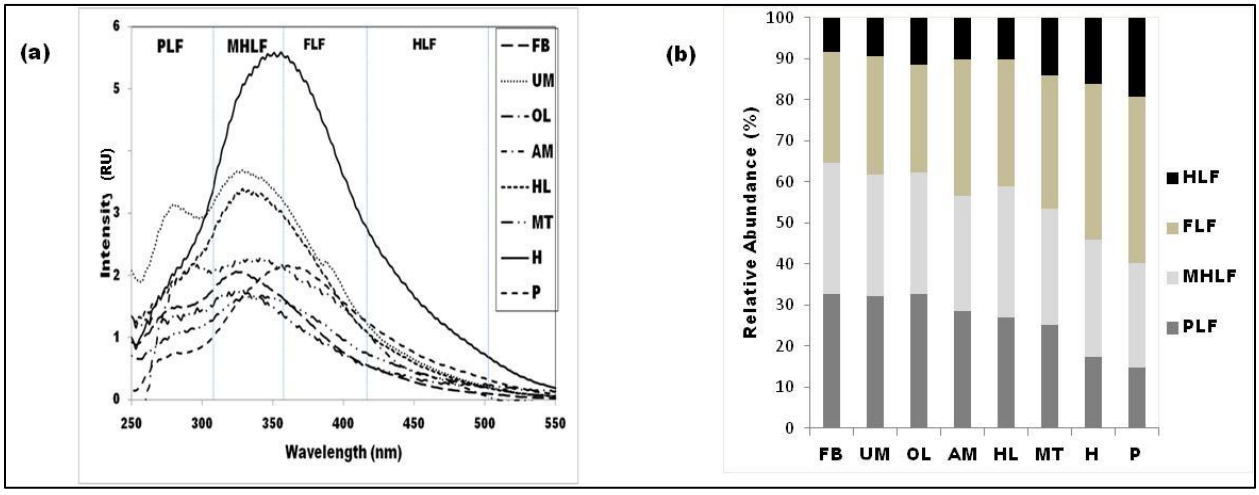

Figure 4. 3: (a) Synchronous scan of raw water sources, (b) relative abundance of NOM fractions in the raw water samples.

The variation of FLF and HLF follow a similar trend, with the highest mean FLF area being established for the coastal plant H (277.92 RU), which was about 5 times greater than the least mean FLF area of the MT plant (76.03 RU) (**Figure 4.3b**). The raw water feeding plant H had high DOC (6.03 mg/L C) and high turbidity (5.32 NTU), thus

indicating high quantities of colloidal and clay material [10]. Water laden with humic acid and fulvic acid is characterized by a brownish-yellow colouration, typical of the surface water on the southwest coast of South Africa [10]. The mean MHLF and PLF areas for plant H (209.78 and 127.50 RU, respectively) was the highest and more than double that of the least mean FLF area for plant MT least plant, MT (66.05 and 58.89 RU, respectively). Although MT had the least MHLF area, it had the highest DOC value (12.51 mg/L C), further confirming the heterogeneity of the NOM. These results suggest that the MT raw water (*FI* = 1.53) is of less microbial origin than that of the H (*FI* = 1.37), and that the source of DOC in MT is largely non-fluorescent and contains mainly biopolymers that are not easily assimilable by microorganisms [24], [25]. Similar results were obtained for biodegradable organic carbon (BDOC) of various South African WTPs [10]. Plant H exhibited the presence of high BDOC fraction (5 mg/L C) compared to other plants, which averaged 2 mg/L C.

4.3.5 Fluorescent Dissolved Organic Matter Components and their Distribution at Source

PARAFAC analysis was conducted using the Aqualog inbuilt SOLO software to study in detail the quantitative removal of FDOM. Save for EB, the inclusion of EB resulted in invalidated results when the split half analysis was used, the PARAFAC model was built from the data acquired from all drinking water sources. For all water sources, modelling was carried out to maximize data collection and data points with the aim of deriving components that represented universal variance between water sources. The objective was to assess the occurrence and distribution of fluorescent components at source and draw correlations with other water quality parameters for predicting occurrence and treatability.

The spectral signatures of the obtained components are shown in **Figure 4.4.a-d**. OpenFluor database was used to cross-reference the derived fluorescence components against those obtained globally [27]. This is, however, a guideline, and the components identified in the study are not necessarily from similar origins. Similarity scores greater than 0.97 were found for each of the four identified components (**Table 4.2**).

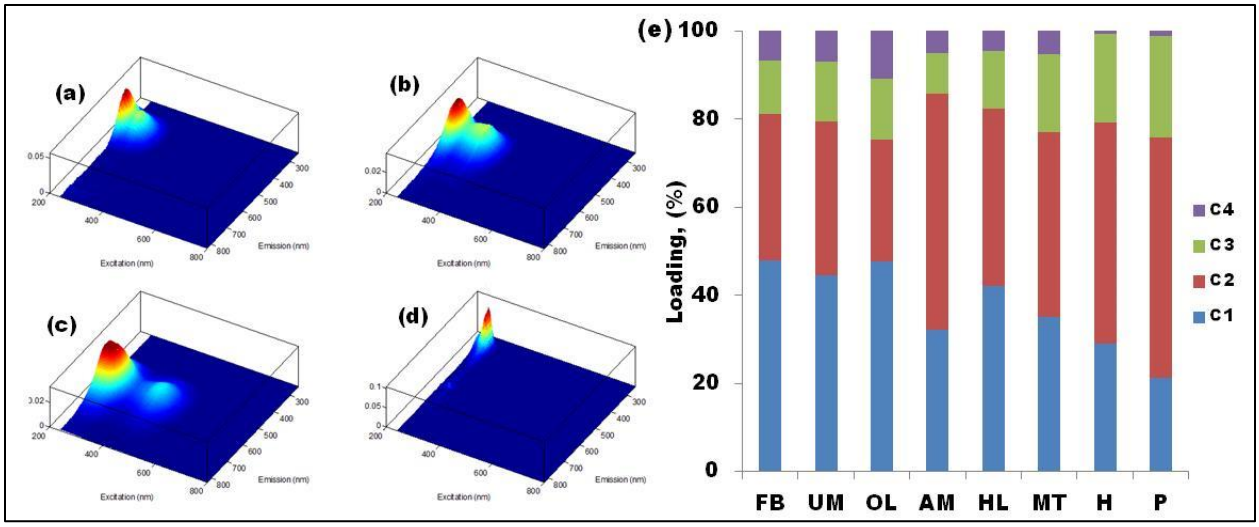

Figure 4. 4: Validated fluorescent components derived from the PARAFAC model on drinking water sources showing (a) component 1 (C1), (b) component 2 (C2), (c) component 3 (C3), and (d) component 4 (C4), and (e) the F_{max} distribution of each component.

Table 4. 2: Identities of similar components using the OpenFluor database

Component	λ_{ex} (nm)	λ_{em} (nm)	Similarity score[a]	Component Identity	Reference
C1	316	<240 (292)	0.97	Terrestrial humic like, reprocessed organic matter	[28]
			0.98	Humic-like, possible photo degradation product	[29]
C2	336	<240 (348)	0.98	Soil derived fulvic acid like	[30]
C3	364	<240 (450)	0.97	Humic acid like	[31]
			0.98	Aromatic, conjugated macromolecular substances of terrestrial origin.	[32]
C4	270	270	0.99	Protein, tryptophan-like	[33]
			0.98	tryptophan-like	[34]

A model fitting four components was established and validated based on the split half criteria as described by Murphy et al., (2013) [27]. After validation, the distribution of the components at each water source was quantified using their maximum fluorescence intensities *(F_{max})*. The value of F_{max} for terrestrial humic-like component (C1) and fulvic like component (C2) was higher than that of humic-like (C3) and protein-like (C4) components (see **Figure 4.4e**) thus suggesting that C1 and C2 have high quantum efficiencies and low responses to quenching effects compared to C3 and C4 [2].

Strikingly, F_{max} for C2 and C3 was higher for plants located on the south west coast of the country (P and H) when compared with the other plants. The raw water feeding these plants has a brown-yellow colouration characteristic of the presence of fulvic acid material, thus corroborating the SFS results (**Section 4.3.4**). It is important to assess the F_{max} of the tryptophan-like component (C4) because it acts as surrogate for wastewater contamination [6]. Unlike the components C1 and C2, which were dominant in reservoirs and rivers, the tryptophan-like component dominated the wastewater effluents [36]. This is because whereas NOM originating from surface water is predominantly terrestrial and mainly from plant matter, sewage-derived NOM originates mostly from autochthonous microbial matter [6]. These distinctions in spectral signatures have facilitated this tracking of wastewater impacted surface waters. Although the level of C4 was always found to be lower than that of any of the other components, C4 presence signals the impact of wastewater contamination. This means plants H and P were less impacted by anthropogenic activities than the other plants.

4.3.6 Pseudo-Quantitative Determination of Polysaccharides in Raw Water

Polysaccharides are of interest to WTPs because they have a high membrane fouling propensity caused by their large molecular size and gelling properties, which enhance filtration resistance and attracts bacteria to adhere to the membranes [37]. Thus, costal plants intending to incorporate membrane technology must critically consider this implication. The usual method of determining polysaccharides is via the LC-OCD method, however this method is costly and laborious. Herewith, a relatively facile spectroscopic method is reported. In brief, polysaccharides are oxidised to UV absorbing furfurals by sulphuric acid, the extent of absorption is relative to the quantity of polysaccharides in the sample [38].

UV-visible scans at 200 - 600 nm of samples prepared using the sulphuric acid-UV method [38][38] is presented in **Figure 4.5**. The maximum absorbance peaks obtained were at slightly shorter wavelength than those reported by Albalasmeh et al. (2013). Whereas this work involved the use of real water samples, which possibly contain a variety of carbohydrates, pure carbohydrates were used in the work reported by Albalasmeh et al. (2013) [13]. This slight hypsochromic shift arises because the range

of chromophores that absorb in *UV-Vis* region is high with varied concentrations giving rise to undistinguishable absorption spectra [13][39]. Additionally, molecular and intermolecular interactions, vibration and rotation distort the absorption spectral signatures in the *UV* spectrum [13]. However, for consistency with literature, *UV* absorbance at 315 nm was used for discussion, and the results are indicative and not absolute.

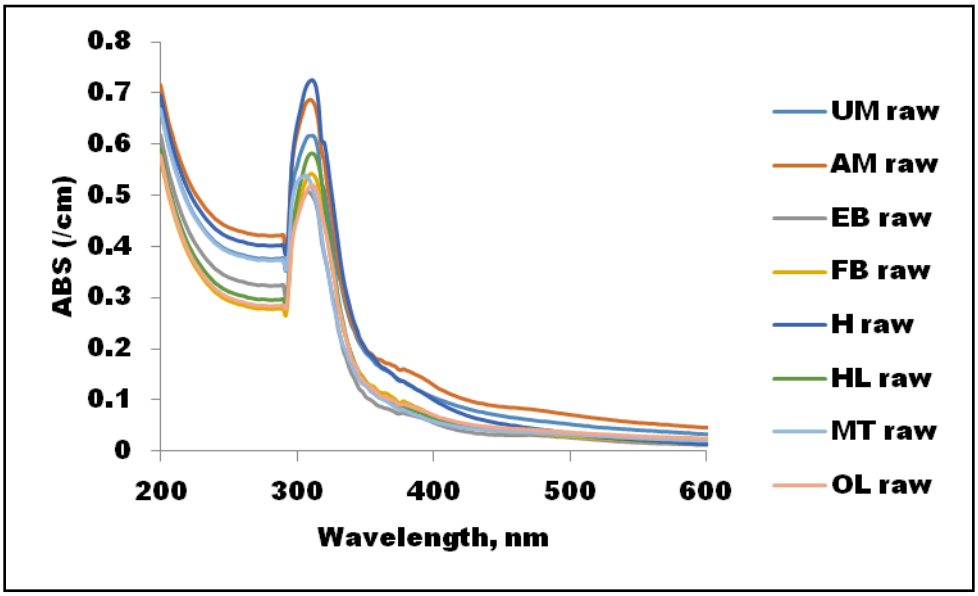

Figure 4. 5: UV absorbance after the sulphuric acid-UV method.

Plant H exhibited the highest UV_{315} absorbance (0.73 cm^{-1}) and EB the lowest (0.46 cm^{-1}) (**Figure 4.5**). Overall, the highest UV_{315} absorbance occurred in the raw water samples of the coastal plants as opposed to the inland plants. A strong correlation (R^2= 0.93) was observed between the *UV* absorbance at 315 nm and the *FI* spectroscopic ratios (**Figure 4.6**) suggesting that the source of polysaccharides in the samples is of aquatic origin due to microbial activities releasing extracellular polymeric substances [40]. Costal plants were found to possess low *FI* index, indicating that microbial NOM has a high UV_{315} absorbance with high polysaccharide content.

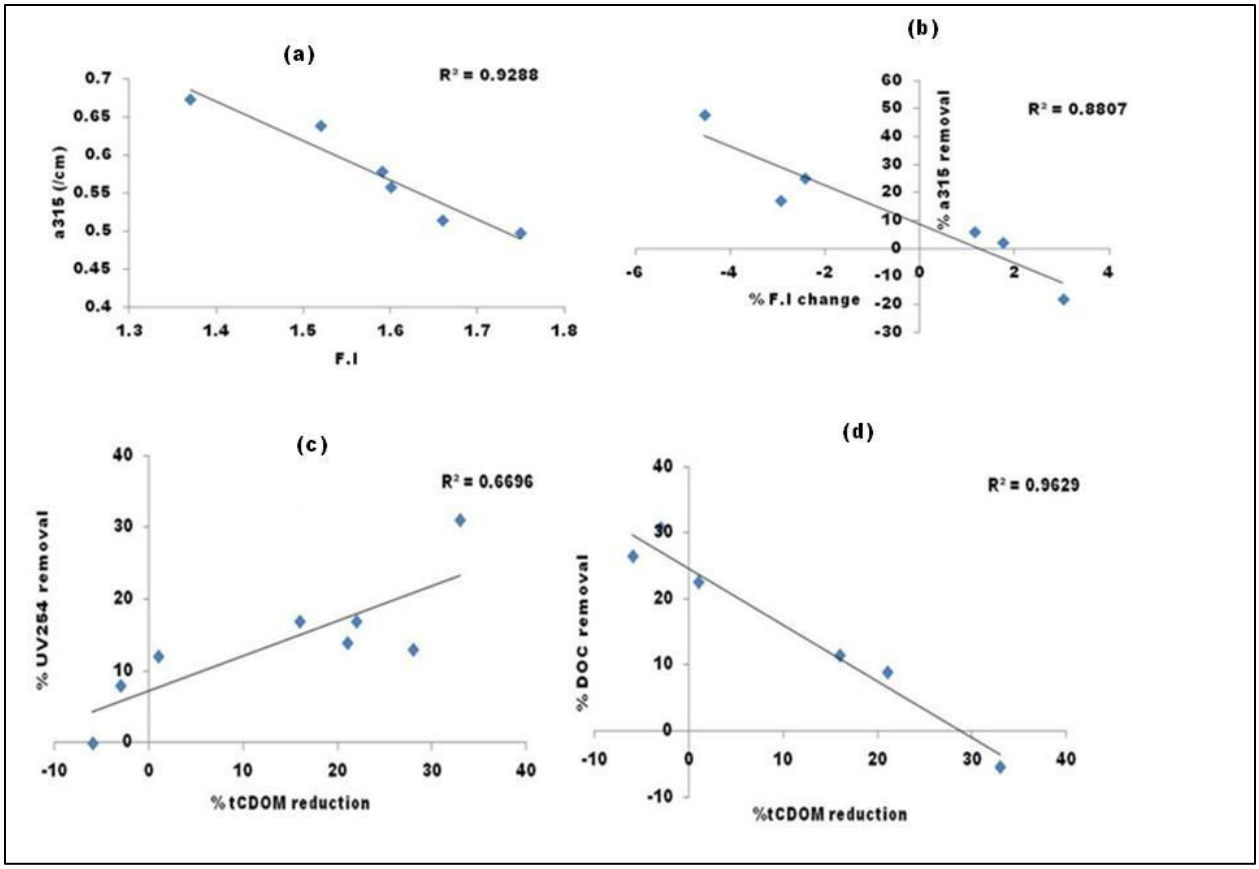

Figure 4. 6: Correlations between parameters: (a) FI and a315, (b) percentage change in FI and a315 removal, (c) percentage *tCDOM* reduction and UV_{254} removal, (d) percentage *tCDOM* reduction and percentage DOC removal.

4.4 SELECTIVITE REMOVAL OF NOM FRACTIONS AT DIFFERENT STAGES OF THE TREATMENT TRAIN

To date, a few studies on the character of NOM found in water treatment plants of South Africa have characterized NOM occurring at individual plants and established the ability of the plants to remove bulk NOM by specific treatment processes (e.g [10][17][41]). Even then, the occurrence, behaviour and removal efficiencies of fluorescent EEM components using specific treatment processes have not been reported in South Africa. Therefore, it is important to assess the treatment efficiency of these plants in the removal of NOM given the variability of the water resources in South Africa [42]. It is expected that the water types influence the occurrence of NOM components and the treatment regimen at the plants influence the behaviour and

removal efficiency of the NOM components. **Table A1** shows the effectiveness of treatment stages in removing parameters such as *DOC, FDOM, UV* and the subsequent changes in spectroscopic ratios at each stage (*F.I, β:α and HIX*). From Table A1, the overall DOC removal from eastern coast (AM, MT, UM and HL) averaged 30.1%, inland plants (FB and OL) averaged 8.4 % and plants from the South West coast (P and H) coast averaged 42.9% removal. Despite the low removal by the plants, the treated water was within the limits of the South African National Standards (SANSs). As these were grab samples, they do not present any reasonable timeframe such as seasonal variations. Our previous studies which incorporated seasonal variations (**Table 2.2** – Literature Review) showed annual averages of 16.7; 33.5 and 73.5 % for inland, South West coast and Eastern coast plants, respectively [53]. Eastern coast plants annual average was higher than global averages, 40% - South Korea [54], 48% - China [55] and 59.8% - Australia [56]. Perhaps the poor removal efficiencies for inland plants may be due to poor optimisation or recalcitrant organics.

4.4.1 Selective Removal of Biogenic NOM at each Treatment Stage

The extent of removal of polysaccharides at different stages of the treatment plant as exemplified by H is shown in **Figure 4.7a**. The characteristic peak is shown for the differential absorbance scans after each treatment stage. Coagulation removed between -21% (OL) to 15.3% (H) of polysaccaharides. No correlation could be established between polysaccahardes and microbial by-product removal at the coagulation stage. Neither could trends relating spatial locations and polysaccharide treatability be established. This can be attributed to many factors such as coagulant type and charge, pH, other charged species that can be entraped within the polysaccharide matrix necessitating its agglomeration into flocs. The negative value for OL (-21%) and FB (-3.7%) indicates a build-up of polysaccharides in the treatment stage. Visual inspection of the abstraction points at these plants showed waxy material characteristic of extracellular polymeric substances (EPS) on the walls of the coagulation/floccultation channels.

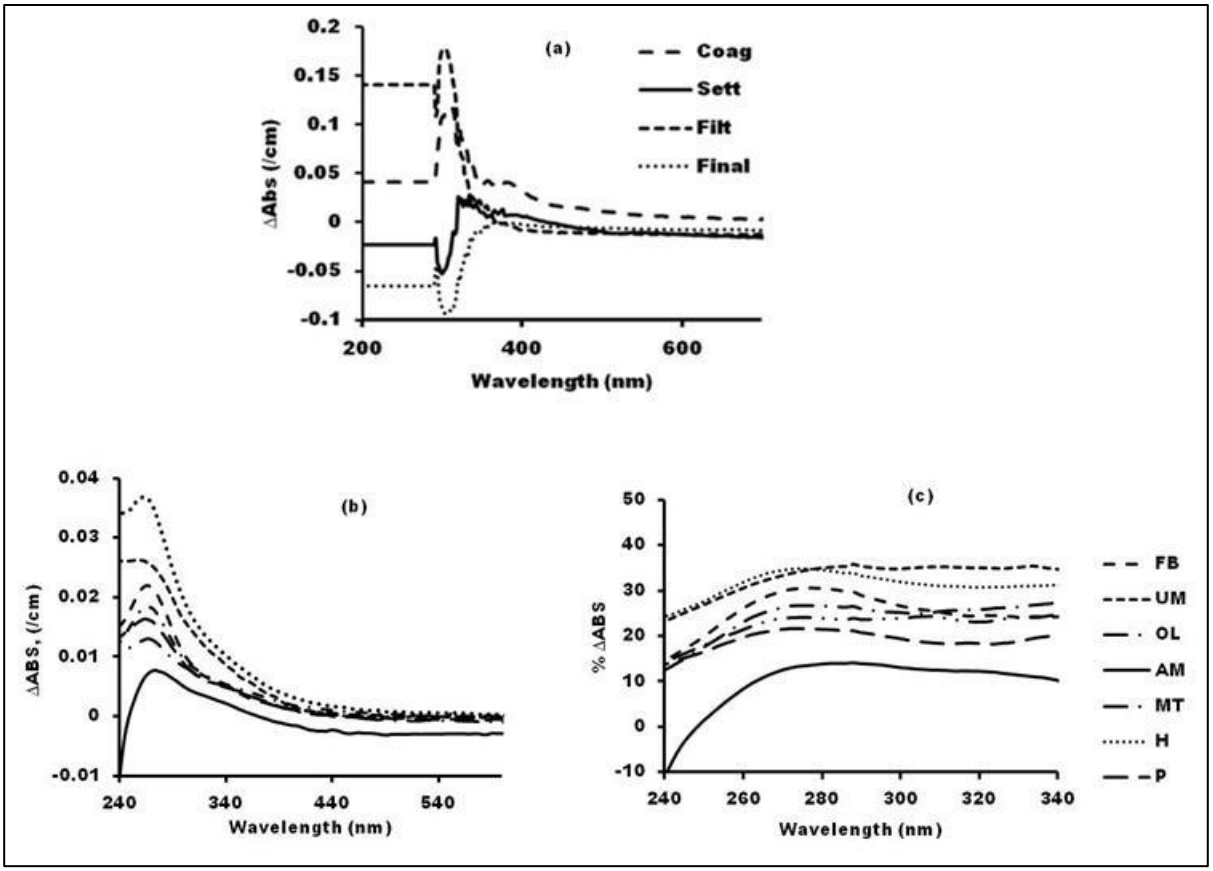

Figure 4. 7: (a) Differential absorbance as exemplified by H for the removal of polysaccharides throughout the treatment train. (b) Differential absorbance (ΔAbs) during disinfection, (c) % ΔABS removed at the disinfection stage

The settlebility of polysaccharides depends on the effctiveness of coagulation so poor coagulation leads to poor settlement of solids consequently translating to poor removal. Further, in comparison to low molecular weight (LMW), high molecular weight (HMW) substances such as polysaccharides are generally easily removed at the sedimentation stage when attached to particles of conventional WTPs [43]. Therefore, the effectiveness of coagulationthe, size and type of the polysaccharide detemine its ability to be suspended or to settle at the bottom of the sedimentation basin. Plants in the east coast of South Africa and inland showed a similar trend with respect to their ability to remove polysaccharides and the following removal percentage values were recorded: HL (22%); AM (22%); MT (19%); UM (18%); OL (21%) and FB (5%). The respective negative removal percentage values of -5 % and -700% that were achieved for the H and P plants located at the South East coast are indicative of a build-up of

polysacchaides at the sedimentation stage, thus suggesting poor settleability at these plants.

Polysaccharide reduction at the sand filtration stage correlated well with change in *FI* (R^2 = 0.88) (**Figure 4.6**). Due to longer residence time in the sand filter, NOM is usually degraded in sand filters [45]. Unexpectedly, there was poor removal efficiencies for HL (-27%); MT (-18%); UM (-12%) and AM (2%), this means there poor degradation of the NOM at the sand filtration stage of the east coast plants. In contrast, the performance of the Inland and South East coast plants was much better and the following removal percentage values were achieved: P (48%); H (25%); FB (17%) and OL (6%). Sand filters function as a habitat for many bacterial species that use dissolved organic carbon as a source of nutrients [44]. The assimilability of NOM depends on molecular weight, with heterotrophic bacteria preferentially degrading LMW over HMW NOM [45]. Polysaccarides are macromolecular polymers with high molecular weight (>20 000 Da) not easily assimilable by heterotrophic bacteria [46]. The results suggest that plants in the East coast receive polysaccharides of high molecular weight, which are not easily degraded by the bacteria.

It was found that polysacaccharides increased at the disinfection stage. This can be attributed to released EPS arising from the bacteria killed by chlorine [45], [47]. All plants showed a build-up of polysaccharides during the disinfection stage and the following removal percentage values were observed for the respective plants: P (-43%); UM (-36%); AM (-19%); H (-19%); OL (-11%); FB (-7%) and HL (-6%).

4.4.2 Selective Removal of Chromophoric DOC at each Treatment Stage

Save for the monotonical absorbance that decreases as wavelength increases, UV-Vis spectra of drinking water samples are nearly featureless. Chemometric techniques such as differential spectra (DS) can therefore be used to gain more insights into latent UV-vis peaks. DS normalises different UV-Vis spectra for ease of comparison and DS can also can be used to calculate and evaluate the dynamics of CDOM properties after coagulation, sedimentation, rapid sand filtration and disinfection stages.

The removal by coagulation for NOM components absorbing at shorter wavelengths (< 290 nm) was relativeley constant, whereas the removal for NOM components absorbing at longer wavelengths (> 290 nm) increased by up to 20% (**Figure 4.8**). There was a steady increase in ΔABS, indicating the transformation of NOM components at the sand filter stage (**Figure 4.8**). This means the sand was biologically active thus allowing the attachment of heterotrophic bacteria as it assimilates the available NOM nutrients transforming it into by products and end products such as humics and fulvic like matter that absorbs UV-Vis at higher wavelengths (>290 nm). A correlation coefficient of 0.67 which was achieved for *tCDOM* removal by coagulation and UV_{254} removal indicates moderate correlation between the two parameters. This was expected, since both parameters measure the part of NOM that is responsible for fluorescence. Intriguingly, the percentage of *tCDOM* removed by coagulation correlated well (R^2 = 0.96) with the DOC removal percentage (**Figure 4.6**). This was totally unexpected because DOC measures all types of both fluorescent and non-fluorescent organic matter [48].

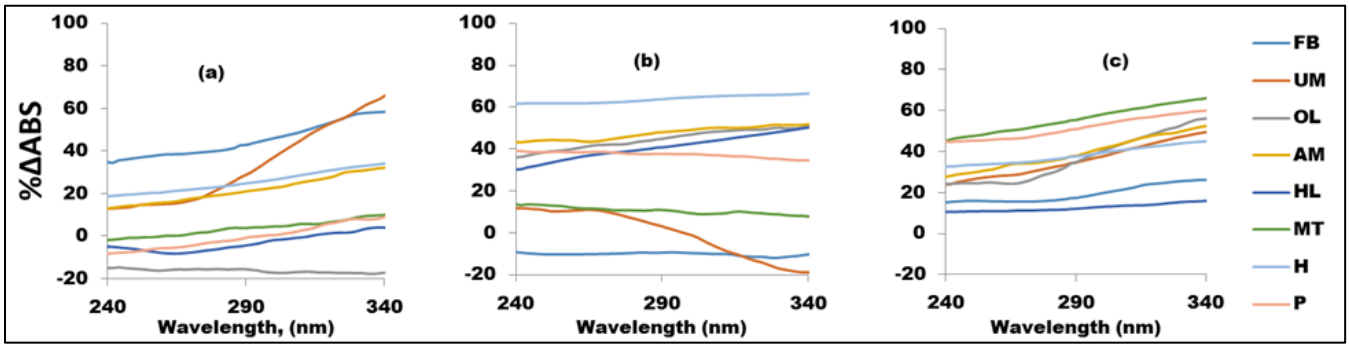

Figure 4. 8: % ΔABS for (a) coagulation, (b) Settled water and (c) filtration stage

While DOC removal varied considerably (5 – 30%) at the sedimentation stage for all plants, only a minimum variation of *tCDOM* (< 10%) was observed (**Table A1**). This could be due to the phase transformation of particulate organic matter (POM) and settling of NOM [45]. Sand filtration followed a trend that is similar to that of sedimentation; however, a smaller *tCDOM* variation of < 5% was achieved.

Differential arbsorbance graph revealed a characteristic absorbance peak in the region 260-270 nm for the disinfection stage (**Figure 4.7b).** Similar results have been reported

in literature [50]. The removal of the characteristic 260-290nm CDOM peak following disinfection is depicted in **Figure 4.7c**. These results are consistent with findings from Lavonen et al., (2015)[50], which suggest that the absorbance in this range is especially reactive during the chlorination and chloramination steps.

4.4.3 Selective Removal of Fluorescent NOM at each Treatment Stage

Coagulation was more effective in the removal of the humic-like fractions when compared with the other fractions (**Figure 4.9a**). Regardless of the location of the plant, bulk DOM removal (in terms of UV_{254}) was found to be higher in comparison to FDOM in the rapid sand filtration stage (**Figure 4.9b**). This suggests that the non-FDOM fractions are removed much more efficiently than the FDOM fraction during the rapid sand filtration (RSF) stage. Although still in agreement with the concept that SUVA > 4 gives rise to more than 50% removal of humics by coagulation, the removal of the humic FDOM ($P_{i,5}$) correlated weakly (R^2 = 0.52) with the SUVA of the raw water. For example, a SUVA value of 15.63 was obtained at source of plant H and a humics removal percentage of 88% through coagulation was achieved. Despite the disinfection stage being efficient in the removal of humic-like fractions, the efficiency of this process when removing other FDOM was low (less than 30%) (**Figure 4.9c**). Chlorination results in chemical modifications of NOM by selectively targeting double bonds and conjugated functional groups. Depending on the number and distribution of these moieties, there are differential removal rates of bulk NOM and FNOM, and differential generation of resultant DBPs [51]. Overall, although the total removal efficiencies of humic-like FNOM is high, removal efficiencies for other FNOM fractions are much lower. This indicates the drinking water treatment processes are lacking in the removal of FNOM compared to bulk NOM removal.

FNOM can be quickly and sensitively detected online using fluorescence spectroscopy techniques [51][18]. An understanding of the dynamics of FNOM fractions in drinking water production is necessary for monitoring and control because the overall removal of NOM is strongly correlated to its fluorescent fractions [52][45].

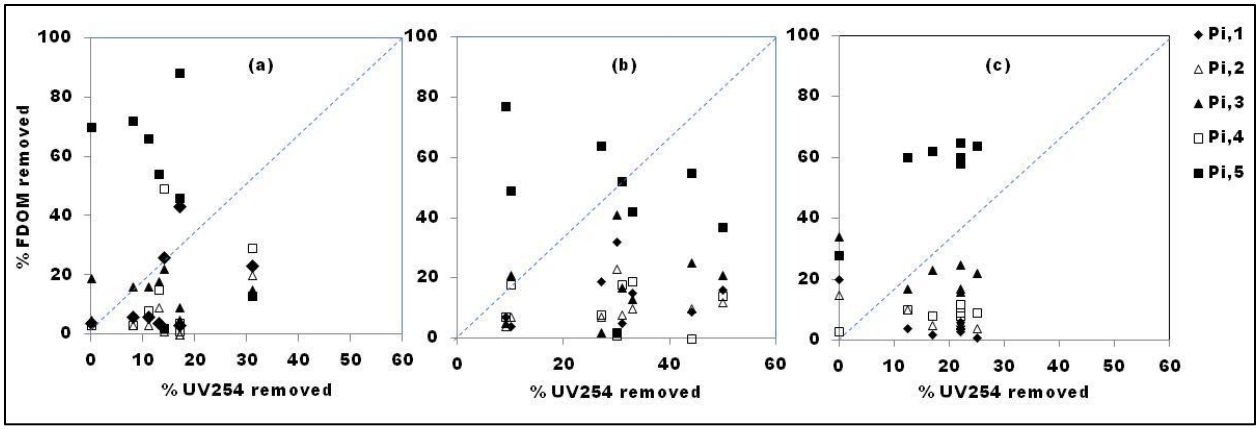

Figure 4. 9: Correlations between the removal FDOM and the removal of NOM in three treatment stages (a) coagulation, (b) slow sand filtration, and (c) disinfection

4.6 CONCLUSION

This study investigated the concentration and chemical profile of NOM in South African drinking water treatment sources as well as the fate of NOM and its transformations throughout the treatment train at various South African plants. This study constitutes the first study conducted in South Africa for the determination of the occurrence, behaviour and removal efficiencies of fluorescent EEM components in the country's water treatment plants. Water samples were analysed for DOC, UV absorbance, SUVA, spectroscopic indices, fluorescence intensity as well as presence of biopolymer (polysaccharides), and the following key findings related to the objectives of this research study were reported:

- The characterisation of NOM using SUVA serves as a valuable prediction tool for the removal of NOM. As expected, a DOC removal efficiency rate exceeding 50% was observed for plants with SUVA > 4, namely plants H, HL and P. Less than 25% DOC removal efficiency rate was observed for plants FB, UM and MT, which had a SUVA < 2.
- A model fitting four components was established and validated based on the slit half criteria, and the distribution of the components at each water source was quantified using their maximum fluorescence intensities *(F_{max})*. The value of F_{max} was higher for terrestrial humic-like (C1) and fulvic like (C2) components in comparison to humic-like (C3) and protein-like (C4) components. This suggests

that C1 and C2 components have high quantum efficiencies and low responses to quenching effects compared to C3 and C4 components.

- Coagulation was more effective for the removal of the humic-like fractions when compared with the other fractions. In the rapid sand filtration stage, bulk DOM removal (in terms of UV_{254}) was found to be higher than that of FDOM, regardless of location of the plant. This suggests that non-FDOM fractions are removed much more effectively than FDOM fraction during the RSF stage. Although disinfection has proven to be efficient in the removal of humic-like fractions, the efficiency of this process in the removal of other FDOM is not as effective.

4.7 REFERENCES

[1] S. L. Leavey-roback, S. W. Krasner, and I. H. Mel (2016). The effect of natural organic matter polarity and molecular weight on NDMA formation from two antibiotics containing dimethylamine functional groups. *Science of the Total Environment, The*., **572**, 1231–1237.

[2] S. A. Baghoth, S. K. Sharma, and G. L. Amy (2010).Tracking natural organic matter (NOM) in a drinking water treatment plant using fluorescence excitation e emission matrices and PARAFAC. *Water Research*, **45**(2), 797–809.

[3] N. P. Sanchez, A. T. Skeriotis, and C. M. Miller (2013). Assessment of dissolved organic matter fluorescence PARAFAC components before and after coagulation e filtration in a full scale water treatment plant. *Water Research*, **47**(4), 1679–1690.

[4] Y. Zhang, X. Zhao, X. Zhang, and S. Peng (2015).A review of different drinking water treatments for natural organic matter removal', *Water Science & Technology: Water Supply*, **15**(3), 442.

[5] J. O. Tijani, O. O. Fatoba, G. Madzivire, and L. F. Petrik (2014). A review of combined advanced oxidation technologies for the removal of organic pollutants

from water. *Water, Air, and Soil Pollution*, **225**(9), 2014.

[6] R. K. Henderson, A. Baker, K. R. Murphy, A. Hambly, R. M. Stuetz, and S. J. Khan (2009). Fluorescence as a potential monitoring tool for recycled water systems : A review. *Water Research*, **43**(4), 863–881.

[7] M. Bieroza, A. Baker, and J. Bridgeman (2011). Exploratory analysis of excitation – emission matrix fluorescence spectra with self-organizing maps — A tutorial. *Education for Chemical Engineers*, **7**(1), 22–31.

[8] J. A. Korak, A. D. Dotson, R. S. Summers, and F. L. Rosario-ortiz (2013). Critical analysis of commonly used fluorescence metrics to characterize dissolved organic matter. *Water Research*, **49**, 327–338.

[9] A. Lidén, A. Keucken, and K. M. Persson (2017). Uses of fluorescence excitation-emissions indices in predicting water treatment efficiency. *Journal of Water Process Engineering*, **16**, 249–257.

[10] T. I. Nkambule, R. W. M. Krause, J. Haarhoff, and B. B. Mamba (2012). Natural organic matter (NOM) in South African waters : NOM characterisation using combined assessment techniques. *Water SA*, **38** (5), 697–706.

[11] D. J. Dryer, G. V. Korshin, and M. Fabbricino (2008). In situ examination of the protonation behavior of fulvic acids using differential absorbance spectroscopy. *Environmental Science and Technology*, **42**(17), 6644–6649.

[12] G. S. Wang and S. T. Hsieh (2001). Monitoring natural organic matter in water with scanning spectrophotometer. *Environment International*, **26**(4), 205–212.

[13] P. Roccaro, M. Yan, and G. V Korshin (2015). Use of log-transformed absorbance spectra for online monitoring of the reactivity of natural organic matter. *Water Research*, **84**, 136–143.

[14] E. Lavonen (2015). Tracking Changes in Dissolved Natural Organic Matter Composition. Doctoral Thesis, Swedish University of Agricultural Sciences.

[15] X. S. He (2013). Fluorescence excitation-emission matrix spectra coupled with parallel factor and regional integration analysis to characterize organic matter humification. *Chemosphere*, **93**(9), 2208–2215.

[16] T. Meyn, J. Altmann, and T. O. Leiknes (2011). In-line coagulation prior to ceramic microfiltration for surface water treatment—minimisation of flocculation pre-treatment. *Disalination and Water Treatment,* **42**(1-3), 163-176

[17] K. P. Lobanga (2012). Natural organic matter removal from surface waters by enhanced coagulation, granular activated carbon adsorption and ion exchange. PhD thesis, University of Johannesburg.

[18] D. Zheng, R. C. Andrews, S. A. Andrews, and L. Taylor-Edmonds (2015). Effects of coagulation on the removal of natural organic matter, genotoxicity, and precursors to halogenated furanones. *Water Research*, **70**, 118–129.

[19] J. Hur, K. Jung, and Y. Mee (2011). Characterization of spectral responses of humic substances upon UV irradiation using two-dimensional correlation spectroscopy. *Water Research*, **45**(9), 2965–2974.

[20] H. Yu, Y. Song, X. Tu, E. Du, R. Liu, and J. Peng (2013). Assessing removal efficiency of dissolved organic matter in wastewater treatment using fluorescence excitation emission matrices with parallel factor analysis and second derivative synchronous fluorescence. *Bioresource Technology*, **144**, 595–601.

[21] H. Yu (2011). Fluorescence Spectroscopic Properties of Dissolved Fulvic Acids from Salined Flavo-aquic Soils around Wuliangsuhai in Hetao Irrigation District , China. *Soil Science Society of America Journal,* **75**(4), 1385–1393.

[22] W. H. Mcdowell *(2006).* A comparison of methods to determine the biodegradable dissolved organic carbon from different terrestrial sources. *Soil Biology and Biochemistry*, **38**,1933–1942.

[23] J. Hur, D. Lee, and H. Shin (2009). Comparison of the structural , spectroscopic and phenanthrene binding characteristics of humic acids from soils and lake

sediments. *Organic Geochemistry*, **40**(10), 1091–1099.

[24] K. Kimura, K. Shikato, Y. Oki, K. Kume, and S. A. Huber (2018). Surface water biopolymer fractionation for fouling mitigation in low-pressure membranes. *Journal of Membrane Science*, **554**(November), 83–89.

[25] K. Kimura and Y. Oki (2017). Efficient control of membrane fouling in MF by removal of biopolymers: Comparison of various pretreatments. *Water Research*, **115**, 172–179.

[26] Z. Filip, W. Pecher, and J. Berthelin (2000). Microbial utilization and transformation of humic acid-like substances extracted from a mixture of municipal refuse and sewage sludge disposed of in a landfill. *Environmental Pollution*, **109**(1), 83–89.

[27] K. R. Murphy, C. A. Stedmon, P. Wenig, and R. Bro (2014). OpenFluor – an online spectral library of auto- fl uorescence by organic compounds in the environment. *Analytical Methods*, 658–661.

[28] U. J. Wu, K. R. Murphy, and C. A. Stedmon (2017). The One-Sample PARAFAC Approach Reveals Molecular Size Distributions of Fluorescent Components in Dissolved Organic Matter. *Environmental Science and Technology*, **51**(20),11900–11908

[29] C. L. Osburn, L. T. Handsel, M. P. Mikan, H. W. Paerl, and M. T. Montgomery, (20120. Fluorescence Tracking of Dissolved and Particulate Organic Matter Quality in a River-Dominated Estuary. *Environmental Science and Technolog*y, **46**(16), 8628-36

[30] C. L. Osburn, T. J. Boyd, M. T. Montgomery, T. S. Bianchi, R. B. Coffin, and H. W. Paerl (2016). Optical Proxies for Terrestrial Dissolved Organic Matter in Estuaries and Coastal Waters. *Frontiers in Marine Science*, **2**(January), 127-135.

[31] K. M. Cawley (2012). Characterising the sources and fate of dissolved organic matter in Shark Bay , Australia : a preliminary study using optical properties and

stable carbon isotopes. *Marine and Freshwater Research*, **63**(11), 1098-1107.

[32] C. L. Osburn, L. T. Handsel, B. L. Peierls, and H. W. Paerl (2016). Predicting Sources of Dissolved Organic Nitrogen to an Estuary from an Agro-Urban Coastal Watershed. *Environmental Science and Technology*, **50**(16), 8473–8484

[33] K. R. Murphy (2011). Organic Matter Fluorescence in Municipal Water Recycling Schemes : Toward a Unified PARAFAC Model. *Environmental Science and Technology*, **45**(7), 2909–2916.

[34] Y. Yamashita, B. D. Kloeppel, J. Knoepp, G. L. Zausen, and R. Jaffe (2011). Effects of Watershed History on Dissolved Organic Matter Characteristics in Headwater Streams. *Ecosystems*, **14**,1110–1122.

[35] K. R. Murphy, C. A. Stedmon, D. Graeber, and R. Bro (2013). Fluorescence spectroscopy and multi-way techniques. PARAFAC. *Analytical Methods*, **5**(23), 6557.

[36] A. D. Pifer and J. L. Fairey (2014). Suitability of Organic Matter Surrogates to Predict Trihalomethane Formation in Drinking Water Sources. *Environmental Engineering and Science*, **31**(3), 117–126.

[37] S. Meng, W. Fan, X. Li, Y. Liu, D. Liang, and X. Liu 92018). Intermolecular interactions of polysaccharides in membrane fouling during micro fi ltration. *Water Research*, **143**, 38–46.

[38] A. A. Albalasmeh, A. A. Berhe, and T. A. Ghezzehei (2013). A new method for rapid determination of carbohydrate and total carbon concentrations using UV spectrophotometry. *Carbohydrate Polymers*, **97**(2), 253–261.

[39] P. Li and J. Hur (2017). Utilization of UV-Vis spectroscopy and related data analyses for dissolved organic matter (DOM) studies: A review. *Critical Reviews in Environmental Science and Technology*, **47**(3), 131–154.

[40] H. Yu *(2015).* Understanding ultrafiltration membrane fouling by soluble microbial

product and effluent organic matter using fluorescence excitation-emission matrix coupled with parallel factor analysis. *International Biodeterioration and Biodegradation*, **102** (August), 56-63

[41] S. S. Marais, E. J. Ncube, T. A. M. Msagati, J. Haarhoff, T. I. Nkambule, and B. B. Mamba (2015). Investigation of natural organic matter (NOM) character and its removal in a chlorinated and chloraminated system at Rand Water, South Africa. *Water Supply* , **17** (5), 1287–1297

[42] N. Chaukura, N. G. Ndlangamandla, W. Moyo, T. A. M. Msagati, B. B. Mamba, and T. T. I. Nkambule (2018). Natural organic matter in aquatic systems – a South African perspective.*Water SA*, **44**(4), 624–635.

[43] Z. Su, T. Liu, W. Yu, X. Li, and N. J. D. Graham (2017). Coagulation of surface water : Observations on the signi fi cance of biopolymers. *Water Research*, **126**, 144–152.

[44] E. I. Prest, F. Hammes, and M. C. M. Van Loosdrecht (2016). Biological Stability of Drinking Water : Controlling Factors , Methods , and Challenges. *Frontiers in Microbilogy*, **7**, (February),1–24.

[45] X. Yang, Z. Zhou, M. N. Raju, X. Cai, and F. Meng (2017). Selective elimination of chromophoric and fluorescent dissolved organic matter in a full-scale municipal wastewater treatment plant. *Journal of Environmental Sciences (China)*, **57**,150–161.

[47] J. Sun (2016).Three-dimensional fluorescence excitation–emission matrix (EEM) spectroscopy with regional integration analysis for assessing waste sludge hydrolysis at different pretreated temperatures. *Environmental Science and Pollution Research*, **23**(23), 24061–24067.

[48] S. A. Baghoth (2012). Characterizing natural organic matter in drinking water treatment processes and trains. PhD Thesis, Technical University of Delft

[49] W. T. Li (2017). Application of UV absorbance and fluorescence indicators to

assess the formation of biodegradable dissolved organic carbon and bromate during ozonation. *Water Research*, **111**(March), 154-162.

[50] E. E. Lavonen, D. N. Kothawala, L. J. Tranvik, M. Gonsior, and P. Schmitt-kopplin (2015). Tracking changes in the optical properties and molecular composition of dissolved organic matter during drinking water production. *Water Research*, **85**, 286–294.

[51] S. Lee. Determination of mass transport characteristics for natural organic matter (NOM) in ultrafiltration (UF) and nanofiltration (NF) membranes. *Water Supply,* **2** (2), 151–160.

[52] S. Shao, H. Liang, F. Qu, H. Yu, K. Li, and G. Li. Fluorescent natural organic matter fractions responsible for ultrafiltration membrane fouling: Identification by adsorption pretreatment coupled with parallel factor analysis of excitation-emission matrices. *Journal of Membrane Science*, **464**(August), 33–42,

[53]N. Chaukura, N. G. Ndlangamandla, W. Moyo, T. A. M. Msagati, B. B. Mamba, and T. T. I. Nkambule (2018). Natural organic matter in aquatic systems – a South African perspective. *Water SA*.,**44**(4), 624–635.

[54]. J. W Park (2016). Influences of NOM composition and bacteriological characteristics on biological stability in a full-scale drinking water treatment plant. *Chemosphere*, **160**(2016), 189-198.

[55]. H Xu, D Zhang, Z Xu, Y Liu, R Jiao, D Wang (2018). Study on the effects of organic matter characteristics on the residual aluminum and flocs in coagulation processes. *Journal of Environmental Science*, **63**(January), 307-317.

[56]. B. A. Lyon, M. J. Farré, G. A. De Vera, J. Keller, A. Roux, H. S. Weinberg and W. Gernjak (2014). Organic matter removal and disinfection byproduct management in South East Queensland's drinking water. *Water Science and Technology: Water Supply*, **14**(4), 681-689

CHAPTER 5*:...*

Characterisation of natural organic matter in South African drinking water treatment plants: Towards integrating ceramic membrane filtration

5.1 INTRODUCTION

South African water treatment plants employ the conventional water treatment processes which include processes such as coagulation/flocculation, sedimentation, filtration and disinfection. However, these traditional unit processes do not effectively remove natural organic matter (NOM) (around 35% at conventional pH) [1]. However, regardless of more than twenty years of use in the water industry and other separation industries, research on their selectivity in removing specific NOM fractions in surface waters is still in its infancy. Moreover there is no reported information on the use of ceramic membranes for NOM removal in South African surface waters. This work seeks to investigate the effectiveness of ceramic membrane filtration technology in treating surface waters from different water quality regions of South Africa. The objectives were to: (1) characterize the NOM found in the different region of South Africa using DOC, UV_{254}, FEEM, BDOC, polarity fractions and fluorescence indices, (2) investigate the removal efficiency of the BDOC, DOC, FDOM, and polarity fractions by ceramic membranes through analysis of the differences in the feed and filtrate water quality; (3) evaluate quality indices as predictors of NOM removal that can be expected from South African water quality types, and (4) use modelling techniques to investigate the dominant fouling mechanism on ceramic membranes by waters from different water quality sources in South Africa.

This chapter is based on:

Moyo W, Motsa M.M, Chaukura N, Msagati T.A.M, Mamba B.B, Heijman S.J.G and Nkambule T.T.I . Characterisation of natural organic matter of South African drinking water treatment plants: Towards integrating ceramic membrane filtration. Water Science and Engineering (Submitted: 26 February 2020*)*

5.2 METHODS AND MATERIALS

5.2.1 Sampling and Sample sites

Sampling was carried according to the method layed out in **Section 3.2**, and the following five surface water sources that are representative of the water quality regions found in South Africa and serving water treatment plants were selected: source water supplying the Plettenberg Bay water treatment plant, namely Keurbooms River in the Southern Cape (PL); Debose Dam, which supplies Veolia Water Treatment Plant and serves Hermanus and parts of Cape Town (H); source water supplying Midvaal Water Treatment plant namely the Vaal River in the North West Province (MV); Hezelmere River which supplies Hezelmere Water Treatment Plant operated by Umngeni Water Treatment Company serving the greater Umngeni municipality (HL) and source water supplying the Mpumalanga Province and parts of Polokwane City, namely the Lepelle River (OL). The location of sampling sites is shown in **Figure 3.1 (Section 3.3).** Turbidity, pH, temperature, and conductivity were measured onsite using potable multimeters.

5.2.2 Determination of DOC and BDOC fractionation of NOM

The organic carbon quantity of the BDOC fraction, raw, concentrate and permeate of all samples was determined in triplicate using a total organic carbon analyser (TOC fusion, Teledyne Tekmar). The in-depth procedure followed is found in **Sections 3.51 and 3.5.5.**

5.2.3 Fluorescence, UV absorbance analysis and polarity fractionation of NOM

UV, DOC and SUVA were analysed according to the method outlined in **Sections 3.51; 3.52 and 3.53**. UV absorbance at 254 nm (UV_{254}) measurement of the permeates and concentrate was carried out after every hour during the filtration experiments to determine UV transmission through the membrane. The UV254 transmission during the filtration process was calculated as the UV_{254} quotient of permeate to that in the feed water.

The character of the three fractions (hydrophobic, hydrophilic, transphilic) obtained through the polarity rapid assessment method (PRAM) was also analysed using UV254 measurement. The modified-polarity rapid assessment method (m-PRAM) was used to partition NOM into three fractions, namely: the hydrophobic (HPI), hydrophilic (HPO) and transphilic (TPI) fractions. A full UV-Vis scan of samples in all filtrate samples was performed for quality assurance and quality control. Readings at representative wavelengths was recorded after each round of cleaning which included eluting 100 mL of deionized water.

5.2.4 Determination of biogenic NOM fraction

Section 3.5.6 describes in detail the method carried out in the determination of biogenic NOM fraction.

5.2.5 Modelling techniques

Section 3.6.3 describes the parallel factor analysis for the identification and quantification of fluorescent NOM fractions from a pool of data obtained from all the water sources under this study.

5.2.6 Determination of Spectroscopic indices

The determination of spectroscopic indices such as humification index, fluorescence index and freshness index is described in detail in **section 3.56**

5.2.7 Membrane and filtration equipment set up

5.2.7.1 Substrate membranes

The description of the membranes used, membrane characterisation and the operation conditions of the filtration runs is described in detail in **Sections 3.7.1, 3.7.2 and 3.8.1.**

5.2.7.2 Fouling Mechanisms and Fouling Resistance Determination

The mathematical determination of fouling mechanisms models is described in detail in **Section 3.8.2**. The membrane fouling behaviour can be described using the resistance-in-series model shown below (**Equation 5.1**) [2].

$$R_t = R_m + R_f = R_m + R_{rev} + R_{irr} = \frac{TMP}{\mu J} \quad (5.1)$$

where R_t is the total resistance during the ceramic membrane NF process (m^{-1}); R_m is the intrinsic membrane resistance (m^{-1}); R_f is the fouling resistance caused by membrane foulants (m^{-1}), including reversible resistance R_{rev} and irreversible resistance R_{irr}; TMP is the trans-membrane pressure, which was maintained at 3 bar in this work; μ is the dynamic viscosity of the feed water (Pa.s); J is the permeate flux of the membrane during the filtration process (m^3/m^2s).

Immediately before the undertaking of the filtration test, pure water flux of the membrane was determined by filtering ultrapure water to determine the initial flux of the membrane, with which the intrinsic membrane resistance R_m was calculated. Subsequently, the water sample was filtered for 8 hours, with the permeate mass recorded at specific time frames to determine the total fouling resistance R_f. The total fouling resistance obtained in the filtration experiments was expressed in normalized form as R_f/R_m.

5.3 RESULTS AND DISCUSSION

5.3.1 Removal of bulk parameters by ceramic membranes

The UV_{254} removal by the ceramic membranes was largely constant over time for all WTPs, thus giving an indication of a constant output even over extended operation times in real life operations (**Figure 5.1a**). This demonstrates the chemical stability and mechanical strength of ceramic membranes operation over time treating water of different physico-chemical properties. Notably, coastal plants (H and P) had the highest values for UV_{254} removal (both 80% on average) and UV_{254} removal by inland plants was in the range 55 - 60%. Perhaps the lower UV_{254} removal in inland plants was due to the character of NOM that was probably largely non UV absorbing and composed mainly of polysaccharides. Interestingly, a similar trend was observed with DOC removal (**Figure 5.1b**). Coastal plants (PL and H) removed more than 80% of *DOC,*

while inland plants removed between 60 - 75%. The difference in removal efficiency of *DOC* and UV_{254} of inland plants may be attributed to perhaps the differences in measurement instruments. Pyrolysis or chemical oxidation of the organic matter in the sample releases CO_2 and the non-dispersive infra-red detector (NDIR) quantifies the released gas as DOC, whereas UV_{254} measures the absorbance of the fraction of NOM that is chromophoric [3]. UV_{254} values for coastal plants were: 0.17, 0.29, and 0.41 cm^{-1} for HL, H, and PL, respectively, while inland plants had UV_{254} values of 0.14 and 0.21 cm^{-1} for OL and MV, respectively. Remarkably, the UV_{254} removal efficiency followed the order of magnitude of UV_{254} values at respective sources. UV_{254} is a measure of aromaticity of NOM; therefore the results suggest that ceramic membranes are selective depending on the aromaticity of NOM. This finding serves as a prediction tool by water treatment companies to forecast the removal efficiency of NOM by determining the UV_{254} values of the source waters.

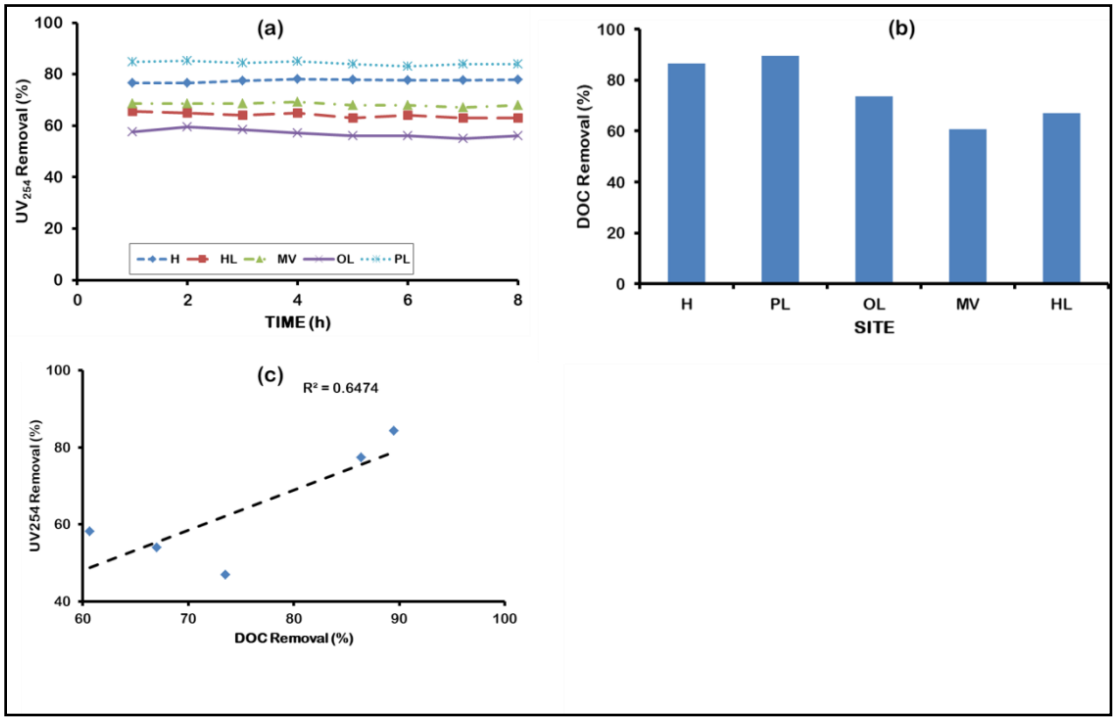

Figure 5. 1: Bulk parameter removal by ceramic membranes: (a) UV_{254} removal; (b) *DOC* removal and (c) correlation between UV_{254} and *DOC* removals.

The SUVA values for the coastal plants were 5.97 and 4.97, 3.97 for PL, H and HL, respectively, while for the inland plants they were in the range 2 – 4. Research has shown that SUVA > 4 indicates high hydrophobicity and SUVA < 2 is an indication of the predominance of non-humics, low molecular mass compounds and hydrophilicity. SUVA between 2 – 4 is exhibited by water which contains roughly an equal mixture of hydrophobic and hydrophilic moieties [4]. Therefore the results suggest ceramic membranes are particularly selective to retaining hydrophobic NOM as demonstrated by high *DOC* and UV_{254} removals by coastal plants. In general, the hydrophilic fraction of NOM is reported to be recalcitrant to removal by membrane technology compared to the hydrophobic fraction [5].

Our previous study investigated the removal efficiencies of *DOC* by conventional methods (coagulation, sedimentation, filtration and disinfection) at WTPs in South Africa, including those under current study, and *DOC* removal efficiencies was in the range -35 and 48% [1]. The current study has demonstrated *DOC* removal efficiency of between 60 and 80%, therefore integrating ceramic NF membrane technology with the conventional methods should result in greater *DOC* removal.

Figure 5.1c shows the observed relationship between the DOC and UV_{254} rejections by the ceramic membranes. A poor correlation was observed (R^2 = 0.65) between *DOC* and UV_{254} rejections, suggesting that the rejection mechanisms for *DOC* and UV_{254} may be dissimilar. Perhaps the reason for the difference is primarily about different selectivity and composition of NOM.

5.3.2 Removal of fluorescent fractions by ceramic membranes

Statistically derived components representing *FDOM* were achieved by pooling EEM data from all sources and inputting into the *PARAFAC* model. Therefore, the produced model culminated from diverse data points. The graphical representation of components is shown in **Figure 5.2a-d**. The identification of components was determined by comparing with those in the OpenFluor database that give similarity scores greater than

0.97 (**Table 5.1**). Analysis of the effectiveness of FDOM removal by the ceramic NF membranes showed more than 80% removal regardless of the location of the plant (Table A1). This suggests ceramic membranes have high selectivity towards the removal of fluorescent NOM fractions. The measured water contact angles ranged from 59.5^{o} to 62.4^{o}, these values demonstrated that the membrane surface exhibited a hydrophilic surface. The abundant –OH groups on the pore surface of native TiO_2 NF membranes render ceramic membranes more hydrophilic [21]. This was further corroborated by the computed surface free energy that had an acid-base component greater than 5 mJ/m^2. Surface roughness values from 63 to 71 nm were recorded. This indicates a relatively smooth surface. A smooth surface is ideal for a filtration process because it limits foulant/pollutant adhesion on the surface of the membrane and subsequently enhance the anti-fouling properties [22]. Raw water from coastal plants had a yellowish brown colouration, characteristic of the presence of humic and fulvic acid matter. This finding was further corroborated by high F_{max} for components *C2* and *C3*. Notwithstanding, the removal efficiency of these components was strikingly in the same range as the other plants, suggesting pollutant loading had no bearing on the efficiency of their removal by ceramic membranes. Further studies should investigate the dependence of produced water quality and pollutant loads in terms of character and quantity.

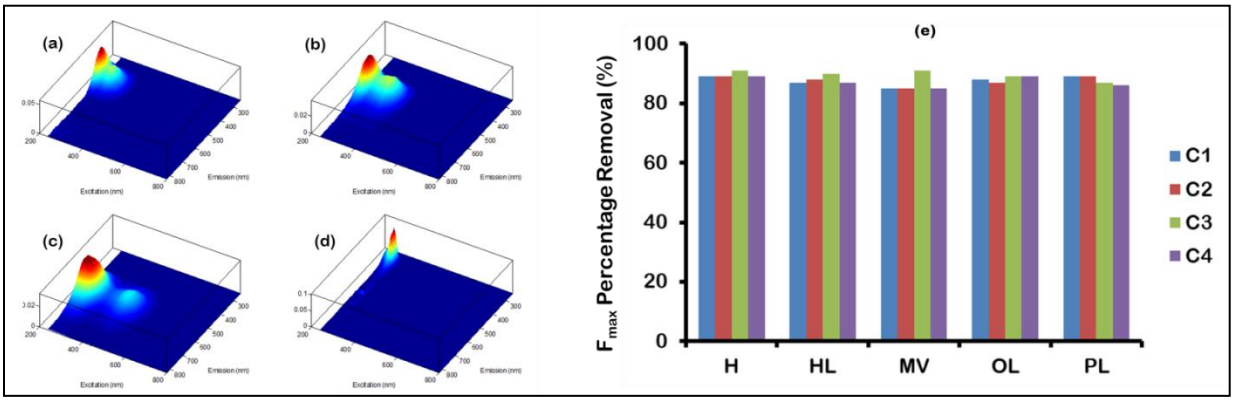

Figure 5. 2: Output of the validated components from the *PARAFAC* model (a) (*C1*), (b) (*C2*), (c) (*C3*), and (d) (*C4*), and (e) the F_{max} removal efficiency by ceramic membranes.

Table 5. 1: Identification of the derived components from the PARAFAC model.

Component	Similarity score	Component identity	Reference
C1	0.97	Reprocessed organic matter, Terrestrial humic like	[5]
max Ex/Em			
316/240(292)	0.98	Photo degradation by-products mimicking humic-like matter	[6]
C2	0.98	Soil derived fulvic acid like	[7]
max Ex/Em			
336/240(348)			
C3	0.97	Humic acid like	[8]
max Ex/Em			
364/240(450)	0.98	Conjugated macromolecular substances of terrestrial origin exhibiting aromatic humic acid like character	[9]
C4	0.99	tryptophan-like, protein	[10]
max Ex/Em			[11]
270/270	0.98	tryptophan-like	

5.3.3 Removal of biodegradable dissolved organic carbon fractions

The removal of *BDOC* by the ceramic membranes was above 85% with coastal plants (PL and H) having the highest removal rate (**Figure 5.3a**). Similar rates of *BDOC* removal (> 90%) by nanofiltration membranes have been reported [13]. Interestingly, the trend in the removal efficiencies of *BDOC* followed that of *DOC* removal (R^2 = 0.97) (**Figure 5.3b**). This implies that the removal of *DOC* can be a predictor of *BDOC* removal by ceramic membranes for the sampled water. The management of the *BDOC* fraction is important because it potentially causes bacterial regrowth in the water distribution system [14]. The *BDOC* fraction is also responsible for the alteration of the

physico-chemical properties of treated water, affecting the taste and odor, elevating turbidity, causing loss of residual chlorine, and subsequently increasing the formation of DBPs [15], [16].

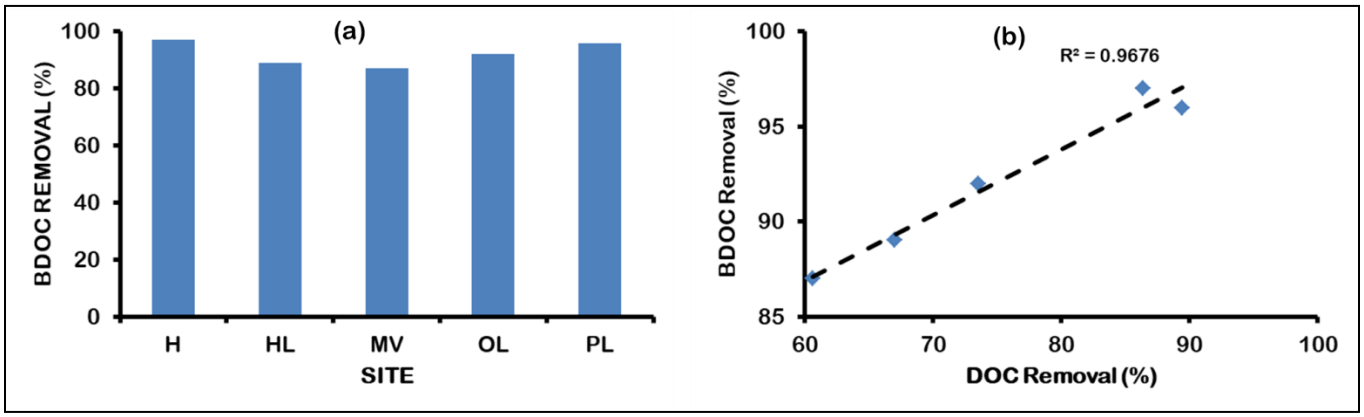

Figure 5. 3: (a) *BDOC* removal by ceramic membrane; correlation of *BDOC* removal; and (b) *DOC* removal

However, it should be noted that the use of membrane-based filtration methods does not completely remove post-treatment microbial proliferation. This is because of the passage of the assimilable organic carbon fraction (AOC) through the pores of the membrane even in the NF range (1 – 10 nm). The AOC fraction can pass through the pores of the membrane and supports bacterial recolonisation by acting as substrate for bacterial growth [17]. Ceramic membranes in the NF range are capable of physically removing bacterial cells, however, nutrients beneficial for the bacterial growth and proliferation can easily pass through NF membranes and promote recolonisation in the distribution system [18].

5.3.4 Removal of NOM polarity fractions

PRAM was used to determine the quantitative difference in organic matter polarity fraction concentration between the feed and effluent of the cartridge. The common problem with the PRAM method is the leaching of water-soluble organic residues and some loose SPE particles get washed off when water is passed through. This exaggerates values of parameters such as *DOC* and UV- vis absorbance. To curb this

problem sufficient cleaning was carried to completely wash off the SPE cartridges of organic matter, uncombined adsorbent chemicals, and methanol (**Figure 5.4**). Several rounds of cleaning guaranteed complete removal of those compounds.

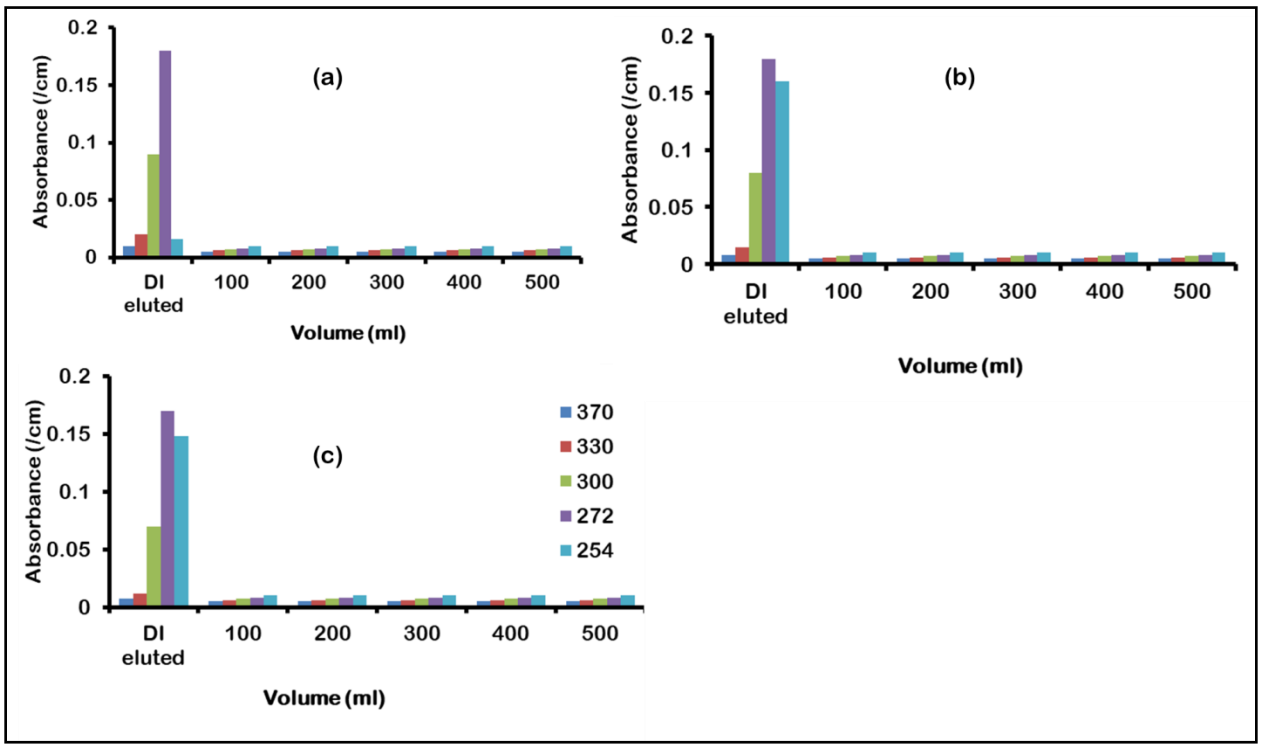

Figure 5. 4: Quality assurance for asserting no further leaching of carbon from SPE cartridges during (a) C18; (b) CN; (c) NH column cleaning

The *HPO* fraction was the most amenable to removal (above 60% for all sites), while the hydrophilic fraction was the least removed 30 - 47% by ceramic NF membranes regardless of the location of the WTP (**Figure 5.5a**). The *HPI* fraction is characterized by a low molecular weight and low C/O ratio, indicative of less aromatic carbon content [19]. The *HPO* fraction was removed by at least 60% by ceramic membranes regardless of the location of the WTP. The high removal of the *HPO* fraction is usually enhanced when the membrane is charged due to charge repulsion between the membrane and the carboxylic and phenolic groups whose pK_a values are in the range 2.5 and 5, while the phenolic hydrogens have pK_a values around 9 and 10 [20]. As a result, *HPO*

fractions are negatively charged due to ionization of carboxylic groups in the pH range of natural waters [5]. Further, *HPO* fractions have a quasi-linear molecular configuration due to intra-charge repulsion caused by the ionized carboxylic groups [5], [21]. Besides charge repulsion, steric repulsion can play a role in the high rejection of *HPO* compared to *HPI* fraction [21].

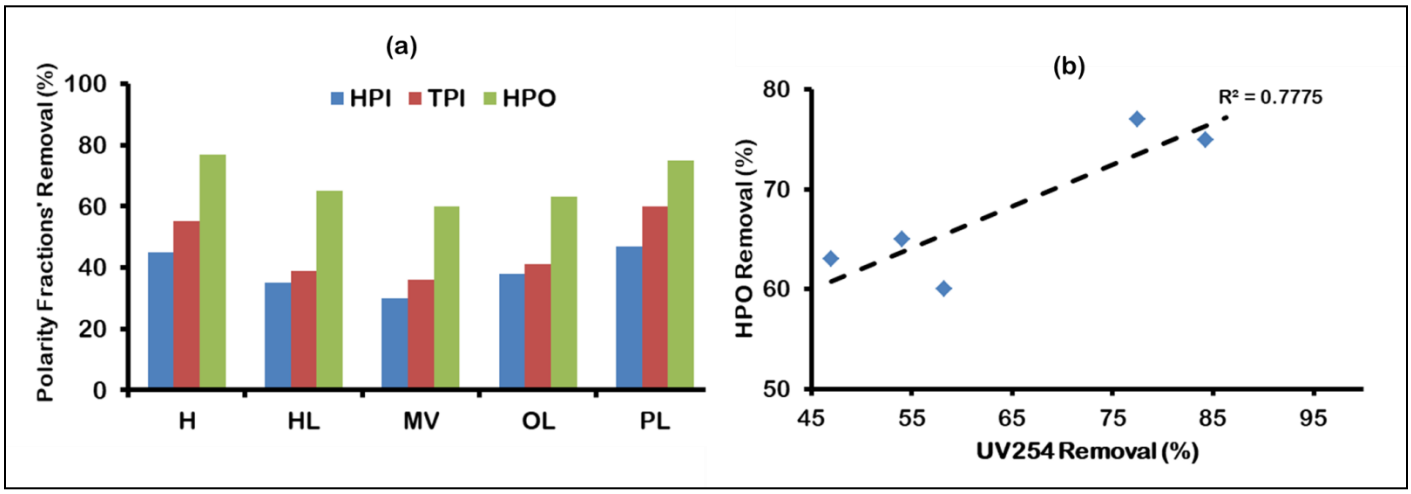

Figure 5. 5: NOM polarity fraction removal by ceramic membranes; (b) correlation between *HPO* removal with UV_{254} removal by ceramic membranes

The removal efficiency for the *HPO* fraction had a modest correlation with the removal of UV_{254} (R^2 = 0.78) (**Figure 5.5b**). Because UV_{254} is a measure of aromaticity and the *HPO* fraction is composed of aromatic groups with conjugated structures it was expected that a linear relationship should exist between the UV_{254} removal and *HPO* removal.

5.3.5 Correlation of fluorescent indices at source to removal of bulk parameters by ceramic membranes.

UV_{254} removal by ceramic membranes and *HIX* of the feed showed a good correlation (R^2 = 0.80) (**Figure 5.6a**). The humification index is reported to be good predictor of NOM removal efficiency [24];[23]. Surface waters with high humic substance content are characterized by high *HIX* value [25]. Therefore, high *HIX* content is equally

susceptible to removal as waters containing high humic substances can be easily removed by membranes [25]. This investigation confirms the aforementioned assertion, whereby higher *HIX* values corresponded to high UV removal (**Figure 5.6a**). A strong correlation between *FI* and UV_{254} was established (R^2 = 0.93) (**Figure 5.6b**). Terrestrially derived NOM (*FI* ≈1.7) susceptibility to removal by ceramic membranes is less than that of microbial derived NOM (*FI* ≈ 1.4) (**Figure 5.6b**). A previous study reported similar findings, when the *FI* index of raw water was greater than 1.5 the NOM in that water was less susceptible to removal by ultrafiltration membranes [23]. A strong correlation was observed between the freshness index *(β:α)* and UV_{254} removal (R^2 = 0.96) (**Figure 5.6c**). Surface water containing aged and condensed humic substances is characterized by low *β:α*, and is amenable to removal by coagulation or membrane filtration [23]. The high correlation of *FI* and *β:α* with UV_{254} removal can be traced to the character of NOM with microbial derived NOM having the greatest influence to the extent of removal by ceramic membranes.

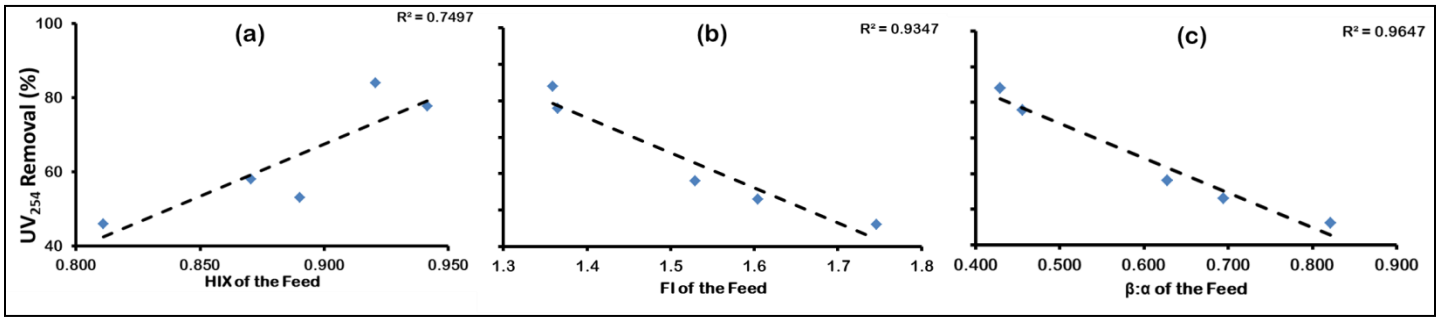

Figure 5. 6: UV_{254} removal by ceramic membranes correlations with (a) HIX, (b) FI and (c) β:*α*

5.3.6 Loss of permeate flux and fouling mechanism of different waters on ceramic membranes

The effect of the physico-chemical properties of water on fouling resistance is shown in F**igure 5.7a.** Plants MV and PL had the similar rates of fouling in the first 75 min, followed by a steady state for the subsequent 30-40 min. However, the rate of UV transmission (i.e the ratio of UV_{254} absorbance of the permeate and the UV_{254}

absorbance of the feed) was different within the same time frames for both plants (**Figure 5.7b**). UV transmission decreased for MV while it remained constant for PL. This suggests the mechanism of fouling was different, probably depending on the character of NOM in each of the sites. Blocking mechanisms which lead to flow reduction have been described by several theoretical models [25]-[28]. Four possible mechanistic models have been proposed, namely: cake filtration, complete blocking, intermediate blocking and standard blocking. Usually, it is not sufficient to designate an individual model to be solely responsible for flux reduction, rather, to different extents, all fouling mechanisms are responsible in flux reduction.

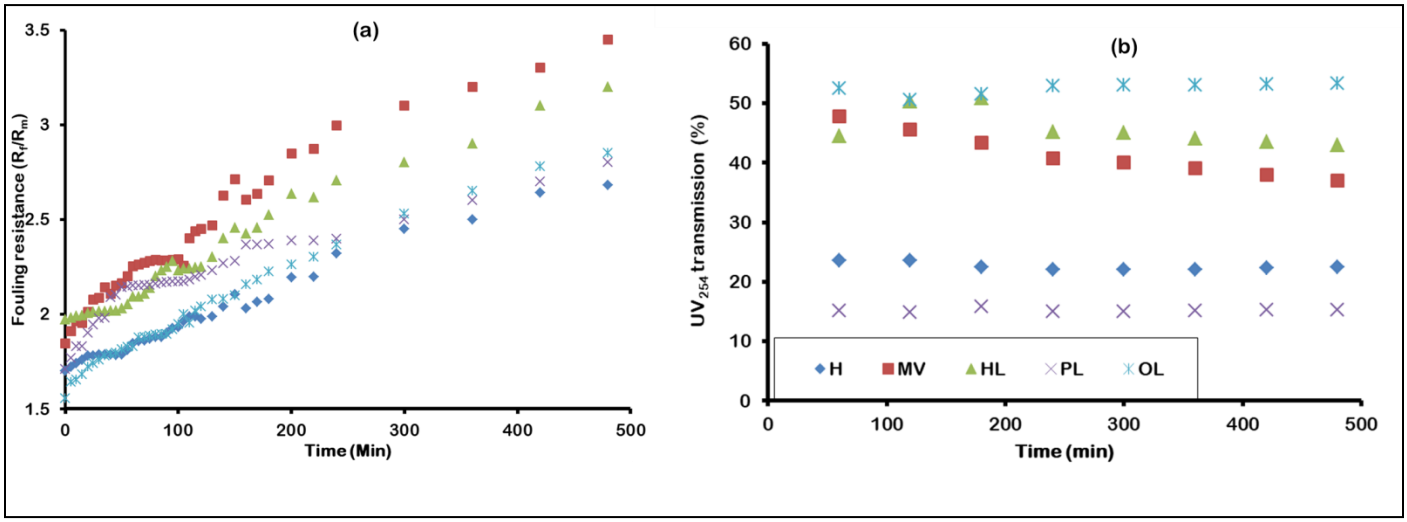

Figure 5. 7: (a) Fouling resistance development during filtration of water from different sites; and (b) UV-vis transmission during filtration of waters from different sites.

The size of the solutes relative to the pores of the membrane determines the extent and progression of each mechanism. For molecules smaller than the mean pore size of the membrane, intermediate blocking is expected to dominate the fouling at the initial phase, the subsequent stage is dominated by cake filtration fouling mechanism [26]. The dominant fouling mechanisms for PL were intermediate fouling and cake filtration (R^2 of 0.85 and 0.83 respectively) (**Table 5.2**). Thus, the UV transmission was constant because after intermediate fouling the cake layer did not allow any further significant

amounts of NOM to pass though. For MV all fouling mechanisms had almost equal contribution on fouling (for complete blocking; standard blocking; cake filtration and intermediate blocking, with R^2 = 0.94; 0.94; 0.98 and 0.79, respectively). However, the UV transmission of MV was higher than that of PL, implying fouling was severe with PL than MV.

Table 5. 2: Summary of the closeness of fit (R^2) of different fouling mechanism of water collected in different regions of South Africa.

	Complete blocking	Standard blocking	Cake filtration	Intermediate blocking
H	0.24	0.23	0.78	0.68
MV	0.94	0.94	0.98	0.79
HL	0.96	0.89	0.80	0.65
PL	0.40	0.40	0.83	0.85
OL	0.42	0.41	0.97	0.90

Plants H, HL and OL showed similar fouling rates in the first 3 h (**Figure 5.7a**). However, the rates of UV transmission at that time frame were different. Complete blocking and standard fouling were the dominant fouling mechanisms for HL (R^2 = 0.96 and 0.89, respectively) (**Table 5.2**). As the buildup of fouling progressed, the UV transmission in the first 3 h increased, implying NOM molecules smaller than the pores of the membranes were passing through.

Whereas for OL and H there was a constant UV transmission within the first 3 hours and there was an initial increase in UV transmission for HL, implying cake filtration was the least fouling mechanism within that time frame (**Figure 5.7b**). However, UV transmission for OL was higher than for all the other sites, implying OL least fouled the ceramic membranes compared to the other sites. Complete blocking (R^2 = 0.24 and 0.42 for H and OL, respectively) and standard blocking (R^2 = 0.23 and 0.41 for H and OL, respectively) were the least fouling mechanisms for H and OL. Intermediate

blocking (R^2 = 0.68 and 0.90 for H and OL, respectively), and cake filtration (R^2 = 0.78 and 0.97 for H and OL, respectively) were the dominant fouling mechanisms. This implies for H and OL an initial phase dominated by intermediate blocking was followed by a transition to cake filtration at a subsequent stage in the filtration process.

5.4 Conclusion

The percent removal of bulk NOM (measured as UV_{254} and DOC removal), the BDOC fraction, polarity fractions and FDOM fractions by ceramic membranes were investigated, and the key findings were:

- Ceramic membranes were more effective in removing bulk NOM for coastal plants than inland plants.
- The removal of FDOM did not depend on the location of the WTP.
- The removal of BDOC was high for coastal plants, and correlated well with DOC removal. Thus DOC removal can be an indicator to predict BDOC removal.
- The HPO fraction was the most amenable to removal by ceramic membranes regardless of the site of the WTP. UV transmission for OL was higher than all the other sites implying OL waters least fouled the ceramic membranes compared to the other sites.

This investigation revealed the dynamics of NOM fractions removal by ceramic membranes, specific to South African waters, and the results serve as an initial appraisal for the application of ceramic membranes in removing NOM in South Africa.

5.5 REREFENCES

[1] P. Tshindane (2019).The occurrence of natural organic matter in South African water treatment plants. *Journal of Water Process Engineering*, **31**(March),100809.

[2] J. Tian, M. Ernst, F. Cui, and M. Jekel (2013). Effect of different cations on UF membrane fouling by NOM fractions. *Chemical Engineering Journal*, **223**, 547–555.

[3] S. A. Baghoth, S. K. Sharma, and G. L. Amy (2010). Tracking natural organic matter (NOM) in a drinking water treatment plant using fluorescence excitation e emission matrices and PARAFAC. *Water Research*,**45**(2), 797–809.

[4] T. I. Nkambule (2012). Natural Organic Matter (Nom) in South African Waters: Characterization of Nom, Treatability and Method Development for Effective Nom Removal From Water. PhD Thesis, University of Johannesburg.

[5] S. Metsämuuronen, M. Sillanpää, A. Bhatnagar, and M. Mänttäri (2014). Natural Organic Matter Removal from Drinking Water by Membrane Technology. *Separation and Purification Technology*, **43**(July), pp. 1–61.

[6] M. A. Zazouli and L. R. Kalankesh (2017). Removal of precursors and disinfection by- products (DBPs) by membrane filtration from water ; a review. *Journal of Environmental Health: Science and Engineering*, **8**;15-25.

[7] U. J. Wu, K. R. Murphy, and C. A. Stedmon (2017). The One-Sample PARAFAC Approach Reveals Molecular Size Distributions of Fluorescent Components in Dissolved Organic Matter. *Environmental Science and Technology*, **51**(20), 11900–11908

[8] C. L. Osburn, L. T. Handsel, M. P. Mikan, H. W. Paerl, and M. T. Montgomery, (2012). Fluorescence Tracking of Dissolved and Particulate Organic Matter Quality in a River-Dominated Estuary. *Environmental Science and Technology*, **46**(16), 8628–8636

[9] C. L. Osburn, T. J. Boyd, M. T. Montgomery, T. S. Bianchi, R. B. Coffin, and H. W. Paerl (2016). Optical Proxies for Terrestrial Dissolved Organic Matter in Estuaries and Coastal Waters. *Frontiers in Marine Science,* **2**(January), 127.

[10] K. M. Cawley (2012). Characterising the sources and fate of dissolved organic

matter in Shark Bay , Australia : a preliminary study using optical properties and stable carbon isotopes. *Marine and Freshwater Research*, **63**, 1098-1107

[11] K. R. Murphy (2011). Organic Matter Fluorescence in Municipal Water Recycling Schemes : Toward a Unified PARAFAC Model. *Environmental Science and Technology*, **45**(7), 2909–2916.

[12] Y. Yamashita, B. D. Kloeppel, J. Knoepp, G. L. Zausen, and R. Jaffe (2011). Effects of Watershed History on Dissolved Organic Matter Characteristics in Headwater Streams. *Ecosystems*,**14**, 1110–1122.

[13] I. C. Escobar and A. A. Randall (2011). Assimilable organic carbon (AOC) and biodegradable dissolved organic carbon (BDOC): complementary measurements. *Water Research,* **35**(18), 4444–4454.

[14] L. G. Terry and R. S. Summers (2018). Biodegradable organic matter and rapid-rate bio fi lter performance : A review. *Water Research*,**128**, 234–245.

[15] W. T. Li (2017). Application of UV absorbance and fluorescence indicators to assess the formation of biodegradable dissolved organic carbon and bromate during ozonation. *Water Research*, **111**(March), 154-162.

[16] M. Vital, D. Stucki, T. Egli, and F. Hammes (2010). Evaluating the growth potential of pathogenic bacteria in water. *Applied and Environmental Microbiology*, **76**(19), 6477–84.

[17] E. I. Prest, F. Hammes, and M. C. M. Van Loosdrecht (2016). Biological Stability of Drinking Water : Controlling Factors , Methods , and Challenges. *Frontiers in Microbiology*, **7**(February), 1–24.

[18] A. Nescerecka, T. Juhna, and F. Hammes (2018). Identifying the underlying causes of biological instability in a full-scale drinking water supply system. *Water Research*,**135**,11–21.

[19] E. Lavonen (2015). Tracking Changes in Dissolved Natural Organic Matter Composition. Doctoral Thesis, Swedish University of Agricultural Sciences.

[20] T. Virtanen (2018). Characterization of membrane–foulant interactions with novel combination of Raman spectroscopy, surface plasmon resonance and molecular dynamics simulation. *Separation and Purification Technology*, **205**, 263–272.

[21] A. W. Zularisam, A. F. Ismail, M. R. Salim, M. Sakinah, and H. Ozaki (2007). The effects of natural organic matter (NOM) fractions on fouling characteristics and flux recovery of ultrafiltration membranes. *Desalination*, **212**(1–3),191–208.

[22] O. E. Trubetskaya, C. Richard, and O. A. Trubetskoj (2016). High amounts of free aromatic amino acids in the protein-like fluorescence of water-dissolved organic matter. *Environmental Chemistry Letters,* **14**, 495–500

[23] A. Lidén, A. Keucken, and K. M. Persson (2017). Uses of fluorescence excitation-emissions indices in predicting water treatment efficiency. *Journal of Water Process Engineering*, **16**, 249–257.

[24] X. S. He (2013). Fluorescence excitation-emission matrix spectra coupled with parallel factor and regional integration analysis to characterize organic matter humification. *Chemosphere*, **93**(9), 2208–2215.

[25] R. Shang (2014). *Ceramic Ultra- and Nanofiltration for Municipal Wastewater Reuse*. PhD Thesis, Technical University of Delft

[26] B. Teychene, G. Collet, and H. Gallard (2016). Modeling of combined particles and natural organic matter fouling of ultrafiltration membrane. *Journal of Membrane Science*, **505**(August), 185–193.

[27] A. W. Mohammad, Y. H. Teow, W. L. Ang, Y. T. Chung, D. L. Oatley-Radcliffe, and N. Hilal (2015). Nanofiltration membranes review: Recent advances and future prospects. *Desalination*, **356** (January), 226-254.

[28] S. J. Lee, M. Dilaver, P. K. Park, and J. H. Kim (2013). Comparative analysis of fouling characteristics of ceramic and polymeric microfiltration membranes using filtration models. *Journal of Membrane Science*, **432**.

[29] L. De Angelis, M. Marta, and F. De Cortalezzi (2013). Ceramic membrane

filtration of organic compounds : Effect of concentration , pH , and mixtures interactions on fouling. *Separation and Purification Technology*, **118**, 762–775.

CHAPTER 6*:...*

Fundamental fouling mechanisms of DOM fractions and their implications on the surface modifications of ceramic nanofiltration membranes. Insights from a laboratory scale application

---

6.1 INTRODUCTION

Although ceramic materials were introduced to the water treatment industry more than a decade ago, little is known about their behaviour during fouling by organic macromolecules. Therefore, in order to advance the use of ceramic membranes in water treatment, it is important to understand the fundamental fouling mechanisms involved during the filtration process. The most commonly used fabrication method for ceramic membranes is the sol-gel method. However, this method poses a challenge in the development of tight ceramic nanofiltration (NF) membranes. Atomic layer deposition (ALD), a gas-solid phase coating procedure for growing atomic-scale thin films, provides a potential solution for addressing sol-gel fabrication deficiencies and for modifying ceramic membranes. The surface reactions of ALD result in exquisitely uniform and conformal pinhole free 3-D coatings of metal oxides on the membrane surface and pore walls, resulting in predetermined pore size. The ALD modified membranes show promise in increased water permeability, however there is no reported study to demonstrate the impact or mechanism of fouling on these membranes compared to the pristine membranes. The purpose of this work was to investigate, model and identify the contributions of each DOM fraction (humic acid, bovine serum albumin, and sodium alginate) in permeate flux decline during ceramic membrane filtration of ALD modified membranes and compare them with those the pristine membranes.

This chapter is based on:

Moyo W, Motsa M.M, Chaukura N, Msagati T.A.M, Mamba B.B, Heijman S.J.G and Nkambule T.T.I (2019). Fundamental fouling mechanisms of DOM fractions and their implications on the surface modifications of ceramic nanofiltration membranes. Insights from a laboratory scale application. *Water Science and Technology*, **80**(9), 1702-1714.

Moyo W, Motsa M.M, Chaukura N, Msagati T.A.M, Mamba B.B, Heijman S.J.G and Nkambule T.T.I. The synergistic fouling of ceramic membranes by particles and natural organic matter fractions using different surface waters in South Africa. Journal of Membrane Science and Research. In Pres

6.2 MATERIALS AND METHODS

The reagents used were of analytical grade and were purchased from Sigma Aldrich, South Africa. Deionized (DI, Milli-Q, Millipore, USA) water was used in all experiments. Humic acid (HA) (50 mg/L), bovine serum albumin (BSA) (20 mg/L), and sodium alginate (SAL) (30 mg/L) were used as model dissolved components of organic matter namely humus substances, protein-like and polysaccharide-like substances, respectively (**Table 6.1**) [1]–[3]. Solutions of 10 mM ionic strength were prepared using NaCl, KCl, $CaCl_2$, and $MgCl_2$ as background electrolytes. Although concentrations of the foulants used here are above those in surface waters [4], they mimic foulant concentrations after extended operation.

Table 6. 1: Compositions of the various feed solution tested during filtration experiments *(n = 3)*

Feed solution	DOC Concentration (mgL^{-1})	pH	Turbidity (NTU)	Conductivity (μSm^{-1})
SAL	13	6.08	0.65	935
BSA	7	5.08	0.68	688
HA	18	6.69	18.88	442
SAL + BSA	27	5.9	0.00	973
SAL + HA	18	6.1	17.89	1237
BSA + HA	22	5.8	16.21	449
SAL + BSA + HA	35	8.5	14.01	1132

6.2.1 Membrane Contact angle and surface energetics

Contact angles of the membranes and surface energetics were determined by method described in **Section 3.7.2**

6.2.2. Membrane characterisation

The membrane surfaces were characterised according to the method described in **Section 3.7.3**

6.2.3 Modification of Ceramic Membranes via the Atomic Layer Deposition

Coating TiO_2 onto substrates was achieved by the use of a flow-type ALD reactor (TU Delft, the Netherlands). Titanium tetrachloride $TiCl_4$ (Sigma-Aldrich/Fluka, the Netherlands) and demineralized water vapour were used as precursors for this reaction. Nitrogen gas (HiQ 5.0, Linde Gas Benelux, the Netherlands) was used as a carrier of the diluted precursors. An infrared lamp connected to a digital temperature probe was used to heat up the ALD reactor to an operating temperature of 70°C. The gaseous precursors deposited on the substrate in a direction perpendicular to its surface. Upon exposure to the substrate, $TiCl_4$ chemisorbed in accordance with **Equation 6.3** [12].

$$n(-OH)^* + TiCl_4\,(g) \rightarrow (-O-)_n\,TiCl_{4-n}{}^* + nHCl(g) \qquad (6.3)$$

** denotes the surface species*

Following the use of N_2 to purge off the excessive $TiCl_4$, hydrochloric acid vapours was produced. As depicted in **Equation 6.4**, the co-reactant H_2O was introduced into the chamber to complete one cycle of coating [12].

$$(-O-)_n\,TiCl_{4-n}{}^* + (4-n)H_2O(g) \rightarrow (-O-)_n\,Ti(OH)_{4-n}{}^* + (4-n)HCl(g) \qquad (6.4)$$

Residual H_2O and the produced HCI vapours were then purged off using dry N_2. The process was carried out to obtain two coats to keep the pore sizes as close as possible to the unmodified membranes so that the only variable for comparison was surface modifications.

6.3 RESULTS AND DISCUSSION

6.3.1 Fouling Characteristics of Single Foulant on the Pristine Membranes

6.3.1.1 Permeate flux loss due to single foulant on the pristine membranes

Permeate flux drop caused by alginate was drastic (54%, J_0 = 11.51 $Lh^{-1}m^{-2}$) (**Figure 6.1, Figure A2(a)**), indicating severe membrane fouling that is consistent with previously reported SAL fouling studies [6]. Complexation with cations could have enhanced the SAL – SAL interactions, leading to their subsequent deposition on the membrane surface. In the early filtration stage, flux decline decreased drastically at a rate of 4.16 x 10^{-2} $Lh^{-1}m^{-2}$ in the first 100 min. Thus, the interplay of permeation drag force generated in the early stages of the filtration process and membrane - SAL interactions promoted the adhesion of SAL onto the membrane surface [2].

The presence of cations promoteed the formation of alginate-cations aggregates, which in turn were responsible for the flux decline and its severity was increased with the increase of the effective size of the alginate molecules. HA-calcium complexes have been shown to form in the presence of Ca^{2+}, and can intensify the HA fouling [7]. Moreover, it has been shown that HA is not preferentially and exclusively selective towards Ca^{2+} cations. In this study, other cations (Na^{+}, K^{+} and Mg^{2+}) present in solution competed for the negative charges in the HA, resulting in the formation of varying sizes of HA aggregates that are not easily deposited onto the membrane surface [7]. In the early filtration stage, flux decline decreased moderately in the first 100 min at a rate of 2.69 x 10^{-2} $Lh^{-1}m^{-2}$ (**Figure 6.1**).

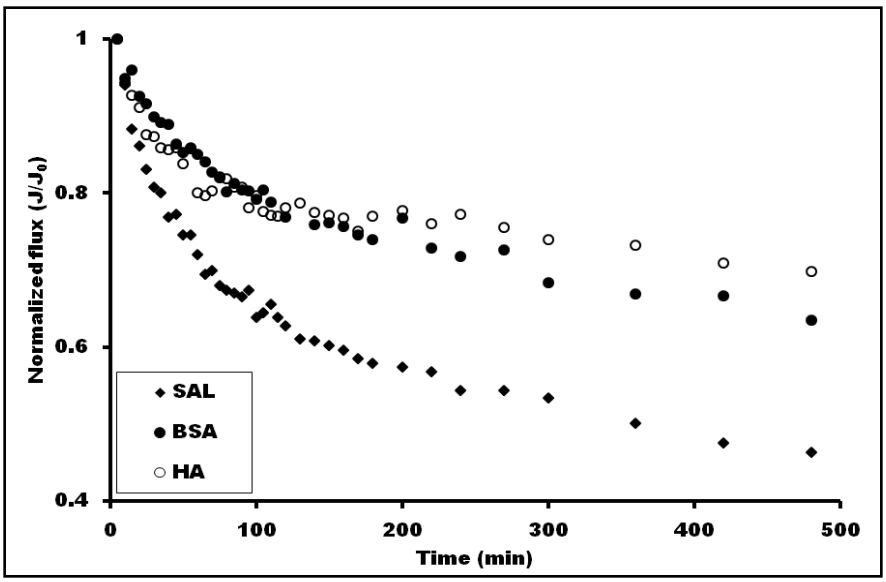

Figure 6. 1: Permeate flux loss due to single model organic foulants on the pristine membrane.

Permeation drag force generated in the early stages of the filtration process and membrane-HA interactions promoted the adhesion of HA onto the membrane surface at different rates. The deposition of HA onto the membrane was moderately stable after the initial 100 min of flux decline, suggesting the small HA-cation aggregates did not favourably form a multilayered structure that could potentially result in increased flux decline.

Membrane fouling due to BSA deposition showed a flux decline rate of 1.60 x 10^{-2} $Lh^{-1}m^{-2}$ (J_0 = 12.87 $Lh^{-1}m^{-2}$) in the first 100 min. Permeate flux remained stable due to the inability of the deposited monolayer BSA which had a negligible effect on the membrane flux. However, as the filtration progressed permeation, drag formed a multi-layered film of protein on the membrane that provided resistance to permeate flow. It can therefore be conjectured that the accumulation of the multi-layered film resulted from the interactions between adsorbed BSA molecules and incoming molecules, and BSA-membrane interactions were at play at the initial stages of the macromolecular adsorption. Polysaccharides and protein-like fractions have previously been reported to

be responsible for severe membrane fouling during wastewater treatment thus corroborating our findings [8]. Results emanating from this study have demonstrated that, for the single foulant, foulant deposition on the membrane surface in the early stages of filtration was primarily governed by membrane-foulant interactions.

6.3.1.2 Modeling fouling mechanisms of single foulant on the pristine membranes

The SAL filtration experiments demonstrated an almost 33% (J_0 = 11.51 $Lh^{-1}m^{-2}$) sharp decrease in the initial flux after only 100 minutes of filtration. Similar behaviour, which is associated with the rapid formation of a gel-like layer that presents an extra resistance to water permeability, was reported for SAL filtration using polymeric membranes [9]. The interpretation of the experimental data using the mechanistic SAL models (**Figure 6.1 a-d**) is consistent with cake filtration mechanism (R^2 = 0.99) that is preceded by intermediate blocking (R^2 = 0.96), whereby not only are the surface pores blocked by particles but also the particles deposit onto each other. The initial large decay of the flux evolution, which ends at a point of blockage of the surface pores, coincides with the commencement of the considerable slower reduction of permeability. The mechanistic fouling models points to cake filtration as the predominant fouling mechanism, thus supporting our findings. Due to the bigger size of the aggregates formed during SAL-Ca^{2+} complexation, a rather loose permeable gel layer is formed on the surface.

In BSA filtration, experimental data adjusted well to standard (R^2 = 0.94) intermediate blocking (R^2 = 0.96) and ultimately complete blocking (R^2 = 0.94) mechanisms, indicating adsorption onto the inner pores of the membrane. Interestingly, as evidenced by an R^2 value of 0.90, cake filtration seems to be the least likely mechanism of fouling (**Figure 6.2 a-d**).

HA fouling mechanisms had almost equal occurrence for complete blocking, standard blocking, and intermediate blocking (R^2 = 0.87; 0.87 and 0.83 respectively) (**Figure 6.3 a-d**). These results suggest an equal interplay of these fouling mechanisms. However, it could not be established whether these fouling mechanisms occurred sequentially or

concurrently. The deposition of small HA-cation aggregates formed a somehow soft cake layer without further formation of multilayers without altering the rate of flux decline.

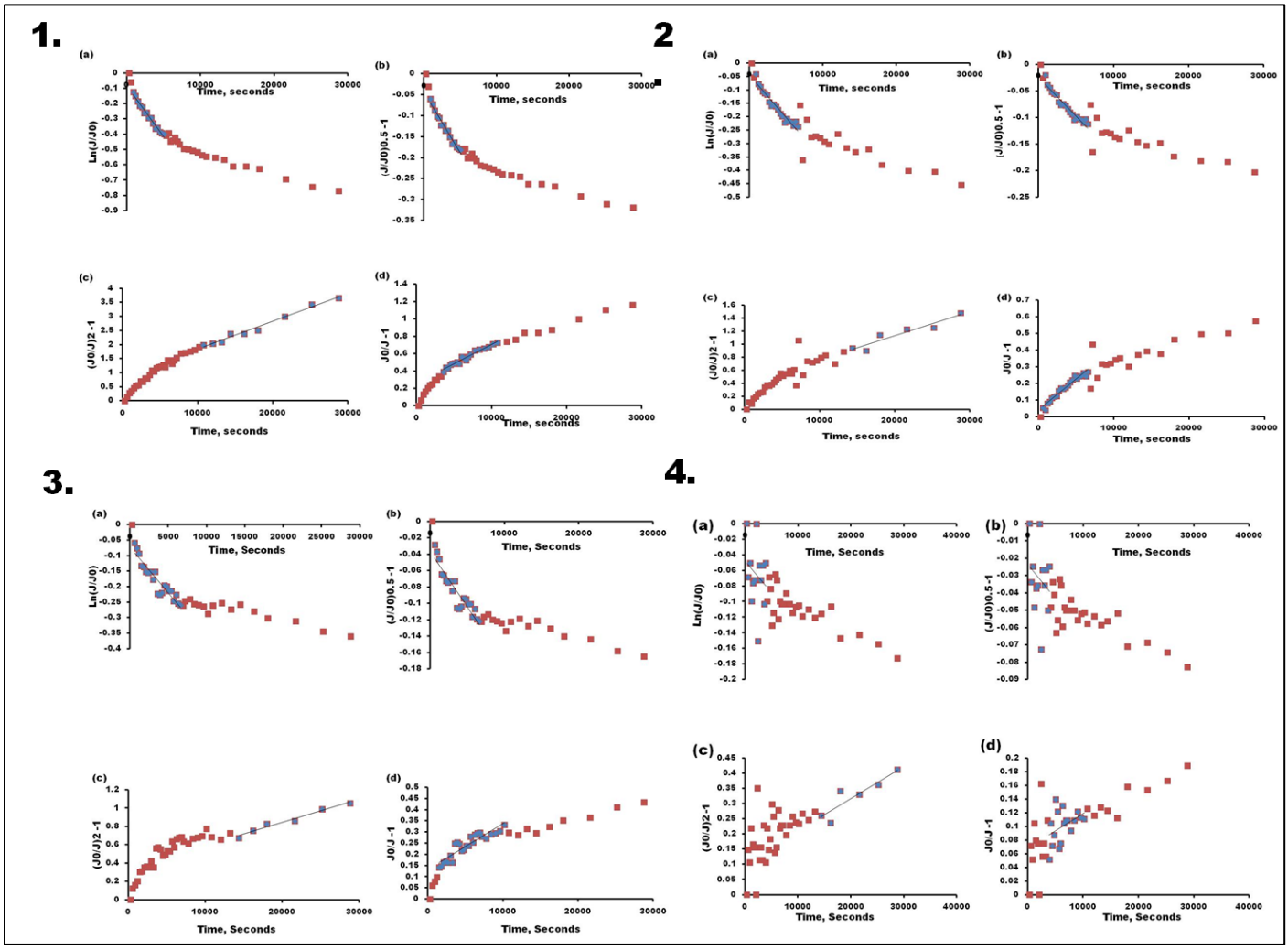

Figure 6. 2: Mechanistic fouling of single foulants on the pristine membrane - 1: SAL; 2: BSA; 3: HA and modified membrane - 4: SAL. Where (a) complete blocking, (b) standard blocking, (c) cake filtration, (d) intermediate fouling.

6.3.1.3 Permeate flux lose due to single foulants tracked by FEEM-PARAFAC model on the pristine membranes

Due to the HA and BSA fluorescing in the UV-Vis regions, it was possible to follow their filtration progress using fluorescence excitation emission matrix (FEEM) spectroscopy. The quantification of the foulants in the concentrate and permeate was monitored using the inbuilt SOLO software for PARAFAC analysis (**Figure 6.3**). As depicted by minimum fluctuations in the F_{max} of the concentrate, the fouling behaviour of BSA was expected constant in the first 120 min. A decrease in the F_{max} signal of the permeate was noted, thus suggesting reduced permeation of BSA through the membrane barrier after 180 to 300 minutes of filtration. This implies more protein molecules, which result from BSA-BSA interactions that form a multi-layered film and thus provide resistance to permeate flow, were deposited onto the adsorbed BSA monolayer (**Figure 6.3a**). A shift in the F_{max} observed from 300th minute until the end of the filtration run suggests a change in the fouling mechanism. This staged filtration character of BSA has been reported by Motsa et al. (2018)[6]. Little variation of F_{max} was observed for HA during the entire filtration run. Although the F_{max} signal was found to be higher in the concentrate, it was almost consistent during the entire filtration run (**Figure 6.3b**). Our results, which are consistent with previously reported findings, suggest that the Ca^{2+} ions chelate with HA-forming aggregates that do not easily settle or pass through the membrane barrier [1], [10], [11].

The fraction of NOM that fluoresces in the UV-Vis range is referred to as fluorescent natural organic matter (FNOM). Since they are the main components of membrane fouling, the FNOM fractions important for NF applications are proteins and humic substances [10]. Therefore, fluorescent NOM fractions have to be monitored and controlled in NF membrane operations.

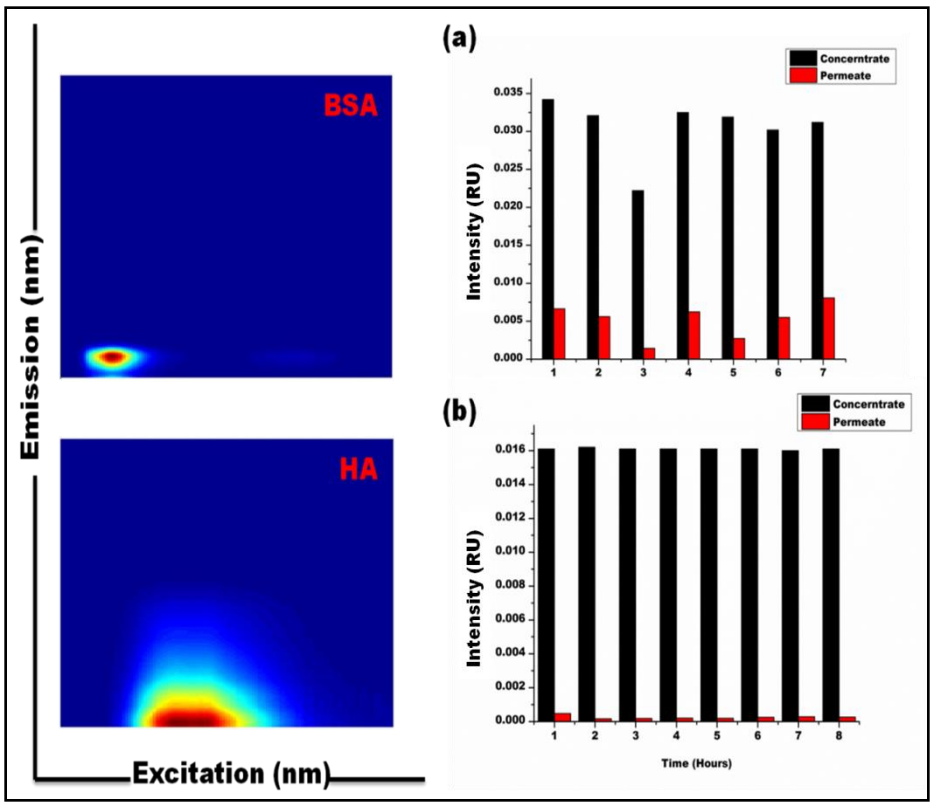

Figure 6. 3: EEM contours of model foulants identified by PARAFAC and their relative abundance in the concentrate and in the permeate of the pristine membrane (a) BSA component and (b) HA component.

6.3.2 Effect of Foulant Mixtures on the Pristine Membranes

6.3.2.1 Permeate flux loss due to combined foulants on the pristine membranes

The HA-SAL-BSA and HA-SAL combinations followed a similar trend and were accompanied by a respective flux loss of 22%, J_0 = 21.61 $Lh^{-1}m^{-2}$ and 25%, J_0 = 20.31 $Lh^{-1}m^{-2}$ within the first 100 minutes, respectively (**Figure 6.4, Figure A2(b)**). Within the same period of time, SAL and BSA led to a flux loss of 38% and 20%, respectively. In the presence of other foulants, SAL reduced its fouling propensity, probably as a result of the competition of the foulants for the cations. The concentration of the cations was therefore significantly reduced compared to the concentrations of the foulants. In this regard, SAL complexation was found to be minimal; instead of forming aggregates that

could settle on membrane surface resulting in lower flux loss compared to the sole application of SAL, the bulk of SAL remained in solution.

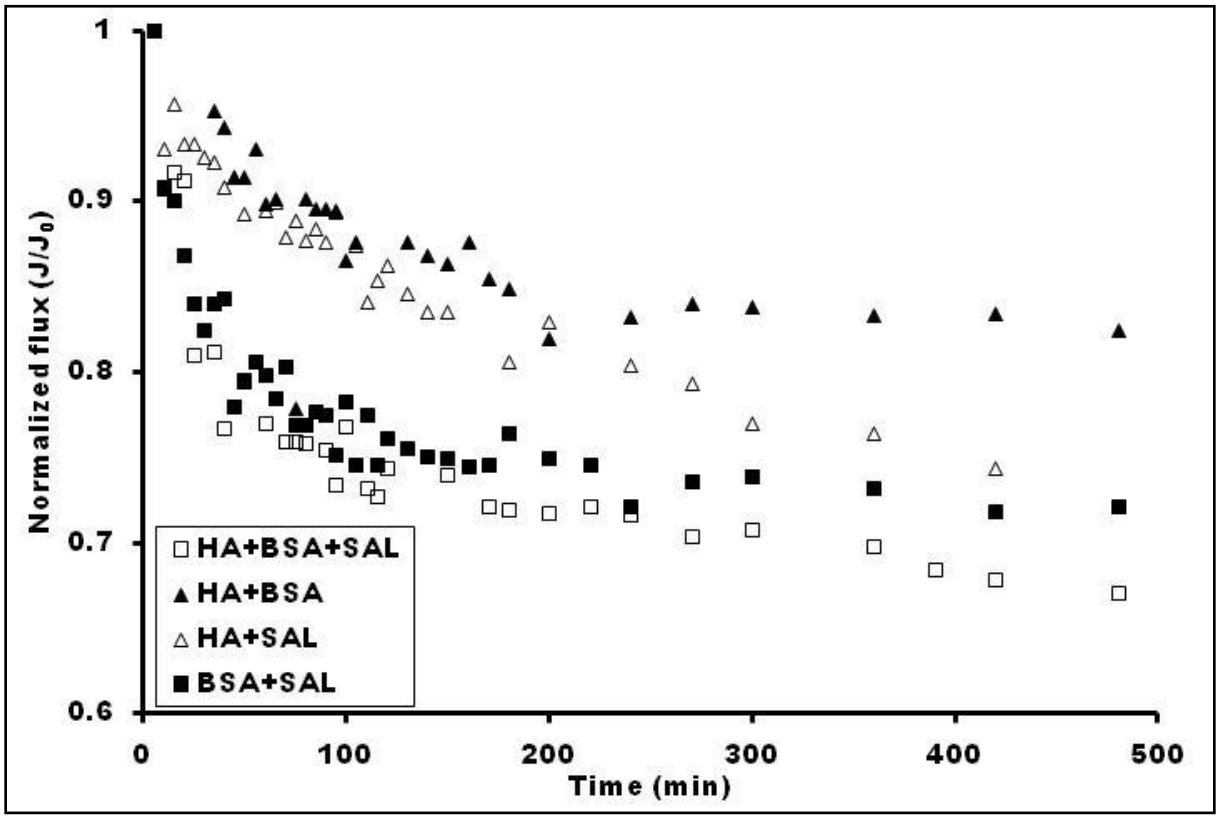

Figure 6. 4: Permeate flux loss profiles due to combined foulants on the pristine membrane.

A summary of the experimental R^2 values is shown in **Table 6.2**. It was interesting to note that cake filtration was least indicated fouling mechanism in feed solutions containing BSA and SAL (R^2 = 0.52, 0.37 for BSA+SAL and BSA+SAL+HA, respectively). This finding is in sharp contrast to the findings reported in the literature, whereby such mixtures supported cake filtration resulting from the incorporation of the BSA macromolecules into the SAL-cation complexes [12]. Feed stream containing HA and SAL indicated cake filtration fouling mechanism (R^2 = 0.97) to be the most likely fouling mechanism, this was ascribed to the complexation of cations to the organics leading to the formation of large HA - cation, SAL - cation and SAL - HA complexes that

settle on the surface of the membrane and increase the resistance to permeate flow. Permeate flux loss was enhanced by the deposition of these large aggregates via permeation drag forming a layer that also reduced the back-diffusion of salts from the membrane surface to the bulk solution. However, previous studies have reported that the surface charges of these foulants are negative, and should therefore repel each other [12]. Depending on the magnitude of the negative charge, the formation of combined macromolecular structures is hindered due to charge repulsion. The presence of cations then necessitates on a competitive basis, the formation of smaller aggregates that do not easily settle on the surface of the membrane thus minimising the cake filtration effect.

Table 6. 2: Summary of the R^2 of the mechanism of fouling for single and combined foulants

	Unmodified membrane							Modified membrane	
	SAL	HA	BSA	HA+ SAL	HA+ BSA	BSA+ SAL	SAL+ HA+ BSA	SAL	SAL+ HA+ BSA
Complete blocking	0.98	0.87	0.94	0.80	0.85	0.78	0.76	0.06	0.74
Standard blocking	0.98	0.87	0.94	0.80	0.85	0.75	0.75	0.06	0.74
Cake filtration	0.98	0.97	0.90	0.97	0.45	0.52	0.37	0.82	0.99
Intermediate blocking	0.96	0.83	0.96	0.80	0.70	0.57	0.60	0.17	0.39

Whereas the combination of BSA+HA and BSA+SAL resulted in a respective flux loss of 15 (J_0 = 15.22 $Lh^{-1}m^{-2}$) and 25 % (J_0 = 8.14 $Lh^{-1}m^{-2}$), the flux loss of individual HA and SAL was 21 (J_0 = 7.89 $Lh^{-1}m^{-2}$) and 54 % (J_0 = 11.51 $Lh^{-1}m^{-2}$), respectively. In addition, of particular interest for this study was the fact that dual combinations containing BSA favoured complete blocking fouling mechanism (R^2 = 0.85 and 0.78 for BSA+HA and BSA+SAL, respectively) and standard blocking fouling mechanism (R^2 = 0.85, 0.75 for

BSA+HA and BSA+SAL respectively). These results suggest the presence of BSA disrupts the formation of large macromolecular structures of organic-cation and organic-organic complexes. This could be because BSA has a larger charge density and smaller size that enhances the attraction of more positive charge towards itself thus leaving the bulkier HA and SAL in solution. The flux loss trend was strikingly similar to that of solitary BSA, which exhibits a two stage fouling behaviour. Firstly, a rapid flux loss in the first 200 minutes for BSA+HA, and 150 minutes for BSA+SAL, followed by a steady state flux that lasts to the end of the experiment.

Although the single and dual combination of HA and SAL favoured cake filtration (R^2 = 0.97; 0.99; 0.97 for HA; SAL and HA+SAL, respectively) (**Table 6.2**), and the flux loss of 21; 54 and 25 % for HA; SAL and HA+SAL, respectively, the co-existence of HA and SAL in the feed reduced the fouling propensity of SAL on its own. This could be attributed to competition for cations in solution, with HA attracting more positively charged species than SAL, thus leaving most of SAL in solution. The resulting trend in flux loss for the combined HA+SAL is dissimilar to that of the single constituent foulants. The trend for HA+SAL fouling showed an almost linear decline whereas single foulants showed a two-part fouling behaviour. Initially, a rapid flux decline was exhibited, which was followed by an almost steady state flux towards the end of the experiment.

6.3.3 Influence of Membrane Surface Modification on Flux Decline

The impact of membrane surface modification was studied with feed solutions that caused the most severe fouling on the pristine membranes, namely: SA and HA+BSA+SAL (**Figure 6.5, Figures A2 (c) and (d))**. When SA was used as the foulant, the rate of flux decline (25%, J_0 = 6.12 $Lh^{-1}m^{-2}$) was similar for both membranes in the first 50 minutes. Thereafter, a steady state flux was observed for the coated membrane whilst a declining flux trend was exhibited by the pristine membrane (**Figure 6.5a**). The modification of the membranes led to a 35% improvement in the flux recovery when SAL was used as the foulant. For both types of membranes, cake filtration was the

favoured fouling mechanism (R^2 = 0.99 and 0.82 for the pristine and coated membranes, respectively). These results suggest modification of the ceramic membranes investigated leads to an improvement in their anti-fouling property. Inherent to the ceramic membrane surface is the presence of the negatively charged OH group [13]. It appears coating introduced a higher number of OH groups onto the surface of the membrane resulting in greater electrostatic repulsion of SAL.

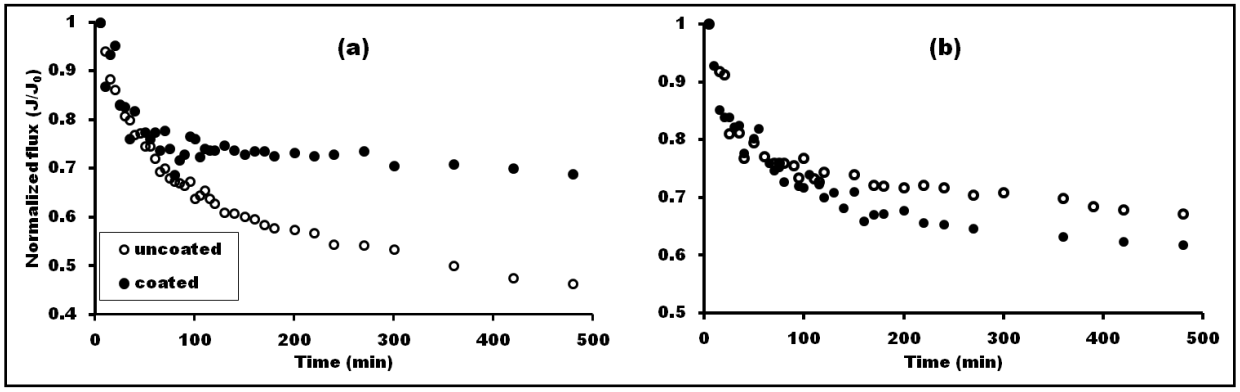

Figure 6. 5: Comparison of fouling profiles of coated and pristine membranes due to (a) SAL foulant and (b) HA+BSA+SAL.

However, no significant difference in flux loss was observed when the foulants were combined in the feed. In fact, the pristine membrane performed better than the coated membrane by a 5% margin in the resultant flux decline (**Figure 6.5b**). The fouling mechanism was almost similar for both membranes. For the coated membrane, R^2 = 0.74; 0.74 and 0.40 for complete blocking, standard blocking, and intermediate blocking, respectively, whilst for the pristine, R^2 = 0.76; 0.75 and 0.60 for complete blocking, standard blocking, and intermediate blocking, respectively. Whereas cake filtration was the most likely fouling mechanism for the coated membrane (R^2 = 0.99), cake filtration was the least likely fouling mechanism for the pristine membrane (R^2 = 0.37). The cations have been reported to act as bridges between the increased OH groups introduced by coating and the foulants in the feed solution, thus promoting the sedimentation of foulants onto the coated membrane [13].

6.3.4 Fundamental Differences Brought About by Modification

6.3.4.1 Contact Angle

Upon additional deposition of TiO_2 layers on the membrane surface, the measured water contact angles dropped from 58° to 38° (**Figure 6.6**), indicating the improved water affinity. This means the membrane could easily be wetted by water during filtration, and this has a positive impact on mass transfer (water transport) and weakening the adhesion forces between the membrane surface and foulants. The anti-fouling properties are thus improved. This observation was further complemented by the surface free energies for the two membranes (**Table 6.3**). After atomic layer deposition of TiO_2, the membrane hydrophilicity was enhanced by the addition of more OH groups. In general, the term "surface hydrophilicity/ hydrophobicity" is defined in terms of the value of the measured contact angle; with an angle of less than 90º considered hydrophilic, and a contact angle of 90º and higher regarded as hydrophobic.

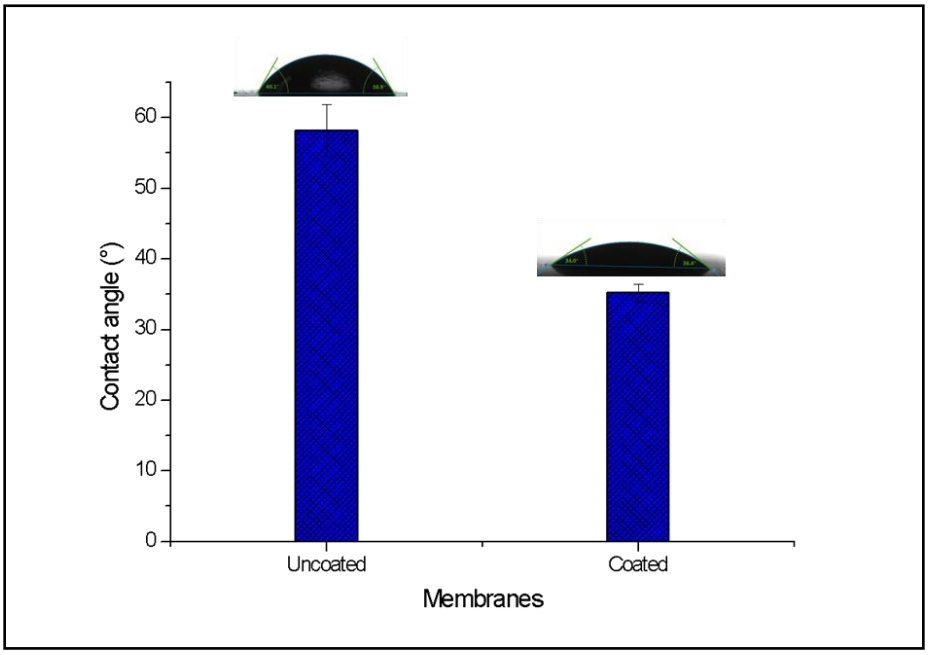

Figure 6. 6: Comparison of contact angle of the coated and uncoated membrane

6.3.4.2 Surface energetics

All the membranes were found to possess a strong electron donor mono-polarity (**Table 6.3**). The values of the surface free energy components correlated with the measured water contact angles. The pristine membranes had a slightly higher Liftshitz-van der Waals component, which corresponds to the contact angle of the apolar liquid (i.e. diiodomethane) and thus the inclined water contact angle. The computed value of the acid-base (γ^{AB}) component, which is an indicator of hydrophilicity was 6.62. This γ^{AB} value increased to 9.06 upon coating with TiO_2, thus confirming the increase in surface hydrophilicity. The deposition of TiO_2 creates favourable interactions between the membrane surface and water molecules, which subsequently lowers the adhesion forces between on-coming foulants and the membrane surface, thus limiting the fouling propensity.

Table 6. 3: Surface free energy components for the unmodified and modified membrane samples

	Surface free energy components				
	γ^{LW}	γ^{+}	γ^{-}	γ^{AB}	γ^{TOT}
Pristine	38.57	0.24	45.09	6.62	45.20
Coated	35.30	0.36	56.69	9.06	44.36

6.3.4.3 Surface elemental composition

The SEM imaging and EDS mapping (**Figure 6.7**) of the coated and pristine membranes indicates that the membrane consists of a porous support that contains a significant amount of Al. The selective layer showed the presence of both Al and Ti, confirming that the ALD process deposited an ultrathin layer on the surface. Interestingly, the cross-sectional elemental analysis of the coated membrane did not show any presence of Ti as a constituting element, thus confirming pore constriction did not occur (**Figure 6.7b**). Hence, the observed change in water affinity was mainly due to

favourable interactions between the TiO_2 on the active layer and the water molecules, which subsequently led to enhanced anti-fouling properties of the membrane

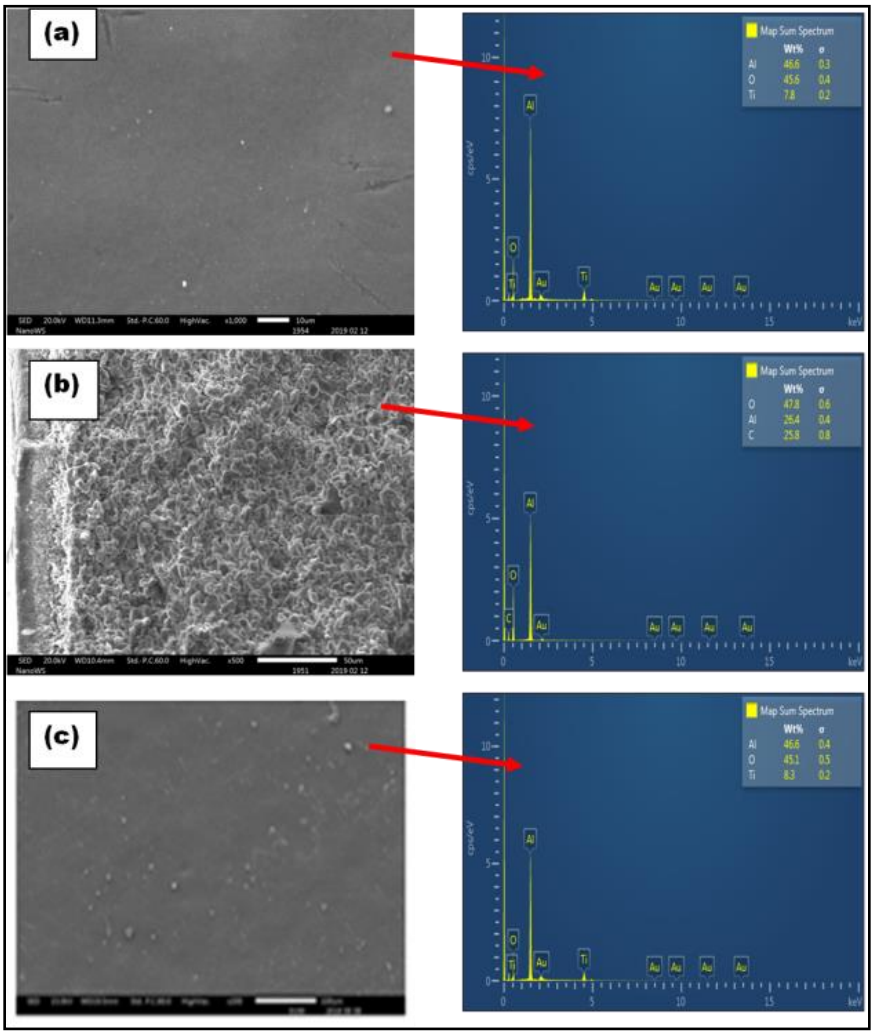

Figure 6. 7: Surface elemental composition of the (a) top side of the coated membrane, (b) cross section of the coated membrane and (c) top side of the pristine membrane

6.4 CONCLUSION

The purpose of this work was to investigate and identify the contributions of each of the individual DOM fraction and their combinations (i.e. SAL, HA and BSA) in permeate flux decline during ceramic membrane filtration. The effect of membrane surface modification on fouling resistance was studied by comparing their performance of both

TiO_2 ALD-coated and pristine membranes. The results showed that SAL caused the most extensive fouling on pristine membranes, and the ALD coating reduced the fouling potential of these membranes by 35%.

Cake filtration was found to be the least likely fouling mechanism occurring in feed solutions composed of BSA and SAL, and the most favourable fouling mechanism of feed solution made up of HA and SAL. The fouling mechanisms were almost similar for both the coated and the pristine membranes. For the coated membrane, R^2 = 0.74; 0.74 and 0.40 was recorded for complete blocking, standard blocking and intermediate blocking, fouling mechanisms, respectively. For the pristine membrane, R^2 values of 0.76; 0.75 and 0.60 were established for the respective fouling mechanisms of complete blocking, standard blocking, and intermediate blocking. However, cake filtration was found to be the most likely fouling mechanism for the coated membrane (R^2 = 0.99), and the least likely fouling mechanism for the pristine membrane (R^2 = 0.37). Coating was found to increase the hydrophilicity of the ceramic membranes; this is evidenced by the contact angle measurements, which showed a 23% decline in hydrophobicity of the coated membrane relative to the uncoated

6.5 REFERENCES

[1] L. De Angelis, M. Marta, and F. De Cortalezzi (2013).Ceramic membrane filtration of organic compounds : Effect of concentration , pH , and mixtures interactions on fouling', *Separation and Purification Technology*, **118**, 762–775.

[2] T. O. Mahlangu, J. M. Thwala, B. B. Mamba, A. D'Haese, and A. R. D. Verliefde (2015). Factors governing combined fouling by organic and colloidal foulants in cross-flow nanofiltration. *Journal of Membrane Science*, **491**(July), 53–62.

[3] M. Schulz, A. Soltani, X. Zheng, and M. Ernst (2016). Effect of inorganic colloidal water constituents on combined low-pressure membrane fouling with natural organic matter (NOM). *Journal of Membrane Science*, **507** (June), 154-164.

[4] W. Sun, J. Nan, J. Xing, and J. Tian (2016). Identifying the major fluorescent components responsible for ultrafiltration membrane fouling in different water sources', *Journal of Environmental Science*, **45**, 215–223.

[5] M. M. Motsa, B. B. Mamba, A. D'Haese, E. M. V Hoek, and A. R. D. Verliefde (2014). Organic fouling in forward osmosis membranes: The role of feed solution chemistry and membrane structural properties. *Journal of Membrane Science*, **460**(July), 99–109.

[6] M. M. Motsa, B. B. Mamba, and A. R. D. Verliefde (2018). Forward osmosis membrane performance during simulated wastewater reclamation: Fouling mechanisms and fouling layer properties. *Journal of Water Process Engineering*, **23**(March), 109–118.

[7] S. Metsämuuronen, M. Sillanpää, A. Bhatnagar, and M. Mänttäri (2014). Natural Organic Matter Removal from Drinking Water by Membrane Technology. *Separation and Purification Technology*, **43**(July) 2012, 1–61.

[8] A. W. Zularisam, A. F. Ismail, M. R. Salim, M. Sakinah, and H. Ozaki (2007). The effects of natural organic matter (NOM) fractions on fouling characteristics and flux recovery of ultrafiltration membranes. *Desalination*, **212**,(1–3), 191–208.

[9] H. C. Kim and B. A. Dempsey (2013). Membrane fouling due to alginate, SMP, EfOM, humic acid, and NOM. *Journal of Membrane Science*, **428** (February), 190-197.

[10] S. Shao, H. Liang, F. Qu, H. Yu, K. Li, and G. Li (2014). Fluorescent natural organic matter fractions responsible for ultrafiltration membrane fouling: Identification by adsorption pretreatment coupled with parallel factor analysis of excitation-emission matrices. *Journal of Membrane Science*, **464**(August), 33–42.

[11] W. Qiao (2017). Characterization of Dissolved Organic Matter in Deep Geothermal Water from Different Burial Depths Based on Three-Dimensional Fluorescence Spectra. *Water*, **9**(4), 266.

[12] T. Nguyen, F. A. Roddick, and L. Fan (2012). Biofouling of water treatment membranes: A review of the underlying causes, monitoring techniques and control measures. *Membranes*, **2**(4), 804–840.

[13] K. Kim and A. Jang (2016). Fouling characteristics of NOM during the ceramic membrane microfiltration process for water treatment. *Desalination and Water Treatment*, **3994**(December), 1–9.

CHAPTER 7

:. Selective removal of natural organic matter fractions by ceramic membranes from water samples obtained from a drinking water treatment plant in South Africa.

7.1 INTRODUCTION

Despite being used for more than two decades in the water industry, very limited data is available on the selectivity of ceramic NF membranes in the removal of specific NOM fractions from untreated and partially treated surface waters. Most of the previous studies have tended to focus on: the removal of bulk NOM using ceramic membranes; a comparison of polymeric and ceramic membranes in the removal of bulk NOM; modifications of ceramic membranes for improved flux or the removal of bulk NOM; and mechanisms of fouling of ceramic membranes by bulk NOM or model NOM fractions [1]–[4]. The effective use of ceramic membranes in water treatment requires a full understanding of the character of NOM fractions found in source surface waters and the removability of these fractions during membrane filtration. Such an understanding will require robust and sensitive analytical instruments that enable real-time characterization and reactivity as well as the treatability of NOM by ceramic membranes to be determined. The objectives of this research study were to: (1) investigate the selectivity and removal of specific NOM fractions (i.e. BDOC, chromophoric, fluorescent and biogenic fractions) from raw and partially treated waters; (2) use modeling techniques to investigate the removal of NOM fractions by ceramic membranes possessing different molecular weight cut-off (MWCO); and (3) investigate the removal of NOM fractions responsible for bacterial regrowth in the distribution system and those responsible for the formation of DBPs.

This chapter is based on:

Moyo W, Motsa M.M, Chaukura N, Msagati T.A.M, Mamba B.B, Heijman S.J.G and Nkambule T.T.I (2020). Investigating the fate of natural organic matter at a drinking water treatment plant in South Africa using optical spectroscopy and chemometric analysis. *Water S.A*, **46**(1), 131-140.

Moyo W, Motsa M.M, Chaukura N, Msagati T.A.M, Mamba B.B, Heijman S.J.G and Nkambule T.T.I. Selective removal of natural organic matter fractions by ceramic membranes from water samples obtained from a drinking water treatment plant in South Africa. *Journal of Membrane Sciences* (Submitted: 30 November 2019)

7.2 MATERIALS AND METHODS

7.2.1 Sampling

Water samples were collected in 25 L containers after each treatment stage at Rietvlei Water Treatment Plant in the Gauteng province of South Africa. The plant has a maximum treatment output of 42 ML/day. The treatment processes involve coagulation/flocculation using a combination of ferric sulphate and a commercial organic flocculant and pH correction using lime, followed by dissolved air floatation filtration (DAFF) through sand beds, and finally chlorination. The turbidity, pH, temperature, and conductivity were measured on-site using potable multimeters. Samples were transported to the laboratory and analyzed within 48 h.

7.2.2 Determination of DOC and BDOC fractionation of NOM

The organic carbon quantity of the BDOC fraction, raw, concentrate and permeate of all samples was determined in triplicate using a total organic carbon analyser (TOC fusion, Teledyne Tekmar). and the rejection of DOC (r_{DOC}) was calculated **(Equation 7.1)** [5]:

$$r_{DOC} = \frac{\left(C_0 - C_p\right)}{C_0} \qquad (7.1)$$

where, C_0 is initial *DOC* concentration in the raw water feed, and C_p is the concentration of *DOC* in the permeate.

The in-depth procedure followed is found in **Sections 3.51 and 3.5.5.**

7.2.3 Fluorescence, UV absorbance analysis and polarity fractionation of NOM

UV, DOC and SUVA were analysed according to the method outlined in **Sections 3.51; 3.52 and 3.53**. UV absorbance at 254 nm (UV_{254}) measurement of the permeates and concentrate was carried out after every hour during the filtration experiments to determine UV transmission through the membrane. The UV_{254} transmission during the filtration process was calculated as the UV_{254} quotient of permeate to that in the feed water.

The character of the three fractions (hydrophobic, hydrophilic, transphilic) obtained through the polarity rapid assessment method (PRAM) was also analysed using UV_{254} measurement. The modified-polarity rapid assessment method (m-PRAM) was used to partition NOM into three fractions, namely: the hydrophobic (HPI), hydrophilic (HPO) and transphilic (TPI) fractions (Nkambule et al., 2012). A full UV-Vis scan of samples in all filtrate samples was performed for quality assurance and quality control (**Appendix A2**). Readings at representative wavelengths was recorded after each round of cleaning which included eluting 100 mL of deionized water (**Appendix A2**).

7.2.4 Determination of biogenic NOM fraction

Section 3.5.6 describes in detail the method carried out in the determination of biogenic NOM fraction.

7.2.5 Modelling techniques

Section 3.6.2 describes the fluorescence regional integration method for the identification and quantification of fluorescent NOM fractions from a pool of data obtained from the feed and permeates. **Section 3.6.4** describes the fitting of Gaussian bands onto the UV spectra of permeates. **Section 3.6.5** describes the 2D-correlation spectroscopy method for the determination of the order of the susceptibility to removal of fluorescent NOM fractions by ceramic membranes of different MWCO.

7.2.6 Membrane and filtration equipment set up

7.2.6.1 Substrate membranes

The description of the membranes used, MWCO characterisation and the operation conditions of the filtration runs is described in detail in **Sections 3.7.1, 3.7.2 and 3.8.1.** Commercial ceramic NF membranes with a TiO_2 active surface layer (TAMI, France) were used in these experiments. The membranes had a disc configuration of 90 mm diameter, 2.5 mm thickness, 30% porosity, an effective filtration area of 0.00563 m^2, and a MWCO of 450 Da. Defects on the membranes were determined using the method developed by Kramer et al., 2019 [6]. The defects values obtained for the membranes were all below 5%. The defects corrected MWCO individual membranes used in the study are shown on **Appendix A7**.

7.2.6.2 Membrane Contact angle and surface energetics

Contact angles of the membranes and surface energetics were determined by method described in **Section 3.7.2**

7.2.6.3 Membrane characterisation

The membrane surfaces were characterised according to the method described in **Section 3.7.3**

7.3. RESULTS AND DISCUSSION

7.3.1 Removal of bulk parameters

Raw water bulk parameters such as DOC, UV and SUVA were 10.72 mg/L.C; 0.16 cm^{-1} and 1.46 $L.mg^{-1}m^{-1}$, respectively. Coagulation contributed 12.7%, respectively to the elimination of UV254 absorbance (**Appendix A7a**). Coagulation is usually the major process for the removal of NOM. However, previous research has shown that SUVA < 2 L/(mg M) implies that the major portion of NOM in the water is composed of non-humic substances and that less than 25% of these substances can be removed [1].The removal of organic matter by the ceramic membranes was in the range 62-68% (**Figure 7.1a**), a result lower than those reported in literature (>90%) by polymeric NF membranes [8]. The polymeric NF membranes used in their study had 200 – 300 Da MWCO, thus denser than the ceramic membranes used in this study. However, the results were consistent with findings which report on lower than normal DOC removal in waters dominated by hydrophilic NOM fractions (**Appendix A1**). For NF membranes, the electrostatic interactions and hydrodynamic conditions between the NOM molecules and membrane surface dictate the diffusive and convective transport mechanism of NOM through the pores [7]. Therefore, molecules with a lower dipole moment would be rejected more compared to molecules of higher dipole moment [10]. Consequently, it is expected that hydrophobic fractions will be retained more than the hydrophilic fractions.

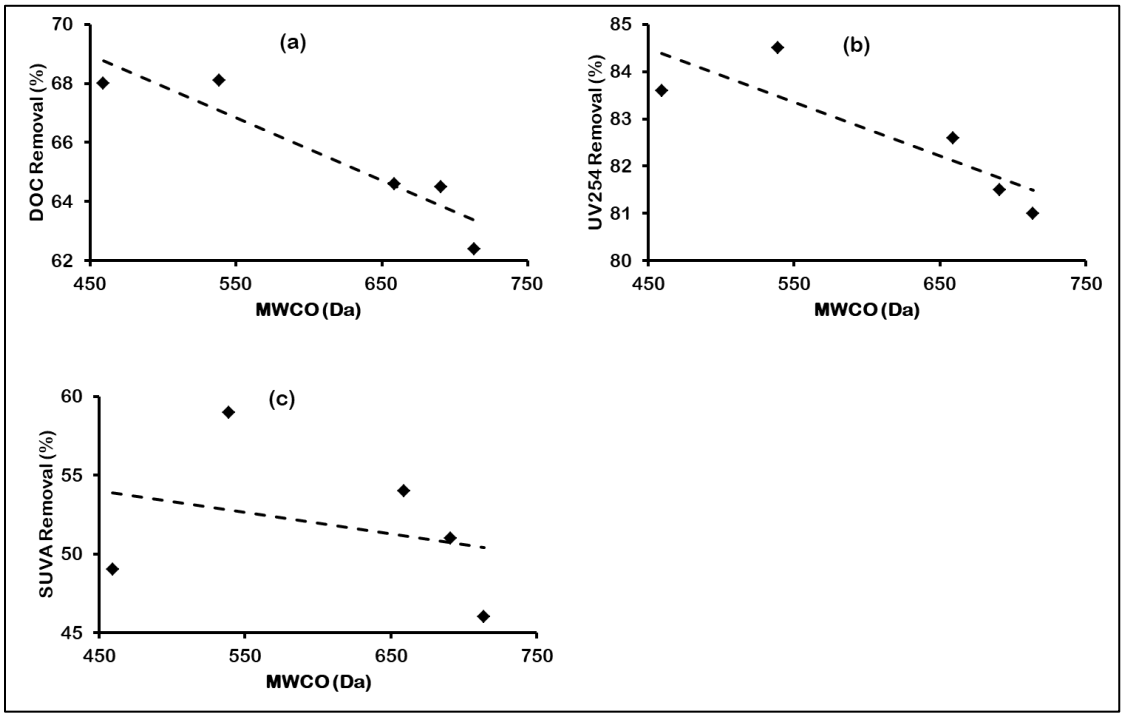

Figure 7. 1: Removal of bulk NOM parameters by membranes of different MWCO (a) DOC, (b) UV_{254}, and (c) SUVA.

Notably, the removal of bulk parameters did not follow a particular order. The measured MWCO ranged from 459 to 714 Da (**Appendix A7a**). Despite a 80 Da difference in MWCO, membranes M1 and M2 removed 68.0 % and 68.1 % organic carbon (**Figure 7.1a**), and 83.6 % and 84.5 % UV_{254} (**Figure 7.1b**), respectively. Similarly, notwithstanding a 32 Da difference in MWCO, membranes M3 and M4 removed 64.5% and 64.6% DOC, and 81.5% and 84.6% UV_{254}, respectively. In contrast, despite a difference in the MWCO of 55 Da, very low DOC (62.4%) and high UV254 (81%) removal rates were obtained for the M5 membrane relative to the M3 (64.5% DOC; 81.5% UV_{254}). A comparative analysis of the M5 and M4 (64.6% DOC; 84.6% UV_{254}) followed a similar trend despite a 23 Da differences in MWCO. SUVA removal followed the similar trend to UV_{254} removal (**Figure 7.1 c**). The high removal rate of UV_{254} was ascribed to the dependence of the hydrophobicity on aromaticity of the NOM fractions [11]. Of note, MWCO showed strong correlations with UV and DOC (R^2 = 0.74; 0.88, respectively) and poor correlation with SUVA (R^2 = 0.09) **(Figure 7.1 (a)-(c)).** Perhaps the MWCO window was too narrow for meaningful correlations with SUVA removal to

be deduced. Regardless of the membranes being in the NF range, permeation drag cannot be the only factor detecting NOM removal with regards to size, the pore size distribution can be broad, therefore NOM removal cannot exclusively be predicted from size exclusion phenomenon [2]. For instance, although the membranes had different MWCO, similar DOC removal rates were obtained. The interplay between transport and rejection mechanisms of NF membranes is still not well understood [2]. Therefore, further investigations should be directed at studying the connection between pore size distribution and MWCO during the rejection of NOM.

7.3.2 Selective removal of NOM fractions

7.3.2.1 Selective removal of chromophoric dissolved organic matter

The UV-Vis spectra from the feed and permeates of respective membranes were deconvuluted to revel the underlayed Gaussian peaks (**Figure 7.2**). The modelled data and the experimental data showed a strong correlation (R^2 > 0.97). The positions of the bands are consistent with reported literature, and thus are similarly coded A01 to A07 with maxima at λ < 240 nm, 266 nm, 298 nm, 323 nm, 355 nm, 381 nm, and 411 nm for A01, A02, A03, A04, A05, A06 and A07, respectively [43]-[44]. The resolution of the deconvulution of band A01 is spectrally interfered by nitrates, inorganic ions and nitrites because these feature predominantly at λ < 240 nm [45]. For this reason, spectral peaks appearing at λ<240 nm were not regarded in this research.

The intensity of the Gaussian bands decreased from the feed to the permeate samples, however, the maxima position of bands did not shift regardless of the significant reduction (p=0.05) of the UV-Vis spectra from the feed to the permeate samples (**Figure 7.2a-f**). The extent of reduction of the intensity of Gaussian bands from the feed to the permeate is a measure of the ability of the membranes to remove chromophoric fractions of NOM [46]. This implies the membranes are capable of retaining the chromophoric NOM fraction. Bands A05, A06 and A07 did not feature in the UV-Vis spectra for the permeates (**Figure 7.2b-f**). This showed the membranes completely removed chromophoric fractions of NOM that absorb in longer wavelengths. Electron donor/acceptor interactions in intramolecular charge transfer schemes are characteristic

of chemical components that absorb UV-Vis radiation at higher wavelengths. Such interactions are low energy transitions and unstable, are easily removed even by physical means such as membrane filtration [15].

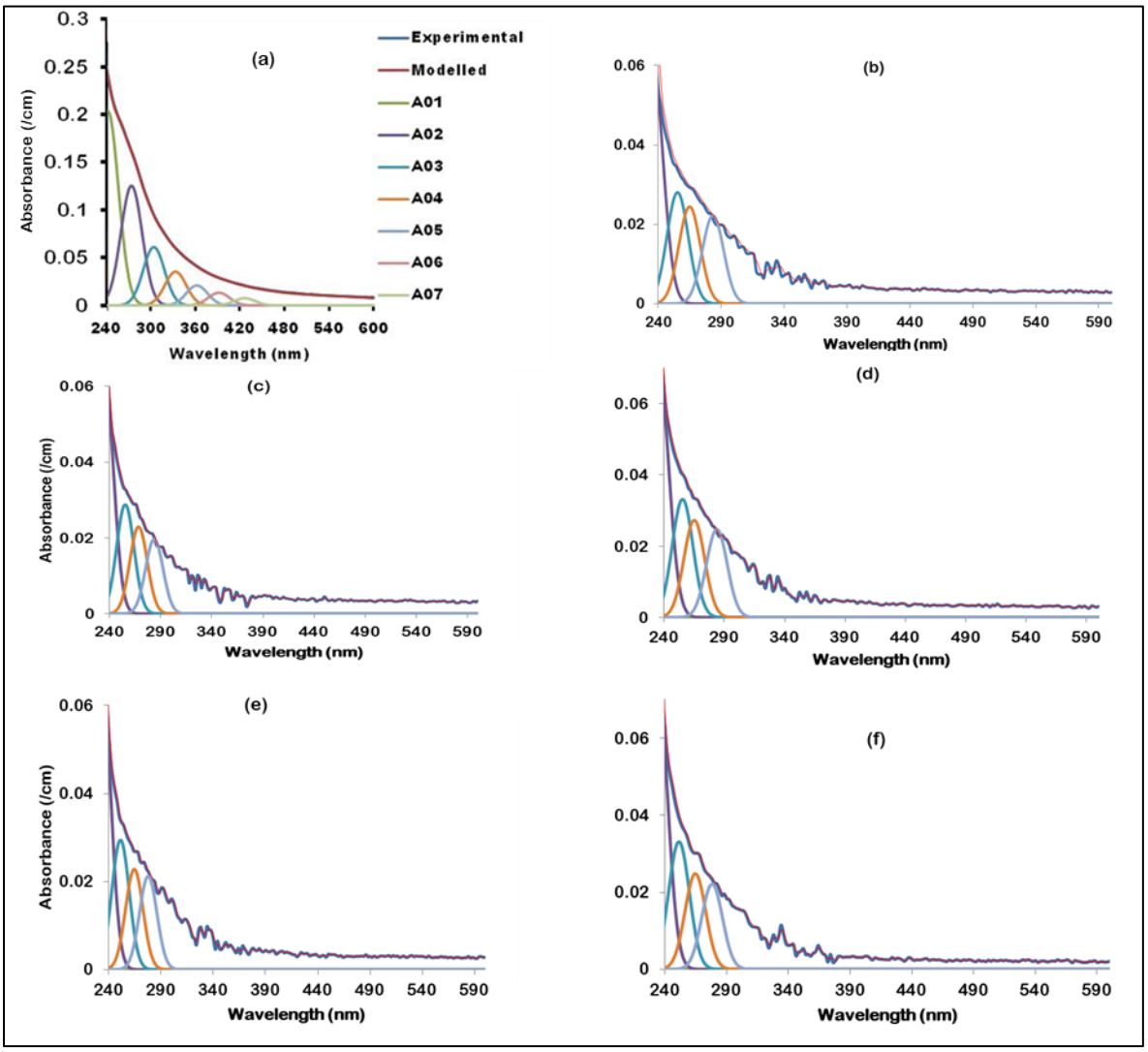

Figure 7. 2: UV-vis spectra of raw and respective membrane permeates fitted with Gaussian bands (a) Feed water; (b) M1 permeate; (c) M2 permeate; (d) M3 permeate; (e) M4 permeate; and (f) M5 permeate.

In this research, band A3 peaked near the range of interest ascribed to $\pi \rightarrow \pi^*$ electron transitions of aniline derivatives and phenolic arenes substituted with a minimum of two rings (270 -280 nm) [15]. At present, there is not enough evidence to assign band A03 to the formation of specific DBPs with certainty. Further research concentrating on

elucidating the correlation of the position, intensity and shape of A03 band and specific DBPs formed is therefore required. However, literature reports a correlation exists between individual DBPs formed and the intensity of the differential absorbance at 272 nm [48]-[49]. **Figure 7.3** shows a strong correlation of the removal of band A03 and MWCO (R^2=0.74). The main aim of this research was to find out if there are significant differences in removal of NOM fractions within a small MWCO window. Although the removal rates of band A03 was within a small range (84.5 – 87.5 %), the population mean was significantly different from the test mean (p=0.05). Furthermore, smaller MWCO membranes are able to retain more constituents of band A03 than higher MWCO membranes. This result is important for WTPs, especially for the targeting of DBP precursors.

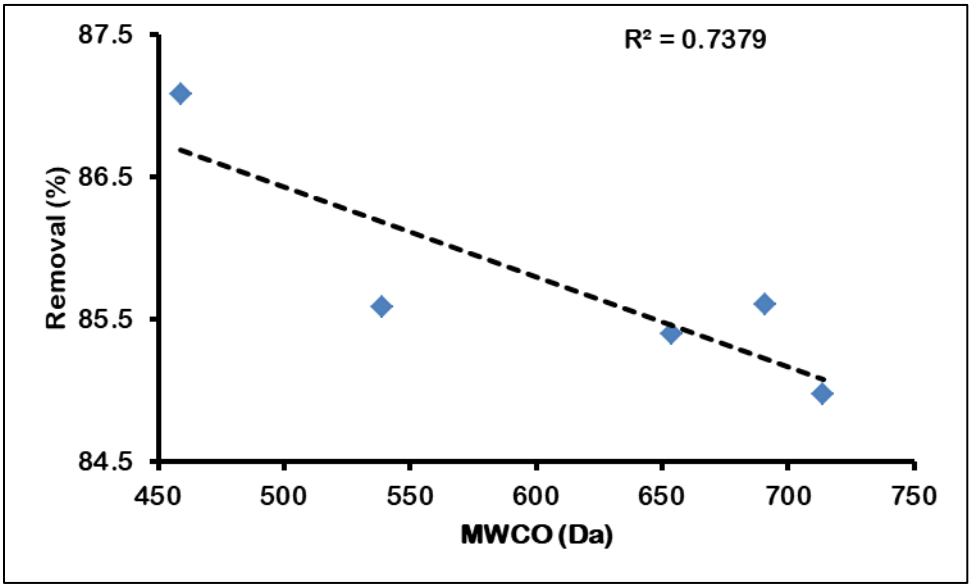

Figure 7. 3: Correlation of removal of band A03 and MWCO

7.3.2.2 Selective removal of biogenic NOM fractions

Raw water exhibited high biopolymer concentration (100.03 µg/L glucose eq). Higher biopolymer concentrations have been reported for highly hydrophilic water compared to hydrophobic water [17]. The membranes under investigation had over 85% removal efficiency for the biopolymers, with M1 ranking the highest at 94.3% (**Appendix A7b**). A fair correlation existed between MWCO and removal efficiency (R^2 = 0.70) (**Figure 7.4**). Since biopolymer sizes are ≥ 10 000 Da, the test membranes were therefore expected to totally reject the biopolymers because MWCO of all membranes in this study were

below 1 kDa. The bulk character of biopolymers depends on the concentrations of its constituent compounds namely polysaccharides, some HL substances and proteins [18]. The sulphuric acid-UV-Vis method is not particularly selective when biopolymers of different constituents exist in solution, and the spectroscopic properties of the derivatives of these constituents could enhance or diminish the response signal [32]. Therefore the measured signals could be from fractions of biopolymers that are small enough to pass through the pores of membrane; such biopolymer fractions are not necessarily representative of the entire population of biopolymeric molecules located on the feed side. In this regard, the results obtained from this study are indicative rather than absolute.

The membrane fouling propensity exacerbated by gelling properties of biopolymers is a nuisance to WTPs with a membrane filtration stage in its regimen. Extended presence of biopolymers on the membrane surface during operation enhances bacterial adhesion and proliferation ultimately increasing filtration resistance [20].

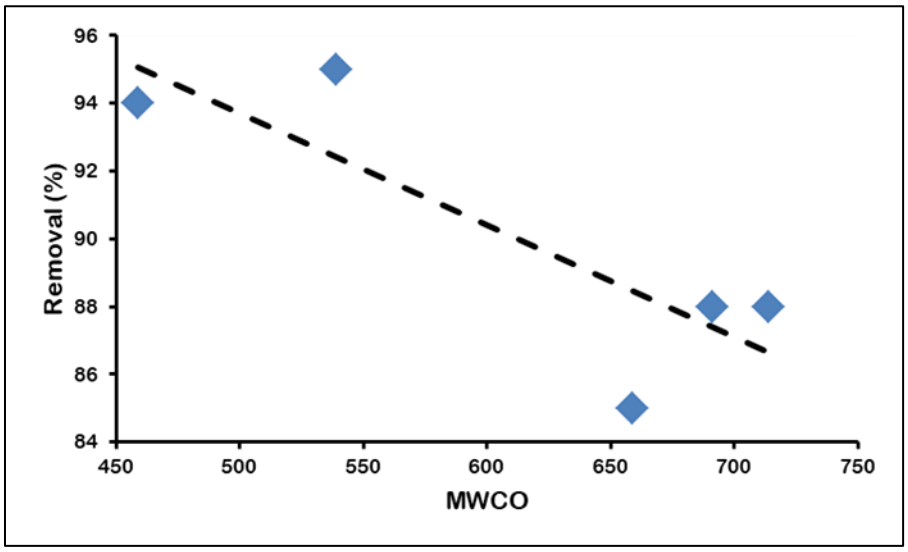

Figure 7. 4: Correlation of polysaccharide removal and MWCO.

7.3.3.3 Selective removal of fluorescent NOM fractions

Figure 7.5 shows the EEM fluorescence spectra for the feed and permeates of the respective membranes. The EEMs for the respective permeates showed a decrease in the intensities of all fluorescent fractions with reference to feed EEM. This shows the ability of ceramic membranes to remove *f*NOM fractions. The measured water contact angles ranged from 59.5^{o} to 62.4^{o}, these values demonstrated that the membrane surface exhibited a hydrophilic surface (**Appendix A5**). The abundant –OH groups on the pore surface of native TiO_2 NF membranes render ceramic membranes more hydrophilic [21]. This was further corroborated by the computed surface free energy that had an acid-base component greater than 5 mJ/m^2. Surface roughness values from 63 to 71 nm were recorded (**Appendix A6**). This indicates a relatively smooth surface. A smooth surface is ideal for a filtration process because it limits foulant/pollutant adhesion on the surface of the membrane and subsequently enhance the anti-fouling properties [22]. On the downside, the inherent –OH groups on the surfaces of the ceramic membranes interact with the polar groups such as phenolic and carboxylic groups thus reducing the transmission of NOM fractions with an abundance of these groups and at the same time fouling the membrane surface and pores [21]. Notably, the HL peak located at 330-350/420-480 nm (Ex/Em) [23] gradually reduced with decreasing MWCO. All *f*NOM fractions were retained to at least 80 % (**Figure 7.5b**). Although the bulk removal of NOM measured as DOC was in the range of 62-68 %, the high removal of *f*NOM fractions confirmed their selectivity towards such types of NOM fractions. For instance, the TPL and HL fractions were removed at a higher rate (> 85 %) compared to the other fractions. These NOM fractions have an abundance of polar carboxylic and phenolic groups which interact with the -OH groups which terminate the membrane surface [21].

Two-dimensional correlation peaks located on the 1:1 slope by convention are auto peaks, and show maxima off the diagonal are termed cross peaks. Only auto peaks are located on the synchronous map while cross peaks, which are either positive or negative, are located on the asynchronous map [28]. Cross peaks give an indication of the order of susceptibility to removal of specific NOM fractions when MWCO is the only

external perturbation. The synchronous spectra showed a single auto peak at the 355/355 nm wavelength pair (**Figure 7.5c**), while peaks appeared at 280/355, and 450/355 nm wavelength pairs in the asynchronous spectra (**Figure 7.6d**). Based on Noda's rule, spectral changes occurring at wavelengths 450 and 280 nm are faster than those at 355 nm. The peak at 450 nm was ascribed to HL substances, while those at 355 and 280 are ascribed to FL and TPL matter, respectively [25]. This implies the HL and TPL fractions are more susceptible to removal than the FL fraction, thus their higher rate of removal compared to other fractions.

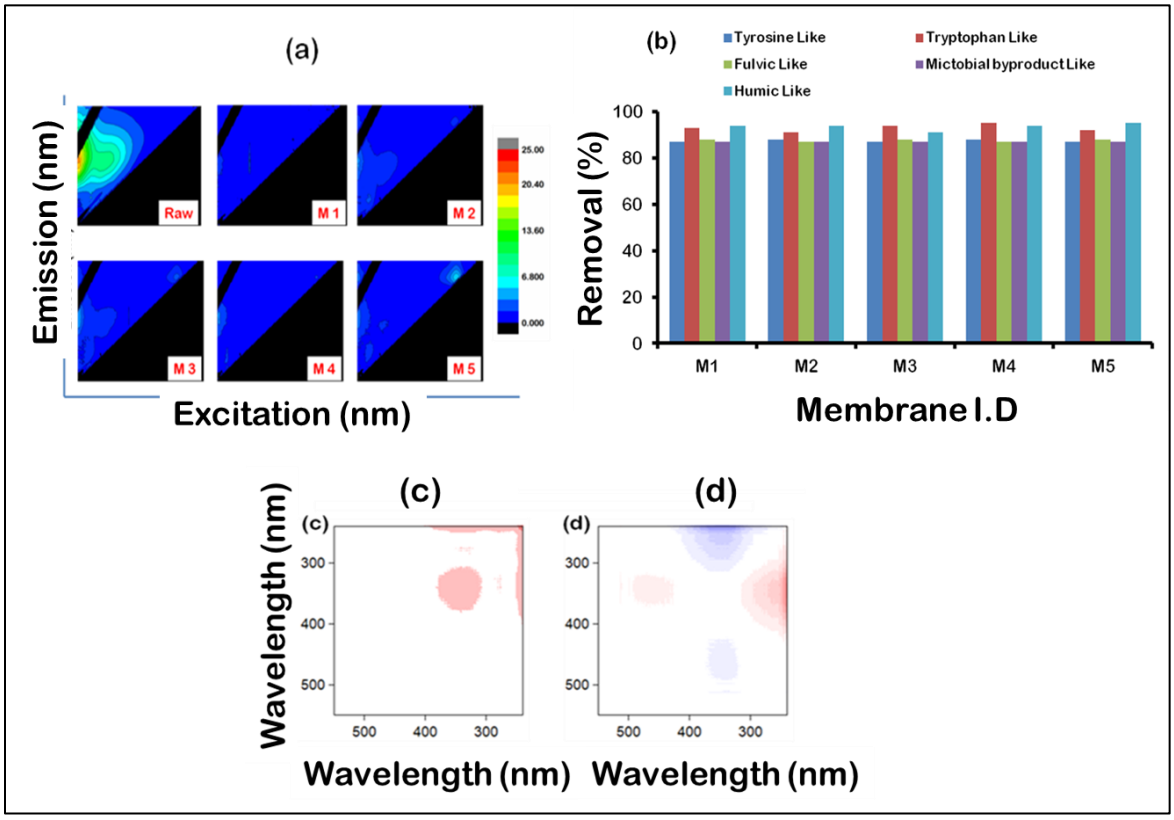

Figure 7. 5: (a) 3D-EEM spectra of the feed raw water and permeates from respective ceramic membranes; (b) quantitative analysis of fluorescent NOM fractions from permeates of respective membranes; (c) Synchronous 2D correlation map; and (d) asynchronous 2D correlation map derived from 260 to 550 nm regions of SFS. A positive correlation is indicated by a red colour while a negative correlation is indicated by a blue colour. A strong negative or positive correlation is indicated by a darker shade.

7.3.3.4 Selective removal of biodegradable dissolved organic matter fraction of NOM

Changes in BDOC components were tracked throughout the water treatment train for the purposes of identifying the components most susceptible for uptake by heterotrophic bacteria and the enabling factors associated by each treatment stage (**Figure 7.7a**). The results showed that the FL and HL fractions declined by 9.5 and 4 %, respectively, while the proteinacious TPL and TYL fractions increased by 5% and 23%, respectively, from the first day to the second day, which corresponded to a 4.4% decrease in DOC during the same time frame. For ease of assimilation of the carbon substrate, in this case the FL and HL components, some species of heterotrophic bacteria secrete extracellular polymeric enzymes, which are proteinacious in nature thus contributing to the spike in TPL and TYL components [55],[57]. It must be noted that the decrease in fluorescent BDOC components does not necessarily imply heterotrophic bacteria are specifically selective to fluorescent BDOC components, even non fluorescent carbon sources can serve as substrate for uptake by heterotrophic bacteria. This was evidenced by a disproportionate decrease in DOC at all the time intervals. DOC is a bulk parameter, encompassing fluorescent and non-fluorescent organic matter fractions. A decreasing trend of all BDOC fluorescent components was observed during days 2 and 3. Whereas the highest decrease was obtained for the FL (28%) and HL (17%) fractions, the least decrease was achieved for the proteinaceous matter (<8% each). This suggests the heterotrophic bacteria At this stage, the implications are that the heterotrophic bacteria have adjusted to the prevailing environment and their preferentially consuming FL and HL components [58]. The HL and FL components of BDOC fraction decreasing trend persisted throughout all time intervals. It was interesting to note the HL was readily assimilable by heterotrophic bacteria as literature indicate that humic matter is a hardly biodegradable material susceptible to uptake by heterotrophic bacteria [59]. Perhaps the combination of the degree of humification (*HIX*), source (*F.I*), age (*β:α*), redox state, size, photochemical and biological reactivity made HL amenable for uptake by heterotrophic bacteria. There was a 26% and 20% increase in TPL and TYL components, respectively, during days 3 and 4, suggesting the beginning of cell die offs due to bacterial population exceeding the available nutrient

quantity. Bacterial DNA and other components of the bacterial cell are made of proteinacious matter, therefore the dead bacterial cells increase the protein signal observed [29]. Interestingly, besides the other fractions, there was a 25% decrease in each of the protein fractions was observed during days 4 to 6. Secondary bacteria, which are higher in the food chain trophic level, consume the dead heterotrophic bacteria cells [59]. Overall, the results point to FL and HL to be the main components of BDOC fraction susceptible to assimilation by heterotrophic bacteria therefore monitoring and controlling these fractions is necessary to curb BDOC concentrations

Removal of BDOC using the membranes investigated in this research study was above 85% with M1 and M5 achieving the highest (94%) and least (88%) BDOC removal efficiencies, respectively (**Appendix A7c**). Similar rates of BDOC removal (>90%) by nanofiltration membranes have been reported [30]. The least MWCO was obtained for M1, which was therefore able to retain higher molecular weight BDOC compared to M5. Perhaps the NOM composed of larger MW components was the main constituent of the bulk BDOC fractions, thus they were rejected to a larger extent (94%) by the least MWCO membrane (M1) (**Figure 7.7b**). Similar findings were reported whereby low MWCO membranes were more efficient in retaining BDOC relative to higher MWCO membranes [31]. The membranes investigated herein were capable of removing more than 90 % of the HL fraction (**Figure 7.7c**). Similarly, the removal of bulk BDOC (**Figure 7.7b**) and the HL fraction of BDOC (**Figure 7.7c**) appeared to be weakly related to the MWCO of the membranes (R^2 = 0.48; 0.63, respectively). The HL fraction is composed of bulky and condensed aromatic structures with carboxylic and phenolic moieties [59]. Consequently, membranes of lower MWCO are able to retain HL fractions through size exclusion. However, because the assimilable organic carbon (AOC) fraction passes through the membranes, membrane-based methods do not completely obliterate post microbial proliferation. The AOC fraction has a smaller molecular size, and can pass through the pores of the membrane, and supports bacterial recolonisation post treatment by acting as substrate for bacterial growth [59]. A significant amount of nutrients can pass through the pores of the membranes, regardless of the MWCO of the membrane, these nutrients serve as substrate for bacteria in the distribution pipes [32].

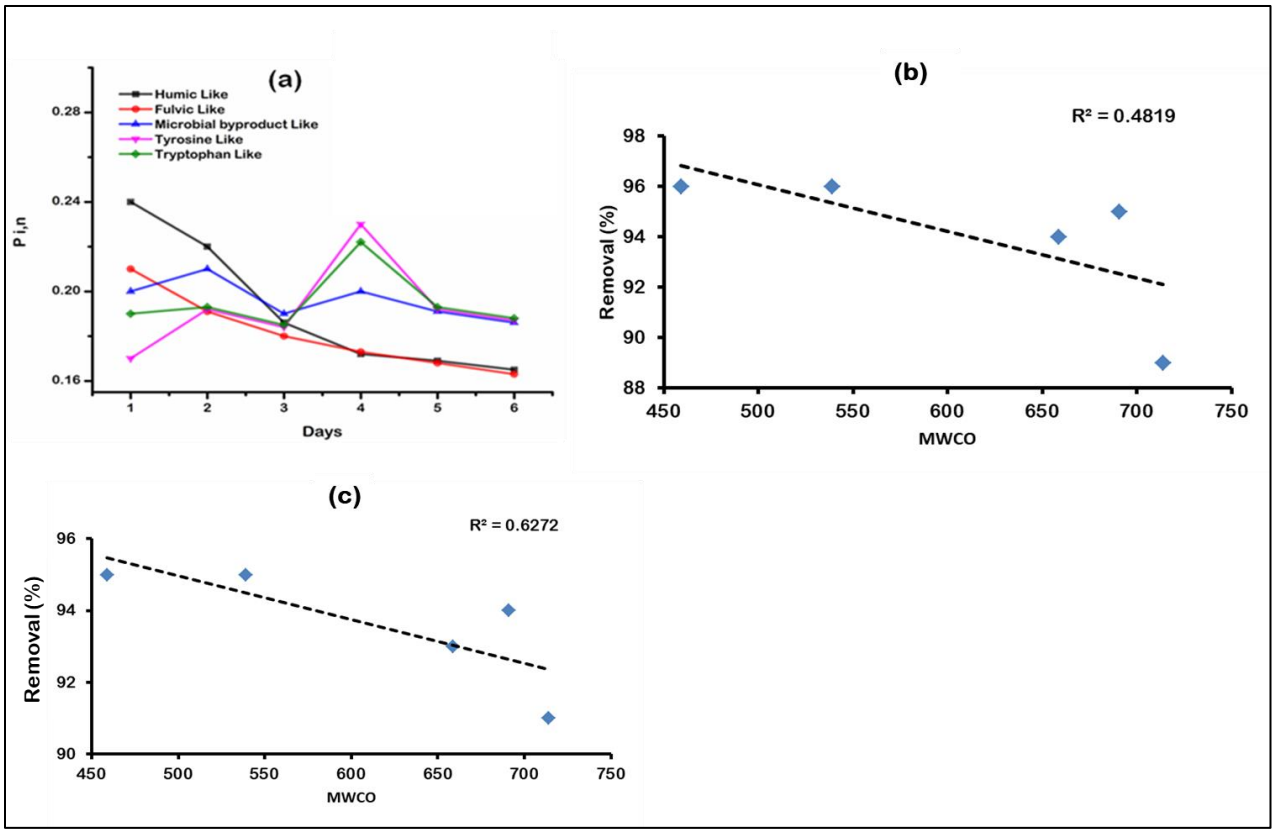

Figure 7. 6: (a) Daily changes in fluorescent DOC fractions; (b) correlation of BDOC removal with MWCO; and (c) correlation of the humic like fraction of BDOC with MWCO.

7.3.3.5 Selective removal of polarity NOM fractions

The distribution of polarity fractions at source was 24, 31 and 45% for TPI, HPI and HPO, respectively (**Figure 7.8a**). These results corroborate previously reported studies, which reported NOM in surface water consisting of about 50% HPO, the HPI fraction contributing between 25-40%, and the TPI fraction occupying the remainder [57]. The WTP regimen reduced the HPO fraction from 45% at source to 36% in the final treated water (**Figure 7.8a**). These results are contrary to literature which report the HPO fraction to be the most amenable to removal by conventional water treatment processes[66]-[69]. The low SUVA values of the raw water indicate minimal HPO quantity to start with and literature states that less than 25 % of HPO fractions are expected to be removed for SUVA<2 L/(mg.m) [37]. The raw and final treated water HPI

fractions did not show significant difference (p<0.01). However, the disinfection stage showed a significant decrease of the HPI fraction (41to 33%; p<0.01) (**Figure 7.8b**). Previous studies report that for low SUVA value waters the HPI fraction has higher disinfection formation potential for haloacetic acid (HAA) and trihalomethane (THM) [38]. It is therefore likely that the decrease of the HPI fraction at the disinfection stage is signaling the formation of the DBPs. The HPI fraction abundance is defined by a SUVA value of less than 2 and low C/O ratio the main indicative characteristics of carbon content which is less aromatic [37].

The fluorescent fractions making up the respective polarity fractions were determined by using the FRI method (**Figure 7.8b**). The intensity of HL fluorescent fraction in the HPO polarity fractions was higher compared to other polarity fractions at all the treatment stages. The HL fraction is the main fingerprint fraction of any hydrophobic NOM fractions, therefore it came as a no surprise that HL component was abundant in the HPO polarity fraction [39]. In light of the HPI polarity fraction conjectured to be the determining precursor for the DBPs formation, it was prudent to investigate the elements making up the HPI polarity fraction. Notably, there was a 14% decrease and an 11% incline of the TYL and HL fluorescent components, respectively, of the HPI polarity fractions at the disinfection stage (**Figure 7.8b**). These results suggest, the TYL fluorescent component to be the limiting reagent in the formation of DBPs and the produced DBPs had a spectral signature similar to the HL fluorescent component. Therefore, proteinaceous material sequestration prior to the disinfection stage is expected to lessen the DBP concentrations in the produced water.

The removal of the HPI fraction was at least 40% (**Appendix A7d**). Because size exclusion is not the only removal mechanism, further research relating membrane charge to the polarity fraction must be explored. A reduction in polarity cannot conclusively explain the impact of size exclusion; other forces such as charge interaction, and non-electrostatic forces, are at play [40]. Inconsistences with MWCO in the removal of the polarity fraction were noted. Such inconsistences are possibly due to chance removal of chemical constituents responsible for impacting the hydrophilic

nature to the sample. The correlation between HPI removal and the MWCO of the membranes was very poor (R^2=0.007), thus supporting the finding that impact of size exclusion is insignificant in the removal of HPI polarity fractions (**Figure 7.8c**). The removal rate, however, of TYL in the HPI fraction was in the range 60-66 % and it followed the order of decreasing MWCO (**Figure 7.8d**). The correlation between the TYL fraction of the HPI and the MWCO of the membranes was modest (R^2=0.502). Furthermore, this finding, as well as results obtained for the removal of chromophoric NOM fractions, is essential for the targeting and elimination of DBP precursor fractions in WTPs.

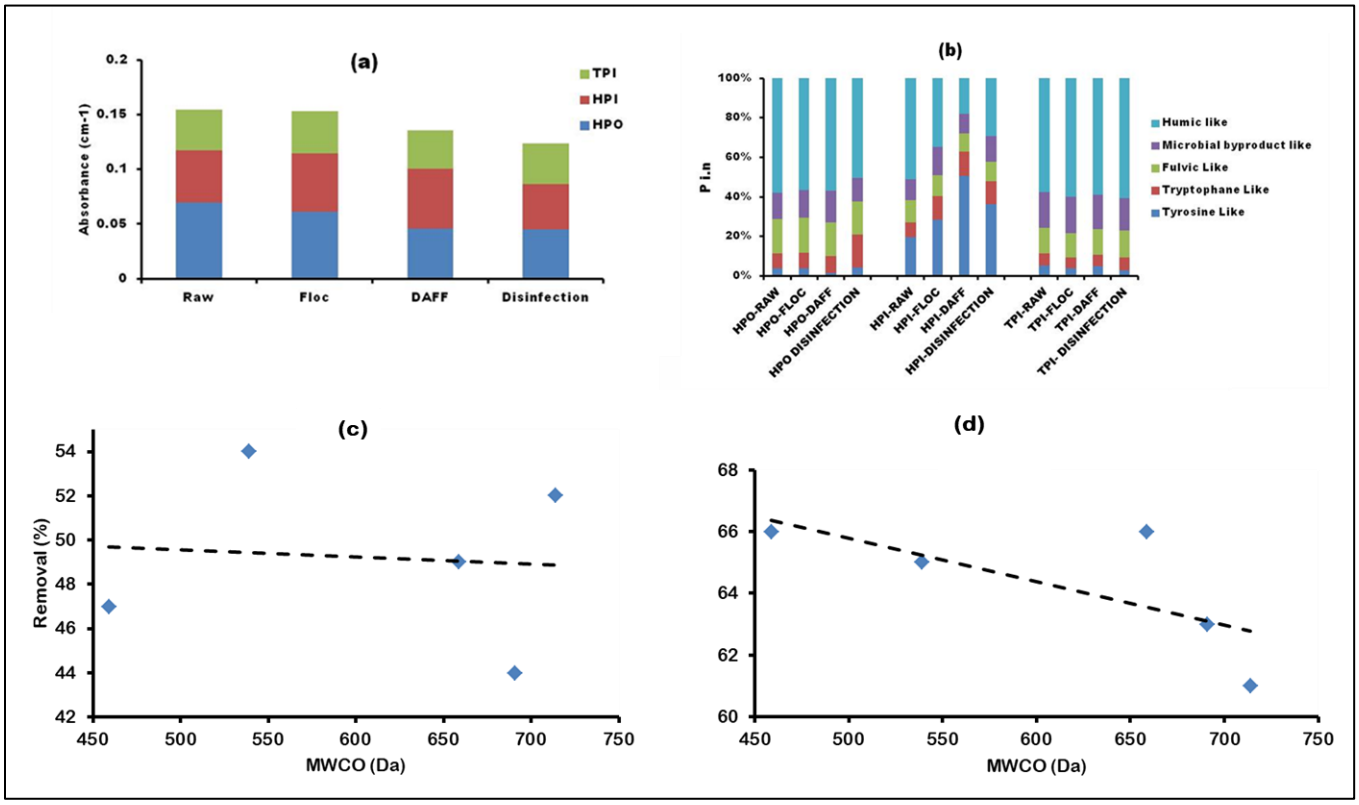

Figure 7. 7: (a) Concentrations of polarity fractions at each water treatment stage; (b) changes in the composition of polarity fractions in response to water treatment regimen; (c) correlation between HPI removal and MWCO; and (d) correlation between tyrosine like fraction and MWCO.

7.4. CONCLUSION

In this study, the removal of various NOM fractions from at bulk water treatment plant in South Africa was investigated using ceramic NF membranes. The key findings were:

1. The FL and HL components of the BDOC fraction were the main substrate susceptible to assimilation by heterotrophic bacterial. The removal of BDOC using a set of membranes was above 85% with the lower MWCO and higher MWCO membranes achieving the highest (94%) and least (88%) BDOC removal efficiencies, respectively. Similarly, the removal of HL fraction of BDOC was directly related to the MWCO of the membranes.

2. There was poor correlation between HPI removal and MWCO of the membranes, and the correlation between the TYL component of the HPI fraction with MWCO of the membranes was modest. Furthermore, the removal of the TYL component of the HPI fraction decreased with decreasing MWCO. These findings as well as results obtained for the removal of chromophoric NOM fractions are essential for the targeting and elimination of problematic NOM fractions in WTPs.

Future research should focus on: (1) investigating the connection between pore size distribution and MWCO during the rejection of NOM, (2) exploring changes in the shape, position and intensity of the characteristics of the A03 band, and (3) investigating the relationship between membrane charge and the polarity fraction, and (4) The 2D-SFS method could be used to determine the sequence or selectivity of removal of NOM fractions at each step. Thus water practitioners can formulate mechanisms of removing problematic NOM fractions by learning the sequence or selectivity of removal by each membrane size placed in sequence.

7.5 REFERENCES.

[1] I. Ivančev-Tumbas (2014). The fate and importance of organics in drinking water treatment: a review. *Environmental Science and Pollution Research*, **21**(20), 11794–11810.

[2] S. Metsämuuronen, M. Sillanpää, A. Bhatnagar, and M. Mänttäri (2014). Natural Organic Matter Removal from Drinking Water by Membrane Technology', *Separation and Purification Technology*, **43**(July),1–61.

[3] R. Liu, T. Xu, and C. an Wang (2015). A review of fabrication strategies and applications of porous ceramics prepared by freeze-casting method. *Ceramics International*, **42**(2), 2907–2925.

[4] N. Shamsuddin, D. B. Das, and V. M. Starov (2015). Filtration of natural organic matter using ultrafiltration membranes for drinking water purposes: Circular cross-flow compared with stirred dead end flow. *Chemical Engineering Journal*, **276**(August), 331–339.

[5] J. Xing (2018). Combined effects of coagulation and adsorption on ultrafiltration membrane fouling control and subsequent disinfection in drinking water treatment. *Environmental Science and Pollution Research*, **26**, 33770–33780.

[6] F. C. Kramer, R. Shang, S. M. Scherrenberg, L. C. Rietveld, and S. J. G. Heijman (2019). Quantifying defects in ceramic tight ultra- and nanofiltration membranes and investigating their robustness. *Separation and Purification Technology*, **219**(January), 159–168.

[7] S. N. Ndiweni (2019). Assessing the impact of environmental activities on natural organic matter in South Africa and Belgium. *Environmental Technology*, **40**(13), 1756-1768.

[8] S. Meylan, F. Hammes, J. Traber, E. Salhi, U. von Gunten, and W. Pronk (2007).

Permeability of low molecular weight organics through nanofiltration membranes', *Water Research*, **41**(17), 3968–3976.

[9] D. R. Ã, M. Rodrı, M. Leo, and D. Prats (2008). Removal of natural organic matter and THM formation potential by ultra- and nanofiltration of surface water. *Water Research,* **42**, 714–722.

[10] B. Van Der Bruggen and C. Vandecasteele (2003). Removal of pollutants from surface water and groundwater by nanofiltration: Overview of possible applications in the drinking water industry. *Environmental Pollution*, **122**(3), 435–445.

[11] S. Zhou (2014). Influence of hydrophobic/hydrophilic fractions of extracellular organic matters of Microcystis aeruginosa on ultrafiltration membrane fouling. *Science of The Total Environment*, (470–471), 201–207.

[12] S. He, M. Yan, and G. V. Korshin (2015). Spectroscopic examination of effects of iodide on the chloramination of natural organic matter. *Water Research*, **70**(August), 449–457.

[13] D. J. Dryer, G. V. Korshin, and M. Fabbricino (2008). In situ examination of the protonation behavior of fulvic acids using differential absorbance spectroscopy', *Environmental Science and Technology*, **42**(17), 6644–6649.

[14] P. Roccaro, M. Yan, and G. V. Korshin (2015). Use of log-transformed absorbance spectra for online monitoring of the reactivity of natural organic matter. *Water Research*, **84**(August), 136–143.

[15] C. M. Sharpless and N. V. Blough (2014). The importance of charge-transfer interactions in determining chromophoric dissolved organic matter (CDOM) optical and photochemical properties. *Environmental Science: Processes Impacts*, **16**(4), 654–671.

[17] H. Yamamura, K. Okimoto, K. Kimura, and Y. Watanabe (2014). Hydrophilic

fraction of natural organic matter causing irreversible fouling of microfiltration and ultrafiltration membranes. *Water Research*, **54**, 123–136.

[18] G. O. Bosire and J. C. Ngila (2016). Assessment of photo-oxidative alterations to natural organic matter in water using fluorescence excitation emission matrices and liquid chromatography-organic carbon detection techniques. *Analytical Methods*, **8**(6), 1415–1424.

[19] A. A. Albalasmeh, A. A. Berhe, and T. A. Ghezzehei (2013). A new method for rapid determination of carbohydrate and total carbon concentrations using UV spectrophotometry. *Carbohydrate Polymers*, **97**(2), 253–261.

[20] S. Meng, W. Fan, X. Li, Y. Liu, D. Liang, and X. Liu (2018). Intermolecular interactions of polysaccharides in membrane fouling during micro fi ltration. *Water Research*, **143**, 38–46.

[21] G. Mustafa, K. Wyns, A. Buekenhoudt, and V. Meynen (2016). Antifouling grafting of ceramic membranes validated in a variety of challenging wastewaters. *Water Research*, **104**, 242–253.

[22] Y. Guo (2018). Coupling continuous sand filtration to ultrafiltration for drinking water treatment: Improved performance and membrane fouling control. *Journal of Membrane Science*, **567**, 18–27.

[23] J. Sun (2016). Three-dimensional fluorescence excitation–emission matrix (EEM) spectroscopy with regional integration analysis for assessing waste sludge hydrolysis at different pretreated temperatures. *Environmental Science and Pollution Research*, **23**(23), 24061–24067.

[24] Z. Chen, M. Li, Q. Wen, and N. Ren (2017). Evolution of molecular weight and fl uorescence of ef fl uent organic matter (EfOM) during oxidation processes revealed by advanced spectrographic and chromatographic tools. *Water Research*, **124**, 566–575.

[25] B. Su, Z. Qu, X. He, Y. Song, and L. Jia (2016). Characterizing the compositional variation of dissolved organic matter over hydrophobicity and polarity using fluorescence spectra combined with principal component analysis and two-dimensional correlation technique. *Environmental Science and Pollution Research*, **23**, 9237–9244.

[26] I. Universiti, H. Abdul, and A. Universiti (2014). Trends on Natural Organic Matter in Drinking Water Sources and its Treatment. *International Journal of Scientific Research in Environmental Sciences*, **2**(3), 94-106

[27] Z. Filip, W. Pecher, and J. Berthelin (2000). Microbial utilization and transformation of humic acid-like substances extracted from a mixture of municipal refuse and sewage sludge disposed of in a landfill. *Environmental Pollution*, **109**(1), 83–89, 2000.

[28] E. I. Prest, F. Hammes, and M. C. M. Van Loosdrecht (2016). Biological Stability of Drinking Water : Controlling Factors , Methods , and Challenges. *Frontiers in Microbiology*, **7**(February), 1–24.

[29] L. G. Terry and R. S. Summers (2018). Biodegradable organic matter and rapid-rate bio fi lter performance : A review. *Water Research*., **128**, 234–245.

[30] I. C. Escobar and A. A. Randall (2001). Assimilable organic carbon (AOC) and biodegradable dissolved organic carbon (BDOC): complementary measurements. *Water Research*, **35**(18), 4444–4454.

[31] I. C. Escobar, S. Hong, and A. A. Randall (2000). Removal of assimilable organic carbon and biodegradable dissolved organic carbon by reverse osmosis and nanofiltration membranes. *Journal of Membrane Science*, **175**(1), 1–17.

[32] A. Nescerecka, T. Juhna, and F. Hammes (2018). Identifying the underlying causes of biological instability in a full-scale drinking water supply system. *Water Research*, **135**, 11–21.

[33] N. Hesham, A. Rahim, and S. Abdel (2013). Fate of Natural Organic Matter and Formation of Disinfection By-Products in a Conventional Water Treatment Plant. *Water Environment Federation*, **2014**(6), 1938-6478

[34] A. D. Knowles (2011). Optimizing the removal of natural organic matter in drinking water while avoiding inintended. PhD Thesis, Dalhousie University

[35] H. Kim and M. Yu (2005). Characterization of natural organic matter in conventional water treatment processes for selection of treatment processes focused on DBPs control. *Water Research,* **39**(19),4779–4789.

[36] S. A. Baghoth (2012). Characterizing natural organic matter in drinking water treatment proCesses and trains. PhD Thesis, Technical University of Delft.

[37] E. Lavonen (2015). Tracking Changes in Dissolved Natural Organic Matter Composition. PhD Thesis, Swedish University of Agricultural Sciences.

[38] N. Karapinar, V. Uyak, S. Soylu, and T. Topal (2014). Seasonal Variations of NOM Composition and their Reactivity in a Low Humic Water. *Environmental Processes ans Sustainability*, **33**(3), 962-971.

[39] C. Chen, X. Zhang, L. Zhu, W. He, and H. Han (2011). Changes in di ff erent organic matter fractions during conventional treatment and advanced treatment', *Journal of Environmental Sciences*, **23**(4), 582–586.

[40] T. O. Mahlangu, J. M. Thwala, B. B. Mamba, A. D'Haese, and A. R. D. Verliefde, (2015). Factors governing combined fouling by organic and colloidal foulants in cross-flow nanofiltration. *Journal of Membrane Science*, **491**(July), 53–62.

[41] J. L. Roe (2011). Characterization of natural organic matter in surface waters and the minimisation of disinfection by-product formation. PhD Thesis, University of Birmimgharm.

CHAPTER 8*:*

Defects in the active layer of ceramic nanofiltration membranes: A facile characterization approach

8.1 INTRODUCTION

The commonly used synthesis route for ceramic membranes is the sol-gel method, which is relatively simple, easy to control, and produces a homogeneous dispersion of particles that results in homogeneity of the physical properties of the membrane [1]. However, the major limitation to this synthesis route is the occurrence of defects. A defect is a crack or pinhole which can occur during membrane fabrication (gelling, drying or firing steps), or during use (sealing or thermal cycling of the membrane) [2]. Defects in the active layer of the membrane can drastically reduce the selectivity of the membranes [3]. The basic and qualitative method of analyzing defects in ceramic membranes is the application of scanning electron microscopy (SEM) or transmission electron microscopy (TEM) images. However, it is difficult to get a general picture of defect size distribution due to limited area of analysis (ca. 100 μm^2) [3]. In addition, given the brittle nature of ceramic membranes, any attempt to break a small piece for SEM/ TEM analysis is likely to result in the total destruction of the whole membrane. Despite the critical effects of defects on membrane performance, this problem has not been widely reported in literature. Most studies on defects are mainly on gas separation membranes [4], [5]. To the best of our knowledge no study has been conducted to analyse defects on ceramic membranes used for water filtration. Bearing this in mind, we present a relatively facile method to characterize defects in the membrane active layer since it is this layer which determines selectivity.

This Chapter is based:

Moyo W, Msagati T.A.M, Chaukura N, Heijman S.J.G, Mamba B.B and Nkambule T.T.I. Defects in the active layer of ceramic membranes: A facile characterization approach. Water Institute of Southern Africa, 2018, Cape Town, South Africa, 24 – 27 June 2018 (**ISBN** 978-0-6399369-2-5 pp.104)

8.2 MATERIALS AND METHODS

8.2.1 Substrate Membranes

Commercial ceramic nanofiltration (NF) membranes with a titanium dioxide active layer purchased from TAMI, France, were used. The membranes had a disc configuration of 90 mm diameter, 2.5 mm thickness, 30% porosity, an effective filtration area of 0.00563 m^2, and MWCO was 1000 Da. Polyethylene glycol of 300 < MW < 6000 Da were purchased from Sigma Aldrich, Germany and used without further purification.

8.2.2 Filtration equipment and operation

The feed was circulated by a gear pump operated at 1100-1180 rpm. The membrane was housed in a circular disc membrane module (TAMI, Germany), and the system was pressurized by adjusting the concentrate valve. Measurements were run under a transmembrane pressure (TMP) of 3 bar and a feed flow of 175 L/h. After equilibration, membranes were conditioned for 5 min for deionised water permeability and 1.5 h for PEG permeability. In the case of deionised water, permeates were collected after 1 min and weighed. In the case of PEG, samples were collected from the feed and permeate side after every 30 min.

Membrane fluxes and water temperature were monitored. The flow rate was correlated to the sample mass, and the flux and temperature-corrected permeability were determined (**Equation 8.1**) [9]:

$$L_p = \frac{J}{\Delta P} \times \frac{\eta_T}{\eta_{20}} = \frac{Je^{-0.0239(T-20)}}{\Delta P} \qquad [8.1]$$

Where ΔP is the measured TMP (bar), J is the measured membrane flux ($Lm^{-2}\ h^{-1}$), Lp is the permeability at 20 ^0C ($Lm^{-2}\ h^{-1}\ bar^{-1}$), and $\eta 20$ and ηT are the permeate viscosity at 20 ^0C and at the measured water temperature.

8.2.3 Molecular weight cut-off

Each PEG solution was prepared by dissolving the polymer in deionised water to give 0.6 g/L. A feed PEG solution was filtered through the virgin membranes at room

temperature and in cross- flow mode. The feed solution permeated the disc membrane under a constant TMP of 3 bar and a cross-flow velocity of 1 ms^{-1}.

Molecular weight cut-off was determined by analyzing both the feed solution and the permeate solution using a high-performance liquid chromatography system (Shimadzu, Japan) coupled to size exclusion chromatography columns (SEC, 5 µm 30 Å, PSS GmbH, Germany). These analyses generated molecular weight distribution curves of the dissolved PEG molecules in the feed and permeate solutions. The corresponding retention curves were then plotted by determining the rejection rate of (R_i) a PEG with certain molecular weight. Thereafter, the experimental rejection curves were described by log-normal distribution model as a function of MW and MWCO (**Equation 8.2**).

8.2.4 Defect Magnitude Determination

In order to characterize the extent of defects, it is necessary to differentiate permeability through membrane pores and through defects. In this work, it is hypothesised that the membrane will reach 100 % rejection when the largest PEG molecules are rejected by the largest defect pore size. In addition, MWCO is the value at which 90% of PEG are retained by the membrane [6], [7]. The rate of rejection *(R)* of PEG of a certain molecular weight is described by **Equation 8.2** [3], [8]:

$$R = \frac{\sigma(1-F)}{1-\sigma F} \qquad [8.2]$$

Where *F* is a solution diffusion constant, and *δ* is the reflection coefficient. To model the retention for a given PEG the log-normal distribution (**Equation 8.3**) is applied [9], [10]:

$$\sigma(MW_S) = \int_o^{MW_S} \frac{1}{S_{MW}\sqrt{2\pi}} \frac{1}{MW} \exp\left[\frac{-((Ln(MW) - Ln(MWCO) + 0.56S_{MW}))^2}{2S_{MW}^2}\right] \qquad [8.3]$$

Where S_{MW} is the standard deviation of the molecular weight *(MW)* distribution.

Molecular weight cut-off without defects was obtained by normalizing the rejection (i.e. rejection of membrane without defects) curve of all the pores by assuming that maximum rejection (plateau of the rejection curve) of the membrane to be that due to proper pores. The actual permeability is the factor of the measured permeability and the magnitude of the defects.

8.3 RESULTS AND DISCUSSION

8.3.1 Molecular Weight Cut-Off Determination

Molecular weight cut-off is the value at which 90 % of PEG is rejected by the membrane [6] (**Figure 8.1**). For the 10 membranes that were investigated, the MWCO including defects ranged from 1439.63 to 5552.39 Da. The least defects (**Figure 8.1a**), average defects (**Figure 8.1b**), and the most defects (**Figure 8.1c**) for the set of membranes were in the range 1131.05-1317.25 Da. In this work, the difference in magnitude of the plateaux (i.e. 3.6-27.1%) gives the magnitude of defects. The MWCO without defects are within the manufacturer's MWCO specification of 1000 Da. However, the experimental values differed from those of the manufacturer by between 13 and 32 %, probably due to the difference in the measurement of the MWCO. Whereas permporometry method was used by the manufacturer, the log-normal distribution method was used in this work. The value of MWCO is therefore an artefact of the measurement technique used. Generally, permporometry is the preferred MWCO determination technique [11], [12].

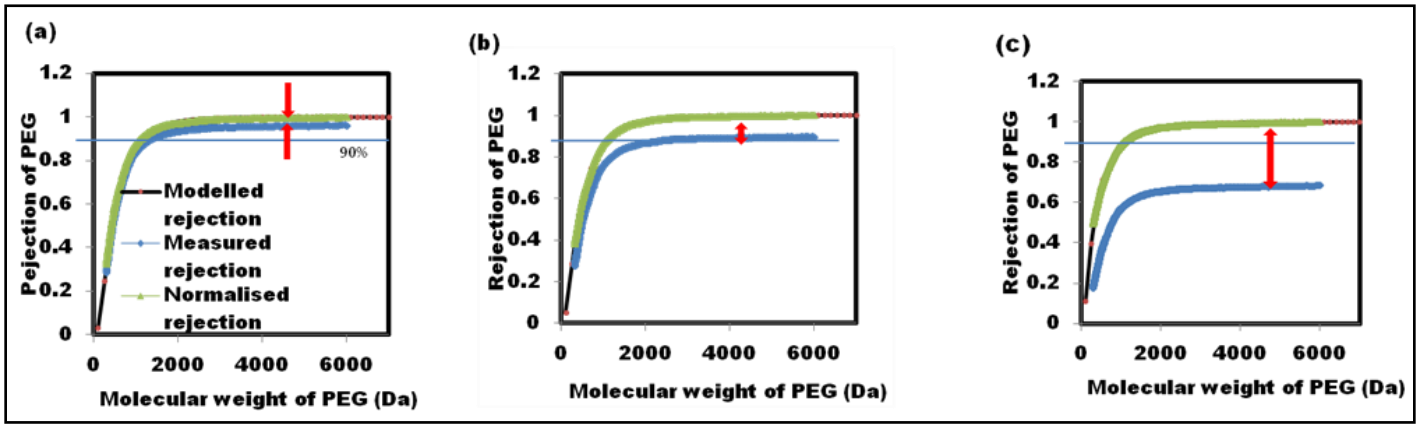

Figure 8. 1: MWCO using PEG for (a) the least defect magnitude, (b) medium defect magnitude, and (c) the most defect magnitude. The red arrow indicates the extent of defects.

The correlation of the extent of defects to the measured MWCO shows that the greater the defect the higher the MWCO (**Figure 8.2a**). Although the defects ranged from 3.6-27.1%, the difference between the measured MWCO with defects and without defects ranged between 27 - 369%. These results show that a small defect can result in the distortion of the measured MWCO. Similar results were obtained by other researchers [13] whereby the permselectivity of the sol-gel silica membranes varied between 3.2 and 52 prior to defect repair and increased to 68 – 308 after defect repair. It is the size and distribution of these artefacts that contribute to the measured MWCO. Similar trends whereby membrane gas permiselectivity due to defects that varied between 3.2 - 52 were reported; however, the permiselectivity increased 5 - 20 fold following repair [14]. No comparative data on defects of ceramic or polymeric membranes for water permeability has been reported in the literature.

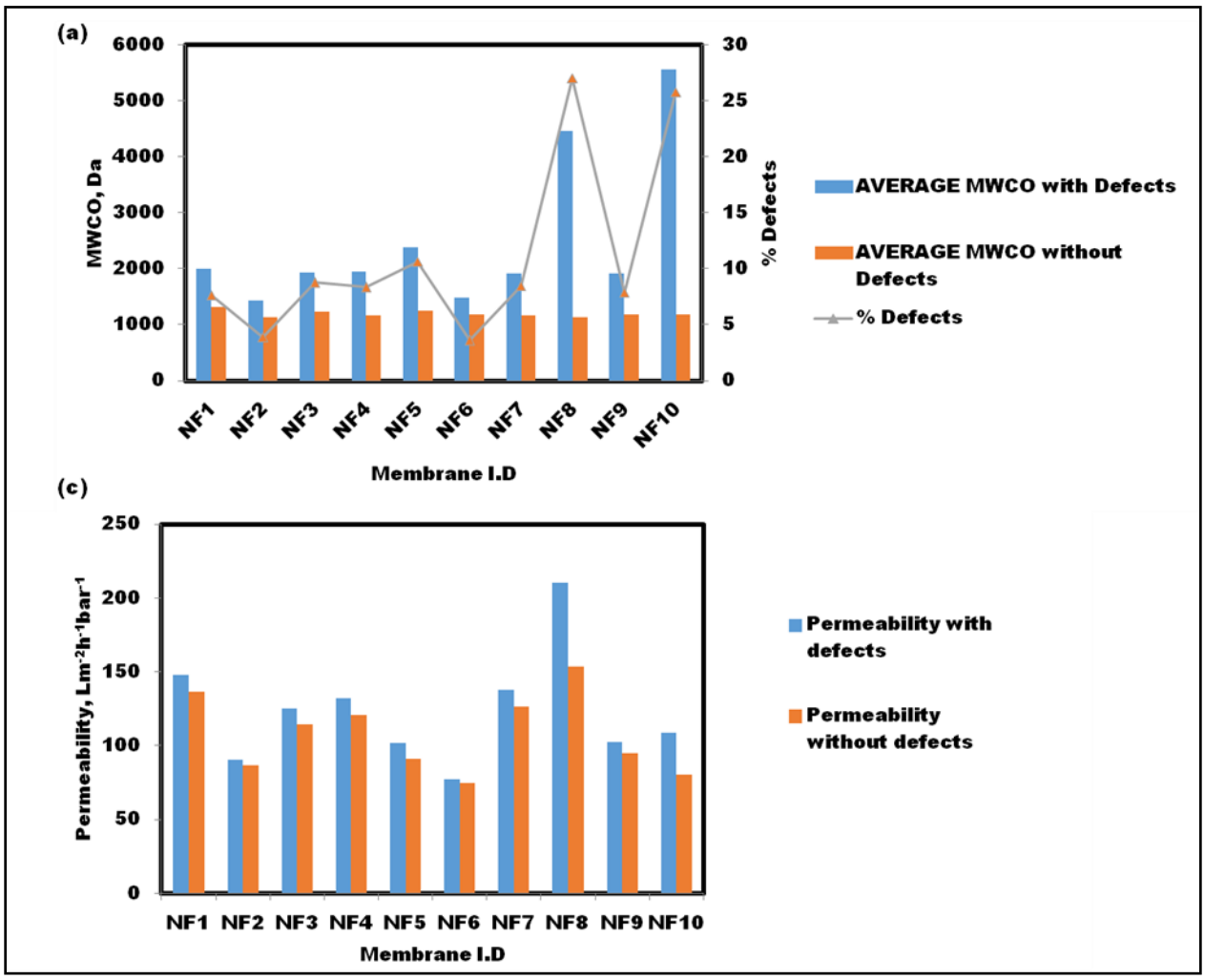

Figure 8. 2: (a) The correlation of the extent of defects to the measured MWCO, and (b) the deionised water permeabilities taking defects into account

8.3.2 Membrane Permeability With and Without Defects

The clean water permeabilities taking defects into account ranged from ~77 to 210 $Lm^{-2}h^{-1}bar^{-1}$ (**Figure 8.2b**). When corrected for defects, the values ranged from ~75 to 153 $Lm^{-2}h^{-1}bar^{-1}$. Solute permeability through the membranes was found to be higher when defects were taken into consideration. This is because defects do not offer any resistance of to the flow of solutes across the membrane because the defected pore sizes are greater than the size of the solute molecules. It was expected that membranes with greater defect magnitude would result in greater water permeability due to unrestricted flow through the defects. However, this was not the

case as the permeability increase due to defects was only ~4-37%. The measured water flux is a result of the combined effect of defect morphology and distribution, which in turn determine the resistance to flow [5].

The ideal permeability in this case is a factor of the magnitude of the defects, and the measured permeability is obtained by subtracting permeability due to defects from the measured permeability. Although the ranges of permeabilities with and without defects are comparable ($p < 0.05$), this trend does not translate into direct comparability of MWCO in that respect. This is because defects can take many forms, they can either be one big hole or several pinholes or a crack or several cracks. Therefore, the permeabilities measured are not within a reasonable range since each type of defect offers variable resistance to flow or the quantity of particles passing through the membrane.

8.4 CONCLUSION

In this study, a simple approach for defect characterization was investigated. The measured defected membrane surface area of the for the 10 disc membranes investigated ranged from about 4 to 27%. This gives an indirect measure of defect distribution on the membrane surface, without taking into account the size and morphology of the defects. This analytical method is non-destructive, generates high precision results, and is potentially useful to the water treatment industry due to ease of use. The method is also much more cost effective when compared with the laborious and expensive permporometry method.

8.5 REFERENCES

[1] J. Malzbender (2016). Mechanical aspects of ceramic membrane materials.

Ceramics International, **42** (7), 7899-7911.

[2] S. P. Cardoso, I. S. Azenha, Z. Lin, I. Portugal, A. E. Rodrigues, and C. M. Silva, (2017). Inorganic Membranes for Hydrogen Separation. *Separation and Purification Reviews*, **47**(3) 1–38.

[3] L. Zheng, H. Li, T. Xu, F. Bao, and H. Xu (2019). Defect size analysis approach combined with silicate gel/ceramic particles for defect repair of Pd composite membranes. *International Journal of Hydrogen Energy*, **41**(41), 18522–18532, 2016.

[4] K. H. Kim, P. G. Ingole, and H. K. Lee (2017). Membrane dehumidification process using defect-free hollow fiber membrane. *International Journal of Hydrogen Energy*, **42** (38) 24205–24212.

[5] J. Yu, J. Zhang, C. Bao, H. Li, H. Xu, and J. Sun (2017). Confined and in-situ zeolite synthesis: A novel strategy for defect reparation over dense Pd membranes for hydrogen separation. *Separation and Purification Technology*, **184**, 43–53, 2017.

[6] J. Shirley, S. Mandale, and V. Kochkodan (2014). Influence of solute concentration and dipole moment on the retention of uncharged molecules with nanofiltration. *Desalination*, **344**, 116–122.

[7] J.I Calvo, R.I Peinador, V Thom, T Schleuss, K T Vinh, P Pradanos and A Hernandex (2017). Comparison of pore size distributions from dextran retention tests and liquid-liquid displacement porosimetry. *Microporous and Mesoporous Materials*, **250**, 170–176.

[8] J. Garcia-ivars, J. Durá-maría, C. Moscardó-carreño, C. Carbonell-alcaina, M. Alcaina-miranda, and M. Iborra-clar (2017). Rejection of trace pharmaceutically active compounds present in municipal wastewaters using ceramic fine ultrafiltration membranes : Effect of feed solution pH and fouling phenomena. *Separation and Purification Technology*, **175**, 58–71.

[9] R. Shang, A. Goulas, C. Y. Tang, X. de Frias Serra, L. C. Rietveld, and S. G. J. Heijman (2017). Atmospheric pressure atomic layer deposition for tight ceramic nanofiltration membranes: Synthesis and application in water purification', *Journal of Membrane Science*, **528** (January), 163–170,.

[10] B. Van der Bruggen and C. Vandecasteele (2002). Modelling of the retention of uncharged molecules with nanofiltration. *Water Research*, **36**(5) 1360–1368.

[11] B. Hofs, J. Ogier, D. Vries, E. F. Beerendonk, and E. R. Cornelissen (2011).Comparison of ceramic and polymeric membrane permeability and fouling using surface water. *Separation and Purification Technology*, **79**(3), 365–374,

[12] S. Zeidler, P. Puhlfürß, U. Kätzel, and I. Voigt (2014). Preparation and characterization of new low MWCO ceramic nanofiltration membranes for organic solvents. *Journal of Membrane Science*, **470**,421–430.

[13] D. Koutsonikolas, S. Kaldis, G. P. Sakellaropoulos, M. H. Van Loon, R. W. J. Dirrix, and R. A. Terpstra (2010). Defects in microporous silica membranes: Analysis and repair. *Separation and Purification Technology*, **73** (1), 20–24.

[14] D. Koutsonikolas, S. Kaldis, and G. P. Sakellaropoulos (2009). A low-temperature CVI method for pore modification of sol-gel silica membranes. *Journal of Membrane Science*, **342**(1–2),131–137.

CHAPTER 9*:..*

CONCLUSION AND RECOMMENDATIONS

The primary aim of this research study was to investigate NOM treatability from South African surface water sources by ceramic NF membranes. This aim was achieved by firstly characterising NOM found in South African surface waters that serve water treatment plants. Secondly, by investigating the extent of treatability of NOM through conventional methods, and then finally by investigating the applicability of ceramic NF membranes in the removal of NOM found in South African water sources. The main findings emanating from this study showed that the NOM found in South African water is variable in terms of character, and the application of ceramic NF membranes produced water of similar permeate quality regardless of the physico-chemical variability of the feed water. It is envisaged that the South African water boards and the potable water treatment industry as a whole will benefit from the findings of this study.

It is expected that the introduction of ceramic NF membrane filtration as a complementary step for the treatment of NOM in South Africa will result in the development of a process that is targeted towards the effective removal of NOM during potable water treatment. In addition, further modifications of the ceramic NF membranes would enhance the targeting and removal of specific problematic NOM fractions.

The proposed technology, is envisioned to:

i) Be tailored to target problematic NOM fractions responsible for the formation of disinfection by-products.

ii) Be modified to target problematic NOM fractions responsible for bacterial proliferation down the treatment stream.

iii) Be robust enough to withstand aggressive waters and be able to continuously produce same quality water regardless of changing physico-chemical properties of the feed waters.

iv) Be able to be integrated into the existing conventional water treatment methods without substantially increasing the carbon foot print of the whole water treatment processes.

9.1 CONCLUSIONS

Samples from five water quality regions of South Africa were used to test the performance of the ceramic membrane filtration technology. Synthetic waters were used for modelling purposes. The major findings of this work, which are presented below, are related to the objectives of the study outlined and the research questions posed in **Chapter 1**.

- **Characterising NOM fractions found in South African surface waters using advanced methods** - Water samples were analysed for DOC, UV absorbance, SUVA, spectroscopic indices, fluorescence intensity as well as presence of biopolymer (polysaccharides), and the following key findings related to the objectives of this research study were reported: The characterisation of NOM using SUVA serves as a valuable prediction tool for the removal of NOM. As expected, a DOC removal efficiency exceeding 50% was observed for plants with SUVA > 4, namely plants H, HL and P. Less than 25% DOC removal efficiency was observed for plants FB, UM and MT, which had a SUVA < 2. A model fitting four components was established and validated based on the slit half criteria, and the distribution of the components at each water source was quantified using their maximum fluorescence intensities *(F_{max})*. The value of F_{max} was higher for terrestrial humic-like (C1) and fulvic like (C2) components in comparison to humic-like (C3) and protein-like (C4) components. This suggests that C1 and C2 components have high quantum efficiencies and low responses to quenching effects compared to C3 and C4 components. Coagulation was more effective for the removal of the humic-like fractions when compared with the other fractions. In the rapid sand filtration stage, bulk DOM removal (in terms of UV_{254}) was found to be higher than that of FDOM, regardless of location of the plant. This suggests that non-FDOM fractions are removed much more effectively than FDOM fraction during the RSF stage. Although disinfection has proven to be efficient in the removal of humic-like fractions by transforming it into a less aromatic and halogenated form, the efficiency of this process in the removal of other FDOM is not as effective.

- **The occurrence and behavior of NOM fractions found in South Africa for the purpose** of investigating the extent of ceramic NF membranes processes in the removal of NOM fractions using multi-faceted characterization techniques. – The rate of removal of bulk NOM (measured as UV_{254} and *DOC* removal), biodegradable dissolved organic carbon (BDOC) fraction, polarity fractions and fluorescent natural organic carbon (FDOM) fractions was investigated. The following conclusions were drawn: Ceramic membranes were more effective in removing bulk NOM (measured as DOC and UV_{254} removal) for coastal plants than for inland plants. The rate of removal of FDOM appears to be generic and applies to all plants investigated and is not dependent on the location of the abstracted water. The removal of BDOC by the ceramic membranes was high for coastal plants and correlated well with DOC removal. DOC removal can therefore be used as predictor of BDOC removal. The hydrophobic (HPO) fraction was the most amenable to removal by ceramic membranes, regardless of the site of sample abstraction. *UV* transmission for OL was higher than for all the other sites thus implying that OL waters least fouled the ceramic membranes compared to the other sites. This investigation revealed the dynamics of the removal of NOM fractions by ceramic membranes, specifically to South African waters. Results generated herein would serve as an appraisal for the application of ceramic membranes in South Africa.

- **Comparative analysis of the fouling of model pollutants and modified membranes and pristine ceramic membranes** under similar hydrodynamic conditions - The results showed that sodium alginate (SAL) caused the most extensive fouling on pristine membranes and atomic layer deposition (ALD) modification reduced its fouling potential by 35%. Cake filtration was the least fouling mechanism in feed solutions composed of bovine serum albumin (BSA) and SAL, and the most favourable fouling mechanism of feed solution, which included humic acid (HA) and SAL. The fouling mechanisms were almost similar for both membranes. For the modified membrane, R^2 = 0.74; 0.74 and 0.40 for complete blocking, standard blocking and intermediate blocking, respectively,

whilst for the pristine, R^2 = 0.76; 0.75 and 0.60 for complete blocking, standard blocking, and intermediate blocking, respectively. However, cake filtration was the favoured fouling mechanism for the modified membrane (R^2 = 0.99), and the least favoured fouling mechanism for the pristine membrane (R^2 = 0.37). Modification of the ceramic membranes led to an increase in their hydrophilicity, as evidenced by the contact angle measurements, which showed a 23 % decline in hydrophobicity from uncoated to coated membrane.

- **Investigate the selectivity of ceramic membranes towards specific NOM fractions and the impact of coupling ceramic membranes to unit operations** (e.g. dissolved air flotation filtration (DAFF)) for purposes of establishing the best unit process combination that gives maximum removal of NOM fractions – Water sample from the DAFF unit process was fractionated and the hydrophilic fraction was conjectured to be responsible for the formation of disinfection by-products (DBP) and the removal of this fraction before chlorination by ceramic membranes was investigated. Correlation between the removal of tyrosine like fraction of the HPI by ceramic membranes and molecular weight cut-off (MWCO) of the membranes was established. Furthermore, the removal of the tyrosine fraction of the HPI fraction followed the order of decreasing MWCO. These findings together with results from the removal of chromophoric NOM fractions are essential to WTPs for the targeting and elimination of the DBP precursor fraction.

The specific conclusions in response to the research questions:

1. *To what extent are NOM fractions removed at each treatment stage?* – In Chapter 4 it was established that the extent of NOM fraction removal at each treatment stage depended on the character of NOM in question and the treatment step itself. The extent of removal of polysaccharides at the caogulation stage was between -21% (OL) to 15.3% (H). This variation was attributed to factors such as coagulant type and charge, pH, other charged species that can be entraped within the polysaccharide matrix necessitating its agglomeration into flocs. It was also found that polysacaccharides increased at the disinfection stage: P (-43%); UM (-36%); AM (-19%); H (-19%); OL (-11%); FB (-7%) and HL

(-6%). This was attributed to an increase of extracellular polymeric substances (EPS) arising from the bacteria killed by chlorine. Coagulation was more effective in the removal of the humic-like fractions than the other FNOM fractions. Regardless of the location of the plant, bulk DOM removal (in terms of UV_{254}) was found to be higher in comparison to FDOM in the rapid sand filtration stage. This suggests that the non-FDOM fractions are removed much more efficiently than the FDOM fraction during the rapid sand filtration (RSF) stage.

2. *To what extent can spectroscopic indices be used as predictors for NOM removal efficiency by conventional unit processes?* – In Chapter 4, when data from all sampled water sources was pooled together a good correlation between *HIX* and UV_{254} removal was established (R^2 = 0.80). At the same time, the freshness index *(β:α)* was correlated to UV_{254} removal (R^2 = 0.79). Microbially derived NOM (*FI* < 1.3) showed greater susceptibility to removal than the terrestrially derived NOM (*FI* >1.7) Specific UV absorbance displayed a mild relationship to the UVA reduction (R^2= 0.75).
3. *What is the removal efficiency of the NOM characteristics (DOC, UV_{254} FNOM, BDOC) found in South African surface waters by ceramic membranes? – In Chapter 5,* it was established that the UV_{254} removal by the ceramic membranes was largely constant over time for all WTPs. This demonstrates the chemical stability and mechanical strength of ceramic membranes operation over time treating water of different physico-chemical properties. Notably, coastal plants (H and P) had the highest values for UV_{254} removal (both 80% on average) and UV_{254} removal by inland plants was in the range 55-60 %. Coastal plants (PL and H) removed more than 80% of *DOC,* while inland plants removed between 60-75%. All fractions were removed to at least 80% of *FDOM* regardless of the location of the plant. This suggests ceramic membranes have high selectivity towards the removal of fluorescent NOM fractions. The removal of *BDOC* by the ceramic membranes was above 85% with coastal plants (PL and H) having the highest removal rate. Interestingly, the trend in the removal efficiencies of *BDOC* followed that of *DOC* removal (R^2 = 0.97). This implies that the removal of *DOC* can be a predictor of *BDOC* removal by ceramic membranes for the sampled

water.

4. *What is the dominant fouling mechanism on ceramic membranes by waters from different water quality sources of South Africa* - In Chapter 5, it was established that the dominant fouling mechanisms for PL were intermediate fouling and cake filtration (R^2 of 0.85 and 0.83 respectively). For MV all fouling mechanisms had almost equal contribution on fouling (for complete blocking; standard blocking; cake filtration and intermediate blocking, with R^2 = 0.94; 0.94; 0.98 and 0.79, respectively). Complete blocking and standard fouling were the dominant fouling mechanisms for HL (R^2 = 0.96 and 0.89, respectively. Complete blocking (R^2 = 0.24 and 0.42 for H and OL, respectively) and standard blocking (R^2 = 0.23 and 0.41 for H and OL, respectively) were the least fouling mechanisms for H and OL. Intermediate blocking (R^2 = 0.68 and 0.90 for H and OL, respectively), and cake filtration (R^2 = 0.78 and 0.97 for H and OL, respectively) were the dominant fouling mechanisms. This implies for H and OL an initial phase dominated by intermediate blocking was followed by a transition to cake filtration at a subsequent stage in the filtration process.
5. *Which model NOM fraction has the highest propensity to foul the membranes and why?* – In Chapter 6 it was established that the most favourable fouling mechanism for cake filtration was for the feed stream containing HA and SAL (R^2 = 0.97), which is ascribed to the complexation of cations to the organics leading to the formation of large HA-cation, SAL-cation and SAL-HA complexes that settle on the surface of the membrane and increase the resistance to permeate flow. Although the single and dual combination of HA and SAL favoured cake filtration (R^2 = 0.97; 0.99; 0.97 for HA; SAL and HA+SAL, respectively) and the flux loss of 21; 54 and 25% for HA; SAL and HA+SAL, respectively, the co-existence of HA and SAL in the feed reduced the fouling propensity of SAL on its own. This could be attributed to competition for cations in solution, with HA attracting more positively charged species than SAL, thus leaving most of SAL in solution.
6. *How does the extent of fouling on the modified ceramic membrane compare with that of pristine membranes?* – In Chapter 6 an investigation of the impact of

membrane surface modification was studied with feed solutions that caused the most severe fouling on the pristine membranes, namely: SA and HA+BSA+SAL. When SA was used as the foulant, the rate of flux decline (25%) was similar for both membranes in the first 50 minutes. Thereafter, a steady state flux was observed for the coated membrane whilst a declining flux trend was exhibited by the pristine membrane. The modification of the membranes led to a 35% improvement in the flux recovery when SAL was used as the foulant. For both types of membranes, cake filtration was the favoured fouling mechanism (R^2 = 0.99 and 0.82 for the pristine and coated membranes, respectively). These results suggest modification of the ceramic membranes investigated leads to an improvement in their anti-fouling property.

7. *What is the extent of selectivity and removal of specific NOM fractions by ceramic membranes (i.e. BDOC, chromophoric, fluorescent and biogenic fractions) from raw and partially treated waters?* – In Chapter 7 the trend in the removal of chromophoric NOM fractions by ceramic membranes was elucidated by applying the Gaussian peak fitting on a UV-Vis spectrum. A very close fit (R^2 > 0.95) of the experimental data and the Gaussian distribution bands were observed. Although the UV-Vis spectra generally reduced significantly from the raw sample to the permeates, the positions of the maxima of the Gaussian bands did not change considerably even though the intensities of the bands reduced. The reduction of intensity of these bands is a measure of the efficiency of the membranes in the removal of chromophoric moieties. Raw water exhibited high biopolymer concentration (100.03 µg/L glucose eq). Higher biopolymer concentration has been reported for highly hydrophilic water compared to hydrophobic water. The membranes under investigation were found to possess over 85% removal efficiency of the biopolymers, with M1 ranking the highest at 94%. The removal efficiency of biopolymers increased following the order of decreasing MWCO (i.e., smaller MWCO membranes were able to retain more biopolymers than larger MWCO membranes due to steric rejection). Removal of BDOC was above 85%, with M1 and M5 achieving the highest (94%) and least (88%) BDOC removal efficiencies, respectively.

8. *To what extent does coupling of the membrane to unit processes improve the effectiveness of the removal of DBP precursors?* - In Chapter 7 it was conjectured that the HPI was the main precursor for the formation of THM and HAA in low-humic water such as in the case under study, an in-depth study of the compositional variation of the HPI was undertaken. The removal of the HPI fraction by the membranes under investigation was at least 40 %. The low removal efficiency of the investigated membranes stems from the fact that these membranes were not charged and the only available mode of removal was based on size exclusion. The removal rate of tyrosine in the hydrophilic fraction was in the range 60-66 %. Through this research study, it has been established that lowest MWCO membrane possesses the highest removal efficiency towards tyrosine-like fraction of the HPI NOM fraction (66.1%). In contrast, the highest MWCO membrane was found to possess the lowest removal efficiency (61%). These findings suggest the tyrosine-like component of the HPI fraction is the DBP limiting reagent. Therefore, sequestration of the proteinacious material prior to the disinfection stage is expected to reduce the DBP concentrations
9. *What are other opportunities for development of simple methods of characterizing ceramic membrane? – In Chapter 8*, the discussion followed the usual and qualitative method of analyzing defects in ceramic membranes namely the application of scanning electron microscopy (SEM) or transmission electron microscopy (TEM) images. However, it is difficult to get a general picture of defect size distribution due to limited area of analysis (ca. 100 μm^2). A relatively facile defect characterisation approach was proposed, from this method, the measured defects quantity for the 10 disc membranes investigated ranged from about 4 to 27%. This gives an indirect measure of defect distribution on the membrane surface, without taking into account the size and morphology of the defects. This analytical method is non-destructive, generates high precision results, and is potentially useful to the water treatment industry due to ease of use. The method is also much more cost effective when compared with the laborious and expensive permporometry method.

9.2 RECOMMENDATIONS

Although the set research aims and objectives of this project have been achieved, it is recommended that further research be undertaken countrywide to address the issues raised in this work. In this regard, the specific research that can be undertaken is as follows:

- **Validating the NOM characterization and monitoring protocol** by incorporating seasonal variabilities.
- **Trihalomethane and Haloacetic acid formation potential of NOM fractions** – Although ceramic membranes were able to significantly reduce the conjectured DBP precursors, further studies need to be carried out to ascertain the extent to which ceramic membranes remove specific DBP precursors.
- **Up scaling to pilot scale** – The study used a laboratory scale ceramic membrane filtration set-up. It would be interesting to upscale the system to pilot scale and using ceramic membranes of different configurations. Additionally, to further assess the robustness of ceramic membranes in terms of fouling resistance, mechanical and chemical integrity longer operation times using feed waters of different physico-chemical properties is envisioned to further appraise ceramic membranes as a technology of choice in South Africa.
- **Quantitative and qualitative analysis of NOM molecular weight fractions using the liquid chromatography coupled with organic carbon detector (LC-OCD)** - lastly, an investigation on the use of LC-OCD as a molecular weight fractionation technique will give further insights into the NOM character of South Africa as well as the selectivity of ceramic membranes towards the removal of specific molecular weight fractions of NOM of South Africa.

Table A1: Average values of DOC concentration and spectrophotometric parameters (n = 3)

WTP		DOC	UV254	SUVA	a315	tCDOM	F.I	β:α	HIX	ΔEEM fraction (RU)				
		(mg/L)	(/cm)	(L/mg.m)	(/cm)	(nm/cm)				$P_{n,1}$	$P_{n,2}$	$P_{n,3}$	$P_{n,4}$	$P_{n,5}$
FB	Raw	5.54	0.13	2.21	0.54	8.78	1.66	0.82	0.84					
	Coag	5.84	0.09	1.69	0.56	5.92	1.64	0.90	0.72	0.23	0.20	0.15	0.29	0.13
	Sett	5.80	0.10	1.78	0.53	6.56	1.70	0.90	0.79					
	RSF	5.54	0.09	1.57	0.44	5.21	1.75	0.89	0.81	0.04	0.07	0.21	0.18	0.49
	Final	5.47	0.07	1.23	0.47	3.86	1.90	0.89	0.76	0.04	0.06	0.17	0.12	0.60
UM	Raw	7.54	0.16	3.09	0.62	13.12	1.59	0.74	0.84					
	Coag	5.23	0.14	1.87	0.51	9.40	1.72	0.69	0.86	0.04	0.09	0.18	0.15	0.54
	Sett	5.12	0.13	2.47	0.42	9.76	1.69	0.70	0.87					
	RSF	4.86	0.09	1.90	0.47	5.86	1.69	0.70	0.88	0.05	0.08	0.17	0.18	0.52
	Final	4.92	0.07	1.33	0.64	3.93	1.82	0.80	0.84	0.03	0.05	0.25	0.09	0.58
OL	Raw	6.01	0.18	3.02	0.52	16.36	1.75	0.82	0.81					
	Coag	5.32	0.15	2.87	0.63	13.73	1.69	0.80	0.83	0.43	0.00	0.09	0.01	0.46
	Sett	5.22	0.11	2.11	0.49	8.68	1.73	0.79	0.83					
	RSF	5.04	0.08	1.65	0.46	4.99	1.71	0.81	0.83	0.19	0.07	0.02	0.08	0.64
	Final	4.92	0.07	1.35	0.51	3.73	1.73	0.83	0.83	0.04	0.10	0.17	0.10	0.60
AM	Raw	4.72	0.21	4.92	0.69	20.53	1.52	0.64	0.87					
	Coag	4.30	0.18	3.90	0.60	16.26	1.70	0.78	0.82	0.26	0.01	0.22	0.49	0.02
	Sett	4.38	0.10	2.33	0.47	8.46	1.70	0.68	0.90					
	RSF	4.46	0.07	1.59	0.46	4.79	1.67	0.68	0.90	0.32	0.23	0.41	0.01	0.02
	Final	4.87	0.07	1.40	0.55	4.34	1.81	0.84	0.77	0.20	0.15	0.34	0.03	0.28
MT	Raw	12.51	0.14	1.12	0.54	12.03	1.53	0.64	0.87					
	Coag	9.20	0.14	1.51	0.54	12.74	1.65	0.74	0.83	0.04	0.05	0.19	0.03	0.70
	Sett	6.51	0.12	1.87	0.44	10.97	1.65	0.72	0.86					
	RSF	5.70	0.06	1.11	0.52	4.42	1.60	0.68	0.89	0.16	0.12	0.21	0.14	0.37
	Final	4.45	0.05	1.14	0.38	3.42	1.83	0.75	0.83	0.02	0.05	0.23	0.08	0.62
H	Raw	6.03	0.58	15.63	0.72	46.27	1.37	0.46	0.94					
	Coag	3.70	0.48	7.99	0.61	36.06	1.55	0.65	0.88	0.03	0.00	0.05	0.04	0.88
	Sett	3.66	0.18	5.02	0.64	12.96	1.65	0.72	0.86					
	RSF	3.22	0.12	3.78	0.48	7.83	1.69	0.68	0.90	0.15	0.10	0.13	0.19	0.42
	Final	3.36	0.09	2.56	0.57	5.32	1.71	0.61	0.87	0.01	0.04	0.22	0.09	0.64
P	Raw	5.88	0.26	4.38	0.08	19.64	1.36	0.44	0.92					
	Coag	4.07	0.24	5.91	0.05	20.20	1.55	0.55	0.89	0.06	0.03	0.16	0.03	0.72
	Sett	3.81	0.16	4.14	0.40	12.52	1.54	0.53	0.92					
	RSF	3.24	0.09	2.65	0.21	5.81	1.61	0.56	0.93	0.09	0.10	0.25	0.00	0.55
	Final	3.44	0.07	2.05	0.30	5.81	1.73	0.54	0.91	0.06	0.05	0.16	0.08	0.65
HL	Raw	2.60	0.17	6.33	0.58	12.81	1.60	0.69	0.89					
	Coag	2.01	0.15	7.62	0.50	12.64	1.69	0.72	0.89	0.06	0.03	0.16	0.09	0.66
	Sett	2.03	0.11	5.33	0.39	7.30	1.70	0.70	0.90					
	RSF	1.94	0.10	4.97	0.50	6.32	1.77	0.69	0.89	0.07	0.04	0.05	0.07	0.77
	Final	1.97	0.16	8.26	0.53	12.66	1.60	0.70	0.89	0.22	0.15	0.26	0.18	0.19

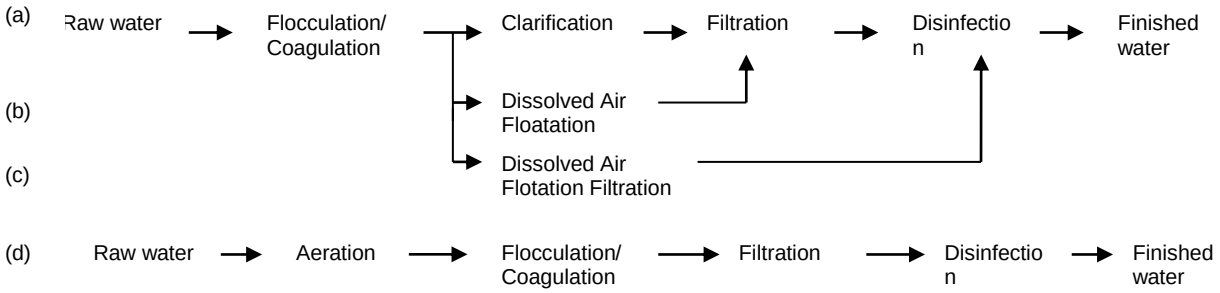

Figure A1: Treatment regimen of sampled WTPs: (a) FB, UM, OL, AM, MT, H, HL; (b) P; (c) RV and (d) EB

Chapter 5: Appendix

Table 1A: Percentage FDOM removal by ceramic NF membranes

	C1 (%)	C2 (%)	C3 (%)	C4 (%)
H	89	89	91	89
HL	87	88	90	87
MV	85	85	91	85
OL	88	87	89	89
PL	89	89	87	86

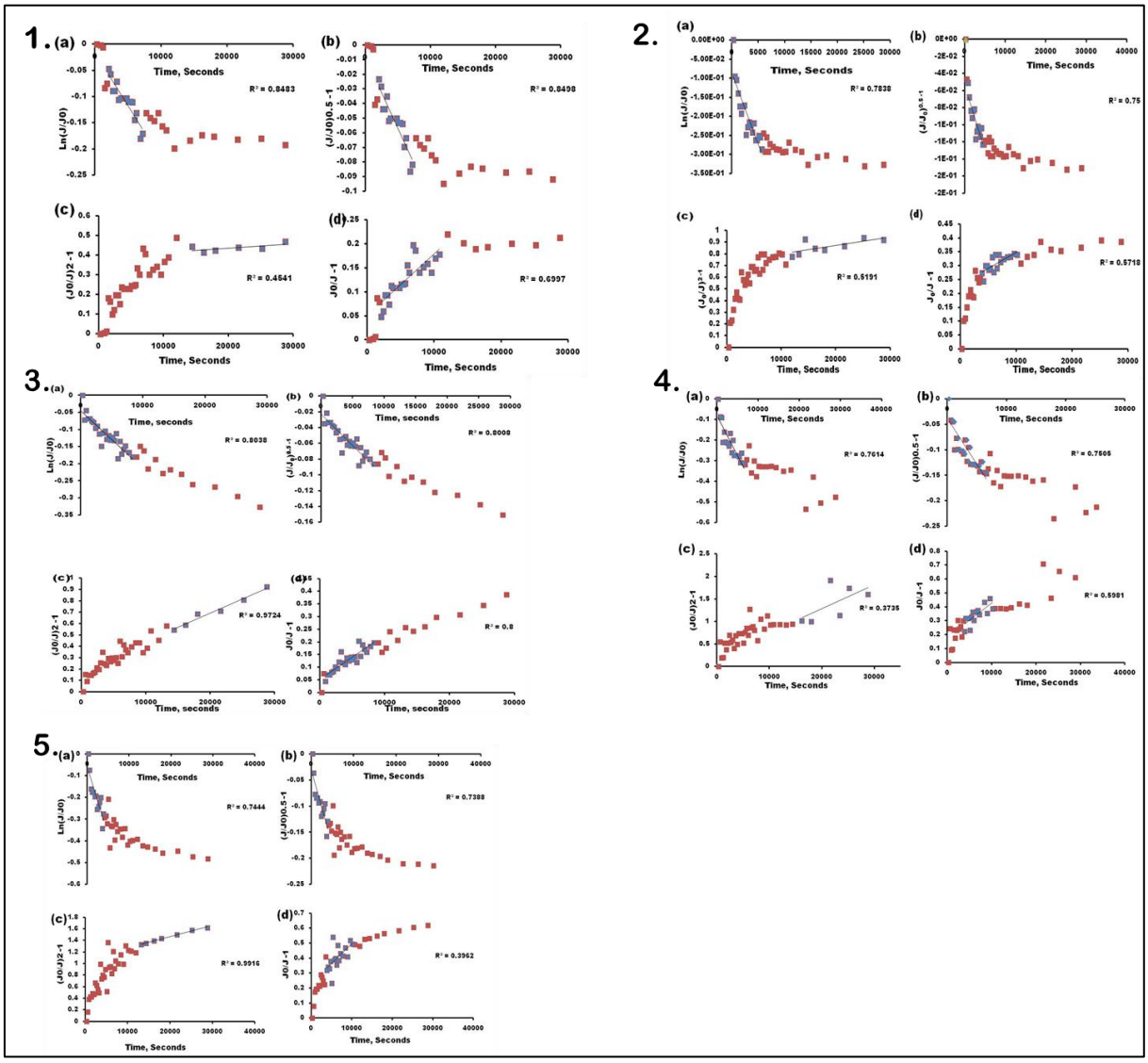

Figure A1: Fouling mechanisms of combined foulants on the unmodified membrane: 1. HA+BSA (a) complete blocking, (b) standard blocking, (c) cake filtration, (d) intermediate fouling; 2. BSA+SAL a) complete blocking, (b) standard blocking, (c) cake filtration, (d) intermediate fouling ; 3. HA+SAL a) complete blocking, (b) standard blocking, (c) cake filtration, (d) intermediate fouling; 4. HA+BSA+SAL fouling on the unmodified membrane a) complete blocking, (b) standard blocking, (c) cake filtration, (d) intermediate fouling**;** 5. HA+BSA+SAL fouling on the modified membrane a) complete blocking, (b) standard blocking, (c) cake filtration, (d) intermediate fouling

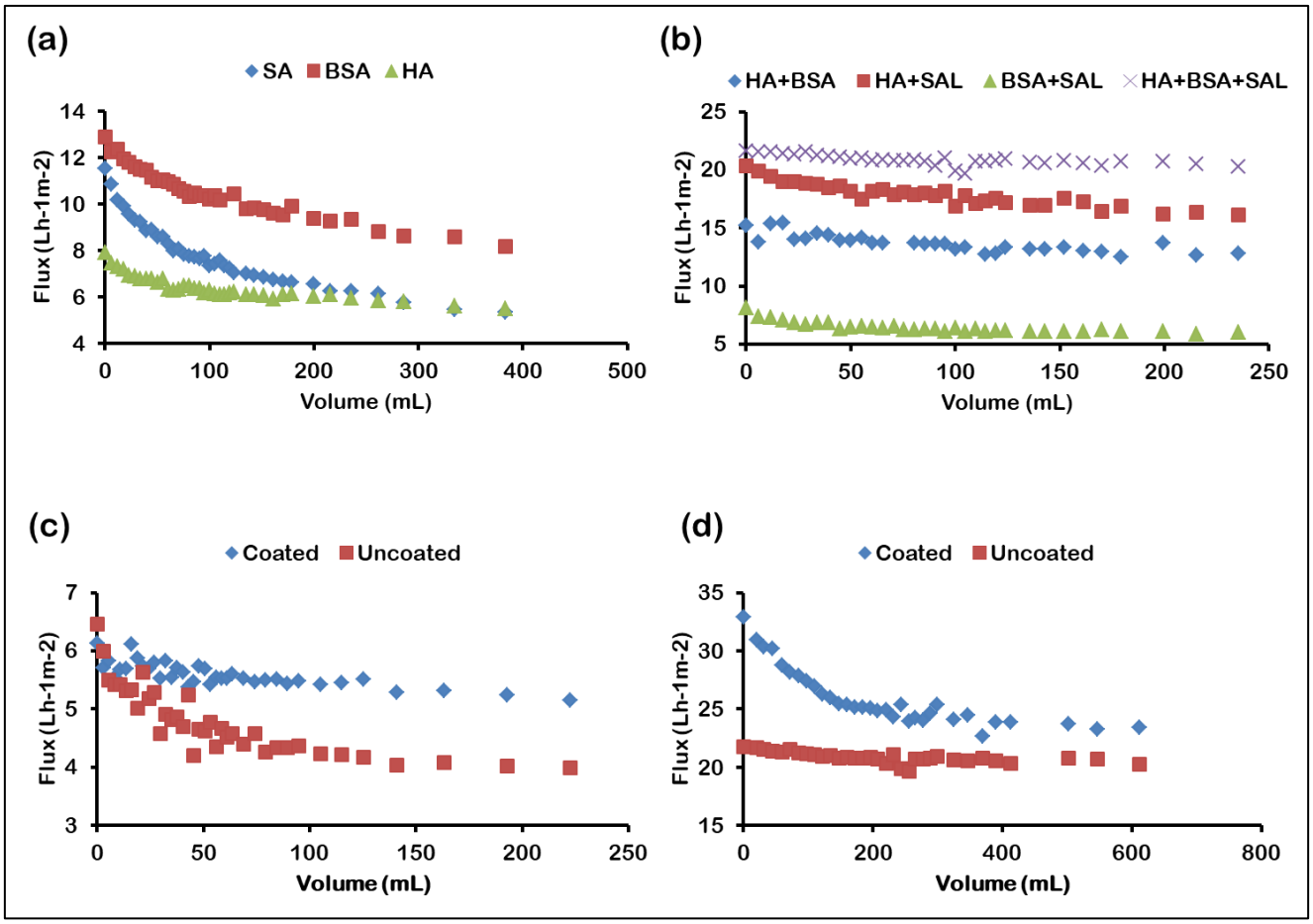

Figure A2: Fouling decline profiles: (a) single foulants on the uncoated membrane; (b) combined foulants on the uncoated membrane; (c) SA fouling profile on the coated membrane; and (d) HA+SAL+BSA fouling profile on the coated membrane

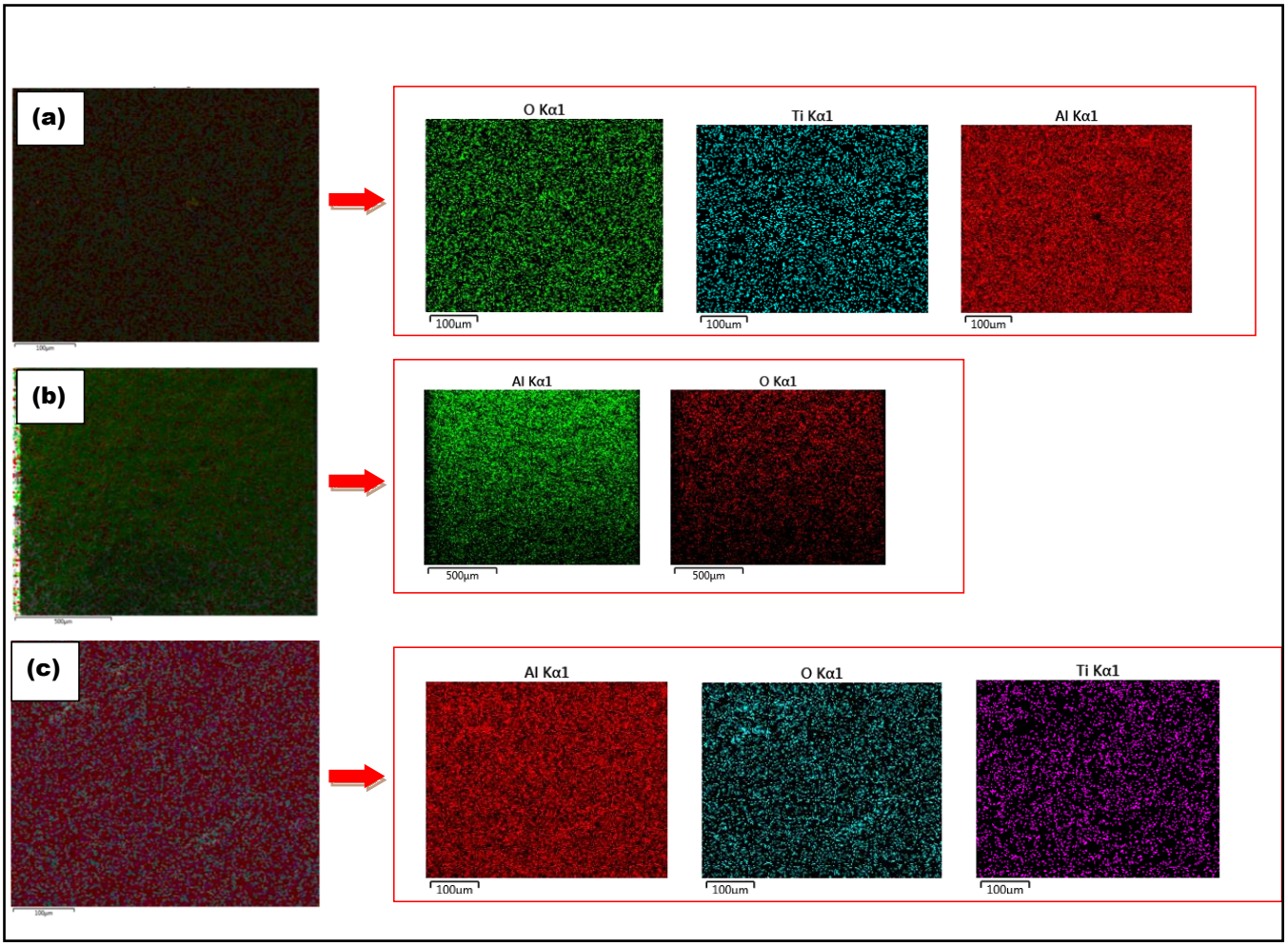

Figure A3: Surface elemental mapping of the (a) top side, (b) cross section of the coated membrane and (c) top side of the uncoated membrane

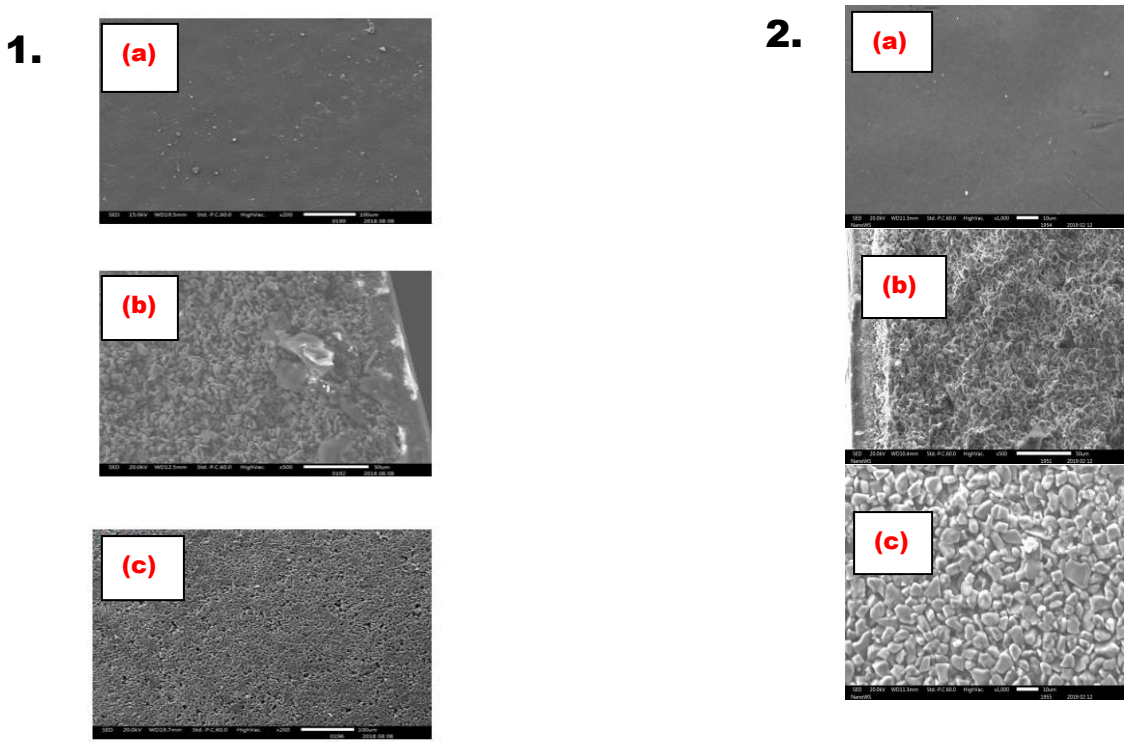

Figure A4: Scanning electron microscope (SEM) micrographs of the (1) uncoated membrane and (2) coated: (a) separation layer; (b) cross sectional layers, and (c) support layer

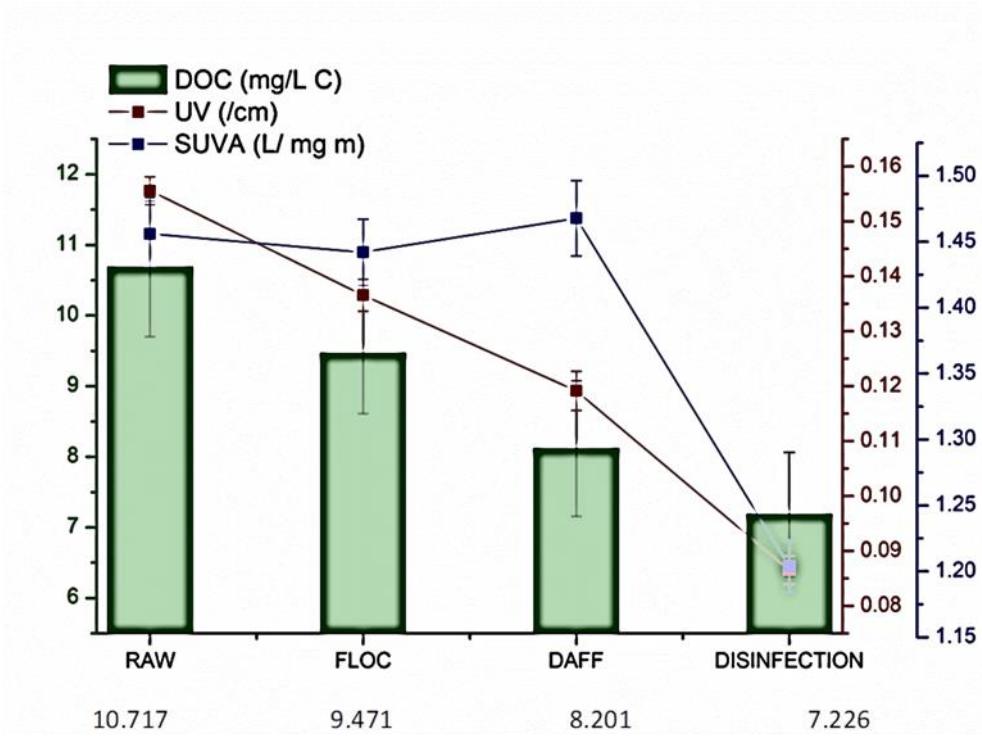

DOC	10.717	9.471	8.201	7.226
UV	0.156	0.137	0.119	0.087
SUVA	1.456	1.447	1.451	1.204

Figure A1: Water quality parameters at different treatment stages

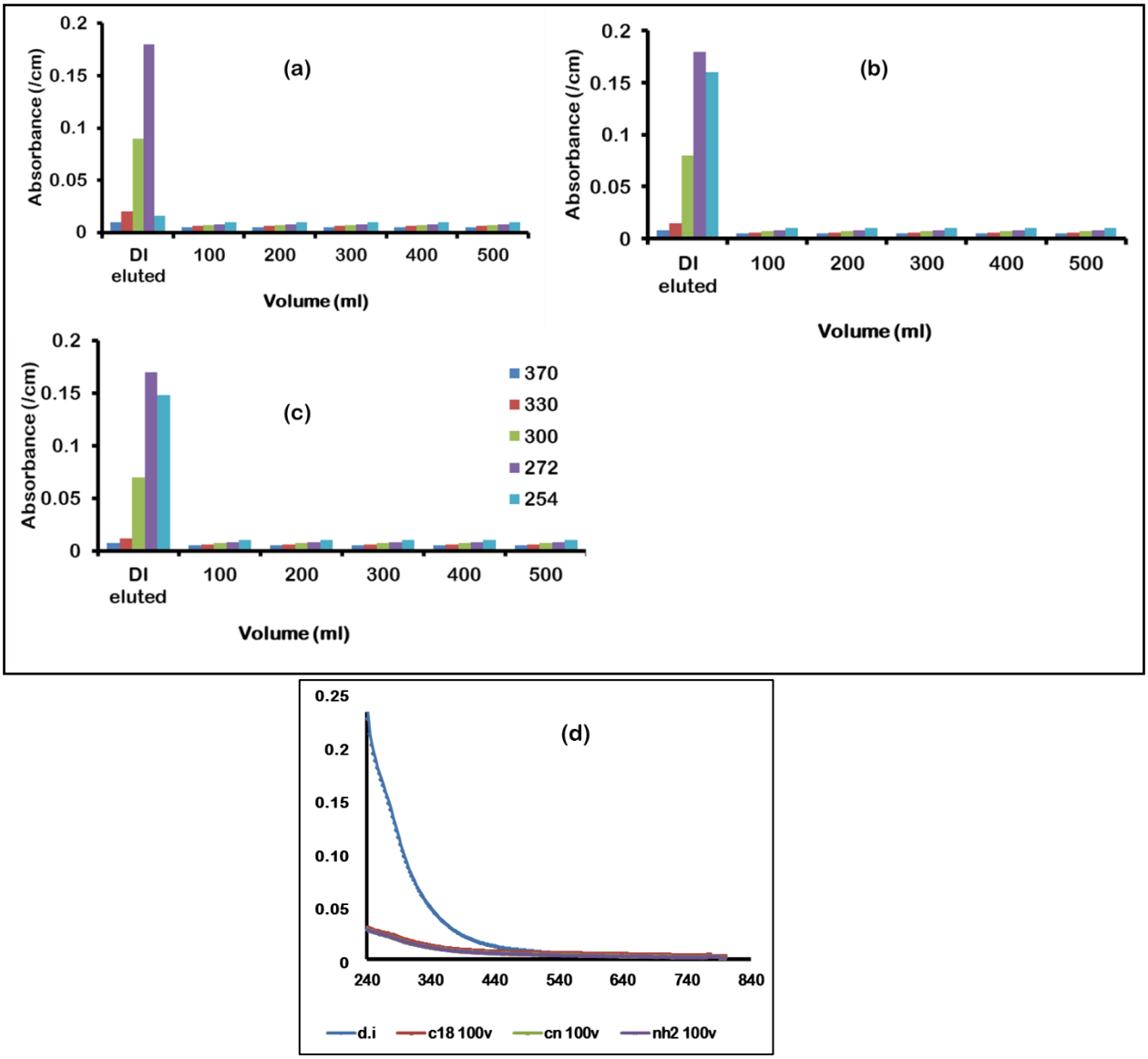

Figure A2: Quality assurance for asserting no further leaching of carbon from SPE cartridges during (a) C18; (b) CN; (c) NH column cleaning; and (d) UV-Vis absorbance after eluting 100 mL of deionized water

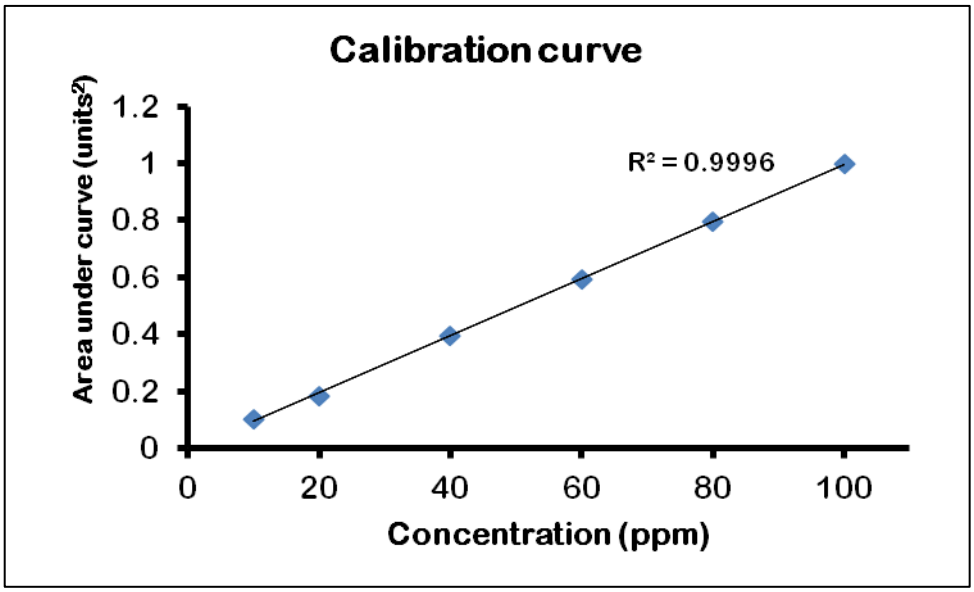

Figure A3: Calibration curve obtained by using glucose standard of known concentration

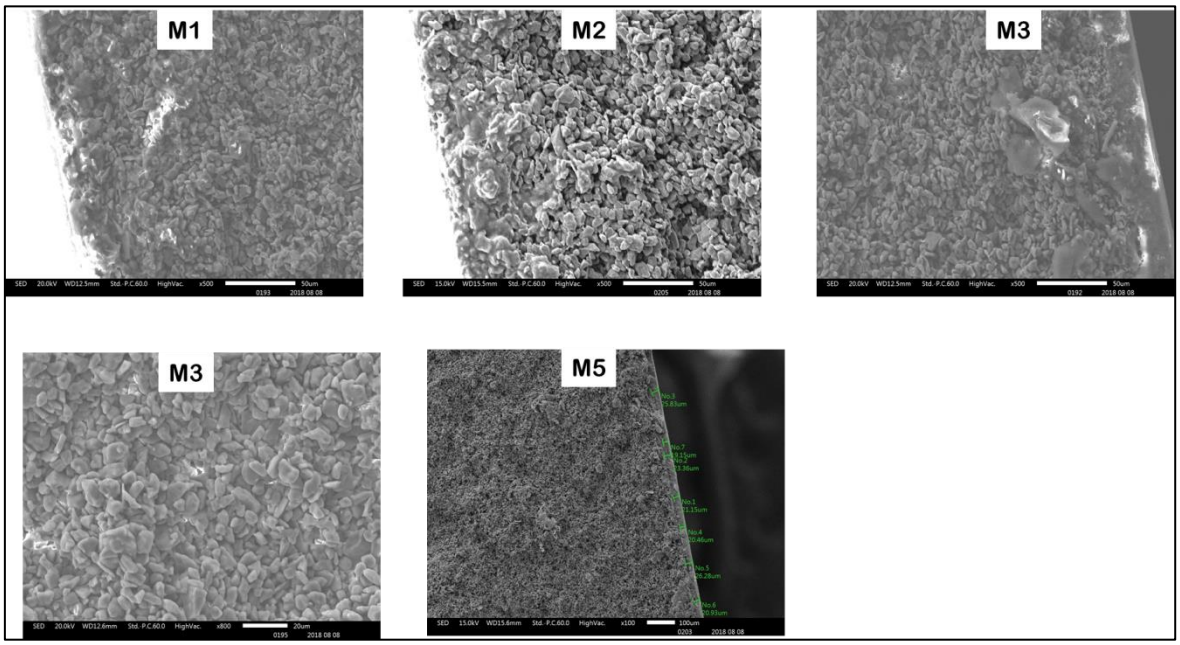

Figure A4: Scanning micrographs of the cross sectional layer of the ceramic membrane.

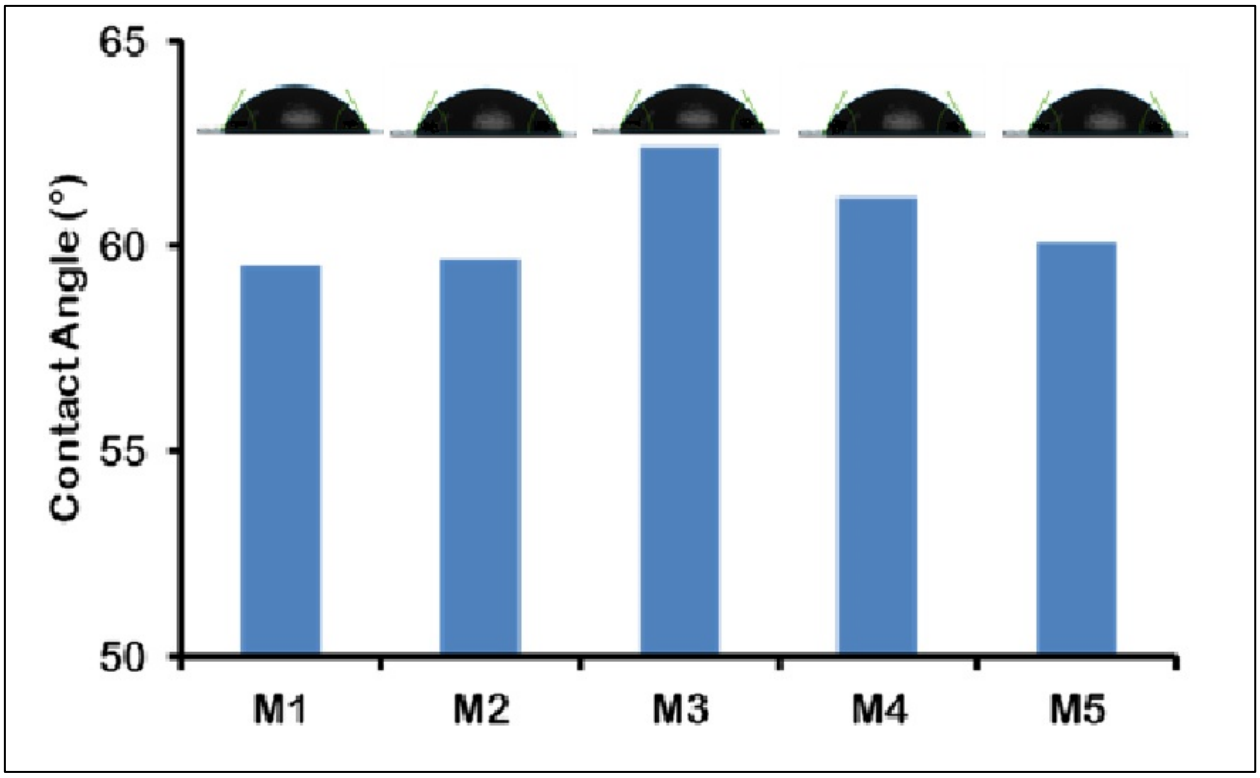

Figure A5: Contact Angles of the ceramic membranes

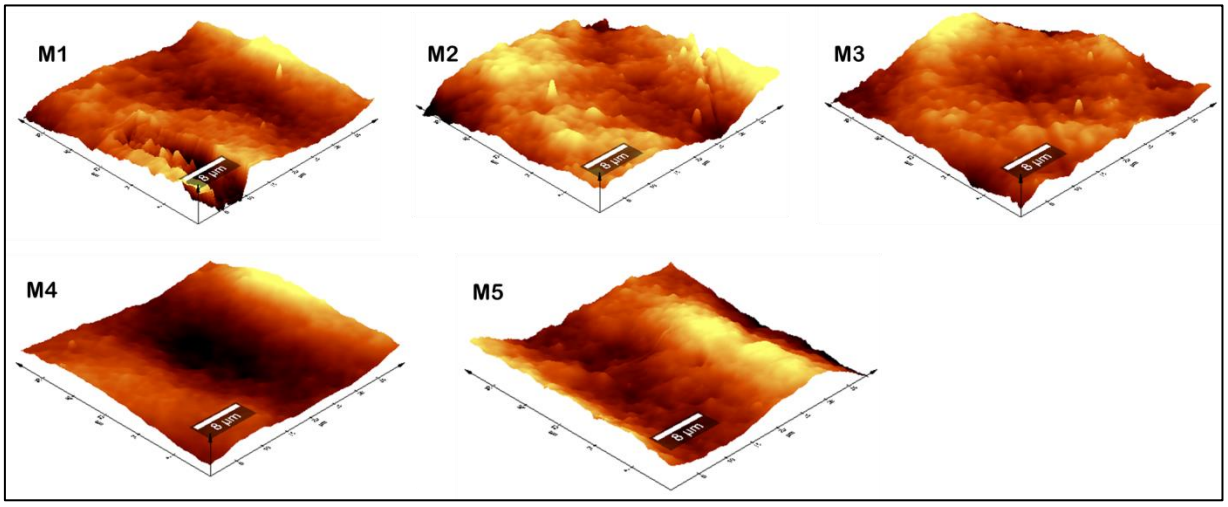

Figure A6: AFM micrographs of the top surface of the ceramic membranes

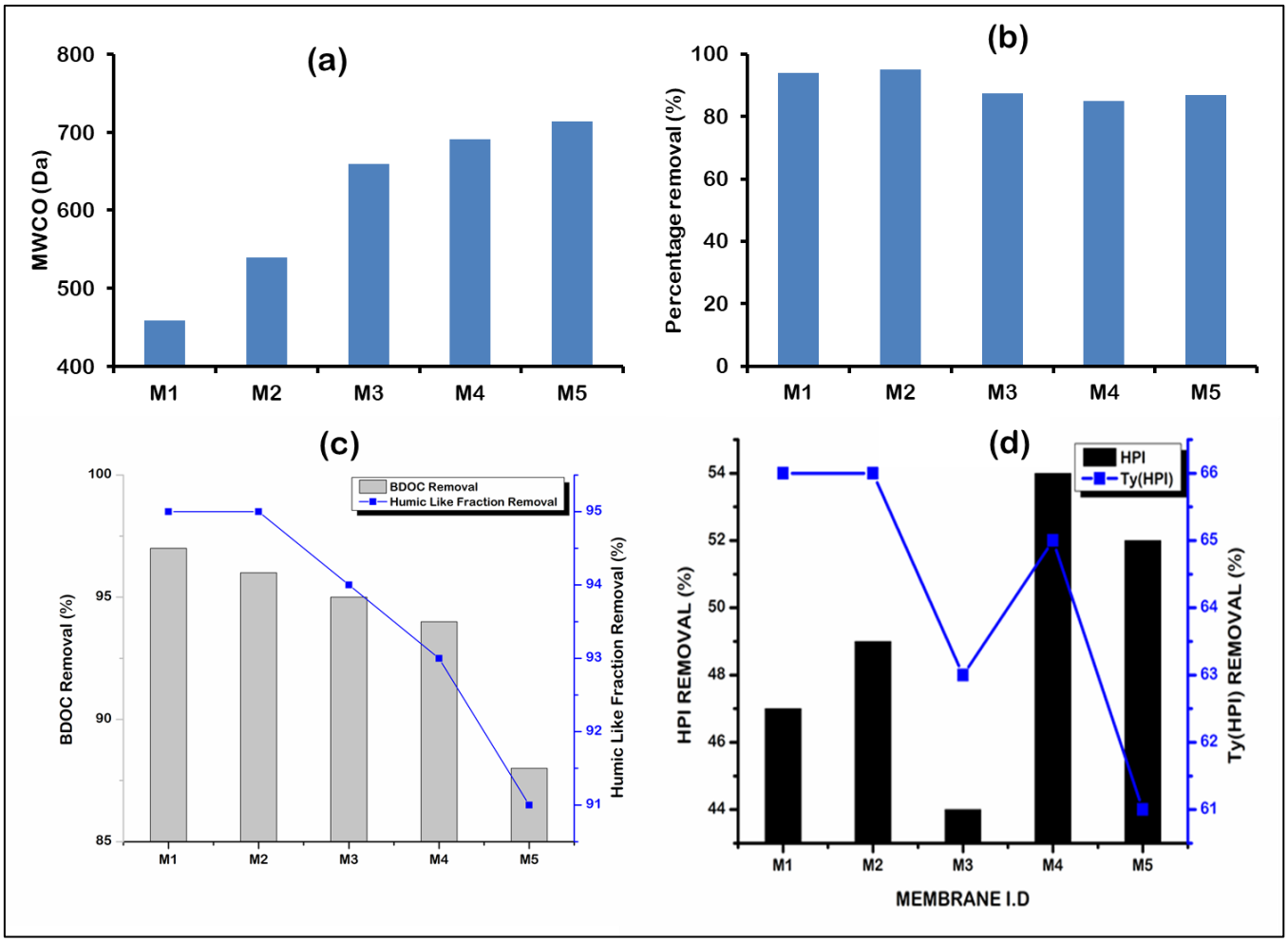

Figure A7: MWCO and removal of NOM fractions by ceramic membranes: (a) MWCO of the membranes (b) Determination of polysaccharide (biopolymer) removal measured as glucose equivalent; (c) BDOC and humic-like fraction of BDOC removal by ceramic membranes, and (d) removal of HPI and tyrosine like fraction of HPI by ceramic membranes.